IAEA-TECDOC-1878

IAEA TECDOC SERIES

IAEA-TECDOC-1878

Demonstrating Performance of Spent Fuel and Related Storage System Components during Very Long Term Storage

Final Report of a Coordinated Research Project

IAEA
International Atomic Energy Agency

DEMONSTRATING PERFORMANCE OF SPENT FUEL AND RELATED STORAGE SYSTEM COMPONENTS DURING VERY LONG TERM STORAGE

The following States are Members of the International Atomic Energy Agency:

AFGHANISTAN
ALBANIA
ALGERIA
ANGOLA
ANTIGUA AND BARBUDA
ARGENTINA
ARMENIA
AUSTRALIA
AUSTRIA
AZERBAIJAN
BAHAMAS
BAHRAIN
BANGLADESH
BARBADOS
BELARUS
BELGIUM
BELIZE
BENIN
BOLIVIA, PLURINATIONAL STATE OF
BOSNIA AND HERZEGOVINA
BOTSWANA
BRAZIL
BRUNEI DARUSSALAM
BULGARIA
BURKINA FASO
BURUNDI
CAMBODIA
CAMEROON
CANADA
CENTRAL AFRICAN REPUBLIC
CHAD
CHILE
CHINA
COLOMBIA
CONGO
COSTA RICA
CÔTE D'IVOIRE
CROATIA
CUBA
CYPRUS
CZECH REPUBLIC
DEMOCRATIC REPUBLIC OF THE CONGO
DENMARK
DJIBOUTI
DOMINICA
DOMINICAN REPUBLIC
ECUADOR
EGYPT
EL SALVADOR
ERITREA
ESTONIA
ESWATINI
ETHIOPIA
FIJI
FINLAND
FRANCE
GABON
GEORGIA
GERMANY
GHANA
GREECE
GRENADA
GUATEMALA
GUYANA
HAITI
HOLY SEE
HONDURAS
HUNGARY
ICELAND
INDIA
INDONESIA
IRAN, ISLAMIC REPUBLIC OF
IRAQ
IRELAND
ISRAEL
ITALY
JAMAICA
JAPAN
JORDAN
KAZAKHSTAN
KENYA
KOREA, REPUBLIC OF
KUWAIT
KYRGYZSTAN
LAO PEOPLE'S DEMOCRATIC REPUBLIC
LATVIA
LEBANON
LESOTHO
LIBERIA
LIBYA
LIECHTENSTEIN
LITHUANIA
LUXEMBOURG
MADAGASCAR
MALAWI
MALAYSIA
MALI
MALTA
MARSHALL ISLANDS
MAURITANIA
MAURITIUS
MEXICO
MONACO
MONGOLIA
MONTENEGRO
MOROCCO
MOZAMBIQUE
MYANMAR
NAMIBIA
NEPAL
NETHERLANDS
NEW ZEALAND
NICARAGUA
NIGER
NIGERIA
NORTH MACEDONIA
NORWAY
OMAN
PAKISTAN
PALAU
PANAMA
PAPUA NEW GUINEA
PARAGUAY
PERU
PHILIPPINES
POLAND
PORTUGAL
QATAR
REPUBLIC OF MOLDOVA
ROMANIA
RUSSIAN FEDERATION
RWANDA
SAINT LUCIA
SAINT VINCENT AND THE GRENADINES
SAN MARINO
SAUDI ARABIA
SENEGAL
SERBIA
SEYCHELLES
SIERRA LEONE
SINGAPORE
SLOVAKIA
SLOVENIA
SOUTH AFRICA
SPAIN
SRI LANKA
SUDAN
SWEDEN
SWITZERLAND
SYRIAN ARAB REPUBLIC
TAJIKISTAN
THAILAND
TOGO
TRINIDAD AND TOBAGO
TUNISIA
TURKEY
TURKMENISTAN
UGANDA
UKRAINE
UNITED ARAB EMIRATES
UNITED KINGDOM OF GREAT BRITAIN AND NORTHERN IRELAND
UNITED REPUBLIC OF TANZANIA
UNITED STATES OF AMERICA
URUGUAY
UZBEKISTAN
VANUATU
VENEZUELA, BOLIVARIAN REPUBLIC OF
VIET NAM
YEMEN
ZAMBIA
ZIMBABWE

The Agency's Statute was approved on 23 October 1956 by the Conference on the Statute of the IAEA held at United Nations Headquarters, New York; it entered into force on 29 July 1957. The Headquarters of the Agency are situated in Vienna. Its principal objective is "to accelerate and enlarge the contribution of atomic energy to peace, health and prosperity throughout the world".

IAEA-TECDOC-1878

DEMONSTRATING PERFORMANCE OF SPENT FUEL AND RELATED STORAGE SYSTEM COMPONENTS DURING VERY LONG TERM STORAGE

FINAL REPORT OF A COORDINATED RESEARCH PROJECT

INTERNATIONAL ATOMIC ENERGY AGENCY
VIENNA, 2019

For further information on this publication, please contact:

Nuclear Fuel Cycle and Materials Section
International Atomic Energy Agency
Vienna International Centre
PO Box 100
1400 Vienna, Austria
Email: Official.Mail@iaea.org

Printed by the IAEA in Austria
June 2019

IAEA Library Cataloguing in Publication Data

Names: International Atomic Energy Agency.
Title: Demonstrating performance of spent fuel and related storage system components during very long term storage / International Atomic Energy Agency.
Description: Vienna : International Atomic Energy Agency, 2019. | Series: IAEA TECDOC series, ISSN 1011–4289 ; no. 1878 | Includes bibliographical references.
Identifiers: IAEAL 19-01246 | ISBN 978–92–0–103319–2 (paperback : alk. paper)
Subjects: LCSH: Spent reactor fuels — Storage. | Spent reactor fuels. | Radioactive wastes — Storage.

FOREWORD

In many countries with nuclear reactors, the original intent was to manage the spent nuclear fuel (SNF) by transporting it to its final disposition (e.g. reprocessing, geological disposal) within the first decade after its removal from the reactor core. For many reactors designed and constructed prior to about 1990, pool capacity was limited to the volume required to store fuel from roughly ten years of reactor operation.

In the 1990s, many countries that had initially planned to reprocess SNF chose not to do so. In all countries, geological disposal of SNF or high level waste from reprocessing was postponed — initially for periods expected to be no more than 20 years — necessitating additional SNF storage capacity, often outside the spent fuel pools. The SNF was to be transported after this relatively short storage period, often in the same system used for additional storage. Thus the storage and transportation systems were designed accordingly, and the time period considered in the assessment of the behaviour of SNF during storage and transportation was around two decades.

As the duration of SNF storage now extends beyond 20 years, management of SNF has become an increasingly important factor influencing the future of nuclear energy. Storage and transportation systems designed for only a few decades are now being called upon to maintain their safety functions beyond their initial design period. Similarly, the behaviour of SNF needs to be determined for these longer storage periods. It is now essential that degradation of those systems that could lead to the loss of one or more safety functions be understood. The expanding use of nuclear fuel with higher burnup levels requires additional research to improve understanding of its longer term behaviour, as there may be additional issues that may make such fuel more susceptible to embrittlement (especially after a longer storage period prior to transportation).

Most R&D on longer term degradation of SNF storage and transportation systems will necessarily be at a small scale (often using unirradiated fuel or fuel substitutes), owing to resource limitations. However, there is a need for 'demonstrations' of systems at larger scales (concerning both size and time), to ensure that the smaller scale R&D work has not missed any combined effects. There are several considerations in the design of large scale demonstrations to maximize their usefulness.

Safe and secure management of SNF for these longer storage periods will depend on the development of experts in many countries with the skills and training necessary to safely manage SNF prior to its final disposition. Recognizing the benefits of sharing information, experience and lessons learned in this area, the IAEA launched a coordinated research project (CRP) entitled Demonstrating Performance of Spent Fuel and Related Storage System Components during Very Long Term Storage to support its Member States in sharing information, best practices and lessons learned to increase the number of countries with the necessary expertise.

The present publication summarizes the work conducted from 2013 to 2016 as part of that CRP. This work, which was mainly focused on dry storage conditions, contributes to the overall goal of demonstrating the performance of spent nuclear fuel and related storage system components over longer term storage. Confidence in the models developed from the work conducted as part of this CRP, along with a large amount of other data, can be improved via use of larger scale (in both space and time) demonstration testing. The relationship between smaller scale testing and fuller scale demonstration tests is discussed in this publication.

The IAEA gratefully acknowledges the contribution of the CRP participants and the consultants who collaborated in the drafting and reviewing of this publication, in particular J. Kessler (United States of America) for chairing the CRP and the Research Coordination Meetings. This CRP was funded through the Peaceful Uses Initiative (PUI). The IAEA officers responsible for this publication were A. Bevilacqua and A. González Espartero of the Division of Nuclear Fuel Cycle and Waste Technology.

CONTENTS

1. INTRODUCTION

1.1. BACKGROUND

Several decades ago, it was envisioned that spent nuclear fuel (SNF) being discharged from nuclear power reactors would be recycled[1]. Recycling typically includes chemical reprocessing of SNF to separate the fissile material from the non-fissile radionuclides with the fissile material being reconstituted into new fuel. The non-fissile material is primarily high level waste (HLW), considered by-product of reprocessing. HLW was envisioned to be temporarily stored prior to be disposed of in deep geological formations. The designers of the current fleet of commercial reactors assumed that SNF would be stored at the reactor site for a few years prior to subsequent transport for reprocessing. Thus, many SNF pools (SFPs) adjacent to the reactors only have the capability of storing SNF for five to ten years of reactor operation.

A common problem in countries using nuclear power is the current lack of an ultimate disposition pathway (either geological disposal[2] or SNF reprocessing), due to the cancellation of plans for SNF reprocessing in most countries, and decades-long delays in the availability of deep geological disposal facilities in almost all countries. As a result, there is a need for additional storage capacity. As SFPs at reactor sites reach capacity, one or, often both of the following approaches to managing the longer term, but still temporary, storage of SNF have been adopted: the original SNF racks in the SFPs were replaced with higher capacity racks that increased the amount of SNF that could be stored in the SFPs; and/or additional SNF was removed from SFPs and placed in a new storage facility away from reactor site.

Both, away from reactor and at-reactor facilities can employ either wet or dry storage. There is an increasing use of dry storage systems in which the water is removed. The most commonly used dry storage systems can store a few to up to several tens of assemblies.

There are four different dry storage system designs:

(1) Bolted lid cask employing shielding materials in the cask wall (Figs 1.1 and 1.2). In some bolted lid designs, concrete is included in the cask wall;
(2) Steel canisters inside concrete overpacks (horizontal design) (Fig. 1.3);
(3) Steel canisters inside concrete overpacks (vertical design). There are two variants of the vertical design:
    (a) Concrete overpacks exposed to the atmosphere (Fig. 1.4). The exposed concrete surfaces of the concrete cask are coated with a commercial-grade sealant to provide protection to the cask surfaces during current and long term storage operations;
    (b) Concrete overpacks with an outer steel liner (Fig. 1.5);

[1] In this report, only SNF primarily from light water reactors (LWRs) will be discussed. There are many countries that have SNF from other types of reactors and defence activities that will also have to be managed (storage and transportation followed by reprocessing or disposal). Many of the issues related to the need for long term storage summarised in this TECDOC can apply also to them.

[2] While progress is being made in several countries that could change the situation in the next decade or two, as of March 2019 no geological disposal facilities are operating anywhere in the world for SNF.

(4) Concrete vaults (see Figs 1.6 and 1.7 for two examples). This type of storage system uses metal canisters in all-metal silos located inside concrete vaults.

Bolted metal casks employ a set of bolted metal lids, as those shown in Figs 1.1 and 1.2. Figure 1.2 shows the individual cells inside the cask into which the assemblies are placed, the lid bolted in place, the water removed, and the cask dried and filled with an inert atmosphere. The decay heat from the fuel is removed by transfer through the cask wall and to the outside air. A more detailed figure of the bolted lid is shown in Chapter 5 (see Fig. 5.1). Each lid uses two O-ring gaskets to ensure the lid provides an adequate seal to limit the release of gas from inside the cask body where the SNF is placed and enables seal effectiveness to be monitored.

FIG. 1.1. Example of a bolted metal storage cask: CASTOR® V/19 (reproduced courtesy of GNS) [1.1].

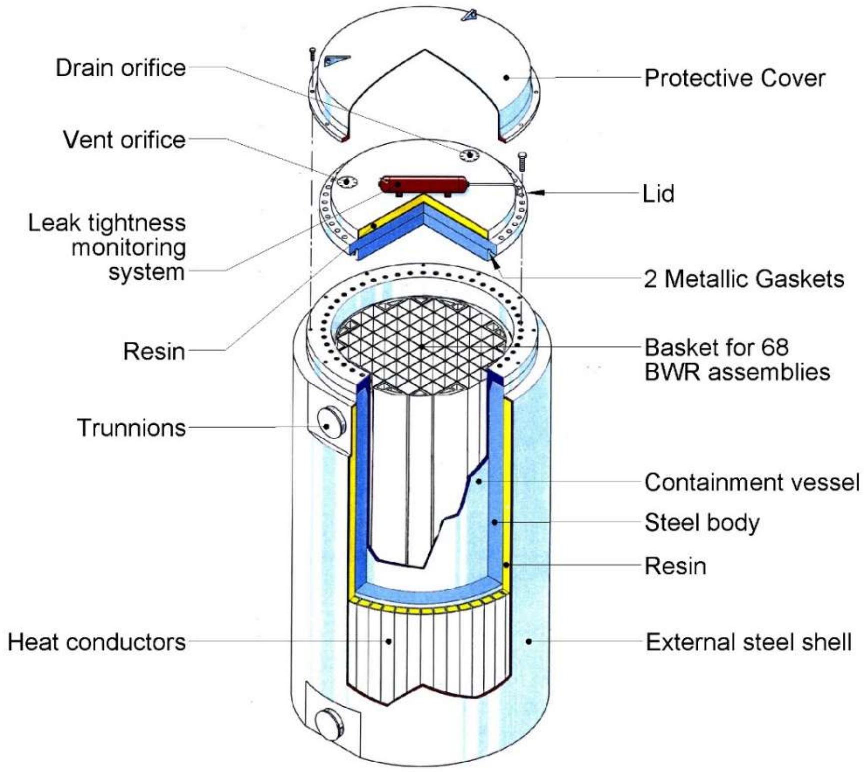

FIG. 1.2. TN-68 transport/storage cask (reproduced courtesy of TN Americas).

The second and third dry storage system types employ a relatively thin-walled welded steel canister with welded lids inside a concrete or metal overpack. Spent fuel is placed into the canister, the lid welded, water removed via vent and siphon ports, and then backfilled with inert gas. The canister is placed into the concrete overpack that has vents to allow air to flow past the canister to remove decay heat via convective flow. The overpack serves to protect the canister from the environment and as shielding from the radioactivity emitted by the SNF. Overpacks are either metal, concrete, or concrete between metal shells. The canister/overpack orientation can be either horizontal (Fig. 1.3) or vertical (Figs 1.4 and 1.5). An exploded view of a welded steel canister for the horizontal system is shown in Fig. 1.3(b). Figure 1.3(a) shows the on-site transfer cask with the canister inside being positioned to insert the canister inside the concrete overpack.

The majority of bolted metal casks are designed for both storage and transportation, so they are called dual purpose casks (DPCs). The metal canisters containing the SNF inside concrete overpacks are also suitable for storage and transport using a different overpack designed specifically for transport, or storage, and potentially disposal (termed multipurpose canisters (MPCs)), each with its different overpack.

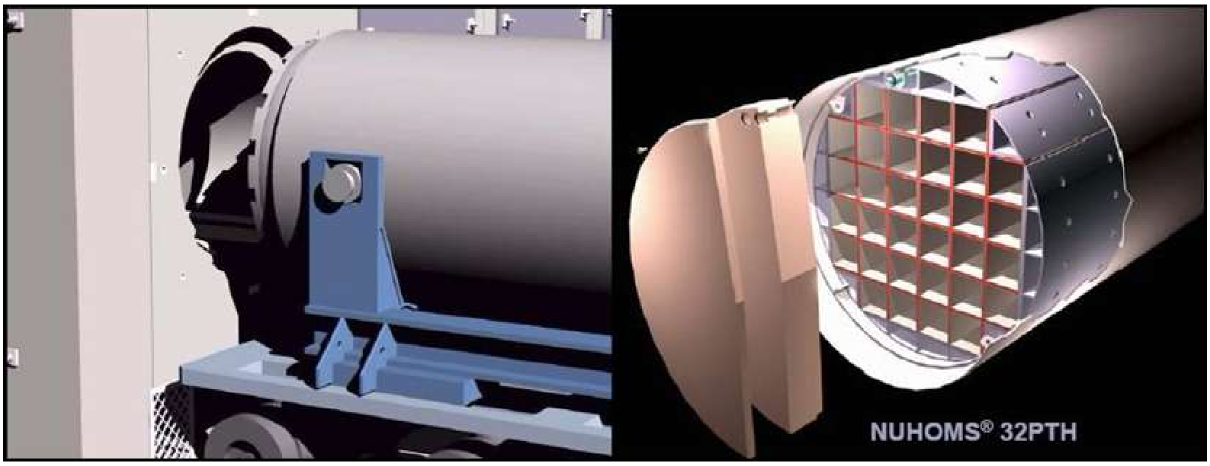

(a) *(b)*

FIG. 1.3. (a) NUHOMS horizontal storage module, transfer trailer (reproduced courtesy of TN Americas); (b) NUHOMS 32PTH dry shielded canister (reproduced courtesy of TN Americas).

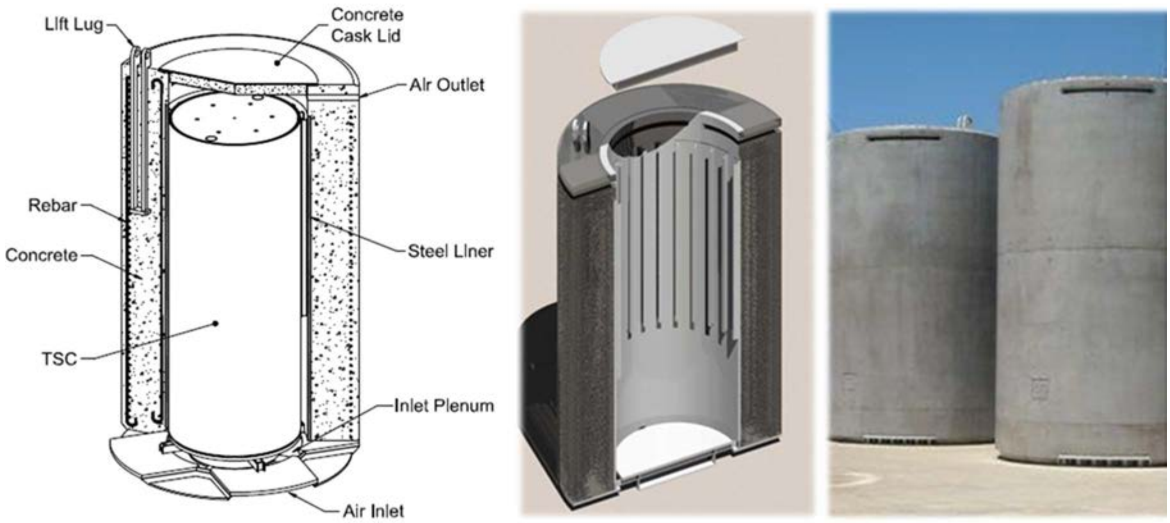

FIG. 1.4. NAC MAGNASTOR system (reproduced courtesy of NAC International) [1.2, 1.3].

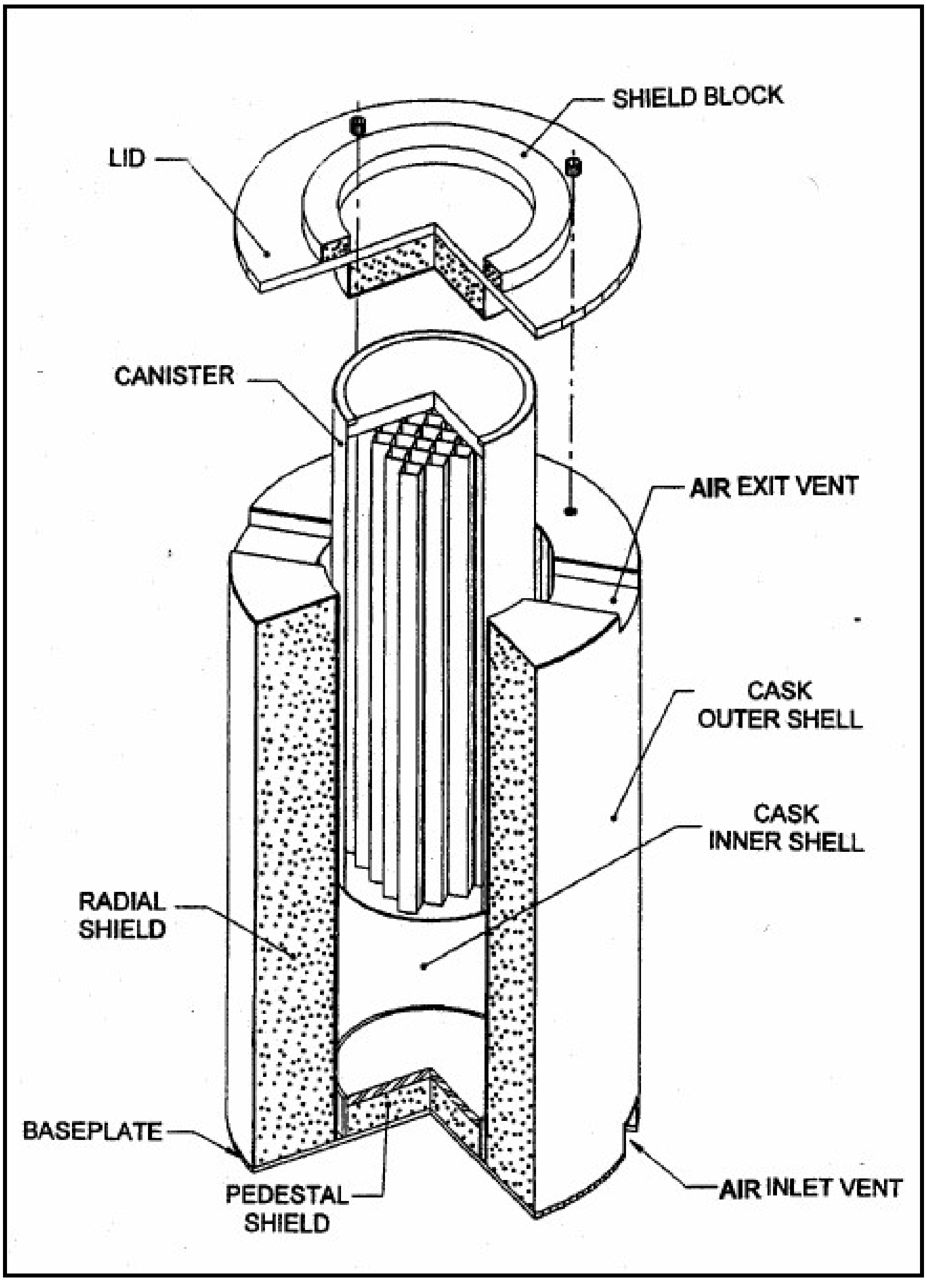

FIG. 1.5. Cross section of the HI-STORM 100 overpack for storage cask (reproduced courtesy of US NRC)[1.4].

A third type of dry storage system is a vault design that employs an array of steel tubes inside a large concrete structure to store the fuel assemblies. For decay heat removal, outdoor air is circulated around the tubes. An example of a vault that will contain SNF is shown in Fig. 1.6 The facility designed by the Spanish waste management organization, Empresa Nacional de Residuos Radiactivos, S.A (ENRESA), consists of LWR SNF first transferred from the transportation overpacks into smaller canisters (left portion in Fig. 1.6). After loading, the canisters will be filled with an inert gas, and welded closed (right-most section in red). The sealed canisters will then be transferred into the vault loading bay (right centre portion in Fig. 1.6) using the canister transfer machine shown on the far right, placed into tubes (drywells), which are long cylinders in stacks, the blue portion of the facility in Fig. 1.6. The drywell cylinders are slightly larger in diameter than the sealed canisters. Once each drywell is completely filled, it will be welded closed, and a shield plug will be placed on top of the drywell. The decay heat from the SNF will be removed via natural convection with the heated air exiting through the tall stacks above the vault.

Vault stores are currently in service at the Paks NPP in Hungary and at Idaho National Laboratory in the United States of America (USA) as shown in Fig. 1.7. The vault at Paks is used to store WWER-1000 spent fuel whilst the Idaho facility contains SNF from the decommissioned Fort Saint Vrain high-temperature gas-cooled reactor. Figure 1.7(b) shows the shield plugs on top of the filled drywells. There is also a dry vault store at the Wylfa NPP in United Kingdom (UK) that stores Magnox fuel. The reactor is now shut down and the vault is being emptied as the spent fuel is being sent for reprocessing. Fig. 1.8 (a) presents an example of a closure system for casks: the typical double barrier bolted closure system of CASTOR® cask types whereas in (b) an example of metal seal is shown.

FIG. 1.6. ENRESA (Spain) planned vault storage (reproduced courtesy of ENRESA) [1.5].

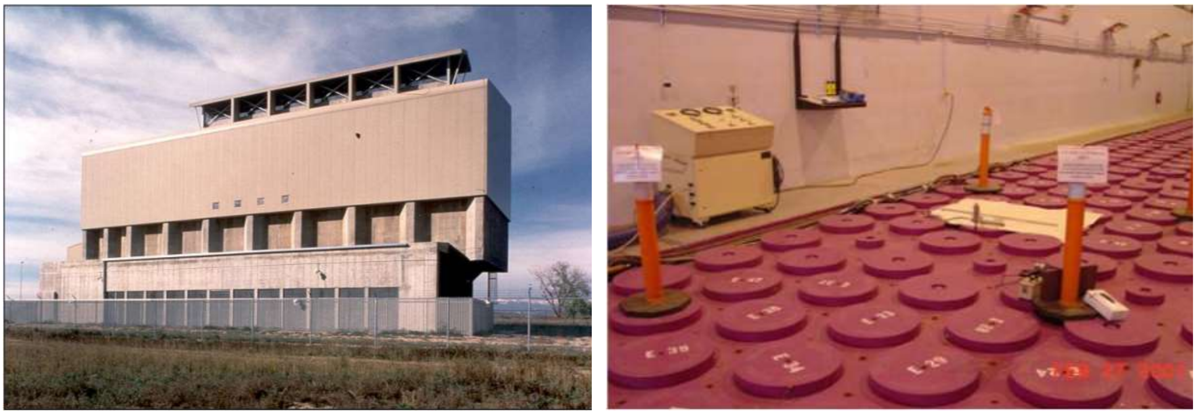

(a) *(b)*

FIG. 1.7. US Department of Energy SNF vault containing SNF from the decommissioned Fort St. Vrain reactor in the US (reproduced courtesy of US DOE) [1.6]: (a) Vault exterior view; (b) Interior charge face.

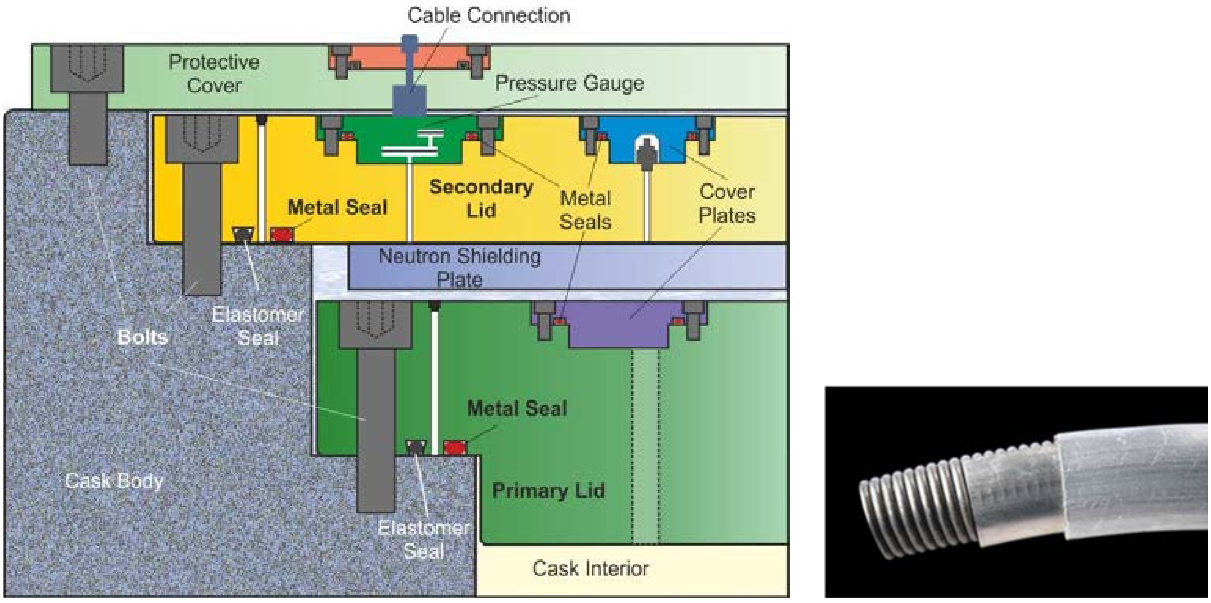

(a) *(b)*

FIG. 1.8. (a) Typical double barrier bolted closure system of CASTOR® cask types [1.7]; (b) A metal seal of the HELICOFLEX® type (reproduced courtesy of Bundesanstalt für Materialforschung und -prüfung (BAM)).

The fact that only few nuclear nations have reprocessing capability and there is so far no deep geological facility under operation is causing the required period of wet and dry storage to be extended. As part of the US Nuclear Regulatory Commission (US NRC)'s 'Continued Storage' ruling, the US NRC evaluated the very long term environmental impacts of time-unlimited storage and found the impacts generally low to medium [1.8]. The US NRC analyses [1.8] assumed monitoring the storage systems for signs of degradation, and mitigation of any degradation that could result in the loss of safety functions. The US NRC [1.8] also assumed near-complete replacement of SNF storage systems would occur every century. These assumptions lead to the need to develop and maintain capabilities to design, monitor, mitigate, and replace storage systems over the course of many decades.

Dry storage systems must meet specific safety functions. The International Atomic Energy Agency (IAEA) Radioactive Waste Management Glossary [1.9] states that a cask for storage or transport "…serves several functions. It provides chemical, mechanical, thermal and radiological protection, and dissipates decay heat during handling, transport and storage." The primary safety function is radiological protection with all the other functions providing a supportive role in maintaining this safety function. The radiological protection safety function is usually sub-divided into three parts:

- Confinement: the IAEA Radioactive Waste Management Glossary [1.9] defines confinement as follows:
  "*A barrier which surrounds the main parts of a facility containing radioactive materials and which is designed to prevent or mitigate the uncontrolled release of radioactive material to the environment. Confinement is similar in meaning to containment, but confinement is typically used to refer to the barriers immediately surrounding the radioactive material, whereas containment refers to the additional layers of defence intended to prevent the radioactive materials reaching the environment if the confinement is breached.*"
  The confinement safety function during dry storage is met using a combination of approaches that may include:
    - Maintaining SNF cladding integrity that would prevent the release of radioactive gases and particulates;
    - 'Canning' of SNF for which the cladding does not prevent radioactive release. Depending on the country, the cans are designed to prevent release of radioactive particulates or prevent release of both particulates and gases.
- Sub-criticality: the SNF must be maintained subcritical. This can be accomplished by using one or more of the following approaches:
    - Ensure that the SNF selected for storage has a sufficiently low reactivity (by limiting the amount of fissile material);
    - Adequate neutron poison capability within the SNF itself due to build-up of fission products that absorb neutrons; supplemental neutron poison material usually located in the storage cell walls;
    - Limiting geometric rearrangement of the SNF assemblies that may cause an increase in k-effective. This is accomplished by maintenance of structural integrity of the SNF assemblies or for the case of assemblies that may have partially lost structural integrity, use of cans that will limit geometric rearrangement.
- Radiation exposure: prevention of radiation exposure that would exceed regulatory limits. This is accomplished by the use of gamma and neutron shielding.

Demonstration of compliance with these safety functions requires knowledge of the behaviour of the SNF and most of the dry storage system 'structures, systems and components' (SSCs) for at least the period of time for which the license has been granted. This requires time-limited aging analyses (TLAAs) based on a variety of models that are developed from mostly smaller scale (in both space and time) testing. Depending on the country, the initial license period for storage ranges from 20 to 100 years. Technical bases to support spent fuel dry storage for the first few decades are mostly in place such that licensing of dry storage systems is proceeding. Some storage systems in some countries need to be used beyond their initial storage periods, which requires revisiting the original TLAAs to ensure the safety functions are still met. This requires knowledge of the condition and behaviour of the SNF and SSCs over a longer period. Therefore, if very long term dry storage followed and/or preceded by transportation is to be achieved to support potential changes in the long term nuclear power program, it will be necessary to confirm that the existing models for dry storage are still adequate to maintain the safety functions during a period well beyond the initial licensing period.

Multiple organizations have performed gap analyses to identify gaps in existing knowledge regarding long term storage and transportation of spent fuel. Gaps due to loss of long term safety functions are either specific to one or more SSCs of the storage system or considered cross-cutting (phenomena that influence the long term behaviour of multiple SSCs). The Electric Power Research Institute (EPRI) summarized the gap analyses conducted by US organizations in early 2011 [1.10]. Gaps identified by the 13 following organizations from 7 participating countries are summarized in [1.11]:

- Germany: Bundesanstalt für Materialforschung und -prüfung (BAM);
- Hungary: Radioaktív Hulladékokat Kezelő Közhasznú; Som System Kft.;
- Japan: Central Research Institute of Electric Power Industry (CRIEPI);
- Republic of Korea: Korea Radioactive Waste Agency (KORAD) and Korea Atomic Energy Research Institute (KAERI);
- Spain: Consejo de Seguridad Nuclear (CSN); Empresa Nacional de Residuos Radiactivos, S.A (ENRESA) and ENUSA Industrias Avanzadas;
- UK: EDF Energy, National Nuclear Laboratory (NNL);
- USA: Sandia National Laboratories (SNL) and Pacific Northwest National Laboratory (PNNL).

Each organization ranked the gaps according to criteria that included the importance to safety and how important it is to perform additional research and development.

Table 1.1 lists only those data gaps whose closure were considered either high or medium priority by at least one of the above organizations. There was near unanimous agreement that three gaps were of high importance in terms of their potential degradation during extended storage and for which additional data is required to assess that potential for storage for very long time periods followed by transportation:

- Fuel cladding, particularly hydride embrittlement;
- Stress corrosion cracking (SCC) of austenitic stainless steel canister welds;
- Fatigue of bolted cask bolts and seals [1.11].

At least one organization considered the following items to be gaps, but considered them to be of low priority for closure:

- Fuel cladding (emissivity changes, fatigue, phase change, wet corrosion);
- Fuel pellets (fragmentation, restructuring/swelling);
- Assembly hardware (corrosion cracking, creep, hydriding effects, metal fatigue);
- Basket (creep, metal fatigue);
- Neutron poison or shielding (poison burnup);
- Concrete casks, overpacks or pads (aggregate growth and reaction, calcium leaching, chemical attack, water decomposition, dry-out, fatigue).

The cross-cutting gaps listed in Table 1.2 are all assessed to be of high importance.

TABLE 1.1. VERY LONG TERM STORAGE TECHNICAL NEEDS FOR STRUCTURES, SYSTEMS AND COMPONENTS (SSCs): SUMMARY OF 'IMPORTANCE TO R&D ASSESSMENTS' (ADAPTED FROM [1.11])

Structures, systems and components (SSCs)	Ageing alteration and/or degradation mechanism	TECDOC chapter in which the gap is addressed
Fuel cladding	Annealing	n.a.
	Hydrogen embrittlement	3
	Hydride cracking	3
	Oxidation	3
	Creep	3
Fuel pellets	Cracking, bonding	n.a.
	Oxidation	3
Fuel assembly hardware	Corrosion and stress corrosion cracking (SCC)	n.a.
Basket	Corrosion, irradiation	n.a.
Neutron shielding	Thermal and radiation ageing	6
	Creep	6
	Corrosion	6
Neutron poison	Creep	n.a.
	Embrittlement	n.a.
	Corrosion	n.a.
Welded canister	Atmospheric corrosion	2
	Aqueous corrosion	n.a.
Moisture absorber	Irradiation, thermal	n.a.
Bolted casks	Fatigue of seals or bolts	5
	Atmospheric corrosion	n.a.
	Aqueous corrosion	n.a.
	Metal seal creep	5
Concrete overpack, cask, or pad	Freeze-thaw	4
	Corrosion (including embedded steel)	4

Note:

A few of these ageing mechanisms are not detrimental to maintaining safety functions.

TABLE 1.2. CROSS-CUTTING DATA NEEDS

Cross-cutting needs note	TECDOC chapter in which the gap is addressed
Monitoring[1] (internal)[2]	7
Monitoring (external)[3]	2, 4, 7
Temperature profile	2–7
Drying issues	3, 7
Subcriticality, burnup credit, moderator exclusion	n.a.
Fuel transfer options	n.a.
Examination[4]	7
Canister weld stress profiles	2, 7
Damage definitions	n.a.
Verification of fuel condition / fuel classification	n.a.

Note:

[1] Monitoring is a general term that includes continuous or periodic measurements or visual observations. This is sometimes referred to as inspection or surveillance.
[2] Internal monitoring is monitoring of the inside of the cask or canister. Examination of the fuel in existing canisters at the Idaho National Laboratory that were put in service in the 1980s into the early 1990s is the one example of internal monitoring that is underway (see Chapter 7).
[3] External monitoring are direct or indirect measurements of the properties of interest. Direct external measurement example: canister exterior surface temperature. Indirect external measurement example: atmospheric chloride concentration as an indication of the amount of chlorides deposited on the outside of canisters.
[4] Examination means post-test measurements or observations of the properties of interest.

The gaps shown in Tables 1.1 and 1.2 can be addressed initially via smaller scale testing. In this case, small scale means tests that are performed for relatively short periods of time compared to actual SNF storage times or tests that are performed using test materials that are smaller in scale and/or use substitute materials than that for real dry storage systems. Usually, models are developed from such smaller scale tests. Ultimate ‘validation’[3] of smaller scale tests and associated models would therefore involve longer time scales and full-size systems.

Hence, it is important to be able to evaluate the relevance of the smaller scale test results to actual dry storage conditions (long time periods and full-size systems). Figure 1.9 illustrates the linkage between smaller scale tests, the models developed from the smaller scale tests, and full-scale behaviour. Laboratory scale experiments (usually short term, small dimensions, and/or substitute materials) are often designed to investigate the effect of individual factors that may contribute to long term alteration of one or more SSCs. These are termed separate effects tests in Fig. 1.9. Predictions are made using models developed from separate effects tests to estimate long term, full-scale behaviour of the actual storage systems. A system demonstration

[3] The term ‘validation’ is commonly used in this context, although the meaning is to provide an evaluation of the behaviour of the full-scale storage systems to determine if the models developed from smaller scale testing adequately project full-scale system behaviour. Such an evaluation is accomplished via demonstration test(s).

is a full- (or at least partially full) scale test to evaluate the adequacy of the models. Data obtained from the system demonstration(s) are compared to the model predictions. If the models are determined to be adequately correct, then the models can be more confidently used to estimate long term behaviour of other dry storage systems. If the models are judged to be deficient (incorrect), then the data from the system demonstration(s) can be used to improve the models. Another type of testing that can be applied to evaluation of models is collection of inspection data from in-service dry storage systems. Chapters 2 through 6 discuss some separate effects tests and inspection data generated as part of this CRP and other data that can be used in the development of models.

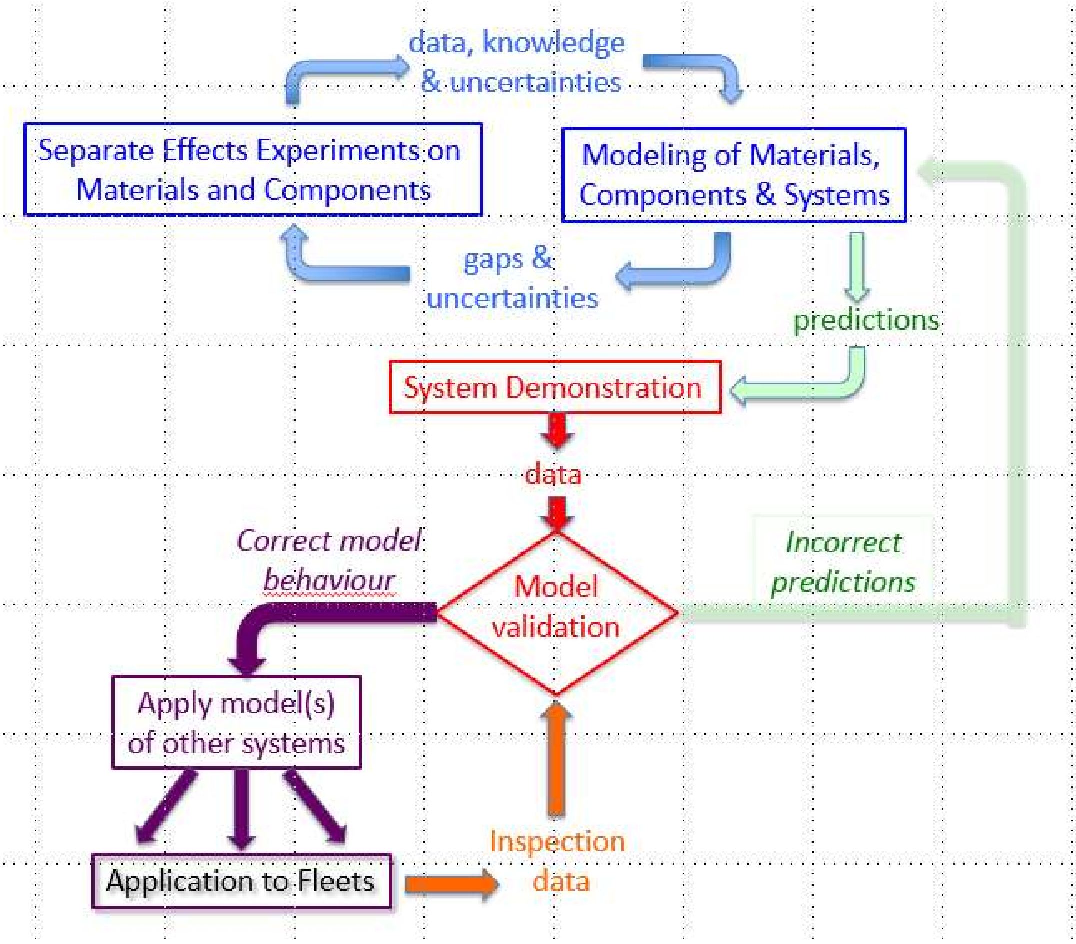

FIG. 1.9. Linkage between separate effects testing, modelling, demonstration large scale, long term testing and inspection data, evaluation criteria, and determination of the extent of application to the fleet of SNF storage systems and the SNF stored in those systems.

Chapter 7 discusses the characteristics of useful system demonstration(s). As described above, the difference between laboratory experiments and demonstration is the prototypical conditions under which a demonstration test should be performed. Prototypical conditions are dependent on the guidance given by the country storing the fuel and doing the demonstration, the type of dry storage system(s) being used, and the types of spent fuel to be stored. A comparison of the attributes of various types of tests from the smallest scale (laboratory scale) to partially full-scale in either time or size (partial demonstration) to full-scale in both time and size (full demonstration) is provided in Table 1.3. The details provided in this table are discussed in Chapter 7.

TABLE 1.3. ATTRIBUTES OF TESTS AT VARIOUS TIME AND SIZE SCALES WITH RESPECT TO DEVELOPMENT OF MODELS INCORPORATING IMPORTANT MECHANISMS INFLUENCING LONG TERM BEHAVIOUR OF ACTUAL SPENT FUEL DRY STORAGE SYSTEMS

Attribute of the demonstration	Laboratory scale test	Partial demonstration	Full demonstration
Purpose	Identify and study mechanisms, develop models	Identify unexpected mechanisms, confirm models (integration of effects), scaling effects	Identify unexpected mechanisms, confirm models (integration of effects), scaling effects
Physical scale (specimen size) (e.g. rod length, components size)	Generally small	Structures, systems and components (SSCs) of interest are near full-scale	Full
Time scale	Short	Long enough to extrapolate data	Long enough to extrapolate data
Instrumented or inspection capability	Yes	Mostly yes	If possible
Acceleration of effects (e.g. time, stress, temperature, bounding conditions)	Yes	Depends on purpose	No
Test conditions (e.g. stress, atmosphere, chemical, thermal)	Can be varied	Most of the conditions are realistic	Realistic
Specimen material and condition (e.g. irradiation, surrogate materials)	If possible	Yes, if possible	Yes
Cost	Low	Moderate	High

1.2 OBJECTIVE

The overall objective of the CRPs summarized in this TECDOC is to supplement and share the tests and models that form the nuclear power community's technical bases for LWR spent fuel management licences as dry storage durations extend. This involves developing:

- A network of experts working on current research projects to demonstrate the long term performance of spent fuel;
- Experimental data on the very long term performance of spent fuel and related important storage system components (i.e. this TECDOC report);
- Computational and experimental methods to adequately demonstrate very long term performance (i.e. ageing management modelling);
- Capability to assess the impact of higher burnup fuel (HBF) on very long term storage prior to or followed by transportation.

It is important to note that the terms long term performance or long term characteristics cover two different situations: storage and transportation after storage, with normal and accident conditions in both cases.

1.3. SCOPE

This work contributes to technical basis documentation for demonstrating the performance of spent fuel and related important storage system components over long durations, and thereby facilitate the transfer of this knowledge to others including to newcomer countries.

1.4. STRUCTURE

This report contains six chapters that summarize the phenomena of interest, and the funded work related to long term degradation and monitoring of storage systems. The detailed individual project reports are found in the annexes of this report[4]. The relevant work is briefly described here, indicating the corresponding annexes with detailed information.

(a) **Chapter 2**: Chloride Induced Stress Corrosion Cracking in Welded Dry Storage Canisters.

- Outcome of work conducted by **Pakistan Institute of Nuclear Science and Technology (PINSTECH, Pakistan)** with detailed information in **PAK 17283 - Annex VIII:** "*Stress corrosion cracking (SCC) susceptibility of welded stainless steel canister samples under simulated marine environment*". This study investigated chloride SCC phenomenon on both welded and unwelded type 316L stainless steel subject to various tensile stresses and chloride environments using electrochemical techniques. The tensile stress necessary for SCC in chloride environment (in addition to the residual stress present after welding) was applied through U bending for salt spray testing and tensile loading the samples in slow strain rate tests. The SCC susceptibility will be determined as a function of chloride concentration and material treatment. The particular emphasis will be given to the role of welded and heat affected region toward localized corrosion and mechanism of stress corrosion cracking.
- Outcome of work conducted by the **National Centre for Nuclear Research (NCBJ, Poland)** with detailed information in **POL 17290 - Annex IX:** "*The investigation of the gamma irradiation influence on the mechanical and corrosion properties of stainless steel used for spent fuel containers and canisters*". Gamma irradiation of type 316L stainless steel has been performed in the SFP of Research Reactor MARIA for 1, 3 and 18 months. In addition, chemical composition, metallographic investigation, non-destructive and intergranular corrosion (IGC) and SCC studies have been performed. Visible crack propagation can be noticed in each of the studied samples. However, due to the small mechanical differences between virgin samples and those samples irradiated for 18 months, it is hard to find a correlation between crack propagation and mechanical response of the sample. The technique used is an excellent tool for measuring small irradiated samples. However, reported herein technique works the best as a qualitative source of information, therefore, analysis of the results in the case of minor changes might be very difficult to interpret.
- Outcome of work conducted by the **National Nuclear Laboratory (NNL, United Kingdom)** with detailed information in **UK 17420 - Annex XIII:** "*Condition monitoring relevant to long term storage of LWR spent fuel*". A review of corrosion

[4] The Annexes of this report are provided as supplementary material. The names of the files are composed by the country abbreviation followed by the code of the CRP and the number of the Annex. The annexes included are: ARG 17338 – Annex I, ARG 17339 – Annex II, FRA 17270 – Annex III, GFR 17307 – Annex IV, JPN 17308 – Annex V, JPN 17486 – Annex VI, LIT 17275 – Annex VII, PAK 17283 – Annex VIII, POL 17290 – Annex IX, SLO 17810 – Annex X, SPA 17305 – Annex XI, SPA 18996 – Annex XII, UK 17420 – Annex XIII USA 19249 – Annex XIV.

sensing technologies was undertaken to provide an assessment of their applicability to various long term corrosion scenarios associated with interim storage. As a result, one technique was selected to go forward to a technical demonstration. This involved the production of an 'instrumented' corrosion coupon, the purpose of which is to identify environmental conditions that may allow corrosion as well as detect the onset and extent of corrosion once initiated. Requirements for an instrumented corrosion sensing device (SMART Coupon) have been developed and an option for short term development/implementation identified. Although localized metal loss maps show indications of localized corrosion at sites where there is corrosion product on the SMART Coupon, anomalies were also identified at sites where there is no corrosion product, and these are likely to be image artefacts.

Environmental data from the environmental control monitor (ECM) system in the environmental chamber has successfully been logged and reported, providing a basis for reliable measurement of local conditions relevant to determining the onset of corrosion. The ECM system shows promise for the online measurement of temperature, humidity and corrosive attack by the electrical resistance (ER) technique on a replaceable thin metal film. It could provide an indication of the corrosive nature of a storage environment although this would not be directly quantifiable to the impact on waste containers.

Separate work on corrosion of thermally sensitised 304 C-ring samples has shown that field signature method is able to detect onset and propagation of corrosion, and any interruption of the corrosion process. Therefore, further development of the original concept based on smaller coupons geometries is likely to be necessary for reliable monitoring of localized corrosion and hence the SMART Coupon concept warrants optimization for deployment in distributed LWR canister systems.

- Outcome of work conducted by the **Central Research Institute of Electric Power Industry (CRIEPI, Japan)** with detailed information in **JPN 17308 - Annex V:** "*Demonstrating performance of spent fuel and related system components during very long term storage*''. Initiation of chloride induced stress corrosion cracking (CISCC) depends on, among other factors, the relative humidity (RH) and the surface concentration of chlorides (as soluble salts) on the welded austenitic stainless steel surface. CRIEPI conducted experiments to identify both minimum RH and chloride surface concentration threshold values below which CISCC would not initiate. The CRIEPI test matrix investigated:
    - Two types of stainless steel: 304L and 316L;
    - At a constant temperature of 50°C or 80°C;
    - A RH of 35%.

  CRIEPI found that the minimum amount of salt for CISCC initiation for stainless steels of types 304L and 316L should respectively be set to 0.2 g/m^2 and 0.8 g/m^2 as Cl. CRIEPI also measured the rate of crack propagation and determined that the crack initially propagated rapidly before the propagation rate deeper into the samples declined to around 4.4~6.8 × 10^{-12} m/s.
- Field measurements of salt deposition were undertaken to understand their dependency on atmospheric salt concentrations. In parallel, laboratory based experiments were undertaken to relate atmospheric salt concentrations to measured deposition levels on heated canister surfaces. Full-scale mock-up CISCC testing contributed towards confirming whether small scale experimental testing related to 'environmental conditions under which CISCC occurs' remain valid at industrial scale and relevant environmental conditions. It also provides evidence of the effectiveness of processes affecting storage conditions. Using data from both laboratory and field tests, a

correlation for the amount of salt deposition was proposed in the form of the empirical equation as a function of time, the canister surface temperature and airborne salt concentration.

A second, full-scale mock-up of a type 304L stainless steel canister was loaded with chloride salt to a surface concentration of 4000 mg/m^2, which is over 20 times the threshold value reported above. Part of the mock-up was subjected to a low plasticity burnishing (LPB) surface treatment that reduces the residual tensile stress on welded stainless steel surfaces. No CISCC was observed on the part of the mock-up with the LBP treatment, suggesting that LPB may hold promise in mitigating CISCC in austenitic stainless steel dry storage canisters.

- Outcome of work conducted by the **National Building and Civil Engineering Institute (ZAG, Slovenia)** with detailed information in **SLO 17810 - Annex X:** "*Monitoring of material degradation during long term storage of spent fuel*". The goal of the research was to identify a reliable technique for monitoring of CISCC processes in a type 321 stainless steel by showing a correlation between different measurement techniques and microstructural evidence of corrosion processes. In this study, two aggressive aqueous environments were used (0.5 M NaCl + 0.5 M H_2SO_4; 1000 ppm boric acid at 100 bar and 300°C) to evaluate several difference techniques for identifying SCC in an atmospheric (not aqueous) environment: electrochemical noise (EN), acoustic emission (AE), tensile test sample elongation, and digital imaging correlation of the sample surface by charge coupled device camera (DIC). AE shows promise identifying relatively large cracks, although it is vulnerable to signal degradation due to environmental noise. EN and the other electrochemical techniques were determined to be of limited use for storage applications.

(b) **Chapter 3**: Rod behaviour.

- Outcome of work conducted by **Centro Atómico Constituyentes (CAC, Argentina)** with detailed information in **AGR 17339 - Annex II:** "*Materials degradation assessment of power reactor spent fuel and installations during long interim dry storage*". According to the dry storage concept developed for the Atucha 1 NPP, the Zircaloy clad spent fuel elements stored inside the CAN-1 dry storage system must withstand environmental conditions which includes maximum SNF cladding temperature of 200°C, internal spent fuel element (SFE) pin pressure of ~70 bar (value at end of cycle) and SNF assembly weight of ~220 kg. The activities carried out during the development of the CRP includes a state-of-the-art review of spent fuel cladding properties and the onset of experimental work aiming to fill the identified gaps. Some of this work has been completed and some other is still being performed and will continue beyond the reach of the CRP:
  - Oxidation of Zircaloy-4: with the addition of 1M LiOH, oxidation rates increased by a factor of 40;
  - SCC of spent fuel cladding: fission product-induced SCC will not take place in CAN-1 SFE storage;
  - Hydrogen damage to cladding: (1) conditions leading to embrittlement due to the presence of radial hydrides are presented; (2) there is inadequate stress to generate delayed hydride cracking;
  - Cladding creep will not take place for dry storage conditions with peak cladding temperatures lower than 200°C;
  - On-going experimental work on hydride lenses effect generated in unirradiated cladding material.

- Outcome of work conducted by the **JRC Directorate for Nuclear Safety and Security of the European Commission**[5]: "*Degradation of LWR spent fuel during very long term storage*". JRC Directorate for Nuclear Safety and Security of the European Commission investigated spent fuel rod damage due to the long term build-up of helium from alpha decay; severe accident effects on cladding (mechanical load, impact resistance, corrosion, loss of cooling, damage fuel and fuel debris generation, and radionuclide source term for geological disposal). During the time of this CRP, first testing in an improved impact load device of a sample from a duplex-type cladding with a burnup of ~67 GWd/t(HM) was performed. A hammer impact load simulating pinch load conditions was applied to determine the amount and particle size distribution of fuel debris, also possible effects due to rodlet internal pressure were considered. The final goal is to determine criteria and conditions governing the response of SF to impact loads that may be experienced by the rod during handling, transportation, storage and after extended storage.
- Outcome of work conducted by **Consejo de Seguridad Nuclear (CSN, Spain)** with detailed information in **SPA 17305 - Annex XI:** "*Effect of hydrogen contents and hydride orientation on ductility*". CSN investigated the mechanical behaviour of highly hydrided SNF cladding, under normal, abnormal and accident conditions during long term dry storage and subsequent transportation. The main goal is to determine the criteria for the SNF classification as damaged or undamaged, based on whether the cladding integrity can be maintained under these operating conditions. CSN experiments used a Zirlo-type cladding using unirradiated materials. The program is based in the performance of a comprehensive ring compression tests (RCTs) matrix at different test conditions:
  - Temperatures: from 20°C to 300°C;
  - Hydrogen concentrations: from 0 to 2000 ppm;
  - Hydrogen morphologies : circumferential/radial hydrides;
  - Hoop stresses (reorientation): from 0 to 140 MPa;
  - Loading rates: from 0 to 3 m/s.

  A complete set of experimental load-displacement curves has been obtained from these tests delivering conclusive results related to cladding integrity behaviour. Cladding without applied stresses at any temperature remained ductile, while cladding subject to a combination of elevated hoop stress and temperature were more brittle.
- Outcome of work conducted by **Centro de Investigaciones Energéticas Medioambientales y Tecnológicas (CIEMAT, Spain)** with detailed information in **SPA 18996 - Annex XII:** "*Evaluating degradation of the spent fuel and the confinement capability of the spent fuel cladding in a dry storage environment*". Oxygen in the cask could potentially degrade the cladding either by reacting directly with it or by reacting with exposed UO_2 fuel (if cladding breaches are present). Consequently, breached rods could lead to radionuclides release via oxidation of the UO_2 fuel into U_3O_8, which has a higher specific volume. Hydrogen pick-up by the cladding will lead to the formation of zirconium hydrides that have a lower ductility than the base cladding metal. The results obtained, so far, are focused on the design and development of the different characterization techniques proposed in the CRP project. The ongoing activities involve the performance of the prototypes in order to carry out the studies of the spent fuel matrix alteration under dry storage conditions. The second phase is being performed to develop the methods for analysing the proposed material.

[5] JRC Directorate for Nuclear Safety and Security of the European Commission was formerly ITU-JRC.

- Outcome of work conducted by **Orano TN[6] (France)** with detailed information in **FRA 17270 - Annex III:** "*Study of degradation of neutron shielding, information on prediction of very long term performance of spent fuel, evaluation of the effect of drying and storage on spent fuel cladding behaviour*". This study includes the contribution of three spent fuel related research activities performed in France:
    - Degradation of spent fuel and containment issues, mainly addressed in the PRECCI project, partnership between CEA, EDF, Orano[7] and ANDRA, aiming to investigate the spent fuel integrity and retrievability after storage (influence of cladding material, temperature, stress conditions for higher burnup (HBU) fuels, clad embrittlement, hydride effects: ductile-to-brittle transition degradation, irradiation damage and recovery) based on experimental work and development of models to assess clad integrity;
    - Effect of drying and residual water on the cladding, combining sampling from fuel cask cavity atmosphere, drying tests and model development to understand the mechanisms involved and to define the adequate drying before shipment;
    - Transportation accident conditions, supported by the Fuel Integrity Project (FIP), a joint programme developed by Orano TN (France) and INS (UK) for the assessment of the fuel in impact mechanical behaviour (hypothetical transport accident). It includes experimental work with irradiated samples up to 40–50 GWd/t(HM) and analytical work for the development of models.
- Outcome of work conducted by **US Nuclear Regulatory Commission (US NRC, United States of America)** with detailed information in **USA 19249 - Annex XIV:** "*Update on NRC activities related to demonstration of SNF long term storage and transportation*". The work performed addresses different knowledge gaps and CRP objectives as follows:
    - Thermal analysis: an independent computational analysis has been performed to predict the thermal behaviour of dry cask storage systems for periods up to 300 years, using computational fluid dynamics (CFD) methods and 3-D numerical simulations;
    - Vacuum drying: development of a plan to measure the quantity of unbound residual water remaining in a canister following vacuum drying. Reports addressing the determination of residual water effects and typical vacuum drying systems and operational procedures have been prepared;
    - Cladding stress: assessment of the potential for low temperature creep and DHC failures in HBU spent fuel cladding during extended dry storage, using a modified version of the US NRC's steady state fuel performance code FRAPCON;
    - Fatigue fracture: HBF mechanical behaviour study supported by rod testing under static and dynamic loading conditions. Effect of hydride precipitation and high levels of irradiation-damage.

(c) **Chapter 4**: Concrete degradation in dry storage systems during long term spent fuel storage.

- Outcome of work conducted by **Comisión Nacional de Energía Atómica (CNEA, Argentina)** with detailed information in **AGR 17338 - Annex I:** "*Feasibility study of*

[6] Orano TN was formerly AREVA TN International.

[7] Orano was formerly AREVA.

an emission tomography monitoring system for dry-stored spent nuclear fuel". The technology to evaluate the spatial distribution of the radiation within dry storage units does not exist yet. Development of such a technique allows for the study of the radioisotope composition and distribution, the design of more efficient barriers, as well as detection of radioactive waste leaks. The construction of a dry-stored SNF emission tomography scanner involves technical challenges, such as high-sensitivity, high energy resolution, and high-background measurements. Laboratory experiments involved the use of a block of reinforced concrete of 40 cm × 20 cm × 10 cm with 3 rebars of 10 mm diameter. This set was placed at 20 cm from a planar gamma camera head (NaI(Tl) detector) and a point source of 100 µCi ^{137}Cs was placed 55 cm away from the block. The block was positioned in such a way that the bars remain parallel to the longest axis. A second set of field test measurements were taken from an actual concrete storage silo containing SNF.
The results obtained from the laboratory experiments enable the possibility to make planar scintigraphy using a flat panel scintillator detector similar to those used in digital high energy radiation fields. The laboratory experiments also show that it is possible to conduct tomographic assays with low energy resolution detectors in low activity radioactive waste containments with compact volume. For the field tests, this ability is strongly reduced in huge concrete silos. These types of assays analysis techniques need further confirmation.

- Outcome of work conducted by the **National Building and Civil Engineering Institute (ZAG, Slovenia)** with detailed information in **SLO 17810 - Annex X:** "*Monitoring of material degradation during long term storage of spent fuel*". Corrosion of steel reinforcement in concrete is one of the main reasons for the reduced service life of concrete structures. Basic mechanisms of corrosion processes of steel in concrete, as well as the influence of the main parameters, are quite well known. On the other hand, the time and spatial evolution of steel corrosion in concrete is not yet completely understood. Various electrochemical and physical methods for the detection of corrosion in concrete exist, but the advantages and disadvantages of each method mean that usually a combination of several techniques is used. The main aim of the work was to build a basis for reliable monitoring of steel corrosion in concrete. Spatial distribution of anodic and cathodic areas and their evolution/alternation in time have received considerable attention. In order to accomplish this goal, two relatively new methods were combined: measuring with ER probes coupled multi-electrodes and with coupled multi-electrode arrays (CMEA). The measuring techniques can form a reliable corrosion monitoring system in SNF/HLW storage concrete systems. Moreover, comprehensive analysis of results obtained by ER and CMEA, and consequent comparison with conventional techniques, can provide important information about the type and dynamic of steel corrosion in concrete.

(d) **Chapter 5**: Bolted closure systems of dry storage casks.

- Outcome of work conducted by **Bundesanstalt für Materialforschung und -prüfung (BAM, Germany)** with detailed information in **GFR 17307 - Annex IV:** "*Long-term behaviour of sealing systems and neutron shielding material*". Permanent deformation and leak tightness of HELICOFLEX® and elastomeric seals were measured in long term compression tests for time periods of up to 6.5 years at three different temperatures (20°C, 100°C and 150°C). In addition, tests at two more temperatures (75°C and 125°C) are running for two years as of April 2016. For elastomeric seals, the change in hardness with time and temperature was also determined.
  The amount of permanent deformation depends on the applied stress, temperature and time. With that an extrapolation for longer periods of time is possible but has to be verified by continuation of the tests. Leakage rate measurements showed that O-rings remained leak tight even when other properties already indicated substantial degradation. This highlights that the choice of the end-of-lifetime criterion has a large influence on the predicted lifetime and that standard criteria referring to material properties do not necessarily correlate with component functions such as leakage rate under static application conditions.
- Outcome of work conducted by **Central Research Institute of Electric Power Industry (CRIEPI, Japan)** with detailed information in **JPN 17308 - Annex V:** "*Demonstrating performance of spent fuel and related system components during very long term storage*". A creep constitutive formula for the metal gasket cover layer to use in numerical tools was proposed by tensile creep tests at high temperature with the aluminium and silver material. In addition, compressive creep tests at high temperature were performed to make the creep constitutive formula because the stress condition of the gasket is compressive. Comparing two formulae, the better one to evaluate the stress relaxation of the gasket will be selected. Moreover, a life-time estimation method considering the influence of the stress relaxation of the gaskets on the containment performance of the metallic gaskets for a long term usage are being evaluated, and the ageing condition of the metallic gaskets using the temperature profile, appeared during the realistic long term storage, will be estimated.

(e) **Chapter 6**: Neutron shielding in dry storage systems.

- Outcome of work conducted by **Orano TN (France)** with detailed information in **FRA 17270 - Annex III:** "*Study of degradation of neutron shielding, information on prediction of very long term performance of spent fuel, evaluation of the effect of drying and storage on spent fuel cladding behaviour*". Concerning SRO-5, radiation shielding (neutrons) is an important safety function that must be maintained during very long term storage. Gamma shielding is often provided by metal and therefore not affected by ageing. In-service neutron shielding materials properties changes may be caused by irradiation or thermal oxidation processes taking into account the maximum temperature of the material and cumulative dose (neutron and gamma). Confirmation study was achieved with experimental part and modelling. The new approach allows a great understanding of neutron shielding (polymer based) long term performance. The long term prediction data of neutron shielding for a family of neutron shielding formulation have been validated (thermoset based compounds). It is possible to address degradation of shielding material in the long term and to confirm that sufficient shielding efficiency remains. A synthesis has been made with the other studies done by other member states in the framework of this CRP (studies published by BAM (Germany)).

- Outcome of work conducted by **Bundesanstalt für Materialforschung und -prüfung (BAM, Germany)** with detailed information in **GFR 17307 - Annex IV:** "Long-term behaviour of sealing systems and neutron shielding material". Ultra-high and high molecular weight polyethylenes (U)HMW-PE are used for neutron shielding purposes in casks for storage and transport of radioactive waste due to their extremely high hydrogen content. During their service life as cask components, the PE materials are exposed to gamma irradiation from the radioactive inventory of the casks. This leads to chain scission and subsequent reactions of C-centred radicals and molecular fragments, resulting in crosslinking because of radical recombination, disproportionation, and formation of low molecular weight fragments as well as recrystallization. Thus, it is necessary to understand the influence of gamma irradiation on the material properties. Experimental techniques to measure changes in the (U)HMW-PE included Differential Scanning Calorimetry (DSC), Dynamic Mechanical Analysis, Fourier Transform – Infrared (FTIR) Spectroscopy, and density measurements.
  With the applied methods it is possible to detect structural changes of (U)HMW-PE induced by gamma irradiation. The gamma irradiation led to an increase of the degree of crystallinity and of the plateau value of shear modulus. With regards to the special application of (U)HMW-PE as neutron shielding material in casks for storage and transport of radioactive material, the present detected changes of the irradiated (U)HMW-PE are not safety relevant for long term neutron radiation shielding purposes over a period of 40 years in Germany.
- Outcome of work conducted by the **Lithuanian Energy Institute (LEI, Lithuania)** with detailed information in LIT 17275 - **Annex VII:** "*Investigation of RBMK-1500 spent nuclear fuel and storage casks performance during very long term storage*". Numerical modelling related to very long term storage of spent RBMK-1500 fuel focused on the following topics:
  - Overview and analysis of available investigations on RBMK fuel performance during wet/dry storage including investigations of RBMK fuel cladding resistance to hydride cracking;
  - Modelling of spent RBMK-1500 nuclear fuel (with initial ^{235}U enrichments of 2.0%, 2.4%, 2.6%, 2.8% and without/with Erbium burnable absorber) characteristics (radionuclide content, gamma and neutron sources, decay heat) for very long term storage periods;
  - Dose rate evaluation for prolonged storage period (from 50 to 300 years) of CASTOR®RBMK-1500 and CONSTOR®RBMK-1500 casks;
  - Modelling of neutron transport and fluxes in components of CASTOR®RBMK-1500 and CONSTOR®RBMK-1500 storage casks versus time (for 300 years period);
  - Neutron activation analysis of CASTOR®RBMK-1500 and CONSTOR®RBMK-1500 storage cask components.

  Dose rate calculations for CASTOR®RBMK-1500 and CONSTOR®RBMK-1500 storage cask have revealed that for very long term storage period a dose rate caused by neutrons becomes dominant, therefore, appropriate materials for neutron shielding shall be considered. Obtained results of CONSTOR®RBMK-1500 cask's heavy concrete wall neutron activation provided the activities of specific radionuclides in the concrete. Neutron induced activities in the casks components for both casks meet the free release conditions during analysed 300–600 years decay. However, it must be taken into account that modelling was done for RBMK fuel that has relatively low enrichment and burnup.

(f) **Chapter 7**: Long term demonstration programmes.

- Outcome of the work conducted by **US Nuclear Regulatory Commission (US NRC, United States of America)** with detailed information in **USA 19249 - Annex XIV:** ''*Update on NRC activities related to demonstration of SNF long-term storage and transportation*''. The potential value and desired attributes of a long term 'confirmatory' test was reported by reviewing work conducted primarily by the US NRC. Once it is decided that a demonstration is desired, it must be decided if enough information, such as thermal modelling to know the temperature, and well controlled laboratory data that supports models, is available to interpret the results. Lastly, it must be decided what type of demonstration to do. Experimental and funding limitations will require trade-offs that must be evaluated to understand the effects of these trade-offs on the viability of the demonstration results. Lastly, it must be decided under what conditions will the demonstration be run, and how will the performance parameters be monitored.

  This annex discusses some of the factors that affect these decisions, so a viable and useful demonstration is conducted when needed. Demonstrations can be run for any system or component, but the annex concentrates on demonstrations run for determining HBF performance.
- Outcome of the work conducted by the **Japan Atomic Power Company (JAPC, Japan)** with detailed information in **JPN 17486 - Annex VI:** "*Demonstration test program for long-term dry storage of PWR spent fuel*". The first interim SNF storage facility in Japan, is preparing for storage of SNF in dry metal casks for both transportation and storage. SNF whose integrity is confirmed prior to transportation will be loaded and transported to the facility, and then stored over the long term. To reduce risk of exposure to workers and waste materials, the interim storage facility has no hot cell, such that the SNF integrity will be determined indirectly by monitoring the casks during storage without opening the lid.

  The work included in the annex of this report describes a long term demonstration project being initiated in 2016 involving the storage of two PWR assemblies with burnups of 48 GWd/t(HM) and 55 GWd/t(HM). A special canister was constructed that contains thermocouples on the outside of the canister to monitor temperature during storage. A port has also been installed to obtain gas samples that will be measured for fission product gases, which would be an indication that at least one fuel rod has been breached. This test duration is planned for 60 years. The first assembly will be placed in the canister at the beginning of the test, and the second assembly will be emplaced ten years later.

This TECDOC is not meant to be a comprehensive treatment of all the potential degradation mechanisms that might occur during long term storage of LWR fuel. Rather, a summary of the particular degradation mechanisms is provided, and the work delivered by participants in the CRP is summarized. Final Reports from participants in the CRP are provided in the Annexes.

REFERENCES TO CHAPTER 1

[1.1] GNS, CASTOR® V/19 (2018), http://www.gns.de/language=en/21551/castor-v-19

[1.2] NAC INTERNATIONAL, The MAGNASTOR System: The New Generation in Multipurpose Storage (2014), https://www.nacintl.com/magnastor

[1.3] NAC INTERNATIONAL, MAGNASTOR (2014), https://www.nacintl.com/

[1.4] UNITED STATES NUCLEAR REGULATORY COMMISSION, Final Environmental Impact Statement for the Construction and Operation of an Independent Spent Fuel Storage Installation on the Reservation of the Skull Valley Band of Goshute Indians and the Related Transportation Facility in Tooele County, Utah, Rep. NUREG-1714, Vol. 1, Office of Nuclear Material Safety and Safeguards, Washington, DC (2001).

[1.5] ZULOAGA, P., ‘‘HLW storage and SL-LLW disposal in Spain’’, paper presented at 19th REFORM Group Meeting, Salzburg (2014).

[1.6] HAIN, K., “Idaho site spent nuclear fuel management”, paper presented at 2010 U.S. Nuclear Waste Technical Review Board, Idaho Falls (2010).

[1.7] VÖLZKE, H., PROBST, U., WOLFF, D., NAGELSCHMIDT, S., SCHULZ, S., Long term performance of metal seals for transport and storage casks, Packaging, Transport, Storage & Security of Radioactive Material 25 (2013) 8–15.

[1.8] UNITED STATES NUCLEAR REGULATORY COMMISSION, Generic Environmental Impact Statement for Continued Storage of Spent Nuclear Fuel – Final Report, Rep. NUREG-2157, Vol. 1, Office of Nuclear Material Safety and Safeguards, Washington, DC (2014).

[1.9] INTERNATIONAL ATOMIC ENERGY AGENCY, Radioactive Waste Management Glossary, 2003 Edition, STI/PUB/1155, IAEA, Vienna (2003).

[1.10] ELECTRIC POWER RESEARCH INSTITUTE, Extended Storage Collaboration Program (ESCP) – Progress Report and Review of Gap Analyses, Rep. 1022914, EPRI, CA (2011).

[1.11] ELECTRIC POWER RESEARCH INSTITUTE, Extended Storage Collaboration Program International Subcommittee Report: International Perspectives on Technical Data Gaps Associated with Extended Storage and Transportation of Used Nuclear Fuel, Rep. 1026481, EPRI, CA (2012).

2. CHLORIDE INDUCED STRESS CORROSION CRACKING IN WELDED DRY STORAGE CANISTERS

2.1. INTRODUCTION

This chapter is relevant to those dry storage systems that incorporate a welded austenitic stainless steel canister housed inside either an outer storage cask (e.g. Figs 2.1, 2.2 and 2.3) or a concrete vault (e.g. Figs 2.4 and 2.5). In most concrete-canister systems the canister provides the only engineered containment barrier for the SNF and keeps oxidants, such as air, away from the fuel. Its integrity is therefore critical to meet the system performance requirements and important for ensuring safety, since not all fuel pins will have intact cladding. In these systems the surface of the canister is cooled by atmospheric air, which is drawn across the canister surface by natural convection as shown in Fig. 2.6 [2.1].

Other dry storage systems using welded stainless steel canisters for fuel during storage, such as CANDU silos and vault stores may also be subject to stress corrosion cracking (SCC). However, in such systems the canisters are held within a secondary containment with an inert internal atmosphere and so the conditions to which the canister is exposed will normally be non-condensing and free from salts of aggressive ions, hence SCC should not be a concern as long as such conditions are maintained.

Canisters are typically made from austenitic stainless steel with an all-welded construction as shown in Fig. 2.7 [2.2]. Austenitic steels have good corrosion resistance because of the formation of a passive, chrome-rich oxide layer on the surface of the steel. Damage to this layer normally self-repairs through corrosion of the underlying material until a new Cr-rich layer forms. Whenever the passive surface is degraded, the steel is susceptible to localized corrosion. Chloride induced stress corrosion cracking (CISCC) is a particular concern because it is a form of localized corrosion where cracks can propagate through the material without requiring substantial loss of material. It is therefore difficult to identify in service.

(a) *(b)*

FIG. 2.1. Examples of canister based dry storage systems in service (reproduced courtesy of US DOE) [2.3]: (a) Horizontally stored canister system; (b) Vertically stored canister system.

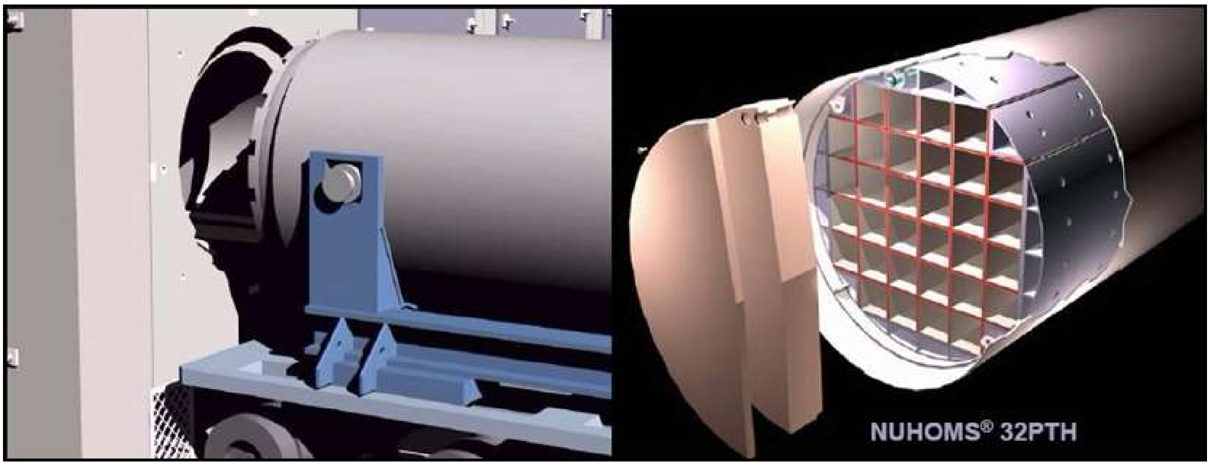

(a) *(b)*

FIG. 2.2. (a) NUHOMS horizontal storage module, transfer trailer (reproduced courtesy of TN Americas); (b) NUHOMS 32PTH dry shielded canister (reproduced courtesy of TN Americas).

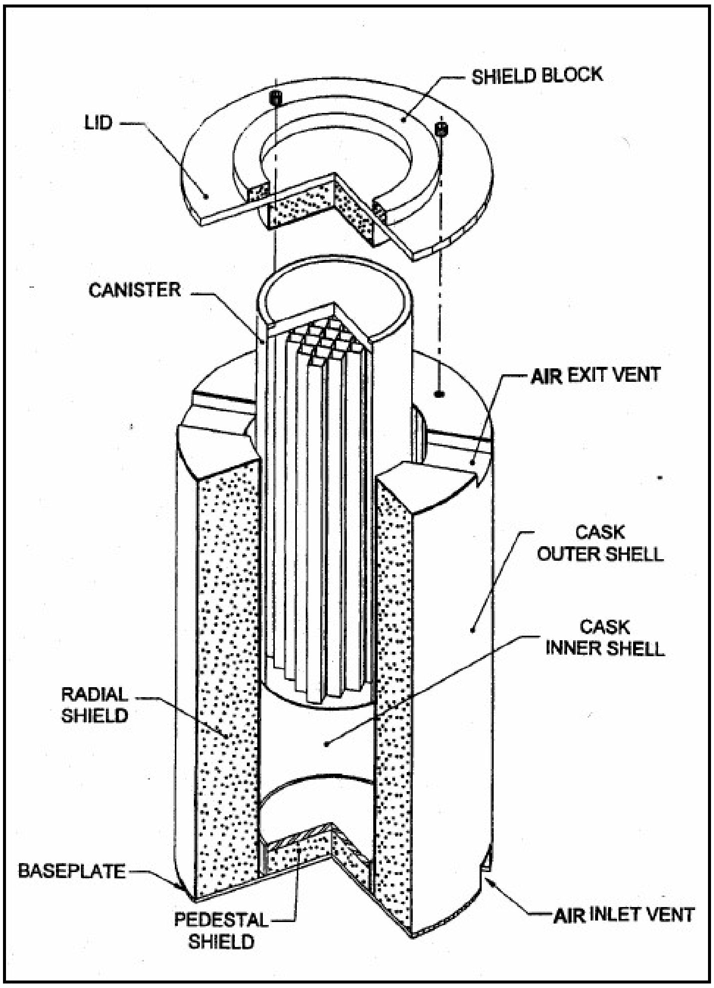

FIG. 2.3. Cross section of the HI-STORM 100 overpack for storage cask (reproduced courtesy of US NRC) [2.4].

FIG. 2.4. ENRESA (Spain) planned vault storage (reproduced courtesy of ENRESA)[2.5].

(a) (b)

FIG. 2.5. US Department of Energy (US DOE) spent nuclear fuel (SNF) vault containing SNF from the decommissioned Fort St. Vrain reactor in the US (reproduced courtesy of US DOE) [2.6]: (a) Vault exterior view; (b) Interior charge face.

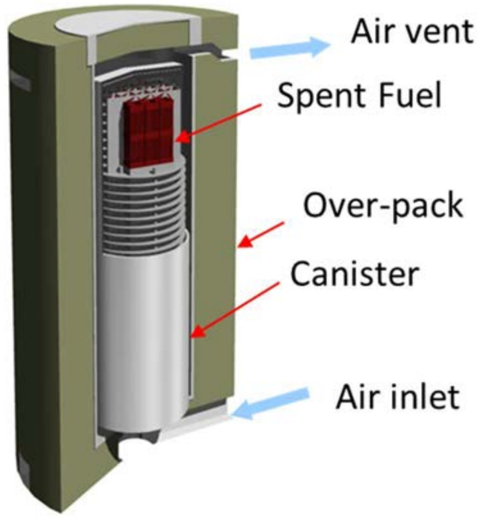

FIG. 2.6. Canister and over-pack arrangement (reproduced courtesy of IAPSAM) [2.1].

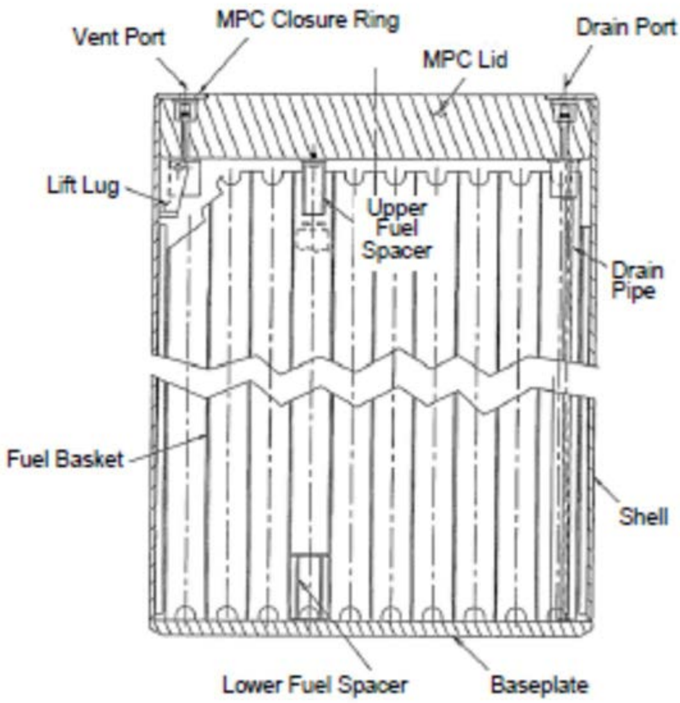

FIG. 2.7. Typical canister construction (reproduced courtesy of US DOE) [2.2].

Through-wall cracking of a canister represents a significant degradation of safety as it can lead directly to a release of radioactivity into the environment. In general, intergranular cracking leads to very narrow, tortuous cracks, which limit the rate at which gasses can escape into the environment and retain all but the very smallest particles that might be present inside the canister. The gas within the canisters is normally at a higher pressure than the outside air and will be slowly released through the crack [2.7], carrying any radioactive gasses that may have been released from fuel with defective cladding with it. Subsequently oxygen can migrate slowly into the canister and may lead to oxidation of exposed fuel, potentially leading to a further release of radioactivity. For this reason, CISCC is considered to be the most important degradation mechanism for LWR fuel storage canisters [2.3, 2.8, 2.9–2.13].

2.1.1. Dry storage systems characteristics

The materials typically used in the manufacture of welded canisters are austenitic stainless steels, typically 304, 304L, 304LN, 316, 316L and 316LN. Typical canister dimensions are 1.6–1.8 m diameter and 4.2–4.9 m long, with wall thicknesses between 13 mm (0.5 in) and 16 mm (0.625 in) [2.2].

Canisters are manufactured from lengths of plate steel, which are rolled then welded to form the canister body. In some designs, the canister shell is formed from a number of rings that are then welded together to form the canister body, in which case the longitudinal welds in adjacent rings are normally aligned so as to be 180° apart. A base plate is then welded to the shell to form the canister body, which is the assembly that is loaded with fuel in the reactor pool. For current welded steel canister designs, fabrication and closure welds are not stress relieved. Final closure welds between the lid and canister body are performed in the reactor building, with the loaded canister in a semi-remote configuration.

The stress levels in canister welds have been measured by X-ray diffraction (XRD) [2.1]. These indicate that there are tensile stresses in the weld regions at the outer surface of the canister that were considered to be greater than that required for SCC, however in many cases there are indications that the stresses become compressive towards the inner surface. On the other hand, recent modelling work [2.13] indicated that through-wall tensile stress fields could be expected and work to analyse stresses in prototypical canister welds is underway. Initial indications are that through-wall tensile stresses exit in the weld and associated heat affected zone (HAZ) [2.14, 2.15].

2.1.2. Environmental conditions

As a result of the natural convection cooling, the temperature of the canister increases from the base toward the top. Over time the canister cools as the radioactivity within the fuel decays away. Illustrative temperature and dose rates at the canister surface, obtained by modelling [2.16], are shown in Table 2.1 and Fig. 2.10. A comparison of predictions and measurements on a vertical storage system are shown in Fig. 2.11.

TABLE 2.1. ILLUSTRATIVE CANISTER SURFACE TEMPERATURE AND DOSE RATE RANGES (reproduced courtesy of US DOE) [2.16]

Canister type	Temperature at loading (°C)		Temperature at ~30 years (°C)		Temperature at ~125 years (°C)		Initial heat load (kW)	Ambient inlet air temperature (°C)
	Max.	Min.	Max.	Min.	Max.	Min.		
Vertical	220	95	145	70	75	45	30	27
Horizontal	220	140	155	110	85	55	42	38
Dose rate (Sv/h)	470		210		23			

Note:

Temperatures in Table 2.1 (from [2.16]) are intended to be illustrative, based on a single heat load and warm ambient conditions. They should not be considered to be definitive or bounding estimates or ranges. Dose rates are an estimate at the centre of a square array of 9 assemblies containing 4% ^{235}U enriched fuel with a burnup of 45–48 GWd/t(HM) after 20 years cooling [2.17].

Thermal modelling predictions are dependent on assumptions in decay heat production, assumption in the distribution of burnup of fuel loaded in a cask and in some aspects of thermo-hydraulic phenomena that are accounted for. Industry codes typically overestimate heat output to ensure conservatism and licensing documents evaluate the maximum possible heat load configurations. Both can lead to temperatures being a few tens of °C higher than a realistic model would predict. The maximum permitted fuel temperature during drying and dry storage often differs between countries, which can substantially affect the maximum canister temperature and the time required for the canister surface to reach any particular temperature, however the general profiles and variations with time are likely to be similar.

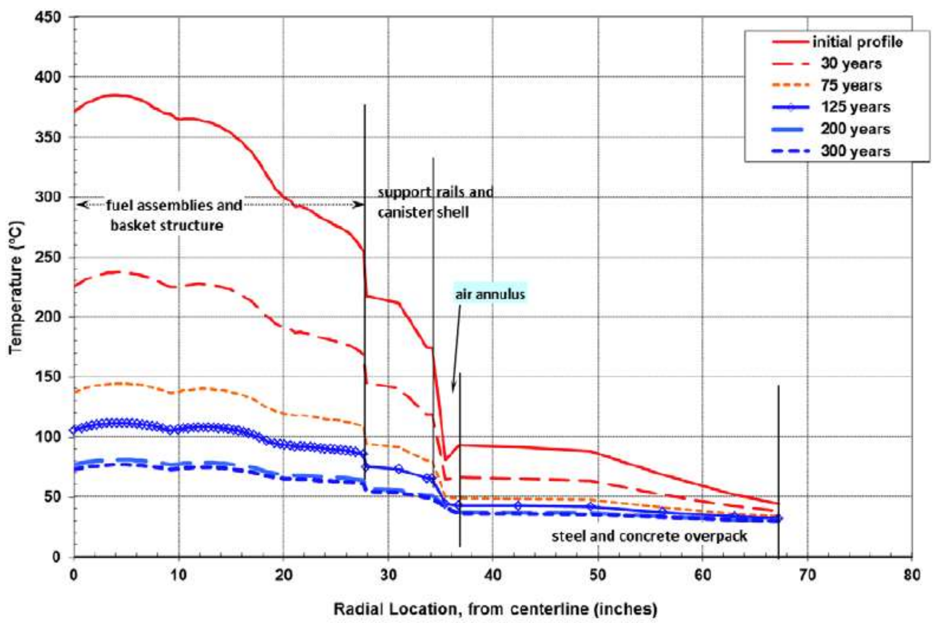

FIG. 2.10. (a) Radial temperature distribution through the canister and overpack at the peak clad temperature location for projected decay heat decrease over time in vertical storage. (1 in = 2.54 cm)

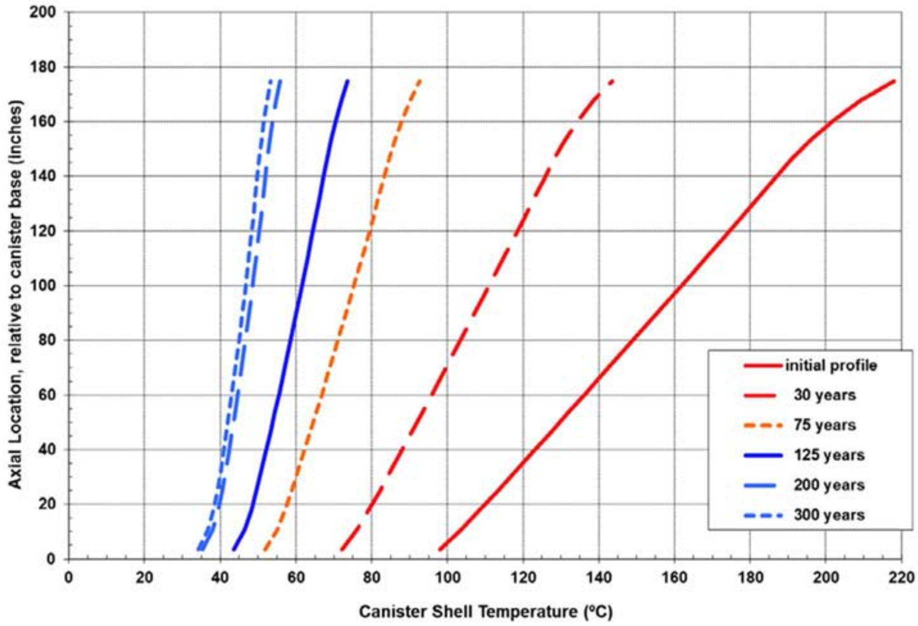

FIG. 2.10. (b) Axial temperature distribution on the canister shell, for projected decay heat decrease over time in vertical storage. (1 in = 2.54 cm)

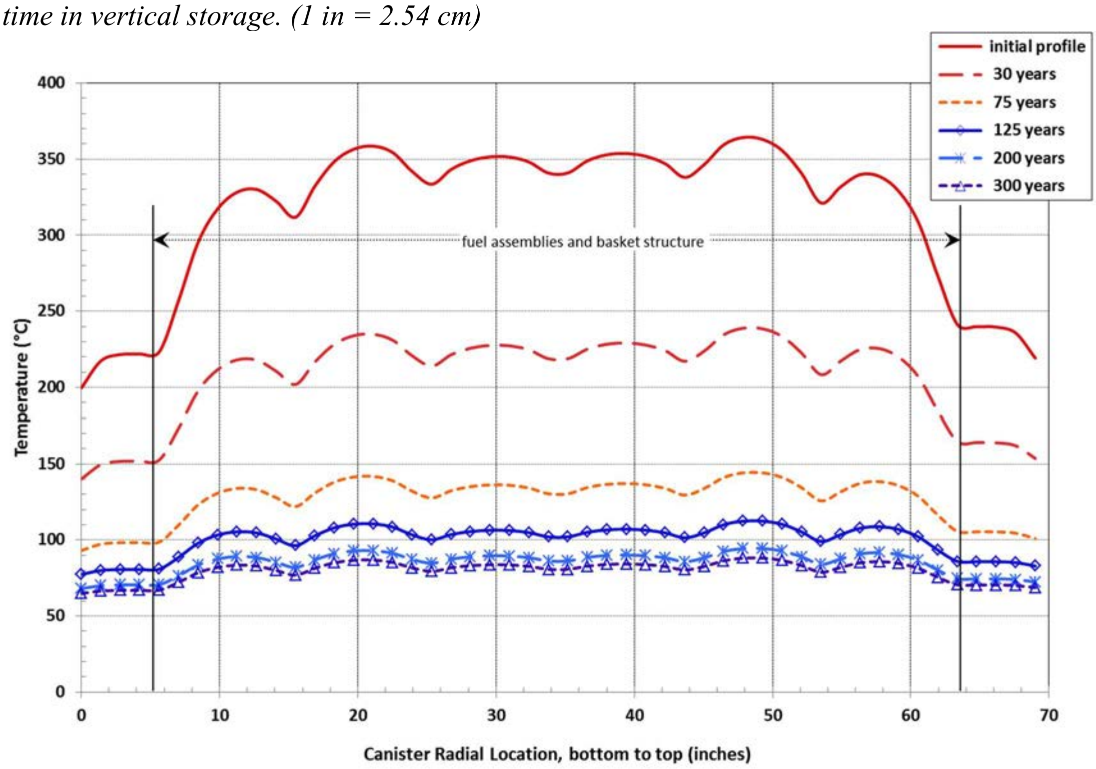

FIG. 2.10. (c) Radial temperature distribution through the canister at the peak clad temperature location for projected decay heat decrease over time in horizontal storage. (1 in = 2.54 cm)

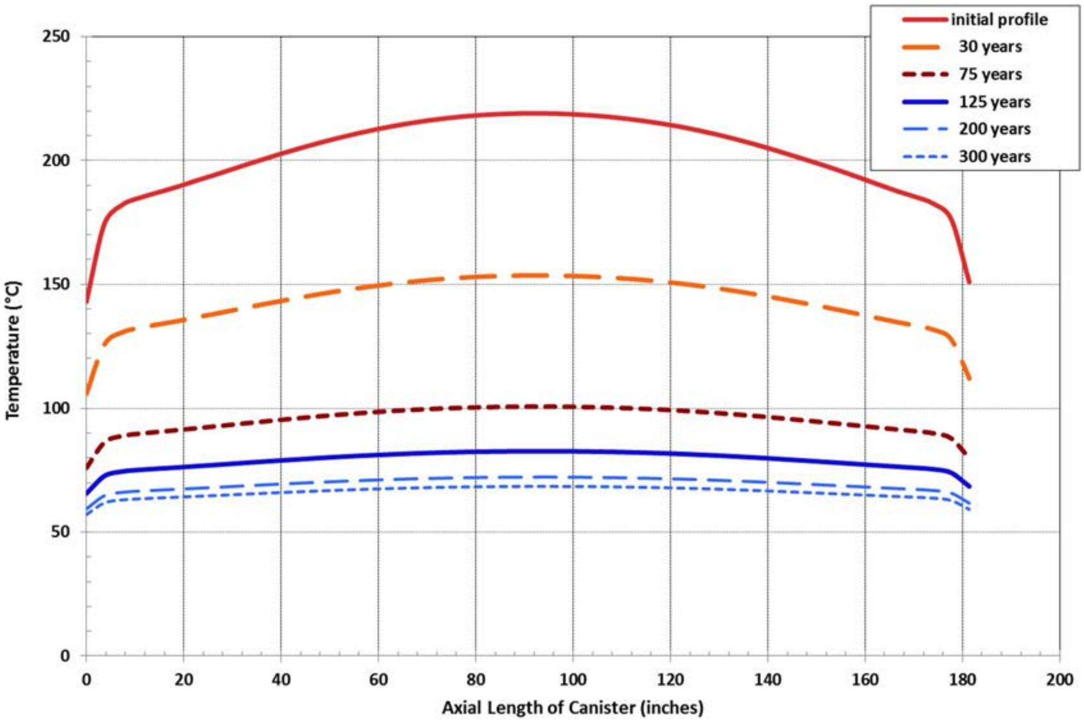

FIG. 2.10. (d) Axial temperature distribution at the canister shell surface along the top, for projected decay heat values over time in horizontal storage. (1 in = 2.54 cm)

FIG. 2.10. Canister temperature distribution (reproduced courtesy of US DOE) [2.16].

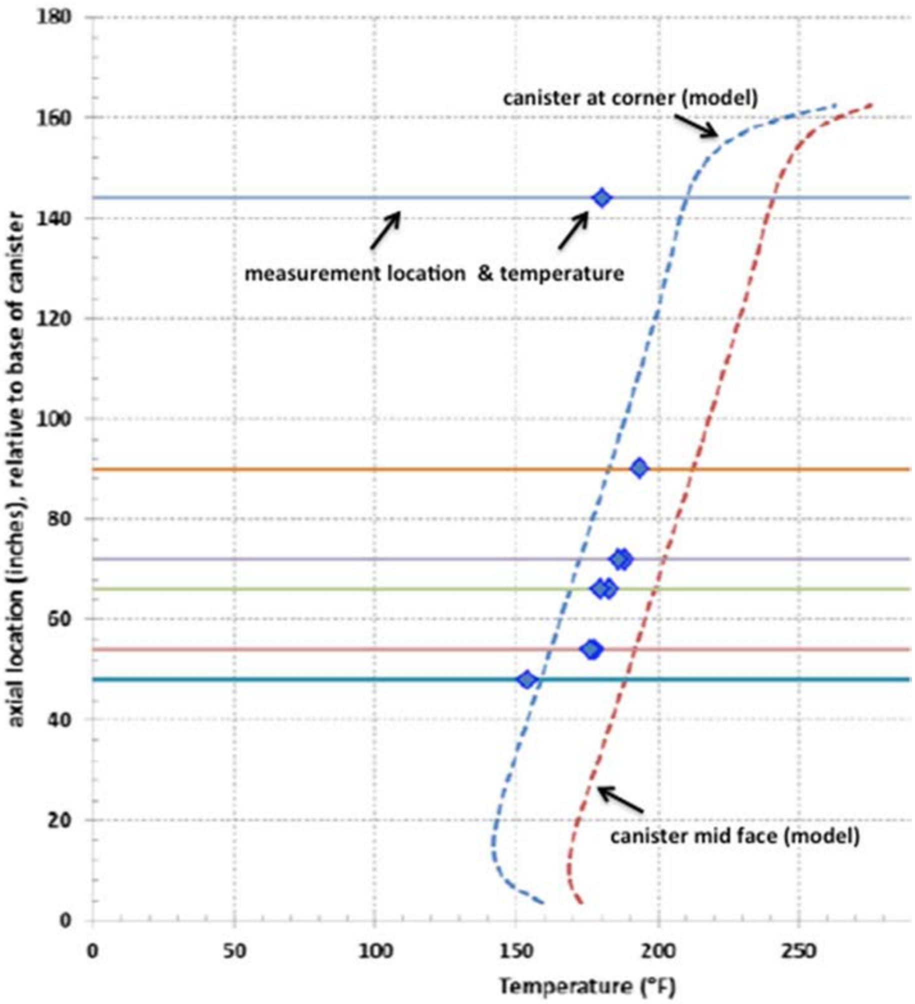

FIG. 2.11. Example comparison of measured and modelled canister temperature for a vertical storage system ([°F] = [°C] × 9⁄5 + 32; 1 in= 2.54 cm) (reproduced courtesy of US DOE)[2.18].

2.1.3. Mechanism(s) for stress corrosion cracking

Where SNF is stored in canister-based dry storage systems, the surrounding concrete structures provide shielding and the stainless steel canisters act as the containment barrier, retaining the inert atmosphere that surrounds the fuel and the radioactive materials associated with the fuel and its structural components. The decay heat from the SNF is mostly convected by the inert gas to the canister wall where the majority is dissipated by the atmospheric air that flows over the outer surface of the canister by natural convection. The canister wall is in direct contact with atmospheric air, which will bring with it particulate materials that may include some chloride salts. The chloride salt loading will be particularly high where the interim storage facilities are close to sea coasts, but some level will also be present at in-land sites. Austenitic stainless steels are susceptible to CISCC in certain environments under tensile stress. CISCC induced by sea salt particles and chlorides, for example, has been observed on various structures of chemical plants built in coastal regions.

CISCC occurs when the following three conditions, enough tensile stress, aggressive environment and a susceptible material are satisfied as shown in Fig. 2.12 [2.1]. As for the canister, residual stress by weld, deposition of sea salt particles on the surface and using of austenitic stainless steel are causes of CISCC as shown in Fig. 2.13 [2.1]. If one of these conditions is removed, CISCC will not occur. Removing at least two of them is desirable for long term safe operation.

The process by which CISCC is expected to occur in a canister is schematically drawn in Fig. 2.14 [2.19]. At first sea salt particles attach on the canister surface. Then, sea salt deliquesces drawing water from humid air. Localized corrosion, such as pitting or crevice corrosion, is induced by the resulting salt solution. Finally, cracking occurs if tensile stress exists around the corroded pit. Localized corrosion produces rust spots, so cracking does not occur without some rust formation [2.19].

Each of the three critical factors required for CISCC are considered below.

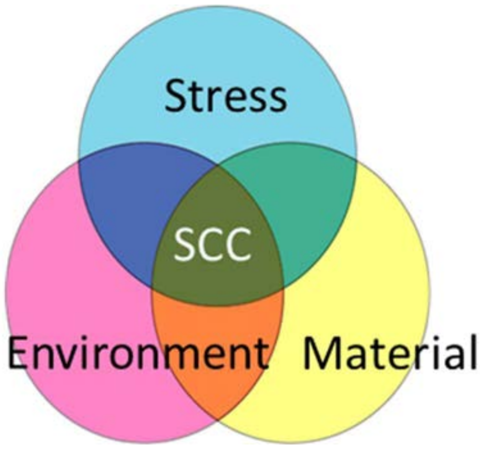

FIG. 2.12. Critical factors for SCC (reproduced courtesy of IAPSAM) [2.1].

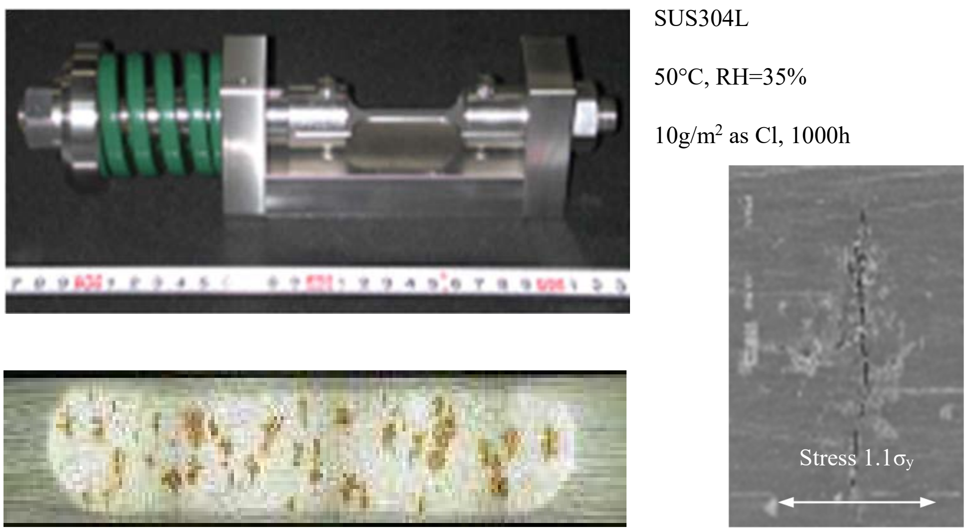

FIG. 2.13. Localized steel corrosion (reproduced courtesy of IAPSAM) [2.1].

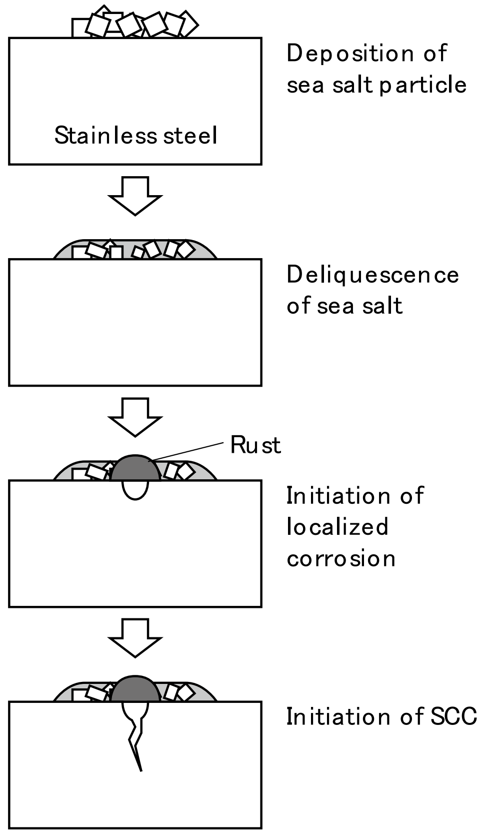

FIG. 2.14. Schematic of CISCC initiation (reproduced courtesy of IAPSAM)[2.19].

2.1.3.1. Stress

Most metals swell during heating. Small, unconstrained grains deform due to the swelling and shrinking at the weld line. In constrained structures like a canister, residual stress emerges instead of deformation. A simplified model for residual stress is shown in Fig. 2.15. Plastic deformation occurs around the weld line during heating followed by shrinkage during cooling, resulting in a tensile stress within the material. The level of residual stress resulting from the welding process can exceed the yield stress. Welding techniques and details of manufacturing processes may also affect residual weld stresses sufficiently to affect CISCC.

Surface finishing with a hand grinder may add additional tensile stress [2.20]. Grinding typically introduces stress in two directions: with the working direction of the grinding tool and along the rotational direction of the grinder head. Surface finishing with a grinder also increases local hardness. It is reported that stress corrosion crack depth increases with surface hardness at operating temperatures typical of LWRs [2.21].

Compressive stresses cannot cause CISCC, as the stress counteracts crack opening. CISCC will be mitigated when the tensile stress is lowered to less than zero (i.e. the stress becomes compressive). Several stress relaxation methods, which are already applied on LWRs, are applicable to canisters. For example, shot peening, laser peening and water-jet peening can be applied to introduce compression stress at and near the canister surface [2.19]. Annealing is another option for mitigation of tensile stress, this time by stress relaxation. Because canister wall thicknesses are small, compared to the diameter, annealing of canisters would require a retainer to prevent deformation of the canister body during the annealing process.

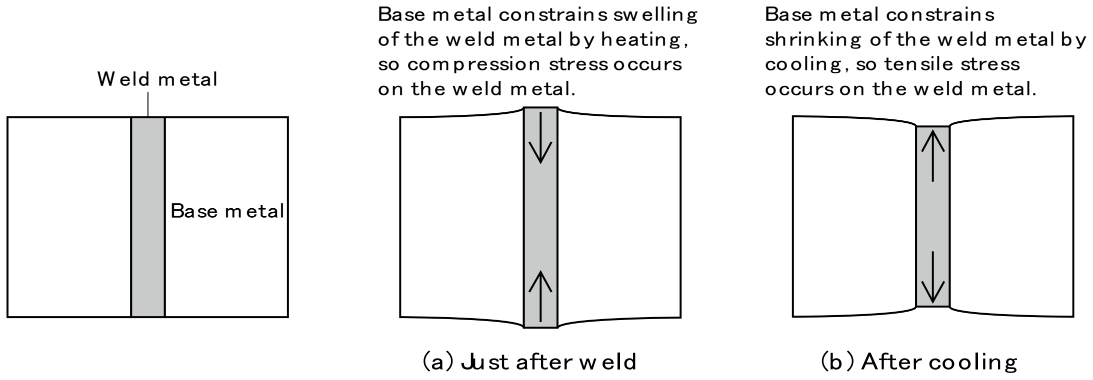

FIG. 2.15. Mechanism of occurrence of residual stress by weld (reproduced courtesy of CRIEPI) [2.19].

2.1.3.2. Environment

Sea salt, transported by cooling air, is a major environmental factor in CISCC because it is a source of aggressive ions that drive local corrosion. The salts also reduce the relative humidity (RH) and hence increase the temperature at which water droplets, necessary for the formation of the electrolytic cells that cause localized corrosion, can form on the canister surface. This effect, called deliquescence, increases the range of 'environmental conditions under which CISCC may occur'.

Sea salt contains a mixture of ionic species, predominantly sodium chloride and magnesium chloride. At room temperature, sodium chloride deliquesces at 75% RH, whilst magnesium chloride deliquesces at a much lower RH of around 30–35% [2.22]. When sea salt is present in air near its deliquescence limit a highly concentrated chloride solution forms on the metal surface that maximize CISCC sensitivity [2.23] (see Fig. 2.14). Other ionic species present in the sea salt, such as calcium chloride, can lower the RH at which deliquescence occurs and a minimum RH for CISCC of type 304 stainless steel at 80°C of 15% has been reported [2.24].

RH is derived from temperature and absolute humidity. If the absolute humidity is constant, RH decreases with increase of temperature, as occurs as air convecting past a canister warms up. Figure 2.16 shows the temperature dependence of RH in air with an absolute humidity of 30 g/m^3 and implies that if the surface temperature on the canister is higher than 70°C, the RH of air with 30 g/m^3 of water vapour will be less than 15% and it will not be possible to initiate CISCC based on the limit identified in [2.24].

It is also worth noting that there is evidence that radiation can reduce the RH threshold for general corrosion of steel from 60–70% in the absence of radiation to around 15–20% [2.25]. It is currently unclear whether this effect would be additive to that of the deliquescent species and hence whether it would affect the initiation of CISCC.

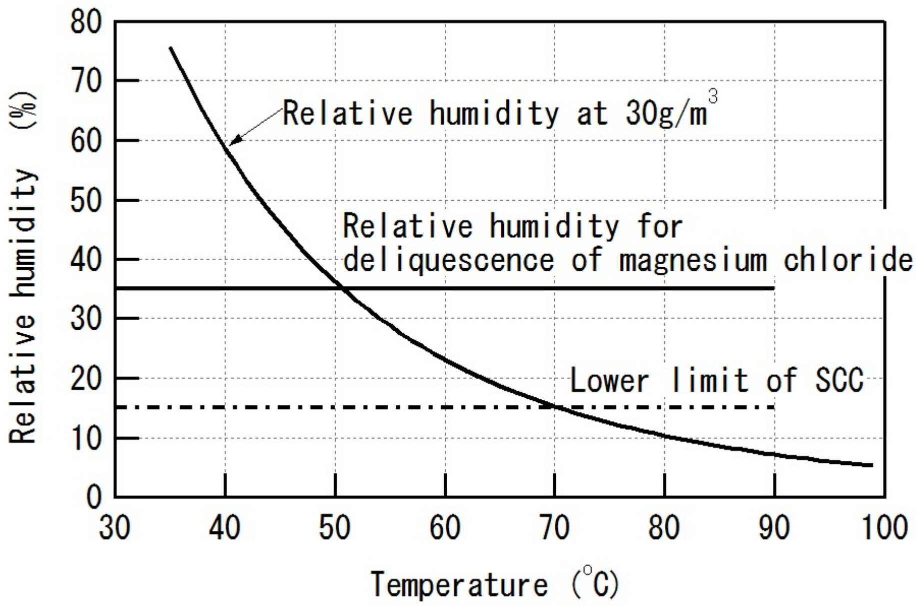

FIG. 2.16. Maximum relative humidity expected on the canister surface (reproduced courtesy of CRIEPI)[2.19].

2.1.3.3. Material

Austenitic stainless steel, such as types 304, 316 and duplex stainless steel, are vulnerable to CISCC. Different alloys display different degrees of resistance to localized corrosion, which, as shown in Fig. 2.14, is normally associated with initiation of CISCC. One measure that provides a qualitative ranking of resistance of stainless steel and nickel based alloys to localized corrosion is the pitting resistance equivalent (PRE) number [2.19], which is calculated as a function of chromium, molybdenum and nitrogen content, from the following equation:

$$\mathrm{PRE} = (\%\mathrm{Cr}) + 3.3(\%\mathrm{Mo}) + 16(\%\mathrm{N}) \tag{2.1}$$

Chemical composition of major alloying elements and PRE numbers for common canister materials are shown in Table 2.2. The PRE number provides an indication of resistance to localized corrosion, but it is not a quantitative measure of initiation time or corrosion rate. Constant load tests for these materials at 80°C, 35% RH with enough sea salt on the specimen surface to ensure a high chloride concentration was conducted. As shown on Fig. 2.17, types 304 and 316 failed at around several hundred hours while S31254 and S31260 did not fail for more than 60 000 hours [2.26, 2.27].

Other grades of stainless steel have been adopted over recent years in applications requiring high resistance to CISCC, such as bridges and structural elements of swimming pools. These materials provide higher resistance to localized corrosion and CISCC, but at higher cost and in some cases, such as 2205 duplex stainless steel, lower creep strength.

Material selection is a complex process requiring evaluation of material properties, vulnerabilities, performance requirements, ageing management requirements, initial and on-going costs. Final selection is normally governed by engineering and safety management policies of the operating organizations [2.19], which can lead to different materials being selected for nominally similar situations.

TABLE 2.2. CHEMICAL COMPOSITION FOR MAJOR ELEMENT OF CANISTER MATERIALS (adapted from [2.28])

Stainless steel		Cr (wt%)	Ni (wt%)	Mo (wt%)	N (wt%)	PRE
Conventional	S30403	18–20	8–12	n.a.	n.a.	18
	S31603	16–18	10–14	2–3	n.a.	23
High corrosion resistance	S31260	24–26	5.5–7.5	2.5–3.5	0.1–0.3	34
	S31254	19.5–20.5	17.5–18.5	6–6.5	0.18–0.22	42

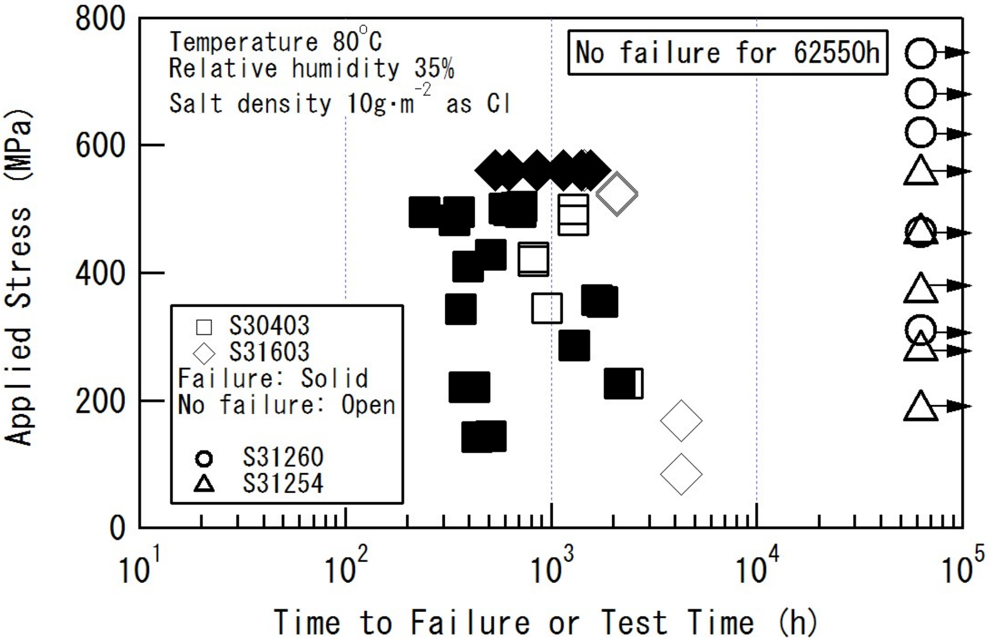

FIG. 2.17. CISCC resistivity of canister materials evaluated with constant load test (reproduced courtesy of CRIEPI) [2.19].

2.1.4. Monitoring and inspection for conditions relevant to stress corrosion cracking

Monitoring and inspection of canisters is challenging because of the limited size of the air vents (e.g. 13 cm × 15 cm for Fig. 2.18 [2.18, 2.29] and 20 cm × 30 cm for Fig. 2.19 [2.30]) and poor access routes to the canister surface. Furthermore, in many designs the gap between the canister surface and surrounding concrete/heat shields is very narrow and internal support features and guides limit access to parts of the canister [2.29].

The environment within these spaces is also hostile, with temperatures over 100°C and high radiation fields of >100 Sv/h for many decades (see Subsection 2.1), which limits the service life and reliability of sophisticated inspection techniques.

A range of inspection techniques have been evaluated for initial canister inspections [2.29, 2.31], including small remotely operated vehicles, non-robotic long-reach tools (Fig. 2.20) and robotic snake arms (Fig. 2.21), and there is on-going work on the development of advanced deployment systems.

CISCC creates cracks that are inter-granular and are therefore of similar width to grain boundaries. Even after stress relaxation the resulting cracks are typically narrow (e.g. Fig. 2.14) and therefore difficult to locate on large items. Initial canister inspections [2.31] also indicated substantial accumulation of inert particulate (e.g. dust, pollen) on the canister surface that could interfere with measurement techniques and affect the ability to detect narrow cracks.

Analysis of initial samples of particulate and salts also indicated the importance of careful sample preservation to avoid evolution of the sample composition prior to measurement [2.32].

A number of techniques to monitor parameters to relevant canister integrity have been proposed and tested, including non-intrusive means to monitor the chlorine attached on the surface of the canister [2.33] and detect loss of canister integrity [2.34].

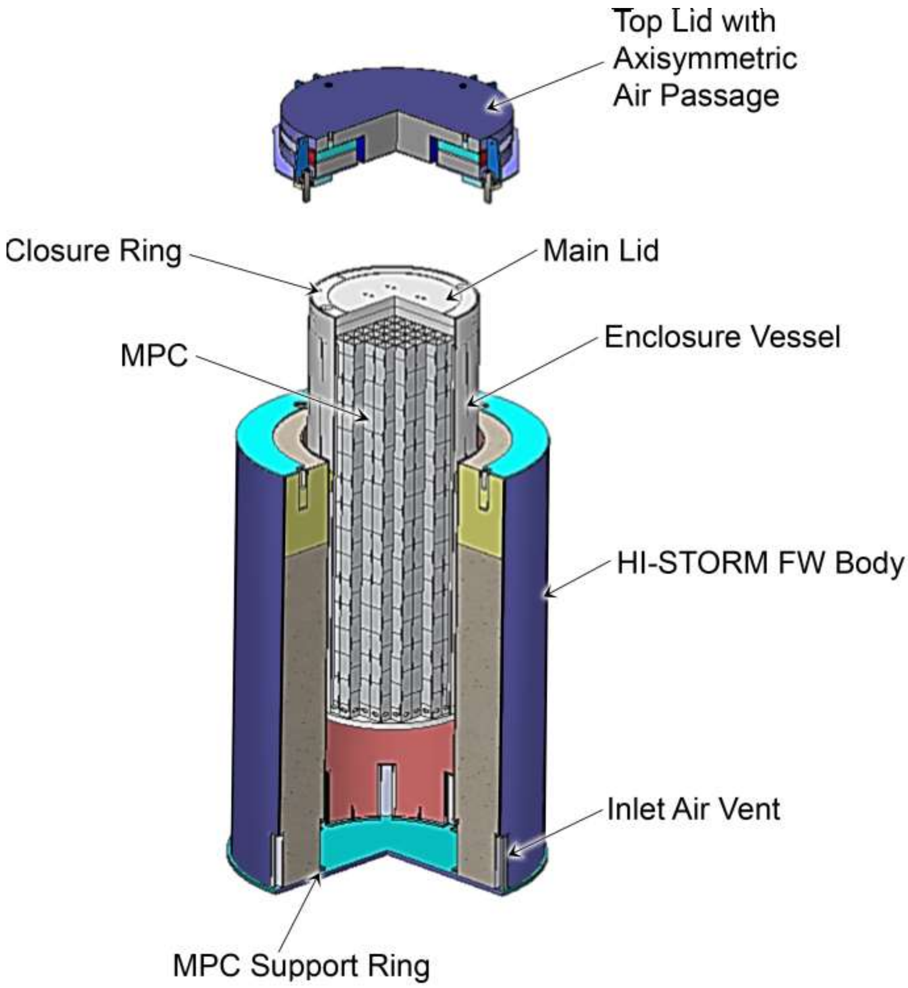

FIG. 2.18. HI-STORM schematic (reproduced courtesy of Holtec International)

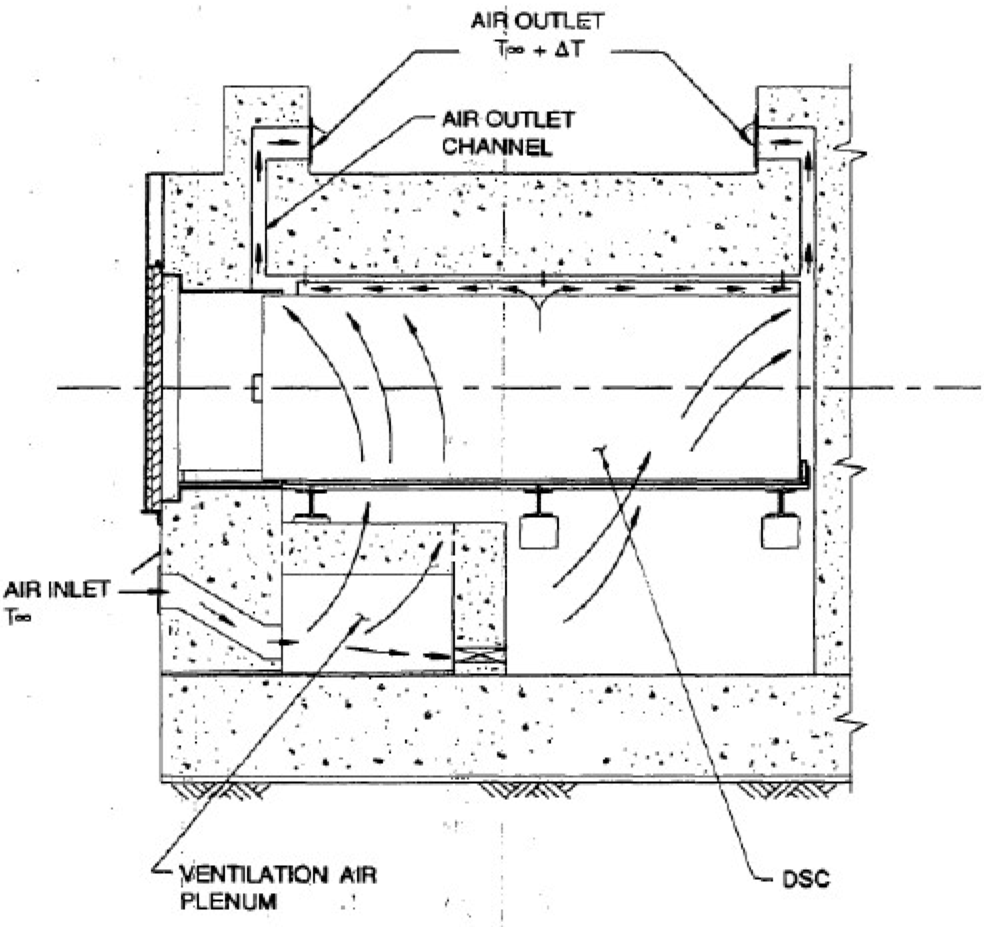

FIG. 2.19. Cross section of horizontal canister system (reproduced courtesy of TN Americas LLC) [2.30].

FIG. 2.20. Non-robotic inspection tool (reproduced courtesy of US DOE)[2.35].

FIG. 2.21. Conceptual robotic snake (reproduced courtesy of OC Robotics).

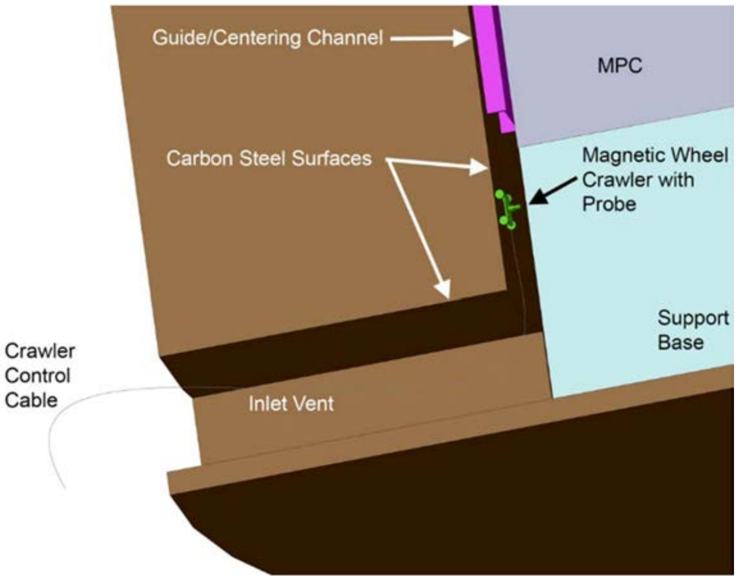

FIG. 2.22. Conceptual magnetic crawler inspection device inserted in the base of a vertical storage system (reproduced courtesy of US DOE) [2.29].

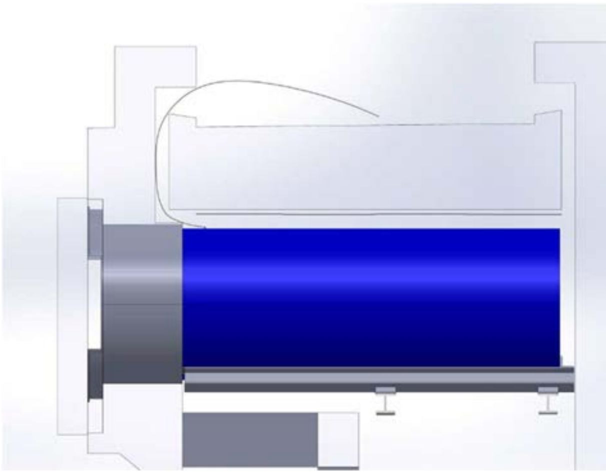

Fig. 2.23. Conceptual spring steel probe inserted into a horizontal storage system (reproduced courtesy of US DOE) [2.29].

2.1.5. Prevention and mitigation

Prevention of CISCC can be achieved by taking action in relation to the principle factors affecting CISCC, which are stress, corrosive environment and material susceptibility.

As discussed earlier, residual stress in the canister body can be relieved by annealing after manufacturing, although this introduces the need to prevent deformation during such processes and cannot be used for the final closure welds, which are made at the reactor building. Alternatively, the canister surface can be treated to introduce compressive stresses that would counteract crack opening at the initiation sites. This approach requires a high degree of control since failure to ensure comprehensive coverage of the canister surface can lead to enhanced stresses in any untreated areas.

The local environment can be made less corrosive by the provision of protection from the environment, e.g. a storage building with air filtration, or removal of salt particulate entering the cooling annulus. It is also possible to provide a secondary containment barrier, e.g. double wall design as proposed for use at Sizewell B in the UK. It is important to remember that the environmental conditions at the canister surface will change with time as the heat load from the fuel and the associated radiation levels fall, due to radioactive decay. There is also some evidence that salts deposited on the canister surface may continue to oxidise and react with their local environment, leading to a change in composition over time.

In addition to common steels identified above, there is continual development of steel formulations to provide resistance to atmospheric corrosion and some super austenitic steels (e.g. ASI 2205) have expected service lives of over 100 years in marine environments, which are substantially more challenging that those likely to be experienced by canisters. Therefore, greater resistance to CISCC can be provided by selection of more resistant materials.

The effects of CISCC could be mitigated by the provision of repairs or replacement of the containment function by over-packing or re-packing into a new canister. Such mitigation requires the ability to detect either CISCC or the consequential effects of a through-wall crack, such as changes in temperature profile in the canister or release of radioactivity from the canister.

2.1.6. Key knowledge gaps and CRP activities

Important gaps in knowledge of CISCC have been identified in international gap analyses, as indicated in Chapter 1 and shown in Table 2.3. To assist in the discussion of results and implications, the CISCC topic has been further broken down into a number of sub-topics. Activities within this CRP that address these subtopics are indicated with a tick and each of the topic areas are then reviewed in turn, below.

TABLE 2.3. POTENTIAL EFFECTS ON SAFETY FUNCTIONS OF CANISTER CISCC

Structures, systems and components (SSCs)	Type: welded canister systems
Sub-SSC	Welded canister
Degradation issue(s)	CISCC
Containment (storage and transportation)	Direct effect
Sub-criticality (storage and transportation)	Indirect (potential for water entry)
Thermal performance	Air ingress leads to lower thermal conductivity
Radiological protection	Radionuclide gas and particulate release possible
Retrievability (storage, transportation & disposal)	Indirect (contamination issues for workers)
IAEA Research Agreement (RA) or IAEA Research Contract (RC)	(see JPN 17308 – Annex V, PAK 17283 – Annex VIII, SLO 17810 – Annex X, UK 17420 – Annex XIII)
Priority knowledge gaps (✓ indicates work was conducted in this CRP)	Material properties: ✓ ‘Environmental conditions under which CISCC occurs’ (e.g. temperature, salt concentration, residual stress) ✓ Impact of radiation on CISCC ✓ Processes affecting storage conditions ✓ Inspection and measurement of important parameters ✓ Detection of CISCC

2.2. ENVIRONMENTAL CONDITIONS UNDER WHICH CHLORIDE INDUCED STRESS CORROSION CRACKING OCCURS

2.2.1. Outcome of work at Central Research Institute of Electric Power Industry (CRIEPI), Japan

CRIEPI undertook work on the mechanisms of CISCC in LWR canister materials to identify RH and chloride thresholds for CISCC. Using test specimens of types 304L and 316L stainless steel cut from welded plates finished by grinding. CISCC initiation tests, as shown in Fig. 2.24, were conducted at a constant temperature of 50°C and RH=35% with different levels of chloride with the aim of deriving a critical chloride threshold after 10 000 hours heating. Crack growth rate (CGR) tests were also conducted using four-point bending test specimens cut from full-scale laser welded canister base, as shown in Fig. 2.25, with a view to improve the estimated time to failure after CISCC has initiated. This testing method was adopted to provide more realistic stress profile in the test specimen, compared to that found in U-bend and C-ring specimens. The test specimens were placed under conditions of constant temperature and humidity in chambers, at 80°C and RH = 35%.

This work addresses the gap related to ‘environmental conditions under which CISCC occurs’. Long term CISCC initiation and CGR tests, as shown in Figs 2.26 and 2.27, were completed and results were reported [2.36].

The CISCC initiation test results indicated that the minimum amount of salt below which CISCC was not initiated in stainless steels of types 304L and 316L was less than 0.2 g/m^2 and

0.8 g/m^2 as Cl, respectively. The CGR was measured by the reverse direct current potential drop (RDCPD) method. The potential drop data was converted to crack depth data, assuming the propagation of a half elliptical crack. It emerged that the crack initially propagated rapidly before the propagation rate declined to around $4.4 \sim 6.8 \times 10^{-12}$ m/s. Allowing a margin for uncertainties in the modelling, this data indicates that a CGR of 2×10^{-11} m/s will be conservative for canister life assessments [2.36]. For a 1.27 cm (0.5 in) thick canister wall this would imply a minimum crack propagation time of just over 20 years. Service life would be greater than this because conditions conducive to localized corrosion would have to occur and then localized corrosion would initiate before the crack propagation time becomes relevant.

Work to refine the understanding of CISCC initiation and CGR in materials relevant to LWR canisters is continuing and will provide important data that will help to underpin canister integrity assessments. Collation of such data with existing information may help resolve current ambiguities with respect to thresholds, however it can be anticipated that further work in this area may be required to assist in understanding the sources of current uncertainties and validation of future test results.

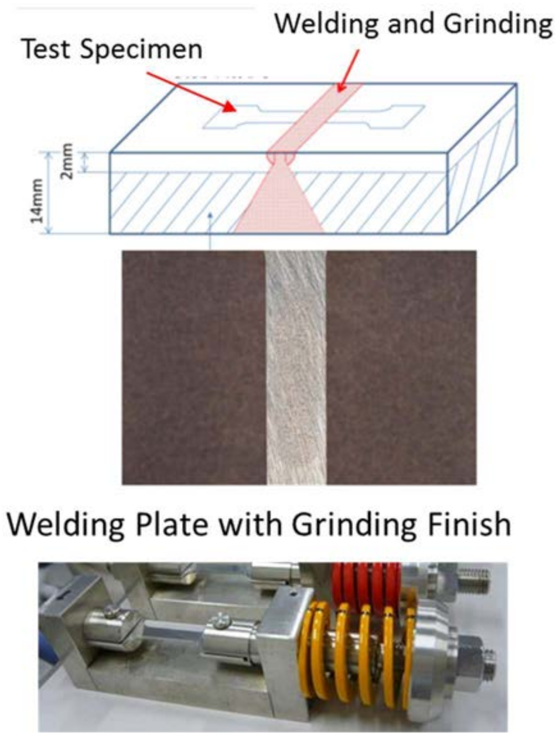

FIG. 2.24. CISCC initiation test (reproduced courtesy of CRIEPI)[2.36].

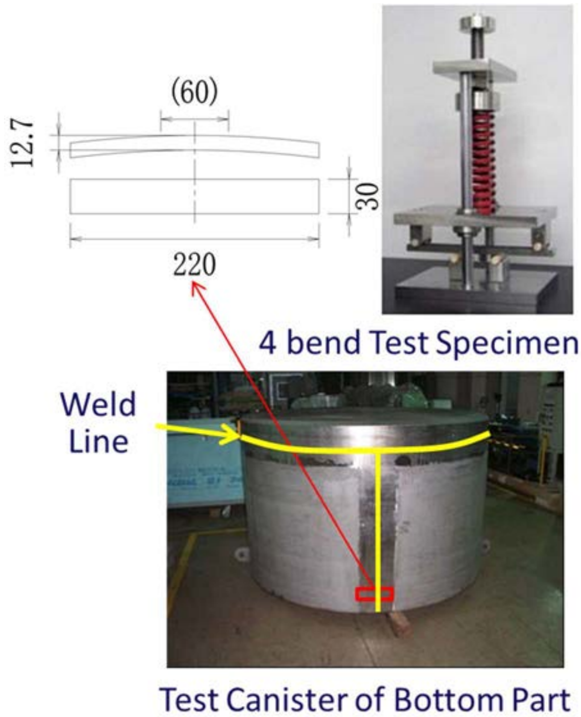

FIG. 2.25. Crack growth rate test apparatus (reproduced courtesy of CRIEPI) [2.36].

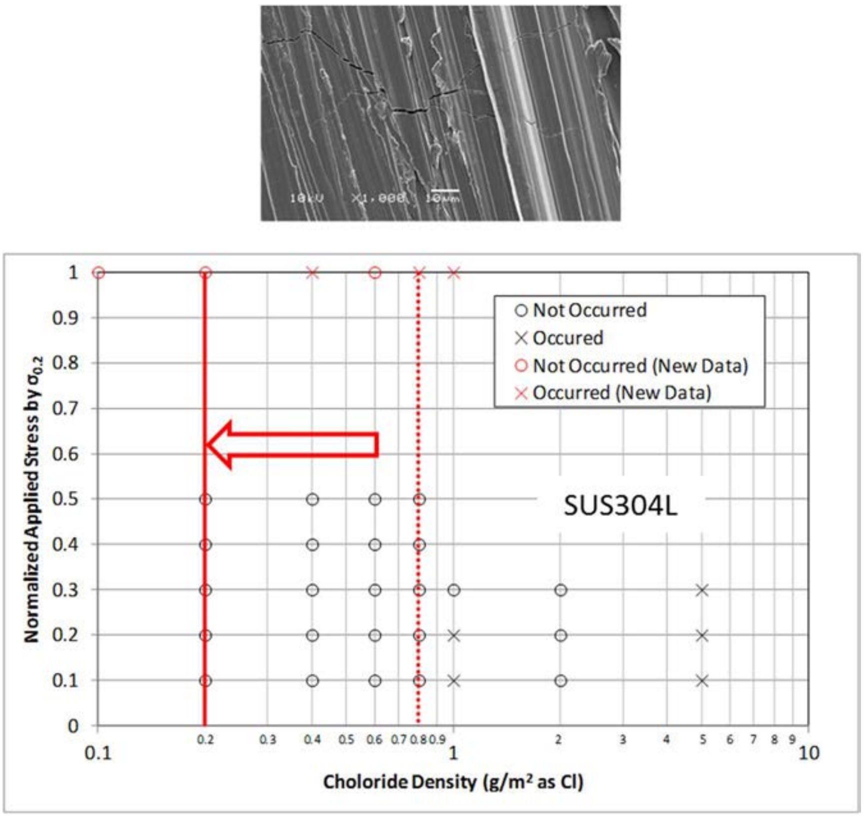

FIG. 2.26. CISCC initiation test results for 304L stainless steel (reproduced courtesy of CRIEPI) [2.36].

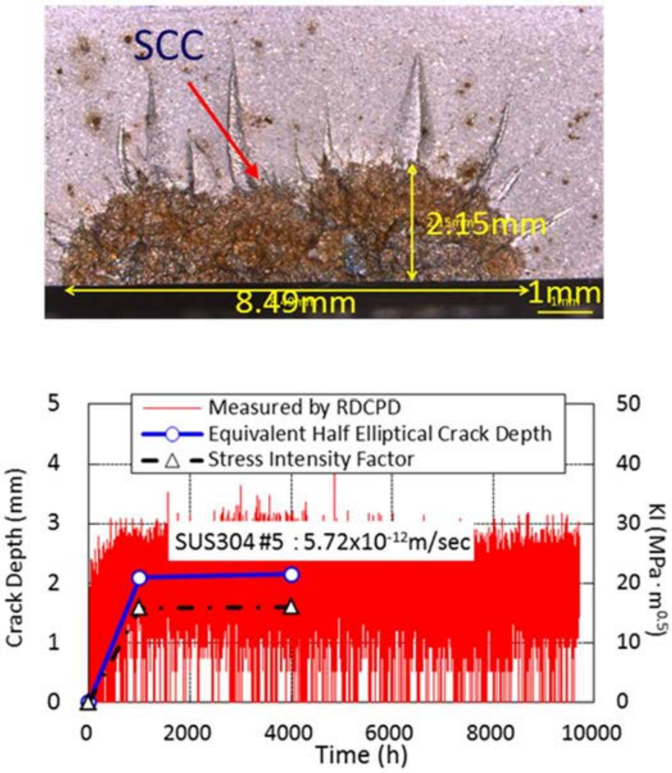

FIG. 2.27. Crack growth rate test results for 304L stainless steel (reproduced courtesy of CRIEPI) [2.36].

2.2.2. Outcome of work at US NRC - Nuclear Waste Technical Review Board (NWTRB)

CISCC of welded stainless steel components including water piping and storage tanks has been observed in operating commercial nuclear power reactors. The US Nuclear Regulatory Commission (US NRC) Information Notice 2012-20 [2.12] documents previous cases of atmospheric CISCC of welded stainless steel piping systems and tanks at operating reactor locations. This includes operating experience for reactors where CISCC was observed as a result of atmospheric deposition and deliquescence of chloride containing salts on welded stainless steel components in reactors that were located close to an open ocean or bay.

The results of laboratory and field testing conducted in the past 30 years has provided a better understanding of the factors that influence atmospheric CISCC susceptibility of welded stainless steel components; however, some important uncertainties such as the critical surface chloride concentration necessary to initiate CISCC, are not well established. While CISCC has been observed in welded stainless steel components at operating nuclear power plants, it remains unclear if the conditions necessary for CISCC to occur will develop on SNF storage canisters.

The US NRC has published the results of a completed investigation of CISCC involving the testing of U-bend specimens of types 304, 304L and 316L stainless steel and welds in NUREG/CR-7170 [2.37]. In these tests, CISCC was observed at temperatures ranging from 35°C to 60°C with surface salt concentrations as low as 0.1 g/m^2 in tests lasting between 1 and 12 months. Under these conditions, the surface temperatures of the test specimens were low enough to allow the relative humidity at a heated surface to increase to the point where deliquescence of some of the chloride containing components of deposited sea salts can occur. Previous US NRC sponsored investigations showed that no SCC occurred on specimens maintained at 85°C even with high salt concentrations after a year of testing (NUREG/CR-7030 [2.38]). These results confirm that the environment necessary for CISCC of stainless steels can occur by the deliquescence of deposited sea salt that contains $MgCl_2$ and $CaCl_2$ salts. However, these studies did not identify the critical surface salt concentration necessary for CISCC and previous reports have widely scatted values of the critical concentration. For example, in Subsection 2.2.1 (above) the work by CRIEPI showed a critical chloride concentration of 0.2 g/m^2 whereas Tokiwai et al. [2.39] reported a value of 0.008 g/m^2.

Several recent reports have been published by Electric Power Research Institute (EPRI) that address the potential for CISCC of welded stainless steel SNF storage canisters including an analysis of the effects of CISCC on welded stainless steel canisters [2.13], a literature review of CISCC that summarizes the results of many previous laboratory investigations [2.40], and a flaw tolerance and growth assessment for CISCC of welded stainless steel canisters for dry storage of SNF [2.7]. It should be noted that the EPRI flaw tolerance and growth assessment does not evaluate the time necessary for conditions for CISCC of the canisters to develop. The EPRI assessment is focused on CISCC growth and the EPRI calculations, based on a very limited set of data, provided an initial indication that the time for cracks to penetrate a welded stainless steel canister may range from 26 to more than 100 years depending on environmental conditions.

With the understanding that CISCC has been observed in practice on welded stainless steels and recognizing that significant uncertainties remain regarding the conditions necessary for CISCC to occur, an inspection based example ageing management programme using guidance from consensus codes and standards to assess the condition of canisters after many years in service was developed. This AMP, which will be included in the US NRC's revision to regulatory guidance on license renewal of dry storage systems NUREG-1927 [2.41] relies on consensus based codes and standards including the in-service inspection requirement for operating nuclear power plants documented in ASME Section XI [2.42].

2.2.3. Outcome of work at Pakistan Institute of Nuclear Science and Technology (PINSTECH), Pakistan

This study employed base metal and welded type 316L strip samples[8]. The electrochemical potential in the presence of seawater, NaCl and $MgCl_2$ solutions was measured in order to determine the potential range at which SCC could be initiated. Passive film rupture was also explored with and without the application of stress by investigation of open circuit potential, polarization resistance of film and phase angle in simulated seawater solution using electrochemical impedance spectroscopy. Salt fog testing of U-bend samples (both welded and unwelded) was carried out to investigate CISCC susceptibility at different temperatures.

This study addressed the knowledge gap related to 'environmental conditions under which SCC occurs' through work focused on mechanistic understanding of initiation via interrogation of film breakdown potential and practical susceptibility testing of stressed samples under controlled conditions.

Mechanical testing of welded and un-welded samples showed the expected stress-strain behaviour for 3xx steels and typical variations in hardness across the weld regions. Microscopy of the weld region microstructures showed typical features: delta ferrite network in the weld zone, equi-axed grains in the HAZ and intermetallic particles on grain boundaries.

Susceptibility testing for SCC was undertaken on U-bend samples over which simulated seawater (3.5% NaCl solution) was sprayed continuously. Testing was undertaken at temperatures between 25°C and 75°C at a RH of 70%. This method is significantly different from that used in testing by US NRC and CRIEPI where samples were loaded with a surface concentration of chloride and exposed to environments at different temperatures and RH. As a result of the test method, areal salt concentrations were not determined. No SCC was observed after 24 weeks exposure at room temperature, 50°C and 75°C or after 32 weeks at 40°C. This is consistent with earlier US NRC work at elevated temperatures [2.38] where no SCC was observed after a year, however this was under conditions of low RH. The conditions reported for these tests have high RH, however the continuous spraying will limit the concentration of chloride in the liquid at the surface of the test specimens well below the equilibrium concentration for deliquescing brines. Therefore, it is perhaps not unexpected that SCC initiation was not observed within the timescales reported more recently by US NRC [2.43] for cyclic RH conditions.

Electrochemical polarisation indicated that 3.5% NaCl solution is more aggressive than 0.5 M $MgCl_2$ solution, with seawater being more aggressive than both. The open circuit potential increased with exposure time towards a higher equilibrium level, due to film thickening. Temporary fluctuations in open circuit potential were indicative of transient corrosion events. Slowly increasing stress increased the susceptibility to corrosion, as seen by a decrease in open-

[8] The composition of which was consistent with AISI standard values.

circuit potential, however subsequent behaviour at a fixed stress showed a transition back to conditions similar to those observed for an unstressed sample.

Overall the electrochemical testing confirmed the known behaviour of 3xx series steels, which show good general corrosion resistance but susceptibility to localized corrosion under some conditions, particularly in the presence of chlorides. The extent to which the data derived from this testing is applicable in dry storage conditions is less clear because of differences between test environments and likely field conditions where, at the onset of corrosion, chloride concentrations in deliquescing brines will be much higher than in seawater.

Salt spray testing for SCC susceptibility showed a reduction in susceptibility compared to recent US NRC tests, however the continuous application of sprayed sea water is likely to have resulted in less aggressive conditions at the sample surface. Further work involving electrochemical techniques should address conditions likely to be prevalent during deliquescence rather than those associated with bulk marine conditions.

2.3. RADIATION EFFECTS

2.3.1. Outcome of work at National Centre for Nuclear Research (NCBJ), Poland

This work studied the effects of gamma and low level neutron irradiation from SNF on the properties of type 316L stainless steel. Cross sections (0.5 mm thick) were taken from a welded section of type 316L stainless steel by electrical discharge machining (EDM) as shown in Fig. 2.28. Punch samples of 3 mm were taken and thinned prior to being and irradiated inside a sealed capsule at temperatures of 30–35°C in the SNF pool of the MARIA test reactor, operated by National Centre for Nuclear Research. Irradiation periods of 1, 3 and 18 months led to estimated gamma exposures of 0.81 MGy, 2.1 MGy and 12 MGy (i.e. at an average dose rate of around 1 kGy/h(γ)). Using data from Table 2.1 (above), the highest exposure is representative of canister exposure over about 20 years. Cumulative exposure for a storage period of 125 years is likely to be around 30–50 MGy.

This study aimed to identify whether gamma irradiation of the canister materials during storage could affect the material properties and hence could affect the initiation or propagation of SCC in aged materials, compared to those in unaged test specimens.

Standard tensile and impact strength studies were performed on the unirradiated samples but detected no significant difference between base material (Site A and E) or HAZ (zones B and D). Corrosion testing of unirradiated material in boiling $CuSO_4$ solutions for up to 144 h indicated no significant difference in corrosion susceptibility between material types (A-E). Comparison of nano-indentation and small punch testing (SPT) for all three materials indicated a good correlation, providing confidence that SPT results would provide reliable measurement of variation in relevant material properties.

SPT was used on irradiated samples to minimize dose rates during testing. SPT data was analysed to produce parameters related to the Young's modulus, tensile strength and plasticity limit. Data averaged over 3–5 samples provided some qualitative indications of a small potential effect of irradiation; however, the differences were within the uncertainty in the measurements and hence trends were not significant.

The study concluded that irradiation up to 18 MGy over 18 months did not cause any significant effects on type 316 stainless steel as shown in Fig. 2.29 and hence the material's susceptibility to SCC was unlikely to be affected by exposure to gamma radiation.

Further testing is proposed to examine the effects of neutron dose on steel properties. For storage applications the total dose needs to reflect the low dose rate uptake associated with sub-critical SNF and the operating temperature range associated with canister materials rather than high doses, dose rates and operating temperatures associated with reactor core applications. Given the low cumulative neutron doses expected during storage and currently available data for neutron damage effects in type 316 stainless steel, it is unlikely that significant effects will be seen and therefore such testing would be of low priority.

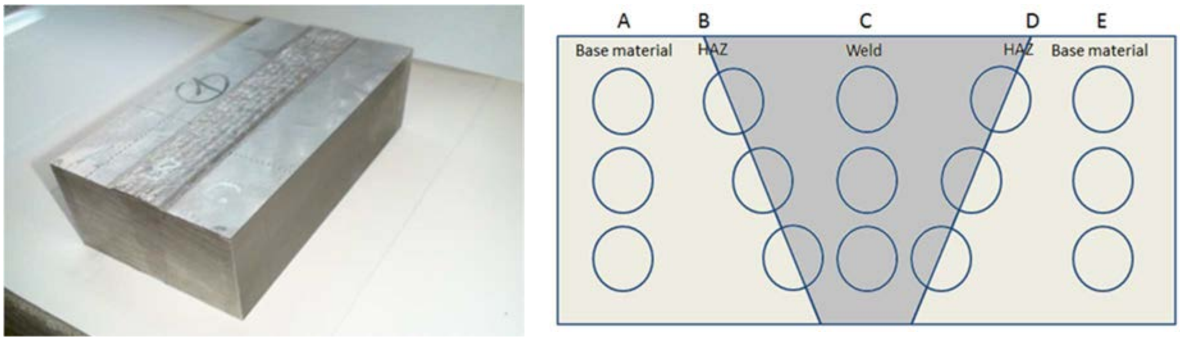

FIG. 2.28. Sample locations for irradiation testing (reproduced courtesy of NCBJ).

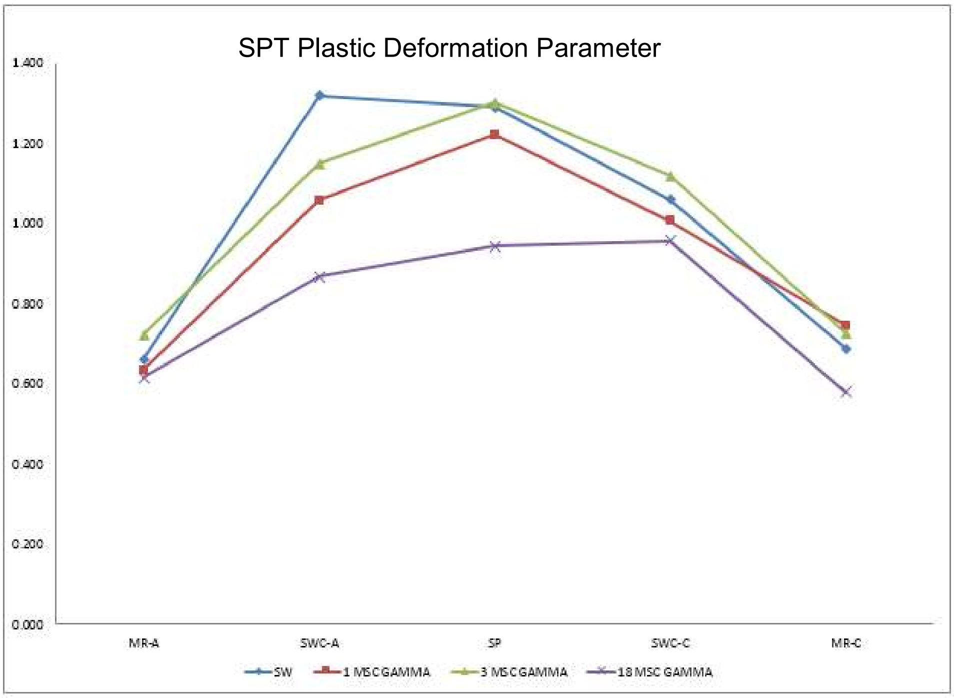

FIG. 2.29. Summarised SPT data at different irradiation levels (reproduced courtesy of NCBJ) [2.44].

2.4. PROCESSES AFFECTING STORAGE CONDITIONS

2.4.1. Outcome of work at Central Research Institute of Electric Power Industry (CRIEPI), Japan

Field measurements of salt deposition were undertaken to understand their dependency on atmospheric salt concentrations. In parallel, laboratory based experiments were undertaken to relate atmospheric salt concentrations to measured deposition levels on heated canister surfaces.

Testing was undertaken on a full-scale mock-up of the top section of a laser-welded canister to provide evidence of CISCC initiation at a scale relevant to operational systems and in relevant environmental conditions. This test also provided evidence of the effectiveness of low plasticity burnishing (LPB) technology as a process to prevent CISCC initiation at the canister surface.

The field testing work provides a better understanding of environmental processes that affect storage conditions: first, by providing information on the levels of airborne salt in the environment where the canisters may be stored and secondly, by providing the relationship between environmental salt concentrations and the level deposited on canister surfaces over time.

Full-scale mock-up CISCC testing contributed towards confirming whether small scale experimental testing related to 'environmental conditions under which CISCC occurs' remain valid at industrial scale and relevant environmental conditions. It also provides evidence of the effectiveness of processes affecting storage conditions.

Using data from both laboratory and field tests of an annulus representing a vertical cask, a correlation for the amount of salt deposition was proposed in the form of the empirical equation as a function of time, the canister surface temperature and airborne salt concentration as shown in Fig. 2.30. Figure 2.31 shows an example of the result calculated for the time taken to reach the minimum amount of salt for CISCC initiation for type 304L stainless steel, which indicates that for these conditions CISCC initiation would not occur for more than 50 years with an airborne salt concentration of 100 $\mu g/m^3$.

In the full-scale mock-up, as shown in Fig. 2.32, the salt concentration on the surface of the top section of a laser-welded canister was set to 4 g/m^2, which is over 20 times of threshold chloride density for CISCC initiation of type 304L stainless steel as described in Subsection 2.1.1. One region of the weld was treated by LPB and the other left after normal finishing.

After 5000 hours of testing at constant temperatures of 80°C with RH=35%, CISCC was observed in the untreated ring plate and the edge of shell near the lid. However, no CISCC was observed in the region treated by LPB providing confirmation of the effectiveness of LPB technology against the CISCC of canister.

These results provide strong evidence of the potential for post-weld treatment to minimize the risk of SCC during service. Further evaluation of options for such treatments and long term effectiveness are therefore warranted to expand the range of potential treatment options and provide sufficient evidence for regulatory acceptance. Assessment or evaluation of other treatment options is also warranted to identify viable candidates for improving long term resistance to CISCC.

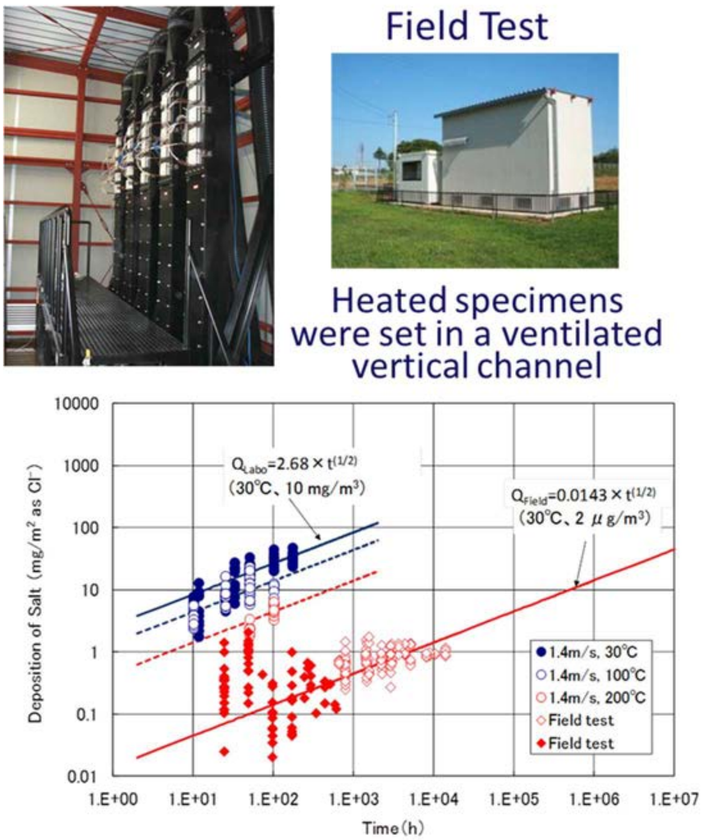

FIG. 2.30. Comparison of accumulated salt amount profile between laboratory and field tests (reproduced courtesy of CRIEPI)[2.36, 2.45].

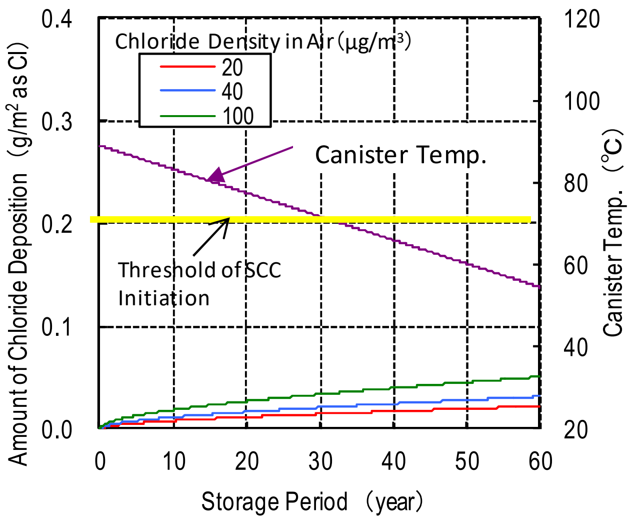

FIG. 2.31. Time to SCC initiation in salty air for type 304L stainless steel (reproduced courtesy of CRIEPI) [2.36].

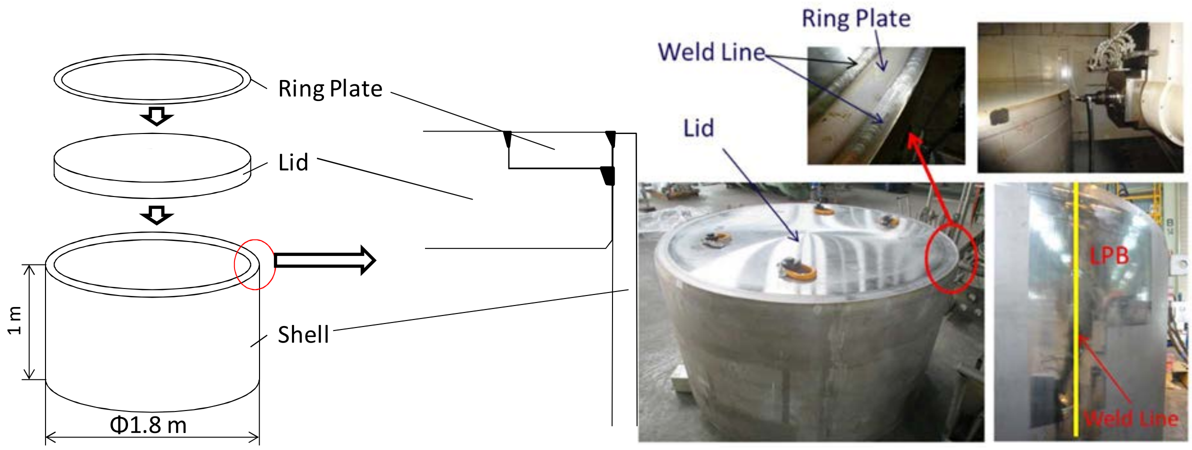

FIG. 2.32. Full-scale mock-up CISCC testing (reproduced courtesy of CRIEPI) [2.36].

2.5. INSPECTION AND MEASUREMENT

2.5.1. Outcome of work at Central Research Institute of Electric Power Industry (CRIEPI), Japan

Progress was made on the development of two detection systems for canister monitoring:

- A full-scale demonstration of temperature measurements to infer He leakage from a canister;
- Development of laser-induced breakdown spectrometry (LIBS) analysis of salt on a steel surface from a bench scale demonstration of capability towards a system suitable for deployment in canister systems.

Both techniques address gaps related to inspection and monitoring techniques, one as a measurement that would indicate CISCC risk and another that provides a retrospective indication of containment failure.

Experimental work on a full-scale heated canister, as shown in Fig. 2.33 [2.46], provided a demonstration that it is possible to obtain a signal indicating loss of containment from temperature sensors located at either the top or the bottom of a canister, as opposed to requiring sensors in both locations as indicated by earlier research.

A prototype compact device for remote LIBS, shown schematically in Fig. 2.34 [2.33], was successfully inserted in the narrow space simulating the space between a concrete overpack and a canister. The results of open pass LIBS measurements under such constraints showed that the chlorine emission spectrum could be measured when the distance from laser device to the measurement points was 5 metres.

Further development and validation of the deployable LIBS system is continuing and is required to provide qualified measurements.

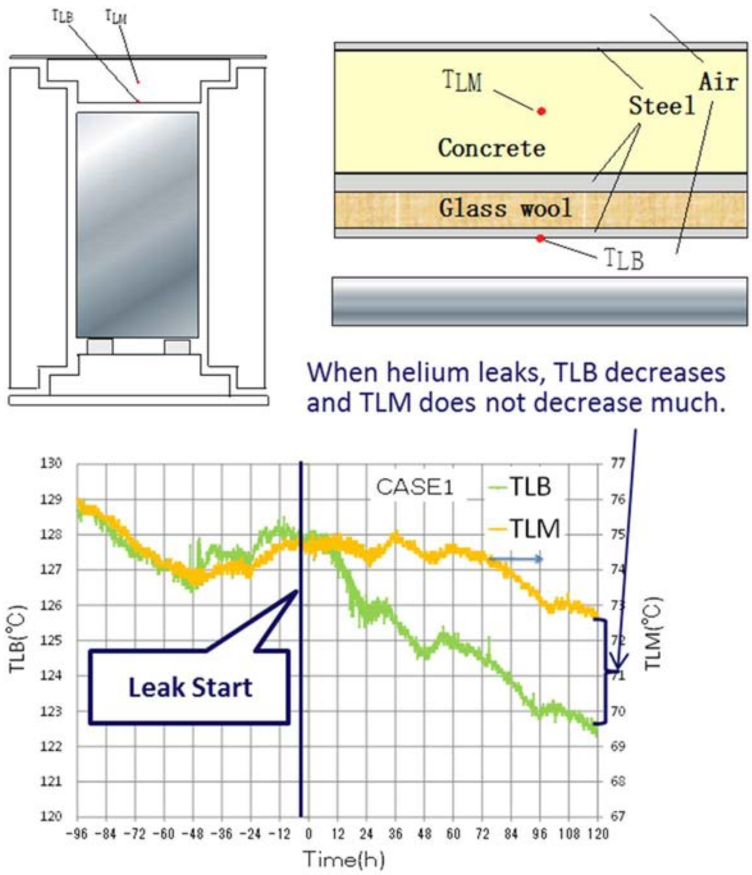

FIG. 2.33. Helium leak detection method of the canister (reproduced courtesy of CRIEPI) [2.46].

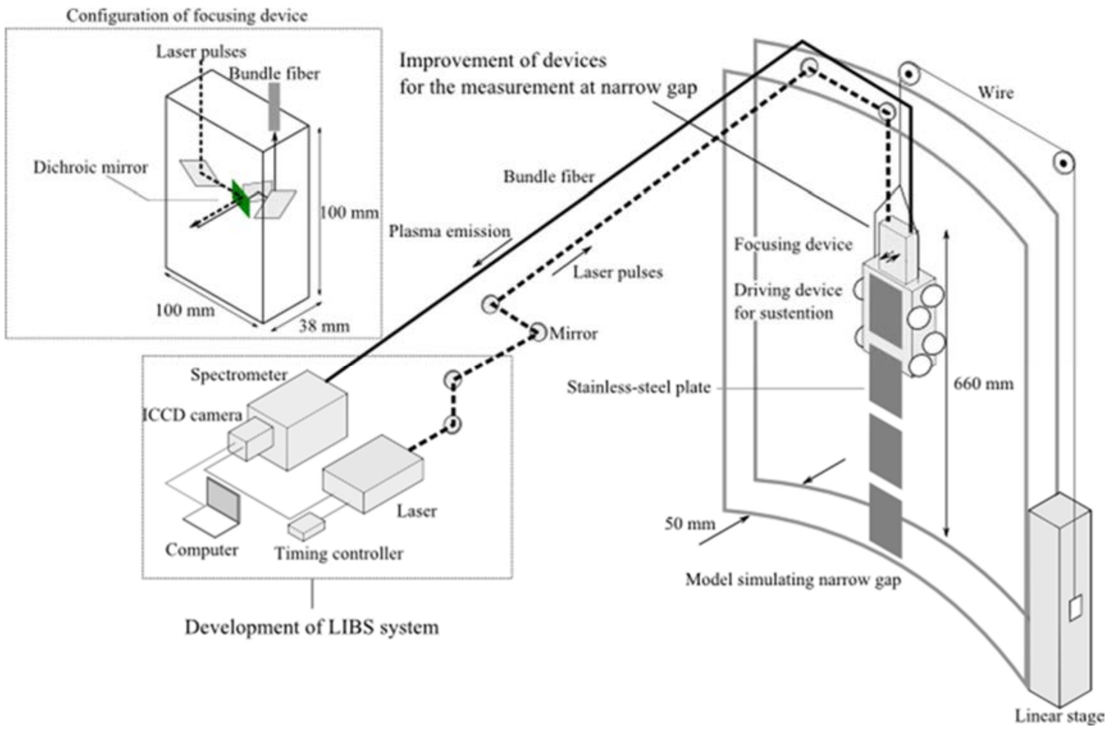

FIG. 2.34. Outline of LIBS System and miniature model simulating the narrow gap between a canister and a concrete over-pack (reproduced courtesy of CRIEPI) [2.33].

2.5.2. Outcome of work at National Building and Civil Engineering Institute (ZAG), Slovenia

Testing was undertaken on type 321 stainless steel in aqueous conditions under two regimes:

- At atmospheric pressure at elevated temperature (up to 70°C) in 0.5M NaCl + 0.5M H_2SO_4 (pH 2);
- At 100 bars in 300°C water with 1000 ppm B, 2 ppm Li (pressurized water reactor (PWR) conditions).

Atmospheric test specimens were subjected to a static load near the yield point to initiate SCC, whilst at PWR conditions slow strain rate tests were used. Monitoring was undertaken using electrochemical noise (EN), acoustic emission (AE) technique, measurement of tensile test sample elongation and simultaneous digital imaging of the surface by charge coupled device camera.

The main aim of the research was to identify a reliable technique for monitoring of CISCC processes by showing a correlation between different measurement techniques and microstructural evidence of corrosion processes. Although the testing was undertaken in aggressive, aqueous conditions, the focus was on the evaluation of AE as a detection technique, which is deployable in non-aqueous contexts and therefore the work contributes towards the provision of reliable techniques for the detection of CISCC.

The testing at low pressure conditions identified a set of AE signals that were associated with CISCC-related ductile fracture of long cracks and a set of signals arising from non-SCC related phenomena related to mechanical damage. These two data sets could be distinguished from each other.

Combined use of EN, digital image correlation (DIC) and AE provided data that elucidated mechanistic details of the SCC process, but many of the techniques were not suitable for deployment in the field. Work at higher pressures indicated that AE signals were susceptible to interference from environmental noise. Environmental sources of acoustic noise were considered to be likely to cause significant degradation of signals derived from cracking in any field deployment.

AE is potentially useful for detection of CISCC associated with large cracks, provided that the active degradation mechanism includes a ductile fracture component. AE can provide surveillance of large areas of canister wall from a single point but is unlikely to be able to determine location of any detected CISCC. The potential for loss of signal due to environmental noise is considered a significant issue. Nevertheless, further work to explore the relative scale of signal and noise levels may be of value.

Electrochemical noise and other electrochemical techniques are of limited use for dry storage applications because of the lack of electrolyte for the required current path.

2.5.3. Outcome of work at National Nuclear Laboratory (NNL), United Kingdom

This project identified desirable characteristics and preferred techniques for incorporation in an instrumented coupon for corrosion monitoring, which would allow real-time monitoring of conditions and localized corrosion of a representative sample of canister material. Preferred options for testing of the concept were those that had already been deployed industrially. A range of testing was undertaken to demonstrate the capability of proposed techniques to identify conditions that were likely to cause corrosion and the ability to detect CISCC.

The purpose of the work was to provide the means to identify conditions under which CISCC might initiate and to detect SCC in representative materials, with the intention of providing early indication that SCC risk was significant. It addresses gaps related to 'Inspection and measurement of important parameters' and 'Detection of CISCC' in Table 2.3, but not detection of CISCC in canisters.

The testing indicated that industrial field signature method systems developed for detection of general corrosion, including mechanisms such as erosion, were not able to reliably detect localized corrosion in the form of pitting or small partial through-wall defects in large samples of material. However other testing indicated that the technique could reliably detect both progression and arrest of CISCC in steel, provided that the specimen and instrument connection geometries were optimized.

Testing of combined techniques to monitor temperature and humidity levels were largely successful and means of confirming deliquescence also showed a good correlation with temperature and relative humidity.

Overall, the work established viability of the concept but pointed towards areas where further development and demonstration were required to produce a system capable of providing a lead indicator for CISCC risk in LWR dry storage canisters. Specific aspects requiring further work include the design of specimens that reliably bound the properties of canister welds without undue conservatism and optimisation of the measurement for detection of CISCC initiation and propagation. Demonstration of long term stability under relevant environmental conditions, including radiation hardness, is also required.

2.6. SUMMARY AND OUTCOMES REFLECTING DATA GAPS FOR LONG TERM STORAGE

The results of work conducted within this CRP have provided evidence that gamma radiation is unlikely to affect the canister material during expected lifetimes and hence confirms that this is not a mechanism of concern.

Results on CISCC initiation conditions have provided new data, which is resolving some of the inconsistencies in previously reported data. An important outcome is evidence of similarity in CISCC initiation between laboratory tests under relevant stress conditions and a full-scale test. Further work is required on susceptibility and crack growth rates under conditions that are relevant for SNF storage canisters. In addition, work is needed to develop mechanistically based models of crack initiation and growth to allow better extrapolation of test data to operationally relevant systems and timescales.

Development of monitoring and inspection techniques within the CRP (LIBS for salt concentration, temperature profiling for loss of canister integrity and instrumented coupons) has shown progress towards systems that are deployable and useful for monitoring canister integrity, although further development and qualification work remains before full value can be obtained in relation to long term management of loaded canisters. Work on AE indicated that it was unlikely to be sufficiently discriminating in real systems to warrant further development at the moment. Given the challenges faced in obtaining reliable data on conditions relevant to SCC, further work in this area is warranted where it complements other ongoing development work. Such work should include activities to raise the technology readiness level of existing techniques and work to demonstrate viability of new techniques.

With respect to a demonstration test, full-scale testing in realistic geometries with representative heating in a representative environment is a valuable step in providing confidence in the scalability of small scale and laboratory tests provided that the canister materials are prototypic. For a demonstration, it is important that the canister materials, manufacturing processes and residual weld stresses are characterized to provide a reliable basis for underpinning its application to other systems and conditions. Such inactive testing avoids the additional costs, dose and difficulties associated with canisters containing SNF and can reproduce the vast majority of relevant conditions. For inspection systems, a demonstration done under radiation fields, as well as under representative temperatures, is an important consideration in demonstrating that in-service inspections will be reliable. Since the potential effects of radiation on deliquescence and corrosion processes have still to be fully understood, a demonstration test on a loaded canister can provide additional data.

REFERENCES TO CHAPTER 2

[2.1] SHIRAI, K., TANI, J., GOTOH, M., WATARU, M., "SCC Evaluation Method of Multi-Purpose Canister in Long Term Storage", 11th International Probabilistic Safety Assessment and Management Conference and the Annual European Safety and Reliability Conference 2012 (PSAM11 ESREL 2012) (Proc. Conf. Helsinki, 2012), IAPSAM & ESRA, New York (2012).

[2.2] CHOPRA, O.K., et al., Managing Aging Effects on Dry Cask Storage Systems for Extended Long-Term Storage and Transportation of Used Fuel, Rep. FCRD-UFD-2013-000294, ANL-13/15, Rev. 1, Argonne Natl Lab., IL (2013).

[2.3] RIGBY, D.B., Evaluation of the Technical Basis for Extended Dry Storage and Transportation of Used Nuclear Fuel, U.S. Nuclear Waste Technical Review Board, VA (2010).

[2.4] UNITED STATES NUCLEAR REGULATORY COMMISSION, Final Environmental Impact Statement for the Construction and Operation of an Independent Spent Fuel Storage Installation on the Reservation of the Skull Valley Band of Goshute Indians and the Related Transportation Facility in Tooele County, Utah, Rep. NUREG-1714, Vol. 1, Office of Nuclear Material Safety and Safeguards, Washington, DC (2001).

[2.5] ZULOAGA, P., ‘‘HLW storage and SL-LLW disposal in Spain’’, paper presented at 19th REFORM Group Meeting, Salzburg (2014).

[2.6] HAIN, K., "Idaho site spent nuclear fuel management", paper presented at 2010 U.S. Nuclear Waste Technical Review Board, Idaho Falls (2010).

[2.7] ELECTRIC POWER RESEARCH INSTITUTE, Flaw Growth and Flaw Tolerance Assessment for Dry Cask Storage Canisters, Rep. 3002002785, EPRI, CA (2014).

[2.8] ELECTRIC POWER RESEARCH INSTITUTE, Extended Storage Collaboration Program International Subcommittee Report: International Perspectives on Technical Data Gaps Associated with Extended Storage and Transportation of Used Nuclear Fuel, Rep. 1026481, EPRI, CA (2012).

[2.9] HANSON, B., et al., Used Fuel Disposition Campaign, Gap Analysis to Support Extended Storage of Used Nuclear Fuel, Rep. FCRD-USED-2011-000136, Rev. 0, Rep. PNNL-20509, Pacific Northwest Natl Lab., WA (2012).

[2.10] HANSON, B., et al., Review of Used Nuclear Fuel Storage and Transportation Data Gap Analysis, Rep. FCRD-USED-2012-000215, Rep. PNNL-21596, Pacific Northwest Natl Lab., WA (2012).
[2.11] NUCLEAR REGULATORY COMMISSION, Identification and Prioritization of the Technical Information Needs Affecting Potential Regulation of Extended Storage and Transportation of Spent Nuclear Fuel, NRC document ML14043A423, Nuclear Regulatory Commission, Washington, DC (2014).
[2.12] NUCLEAR REGULATORY COMMISSION, Potential Chloride-Induced Stress Corrosion Cracking of Austenitic Stainless Steel and Maintenance of Dry Cask Storage System Canisters, NRC document ML12319A440, NRC Information Notice 2012-20, Office of Nuclear Material Safety and Safeguards, Washington, DC (2012).
[2.13] ELECTRIC POWER RESEARCH INSTITUTE, Failure Modes and Effects Analysis (FMEA) of Welded Stainless Steel Canisters for Dry Cask Storage Systems, Rep. 3002000815, EPRI, CA (2013).
[2.14] ENOS, D.G., BRYAN, C.R., Status Report: Characterization of Weld Residual Stresses on a Full-Diameter SNF Interim Storage Canister Mockup, Rep. FCRD-UFD-2015-00123, SAND2015-7068 R, Sandia Natl Labs, NM (2015).
[2.15] Choi, S., Cho, H., Lissenden, C.J., Nondestructive inspection of spent nuclear fuel storage canisters using shear horizontal guided waves, Nuclear Engineering and Technology 50 (2018) 890–898.
[2.16] CUTA, J.M., SUFFIELD, S.R., FORT, J.A., ADKINS, H.E., Thermal Performance Sensitivity Studies in Support of Material Modeling for Extended Storage of Used Nuclear Fuel, Rep. FCRD-UFD-2013-000257, PNNL-22646, Pacific Northwest Natl Lab., WA (2013).
[2.17] WITTMAN, R., Used Fuel Disposition Campaign, Radiolysis Model Sensitivity Analysis for a Used Fuel Storage Canister, Rep. FCRD-UFD-2013-000357, PNNL-22773, Pacific Northwest Natl Lab., WA (2013).
[2.18] CUTA, J.M., ADKINS, H.E., Post-Inspection Thermal Modeling of HI-STORM 100 Storage Modules at Diablo Canyon Power Plant ISFSI, Rep. FCRD-UFD-2015-000492, Rep. PNNL-24771, Pacific Northwest Natl Lab., WA (2015).
[2.19] Central Research Institute of Electric Power Industry, Basis of Spent Nuclear Fuel Storage, ERC Publishing, Tokyo (2015) pp. 237 – 238, 377.
[2.20] SUZUKI, S., et al., Evaluation of SCC morphology on L-grade stainless steels in BWRs, Aturyoku Gijutsu 42 4 (2004) 188–198 (in Japanese).
[2.21] TSUBOTA, M., KANAZAWA, Y., INOUE, H., "The effect of cold work on SCC susceptibility of austenitic stainless steels", 7th International Symposium on Environmental Degradation of Materials in Nuclear Power Systems – Water Reactor (Proc. Int. Symp. Breckenridge, 1995), Vol. 1, NACE International, Houston (1995) 519–528.
[2.22] WEXLER, A., HASEGAWA, S., Relative humidity-temperature relationships of some saturated salt solutions in the temperature range 0° to 50° C, Journal of Research of the National Bureau of Standards 53 1 (1954).
[2.23] SHOJI, S., OHNAKA, N., FURUTANI, Y., SAITO, T., Effects of relative humidity on atmospheric stress corrosion cracking of stainless steels, Boshoku Gijutsu 35 (1986) 559–565 (in Japanese).
[2.24] MAYUZUMI, M., TANI, J., ARAI, T., Chloride induced stress corrosion cracking of candidate canister materials for dry storage of spent fuel, Nuclear Engineering and Design 238 (2008) 1227–1232.

[2.25] Byalobzheskii, A., in Radiation Corrosion, Israel Program for Scientific Translations, Jerusalem (1970) 148–152.
[2.26] TANI, J.-I., MAYUZUMI, M., HARA, N., Initiation and propagation of stress corrosion cracking of stainless steel canister for concrete cask storage of spent nuclear fuel, Corrosion 65 3 (2009) 187–194.
[2.27] TANI, J., MAYUZUMI, M., Stress Corrosion Cracking of Canister Materials for Storage of Spent Nuclear Fuel (Vol. 2) – An Evaluation on the Possibility of SCC Initiation, Rep. Q08007, CRIEPI, Tokyo (2009) (in Japanese).
[2.28] BRITISH STAINLESS STEEL ASSOCIATION, Chemical Compositions of AISI (ASTM/ASME) and UNS Duplex Stainless Steel Grades, 2018 British Stainless Steel Association.
[2.29] MEYER, R.M., et al., NDE to Manage Atmospheric SCC in Canisters for Dry Storage of Spent Fuel: an Assessment, Rep. PNNL-22495, Pacific Northwest Natl Lab., WA (2013).
[2.30] Pacific Nuclear 1991, Topical Report for the Nutech Horizontal Modular Storage System for Irradiated Nuclear Fuel NUHOMS®-24P, NRC ADAMS Accession Number ML 110730769, April 1991.
[2.31] ELECTRIC POWER RESEARCH INSTITUTE, Calvert Cliffs Stainless Steel Dry Storage Canister Inspection, Rep. 1025209, EPRI, CA (2014).
[2.32] BRYAN, C., ENOS, D., Analysis of Dust Samples Collected from an Unused Spent Nuclear Fuel Interim Storage Container at Hope Creek, Delaware, Rep. SAND2015-1746, Sandia Natl Labs, NM (2015).
[2.33] ETO, S., et al., Development of Measurement Technology of Chlorine Attached on Canister Using Laser – Development of Measurement Device and Quantification of Attached Chlorine Concentration for Measurement Scenario during Storage of Spent Fuel, Rep. H14004, CRIEPI, Tokyo (2015) (in Japanese).
[2.34] TAKEDA, H., et al., Development of the detecting method of helium gas leak from canister, Nuclear Engineering and Design 238 5 (2008) 1220–1226.
[2.35] LARSON, N., ‘‘DOE R&D in support of high burnup spent fuel dry storage and transportation’’, paper presented at U.S. NRC RIC, Rockville (2016).
[2.36] WATARU, M., et al., Study on Commercial Realization of Concrete Cask for Interim Storage of Spent Nuclear Fuel – Proposal and Verification of Code Case on SCC Countermeasure of Canister, Rep. N15014, CRIEPI, Tokyo (2016) (in Japanese).
[2.37] HE, X., MINTZ, T.S., PABALAN, R., MILLER, L., OBERSON, G., Assessment of Stress Corrosion Cracking Susceptibility for Austenitic Stainless Steels Exposed to Atmospheric Chloride and Non-Chloride Salts, Rep. NUREG/CR-7170, Nuclear Regulatory Commission, Washington, DC (2014).
[2.38] CASERES, L., MINTZ, T.S., Atmospheric Stress Corrosion Cracking Susceptibility of Welded and Unwelded 304, 304L, and 316L Austenitic Stainless Steels Commonly Used for Dry Cask Storage Containers Exposed to Marine Environments, Rep. NUREG/CR-7030, Nuclear Regulatory Commission, Washington, DC (2010).
[2.39] TOKIWAI, M., KIMURA, H., KUSANAGI. H., The amount of chlorine contamination for prevention of stress corrosion cracking in sensitized type 304 stainless steel, Corrosion Science 25 8–9 (1985) 837–844.
[2.40] ELECTRIC POWER RESEARCH INSTITUTE, Literature Review of Environmental Conditions and Chloride-Induced Degradation Relevant to Stainless Steel Canisters in Dry Cask Storage Systems, Rep. 3002002528, EPRI, CA (2014).

[2.41] NUCLEAR REGULATORY COMMISSION, Standard Review Plan for Renewal of Spent Fuel Dry Cask Storage System Licenses and Certificates of Compliance, Rep. NUREG-1927, Office of Nuclear Material Safety and Safeguards, Washington, DC (2011).

[2.42] THE AMERICAN SOCIETY OF MECHANICAL ENGINEERS, 2007 ASME Boiler & Pressure Vessel Code: an International Code. Section XI, Rules for Inservice Inspection of Nuclear Power Plant Components, ASME, New York (2007).

[2.43] SORENSON, K.B., et al., "Long term storage of used nuclear fuel in the U.S.", PATRAM 2010, 16th Int. Symp. on the Packaging and Transportation of Radioactive Materials (Proc. Int. Symp. London, 2010), London (2010) CD-ROM.

[2.44] KURPASKA, L., "The investigations of the gamma irradiation influence on the mechanical and corrosion properties of stainless steel used for spent fuel containers and canisters'', paper presented at 3rd RCM and Parallel CS on Demonstrating Performance of Spent Fuel and Related Storage System Components during Very Long Term Storage (CRP T13014) embedding the 2016 ESCP International Subcommittee Meeting 11 to 15 April 2015, Santander (2015).

[2.45] WATARU, M., et al., Evaluation of the salt deposition on the canister surface of concrete cask – Measurement test of the salt deposition in the laboratory and the field, Rep. N09023, CRIEPI, Tokyo (2010) (in Japanese).

[2.46] TAKEDA, H., TORIU, D., USHIJIMA, S., Development of Evaluation Method of Long-Term Confinement Performance for Canister (Part 2) – Helium Leak Analyses and Proposition of Simpler Helium Leak Detection Method, Rep. N15006, CRIEPI, Tokyo (2015) (in Japanese).

3. ROD BEHAVIOUR

3.1. INTRODUCTION

As described in Chapter 1, interim storage of spent nuclear fuel (SNF) from power reactors is being performed internationally using different storage options. Given the lack of currently under operation disposal facilities, the temporary storage solutions that were originally envisaged to last for a few decades are now faced with the need for an extension of their service life beyond their intended design life. This extension entails potential challenges for SNF during storage, as well as in the subsequent transportation, and defines the need for additional technical knowledge on SNF behaviour under long term storage conditions. In addition, whatever the fuel cycle option adopted, the SNF would need to be transported after the extended period of storage. Hence, the potential changes in the condition of SNF during storage may affect the capability to fulfil the transportation safety functions.

The specific research objective of this Coordinated Research Project (CRP) regarding SNF is to review the impact of long storage periods on the fuel behaviour, as a function of the different cladding materials and of the different storage and subsequent transportation conditions. More specifically, the degradation of the SNF and cladding confinement capability (avoiding penetrations that could compromise the cladding integrity) are addressed in this CRP.

Loss of cladding integrity may allow the release of gases, fuel particulates and pellet fragments. As a result, the geometric distribution of the radioactive material in the cask may be different of that assumed in the safety analysis, thus limiting its validity. The effect of this potential redistribution of the material on the compliance with the storage and transportation safety functions is reflected in Table 3.1 below. It is observed that all the safety functions may be affected, most of them directly, if the cladding integrity is challenged. Thus, maintaining the long term performance of the fuel cladding during dry storage and transportation in casks is important, and an accurate prediction of its behaviour is key to provide an adequate demonstration of the safety functions fulfilment in the long term.

TABLE 3.1. EFFECT OF LOSS OF CLADDING INTEGRITY ON SAFETY FUNCTIONS

Safety function	Effect on the safety function
Subcriticality	Direct effect (potential for non-analyzed configurations due to loss of geometry)
Confinement	Indirect effect (higher activity inventory available for release)
Radiation protection	Direct effect (potential for non-analyzed configurations due to loss of geometry)
Heat removal	Direct effect (potential for non-analyzed configurations due to loss of geometry)
Retrievability	Direct effect

Figure 3.1 shows several potentially important mechanisms that may degrade the cladding barrier over the long term. The conditions that govern these degradation mechanisms are strongly dependent on the initial physical states, temperature, and in situ mechanical stress state of the cladding when fuel rods are first placed in dry storage.

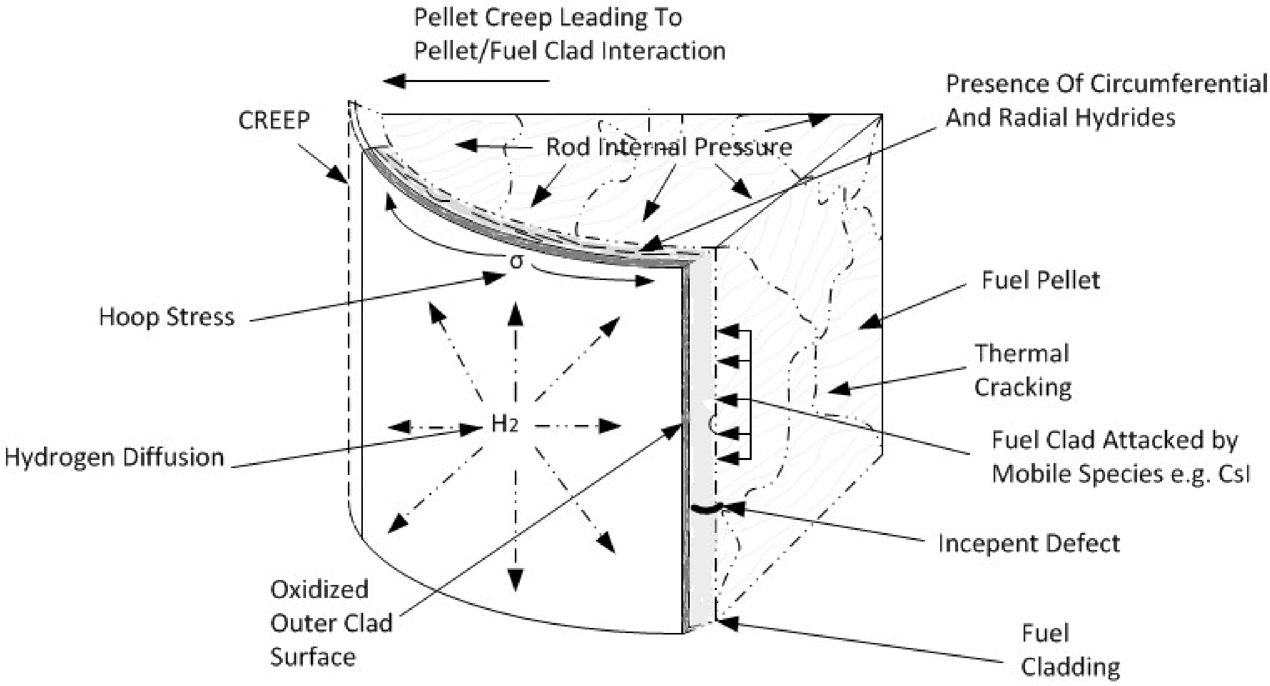

FIG. 3.1. Mechanisms affecting SNF cladding performance during dry storage [3.1].

The importance of R&D activities towards understanding each degradation mechanism has already been presented in Chapter 1 (see Table 3.2). Regarding fuel behaviour, higher importance has been assigned to those mechanisms related to hydrogen embrittlement of the cladding, followed by hydride cracking and cladding and pellet oxidation.

TABLE 3.2. VERY LONG TERM STORAGE TECHNICAL NEEDS FOR STRUCTURES, SYSTEMS AND COMPONENTS (SSCs): SUMMARY OF 'IMPORTANCE TO R&D ASSESSMENTS' (ADAPTED FROM [3.2])

Structures, systems and components (SSCs)	**Ageing alteration and/or degradation mechanism**	**TECDOC chapter in which the gap is addressed**
Fuel cladding	Annealing	n.a.
	Hydrogen embrittlement	3
	Hydride cracking	3
	Oxidation	3
	Creep	3
Fuel pellets	Cracking, bonding	n.a.
	Oxidation	3
Fuel assembly hardware	Corrosion and stress corrosion cracking (SCC)	n.a.
Basket	Corrosion, irradiation	n.a.
Neutron shielding	Thermal and radiation ageing	6
	Creep	6
	Corrosion	6
Neutron poison	Creep	n.a.
	Embrittlement	n.a.
	Corrosion	n.a.
Welded canister	Atmospheric corrosion	2
	Aqueous corrosion	n.a.
Moisture absorber	Irradiation, thermal	n.a.
Bolted casks	Fatigue of seals or bolts	5
	Atmospheric corrosion	n.a.
	Aqueous corrosion	n.a.
	Metal seal creep	5
Concrete overpack, cask, or pad	Freeze-thaw	4
	Corrosion (including embedded steel)	4

Note:

A few of these ageing mechanisms are not detrimental to maintaining safety functions.

While the list of potential cladding degradation mechanisms included in Table 3.2 is exhaustive to characterize the long term behaviour, the contributions to this CRP focus on a limited set of issues which have been included in Table 3.3. A summary of the individual contributions is provided in the following paragraphs. The full text of all technical reports of this CRP is found in the annexes.[9]

TABLE 3.3. GAPS ADDRESSED BY THE CONTRIBUTIONS TO THE CRP

Knowledge gaps	Contributors
Cladding embrittlement due to hydrogen	Argentina (AGR 173–9 - Annex II), France (FRA 172–0 - Annex III), Spain (SPA 173–5 - Annex XI, SPA 18996 – Annex XII), USA (USA 192–9 - Annex XIV), Germany (GFR 173–7 - Annex IV)
Delayed hydride cracking (DHC), stress corrosion cracking (SCC)	Argentina (AGR 173–9 - Annex II)
Cladding oxidation	Argentina (AGR 173–9 - Annex II)
Cladding creep	Argentina (AGR 173–9 - Annex II)
Pellet oxidation	Spain (SPA 189–6 - Annex XII)
Fuel drying	France (FRA 172–0 - Annex III), USA (USA 192–9 - Annex XIV)

3.1.1. Effects of cladding corrosion and hydriding: embrittlement and hydride reorientation

The zirconium-based cladding undergoes outer surface corrosion during in-reactor operation as the high-temperature water reacts with the cladding, producing a zirconium oxide layer. This is shown in Fig. 3.2 along the upper right part of the figure, which is the outside of the cladding. A thick oxide layer is also shown in the upper part of Fig. 3.3. A number of factors, notably the alloy composition and cladding tube manufacturing method, influence the rate of oxide layer formation. A primary effect of cladding corrosion is a reduction in the thickness of cladding, which may affect its mechanical strength during the postulated operation conditions.

[9] The Annexes of this report are provided as supplementary material. The names of the files are composed by the country abbreviation followed by the code of the CRP and the number of the Annex. The annexes included are: ARG 17338 – Annex I, ARG 17339 – Annex II, FRA 17270 – Annex III, GFR 17307 – Annex IV, JPN 17308 – Annex V, JPN 17486 – Annex VI, LIT 17275 – Annex VII, PAK 17283 – Annex VIII, POL 17290 – Annex IX, SLO 17810 – Annex X, SPA 17305 – Annex XI, SPA 18996 – Annex XII, UK 17420 – Annex XIII USA 19249 – Annex XIV.

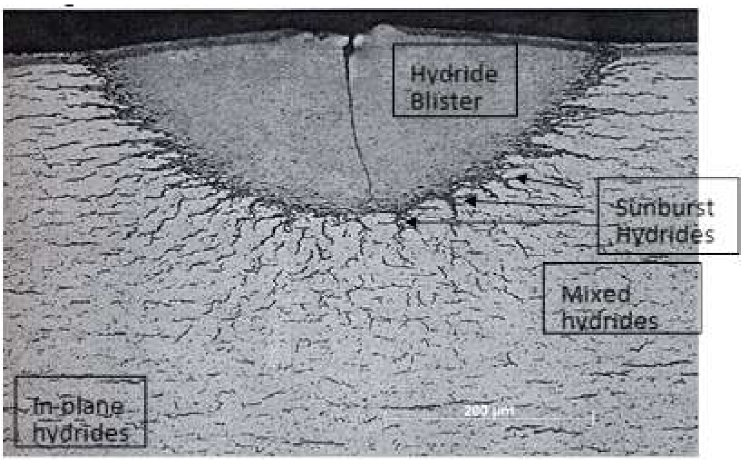

FIG. 3.2. Hydride blister created on pre-hydrided non-irradiated material (reproduced courtesy of Canadian Nuclear Society/Société Nucléaire Canadienne)[3.3].

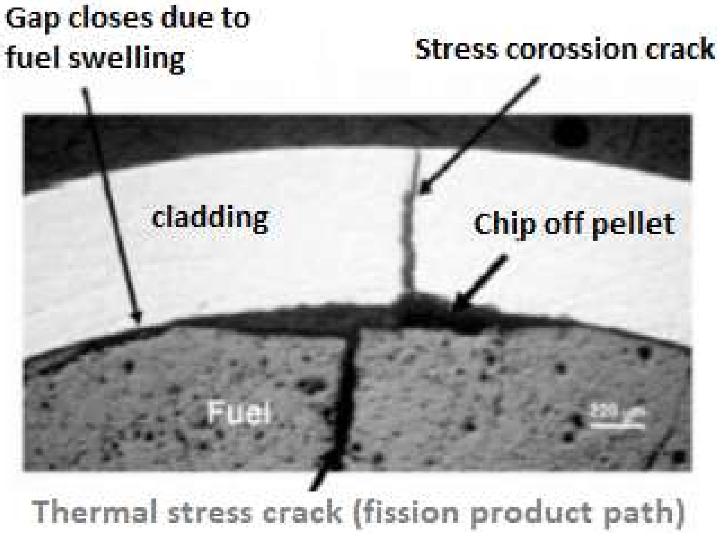

FIG. 3.3. Stress corrosion cracking of cladding (reproduced courtesy of US NRC) [3.4].

The hydrogen released during this chemical reaction is partially absorbed by the cladding material (hydrogen pickup). When the concentration of hydrogen in the zirconium metal exceeds the solubility limit, zirconium hydrides are formed. The zirconium hydrides usually form in relatively flat platelets between the grains of the zirconium alloy. These platelets appear as black lamellae in Figs 3.2, 3.4 and 3.5. In general, the amount of hydrides in the cladding increases with burnup such that the cladding of higher burnup (HBU)[10] fuel will have more hydrides than for lower burnup fuel. Depending on the size, distribution, and orientation, these hydrides can embrittle the cladding to a greater or lesser degree and reduce its ductility. Furthermore, the presence of hydrides can facilitate propagation of cracks if the hydrides are aligned radially, perpendicular to the tensile stress field, as some of the hydrides are in the right photo of Fig. 3.5. The potential for reorientation of some zirconium hydrides from the initial circumferential direction (left-hand photo in Fig. 3.5) into the radial direction (right-hand photo in Fig. 3.5) increases with increasing burnup, cladding hoop stress and temperature. These

[10] High burnup (HBU) is generally considered to be burnup levels exceeding 45 GWd/t(HM).

conditions may be enough to cause hydride reorientation. Since zirconium hydrides are relatively brittle, a large amount of these hydrides oriented in the radial direction would make the cladding more susceptible to cracking if mechanically stressed, such as would occur during SNF transportation. A detailed discussion of the effects of hydride reorientation is provided in [3.5].

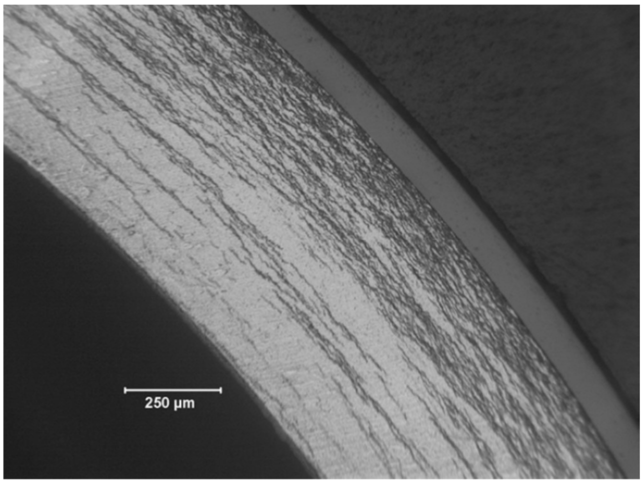

FIG. 3.4. Typical appearance of HBU fuel. Top right: outer corrosion layer. The black lamellae in the zirconium metal are zirconium hydrides (reproduced courtesy of Elsevier) [3.6].

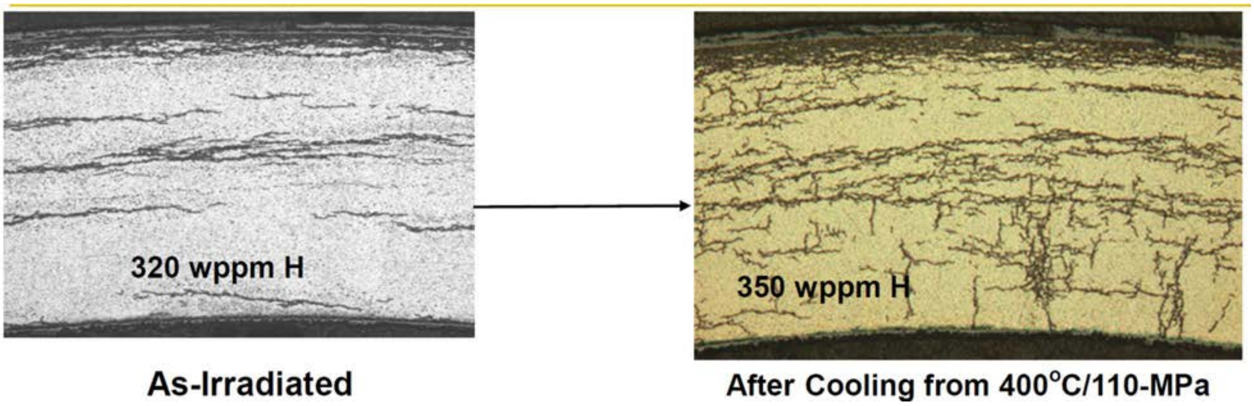

FIG. 3.5. Metallography showing hydride reorientation after cooling under hoop stress in the cladding (reproduced courtesy of US DOE) [3.7].

Although comprehensive experimental and modelling programs have been performed both with fresh (pre-hydrided) and irradiated cladding, the hydride reorientation requires additional studies. The results obtained in limiting conditions of temperature and hoop stress indicate that hydride reorientation and cladding embrittlement may still be an issue, but when more realistic conditions are examined it appears that the associated risks may be less than previously thought.

Some HBU fuel cladding is characterized by an increased outer corrosion layer, larger amounts of hydrogen precipitated into zirconium hydrides, a dense hydride rim and a radiation-hardened zirconium-alloy cladding (Fig. 3.4). Hence, burnup is a factor for the hydrogen effects in the cladding. HBU fuel has higher decay heat, higher rod internal pressure, and higher hydrogen content than low burnup fuel. Therefore, HBU fuel is more susceptible to radial hydride formation, and the difference has been reflected in the applicable regulations.

As shown in Fig. 3.4, hydrides precipitate preferentially near the outer surface of cladding because the outer cladding surface is at a lower temperature than the rest of the cladding material. The hydrogen precipitation near the surface can be enhanced if there is a thermal gradient created by oxide spallation. In this case, the spalled area becomes a cold spot in the cladding, enhancing hydrogen migration to that zone and hydride precipitation. In some instances, a hydride blister containing high concentration of hydrides can be created in the outer cladding surface, as shown in Fig. 3.2. These blisters are essentially brittle and may jeopardize the capability of the cladding to withstand the loads associated to drying, storage and transportation.

As stated in prior paragraphs, the mechanical properties of the irradiated cladding material after a long storage period are affected by different mechanisms, mostly related to the effect of the presence of hydrogen. This may especially be true for HBU fuel, though it is important to note that even if a material is considered brittle, a sufficiently large load must still be applied to result in failure. The mechanical loads associated with normal transportation (i.e. vibration and shock impacts), have recently been determined through tests and analysis, and the results show that HBU fuel cladding would likely not fail due to stresses caused by normal conditions of transport [3.8]. Additional work in this field is reported in Subsection 7.2.3 of this TECDOC.

The hypothetical transportation accident conditions (as well as hypothetical cask drops during handling in storage) are the most demanding scenarios for irradiated fuel from this perspective. Dynamic mechanical modelling, and laboratory and field measurements of cladding stresses have been conducted for many years. Nevertheless, there is still room for improvement in both the existing database and the accuracy of the models.

3.1.2. Fuel drying

Fuel drying is a key process that may contribute to the detrimental effect of hydrogen on the cladding mechanical properties. As already described, cladding hydrides are typically observed to be oriented in the circumferential direction after in-reactor operation. Some of the hydrogen dissolved during fuel drying at high temperature will precipitate as the temperature drops during storage. As the cladding is subject to a circumferential hoop stress during cooling due to the rod internal pressure, at least part of the precipitated hydrides will be oriented radially, contributing to cladding embrittlement if temperatures are low enough to precipitate a sufficient amount of hydrogen in the radial direction. The low temperature threshold for embrittlement due to radial hydrides has been found to be dependent on the cladding material and several other factors, and it is usually termed as ductile-to-brittle transition temperature (DBTT). However, this term is misleading, because the physical process is different from the ductile-to-brittle transition affecting the metallic materials.

The relevant parameters for potential hydride reorientation to the radial direction followed by transition from ductile-to-brittle behaviour are: the initial hydrogen content in the cladding material, the maximum cladding temperature during drying, the minimum temperatures reached during storage and the cladding hoop stress during cooling. Investigation programmes have been and are being performed, both with irradiated and fresh pre-hydrided cladding material, to understand the cladding behaviour in the long term, simulating the mechanisms involved under temperature and loading conditions (pressure/stress, static/dynamic) representative of fuel drying, long term storage and subsequent transportation phases. However, the behaviour and relevance of the parameters governing the process have not been well established yet, and additional experimental work might be necessary.

For the time being, the regulations applicable in the different countries define limits in the maximum cladding temperature during drying and in the acceptable cladding hoop stress, in order to reduce the potential for radial hydride formation causing embrittlement and loss of ductility. This is, for instance, the case of Interim Staff Guidance 11 [3.9] of the US Nuclear Regulatory Commission (US NRC).

The water remaining in the cask cavity after the drying process may lead to cladding oxidation during storage, and hence this is a factor to take into account in order to avoid fuel degradation during long term storage. Although this issue is considered to be of secondary importance, little information on this matter is currently available.

3.1.3. Delayed hydride cracking

DHC is a crack growth mechanism occurring in zirconium alloys as well as other hydride-forming materials that requires the formation of brittle hydrides at the tip of a crack and subsequent failure of that hydride resulting in crack extension. Hydrogen in solution in the zirconium alloy is transported to the crack tip by diffusion processes where it precipitates as a hydride phase. If the precipitate attains a critical condition, related to its size and the applied stress intensity factor, fracture ensues and the crack extends through the brittle hydride and arrests in the matrix. Each step of crack propagation results in crack extension by a distance approximately the length of the hydride.

The velocity of the crack propagation has been found to have a strong temperature dependence, which reflects both the rate at which hydrogen in solution can be transported to the crack tip and the amount of hydride required to be formed for each fracture step in the propagation. Because the diffusion coefficient and the maximum amount of hydrogen available to be transported are both thermally activated phenomena, the crack velocity has the temperature dependence of a thermally activated process, decreasing with decreasing temperature.

3.1.4. Cladding creep

Cladding creep outwards of the fuel rod is the deformation of the cladding material due to stress. Hoop stress in the cladding, which is due to the differential pressure across the fuel rod cladding during storage, is the primary driving force for cladding creep, but creep also increases with temperature. The internal gas pressure is due primarily to the initial helium fill gas and, to a lesser extent, to the fission gas released from the fuel into the fuel rod gas space. This internal pressure is not countered by any external pressure on the rod, and the pressure difference is highest during fuel drying. Cladding rupture may occur during fuel drying when hoop stresses and cladding temperature are sufficiently high.

During the years in dry storage, the fuel rod temperature tends to decrease following the decay heat evolution with time, and the internal fuel rod pressure generally decreases because of larger volume available inside the fuel rod due to creep and the decaying temperature (although gas release from the fuel could increase pressures somewhat in specific cases). Consequently, over time the cladding hoop stress decreases, which in turn will decrease the creep rate, the total creep, and the potential for gross cladding rupture if a small breach occurs.

3.1.5. Stress corrosion cracking

During irradiation of the fuel in the reactor, cracks are generated in the interior surface of the cladding because of fuel-pellet-to-cladding thermomechanical interaction. These incipient cracks may propagate due to stress corrosion, by a combination of volatile-fission-product chemistry (e.g. iodine) and large tensile hoop stresses. The propagation of such cracks may result in effective increases in hoop stress, which would accelerate cladding-creep rupture. The mechanism of crack propagation due to stress corrosion is schematically shown in Fig. 3.3. The figure shows a typical stress corrosion crack in the cladding facilitated by a thermally-cracked pellet providing a pathway for fission gases and a non-circular pellet shape because of chipping during fabrication. The stresses that help initiate corrosion cracking arise from the phenomenon of pellet-cladding interaction in which pellet swelling tends to close the pellet-cladding gap and increases the cladding stresses.

3.1.6. Fuel pellet oxidation

Oxidation of UO_2 in air is a concern for SNF management. In case of a loss of cladding integrity (such as a pinhole or hairline cracks) in an air atmosphere, the UO_2 oxidizes to some intermediate oxide species and the end of the oxidation process is the production of U_3O_8. This uranium oxide is less dense than UO_2. Hence, the fuel will swell because of the oxidation process, and swelling may help propagate the original cladding defect (cladding unzipping). In case oxygen is present during SNF handling or storage, the cladding failure due to oxidation could affect the retrievability, confinement, radiation shielding and subcriticality safety functions.

Furthermore, the transformation of UO_2 to U_3O_8 destroys the ceramic structure of the pellet, reducing the material to a grain-size very fine powder. This may result in additional fission gas release to the atmosphere and production of a higher amount of fine particulates of fuel available for dispersal.

For fuel oxidation to occur, an oxidizing environment must be present. This can happen if the fuel with the cladding defect is handled in dry facilities in a non-inert atmosphere or if air can enter the cask cavity or the hot cell where the cask is located. An oxidizing environment could also be present if a certain amount of residual water was left in the cask after drying. The water could then undergo radiolysis and form hydrogen, oxygen and other oxidizing species, which may be sufficient to provide the oxidizing environment for the fuel in case there is a crack in the cladding.

The rate of air oxidation of UO_2 fuel depends on several factors, including fuel temperature, burnup, oxygen concentration in air, air humidity and nitrogen contents among others. A rather extensive review of the information available on the sensitivity of the oxidation rate to the different parameters can be found in [3.10, 3.11].

3.2. CRP CONTRIBUTORS SCOPE AND OUTCOME

3.2.1. Outcome of work at Centro Atómico Constituyentes (CAC), Argentina

The objective of this contribution is the analysis of the potential ageing degradation mechanisms for very long term (more than 100 years) of Atucha 1 spent fuel, in relation with its transport from storage pool to a dry storage facility. Atucha 1 is a pressurized heavy water reactor (PHWR) using slightly enriched uranium oxide fuel with Zircaloy-4 cladding. In addition, other important aspects related to the performance of the facility in this timeframe have been addressed within this CRP, as ageing degradation of concrete structures (see Chapter 4).

The activities in this contribution carried out during the development of the CRP include a bibliographic state-of-the-art review on SNF Zircaloy-4 cladding ageing degradation mechanisms, as well as experimental work aimed at filling the identified gaps.

The review of the information available has pointed out several scientific issues, such as cladding oxidation, creep, SCC and hydrogen effects (embrittlement, DHC, generation and properties of hydride blisters). The outcome of this review has provided the basis to conclude, among other things, that SCC and DHC will not occur in the conditions present in the dry storage concept of Atucha NPP. Likewise, cladding creep can also be excluded given the 200°C maximum cladding temperature allowed in the fuel storage. It is deemed that the temperature condition for thermal creep is to be higher than 0.3 of the melting point (0.3 × the melting point temperature in kelvin), which would be ~360°C for steady state creep. The closest available experimental data indicate that the deformation level at 200°C will not reach 1%.

SCC will not occur in the specific conditions of the Atucha NPP storage concept: temperature and tensile stresses would not be high enough to allow for crack initiation in intact Atucha fuel assemblies. For those assemblies with defects, an analysis of the stress intensity factor limit for SCC and fracture toughness of the material value to 200°C leads to the conclusion that concern about the SCC mechanism can be discarded: the tube would burst before a crack could propagate (see AGR 173–9 - Annex II).

Additional laboratory work has been performed regarding the cladding conditions needed for hydride reorientation to the radial direction. Conclusions obtained regarding hydride reorientation are the following:

- Cladding embrittlement due to hydrogen is relevant only if radial hydrides are formed;
- Hydrides precipitated in the circumferential direction do not lead to a ductility reduction if the average hydrogen concentration in the cladding is below 700 ppm;
- The cladding hoop stress needed to reorient hydrides in Zircaloy-4 is above 100 MPa.

Experimental work has been carried out to study the impact of hydride blisters on the mechanical properties of the cladding. Blisters have been artificially generated (see Fig. 3.6) in as-received (unirradiated) cladding material by cathodic charging up to 250 ppm of hydrogen. A cold spot in the cladding promotes hydrogen migration and massive precipitation, mimicking the conditions in which blisters are generated during the fuel in-reactor operation. Afterwards, hydride reorientation testing at different hoop stresses have been performed in some specimens. Only part of this work has been completed during the CRP, while the remaining studies are still being performed, and will continue beyond the reach of the CRP.

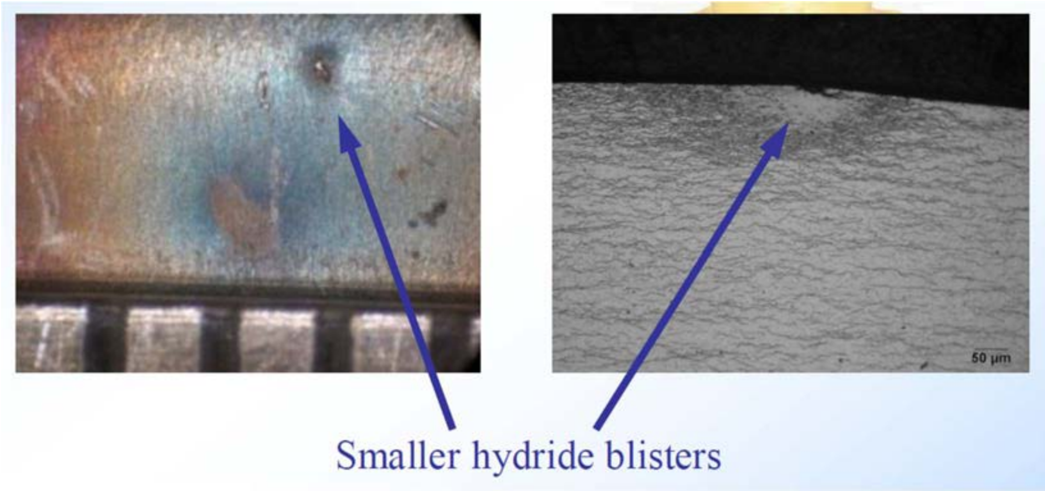

FIG. 3.6. Artificially generated blisters (reproduced courtesy of Centro Atómico Constituyentes (CAC)).

3.2.2. Outcome of work at Orano TN, France

This contribution briefly describes three research activities related to SNF performed by Orano TN[11], in France, with the general objective of investigating basic fuel behaviour properties in dry storage systems and gathering data on dry storage environment and cask materials in order to evaluate long term behaviour of cask materials.

Prediction of very long term performance of spent fuel

This first activity is supported by the PRECCI project contribution, a collaboration between CEA, EDF, Orano and ANDRA to investigate ageing degradation of SNF, including HBU fuel and containment issues. This project covers a broad scope, from fuel in-reactor behaviour, SNF wet and dry storage issues, to SNF transport and deep geological disposal. SNF performance is studied, especially with regard to the preservation of the retrievability safety function and of the fuel rod cladding integrity.

Although the operational experience tends to show that there is no cladding embrittlement even for HBU, the work performed has determined that:

- Hydride embrittlement might occur during dry storage due to hydride reorientation, and if so;
- DBTT for transportation of HBU fuel is the most relevant issue needing further work (Table 3.2).

The activities of Orano within the US Department of Energy (US DOE) SNF Storage Demonstration Program to determine long term fuel performance are described in this contribution. The Orano design TN-32B cask is being used for this demonstration, which is described in Chapter 7 of this TECDOC.

[11] Orano TN was formerly AREVA TN International.

Evaluation of the effect of drying and storage on safety during subsequent normal conditions of transport

This second activity focuses on the gas pressure and composition in the cask cavity during extended storage and their effect on the SNF cladding behaviour. This contribution includes a number of different ongoing activities:

- Development of mitigation systems for hydrogen scavenging in storage casks;
- Investigation of adequate drying methods and controls before shipment, based on the cask cavity atmosphere sampling performed at La Hague reprocessing plant upon cask arrival [3.12]. Sampling includes moisture measurements, as well as checks of the presence of some individual isotopes (oxygen, hydrogen and noble gases). The work includes drying tests to investigate the drying systems performance, i.e. how much residual water remains in the cavity after the drying process;
- Development of models to assess SNF behaviour during long dry storage period, including the influence of irradiation recovery in radially hydrided cladding.

Accidental conditions of transport

This third activity is supported by the Fuel Integrity Project (FIP), a joint programme developed by Orano[12] (France) and INS (UK) for the assessment of the fuel mechanical behaviour in impact (hypothetical transport accident) and for the confirmation of safety-criticality studies assumptions. The project includes experimental work with irradiated samples up to 40–50 GWd/t(HM) and analytical work for the development of models. A new methodology has been finalized for the assessment of the SNF in impact and criticality safety of transportation packages during regulatory drop axial or lateral accidents, showing different levels of deformation. Measurements of the amount of fuel material dispersed in case of cladding rupture have been performed, finding that the quantity is limited to a few grams. The methodology allows for determination of the maximum allowable acceleration for a fuel assembly in case of a hypothetical transport accident.

3.2.3. Outcome of work at the JRC Directorate for Nuclear Safety and Security of the European Commission

This contribution was done by the JRC Directorate for Nuclear Safety and Security of the European Commission[13]. This contribution evaluates the degradation of SNF associated with long term storage, and in particular, the ability of fuel rods to withstand handling and transportation after long term storage by means of post-irradiation examinations combined with separate effect studies.

Previous studies on SNF extended storage basic properties focused on the cumulative effects of alpha-decay damage and helium accumulation and are complemented in this contribution by integral macroscopic SNF rod characterization aimed at determining safety-relevant aspects which would affect the behaviour during off-normal and accident conditions.

---

[12] Orano was formerly AREVA.

[13] JRC Directorate for Nuclear Safety and Security of the European Commission was formerly ITU-JRC.

A new and improved impact load device was built for hot cell testing of SNF rodlets and was used to perform the new campaign of measurements. The new setup can provide special impact modes (e.g. vibration not causing fracture) and is used in this new SNF testing campaign to extend and deepen the characterization of the SNF rod response to impact loads. The behaviour of the hydrides in the cladding is also assessed, and the impact tests are combined with thermal treatments reproducing conditions representative of various stages of the SNF rod history after discharge from the reactor.

The first impact loading test has been performed on an HBU 67 GWd/t(HM) rodlet (Westinghouse duplex alloy, hydrogen concentration of 300 wt. ppm), under simulated pinch load conditions associated with accident scenarios, to study fracturing behaviour and fuel dispersion (see Fig. 3.7). Macroscopic and microstructure properties of the irradiated fuel and the cladding are studied and compared before and after the tests. The amount and particle size distribution of the fuel released during the impact tests are characterized, together with the fracture surfaces of the fuel and cladding.

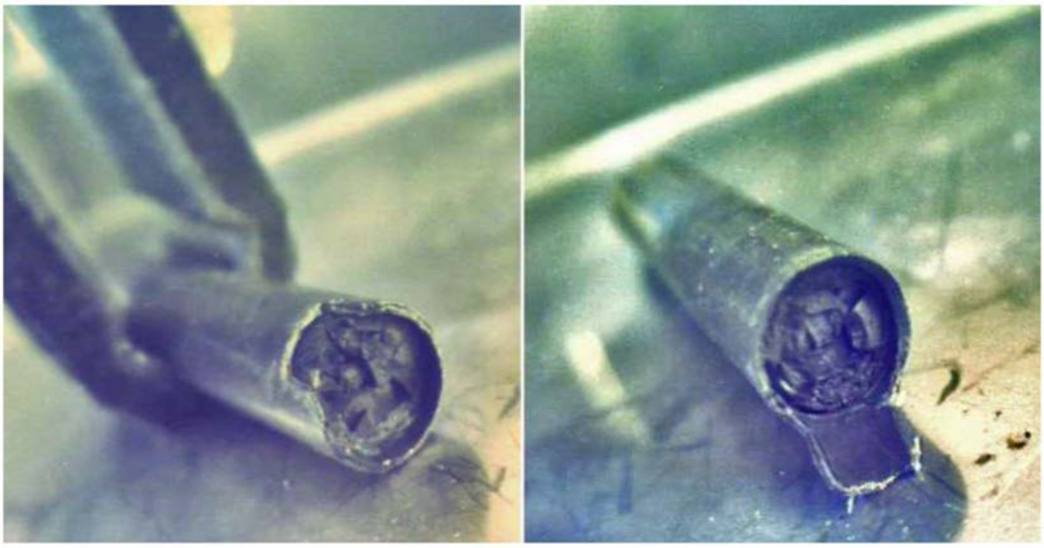

FIG. 3.7. Fragments of the 67 GWd/t(HM) PWR fuel rodlet after the impact test; corresponding surfaces of the central fracture are shown [3.13].

During the time span of this CRP, the preparation work for the investigations described above and for the initial hot cell testing was performed. The analysis of the experimental results which were performed during the reporting period is still ongoing.

3.2.4. Outcome of work at Centro de Investigaciones Energéticas Medioambientales y Tecnológicas (CIEMAT), Spain

This contribution studies the potential degradation of the SNF cladding due to the corrosion under dry storage conditions exposed to an environment with a low concentration of oxygen. The oxygen reacts directly with the cladding or with exposed UO_2 pellets if cladding breaches are present. The results obtained in this contribution so far are focused on the design and development of different characterization techniques and systems for monitoring the cladding degradation through one of two possible ways:

- Cladding oxidation due to direct reaction with oxygen present in the cask cavity gas. This would lead to the thinning of the remaining cladding;

– Cladding degradation due to oxidation of UO_2 fuel to U_3O_8, which has a higher specific volume than UO_2, followed by axial splitting of the cladding.

Regarding these two mechanisms, CIEMAT conducted the following work:

- Cladding oxidation due to direct oxygen reaction:
  – Sample preparation: CIEMAT used as-received (unirradiated) cladding material that was hydrided by cathodic charging. Following hydriding, a thermal treatment was applied to reach a homogeneous hydride distribution. Mechanical polishing and chemical etching were then performed to reveal the hydride distributions. The final average hydrogen concentration obtained was 250 wt. ppm;
  – Sample characterization:
    - o Experimental methods: a new system for cladding hardness measurements was set-up using a Microindentation Tester, MTR3, which is designed to characterize the surface, the mechanical properties of thin films, and the influence of the substrate and coatings. The MTR3 applies a progressive force at a specific point. Furthermore, during this test, the MTR3 was fitted with an optical microscope, digital video-camera and light source. Samples were also characterized using surface techniques such as scanning electron microscopy (SEM) and X-ray diffraction (XRD);
    - o Results: the microindentation tests were performed using both as-received, un-hydrided and pre-hydrided material for comparison. There was a small increase in hardness for the hydrided samples;
- Cladding splitting due to oxidation of UO_2 fuel:
  – An autoclave was designed and used to expose the simulated SNF to high temperature, high pressure and controlled atmosphere tests simulating dry storage conditions. Demonstration tests were performed with UO_2 which was heated up to 700°C in air;
  – A Raman microspectrometer was used to obtain the material spectra, observing material changes during the sequential oxidation of UO_2 up to the total conversion into U_3O_8. The results were compared with prior thermogravimetric experiments to check consistency.

Based on the tests described above, the ongoing activities involve definition of the SNF matrix test to study oxygen-related degradation mechanisms under dry storage conditions. The second phase is being performed to develop the methods for analysing the proposed material.

3.2.5. Outcome of work at Consejo de Seguridad Nuclear (CSN), Spain

This contribution investigates the mechanical behaviour of highly hydrided cladding material under normal, off-normal and accident conditions during long term dry storage and subsequent transportation. The main goal is to determine the criteria for the SNF cladding integrity under the operating conditions with which to be able to classify SNF as either intact, undamaged or damaged.

This study uses unirradiated cold-worked, stress relieved (CWSR) ZIRLO cladding samples subjected to different experimental techniques to reproduce the material and mechanical properties found in real irradiated, hydride-embrittled cladding. Specific experimental devices were designed and fabricated in the framework of this project (Fig. 3.8).

The following treatments were applied to the unirradiated samples:

- Hydrogen charging up to average concentrations of 2000 wt. ppm using the cathodic charging technique;
- Generation of a uniform circumferential hydride distribution using an adequate thermal treatment;
- Hydride reorientation by thermo-mechanical treatment to dissolve and reorient part of the hydrides along the radial direction of the cladding, under a range of hoop stress and temperature conditions.

Samples reoriented under hoop stresses up to 140 MPa are subject to ring compression tests (RCTs) performed at different temperatures (20ºC, 135ºC and 300ºC) and using loading rates representative of storage conditions (low loading rates: 0.5 mm/min, 100 mm/min and 1000 mm/min) and transportation (high loading rates: 3 m/s). The tests results, in terms of load/displacement curves for each sample condition, complemented by metallographic and fractographic post-test examinations, allow the characterization of the cladding material under each condition.

FIG. 3.8. Furnace and ring compression test devices at UPM (reproduced courtesy of UPM).

Analytical activities have been conducted in parallel with the laboratory work. Numerical simulations of the experiments are focused on the development and improvement of a methodology to define failure criteria and to obtain fracture energy data from RCTs testing results.

From the simulation and analysis of the results, it can be concluded that:

At low loading rates representative of storage conditions:

- For samples containing circumferential hydrides only, the material is always ductile, even for hydrogen contents as high as 2000 wt. ppm and 20°C;

– For samples containing radial hydrides, the key parameters driving the ductile-to-brittle transition temperature (DBTT) process are the hydrogen content, the fraction of hydrides reoriented (which is in turn a function of hoop stress), and temperature. Some unstable failures have been observed for small displacement values (δ<1 mm) at 20°C and 135°C. Overall, the results demonstrate the following:
    - At low temperatures (20°C), brittle failure is obtained if the reorientation stress is above 90 MPa regardless of the hydrogen concentration (between 150 and 2000 ppm);
    - At 135°C, the transition from ductile-to-brittle behaviour occurs if the reorientation stress is on the order of 120 MPa and the hydrogen concentration is low (150 ppm);
    - Ductile behaviour is always observed if the reorientation hoop stress is 90 MPa or less, and always observed for higher sample temperatures.

At high loading rate (3 m/s) representative of transportation conditions, ductile behaviour was observed for low hydrogen concentration (0–500 ppm) samples in all the temperature range (20–300°C).

Taking into account the parameters used and the results obtained from the numerical simulations of the experiments, the contributors propose two new failure criteria that provide consistent results and a clear limit between ductile and brittle behaviour:

- Based on strain energy density (SED): SED at maximum loads higher than 25 N/mm^2;
- Based on an equivalent plastic strain (EPS) criterion: EPS higher than 3%.

3.2.6. Outcome of work at US Nuclear Regulatory Commission (US NRC), USA

This contribution presents a review of work performed in the USA. It addresses different knowledge gaps and CRP objectives.

Thermal analysis

Once a sufficient knowledge of the DBTT values for the entire, applicable range of controlling parameters is acquired in due course, the capability to perform an accurate calculation of the highest and the lowest cladding temperatures during long term storage is crucial to evaluate the cladding integrity in postulated scenarios involving mechanical stresses on cladding. An independent computational analysis has been performed to predict the thermal behaviour of dry cask storage systems for periods of up to 300 years [3.14]. Three-dimensional (3D) numerical simulations were performed using computational fluid dynamics (CFD) methods to model the temperature distribution in and around horizontal storage modules (see Fig. 3.9 for an example of a horizontal storage module). A baseline model was developed, and the temperature values calculated were compared with available measured data. The computational model was then used to predict the thermal behaviour of the dry storage modules over 300 years of storage.

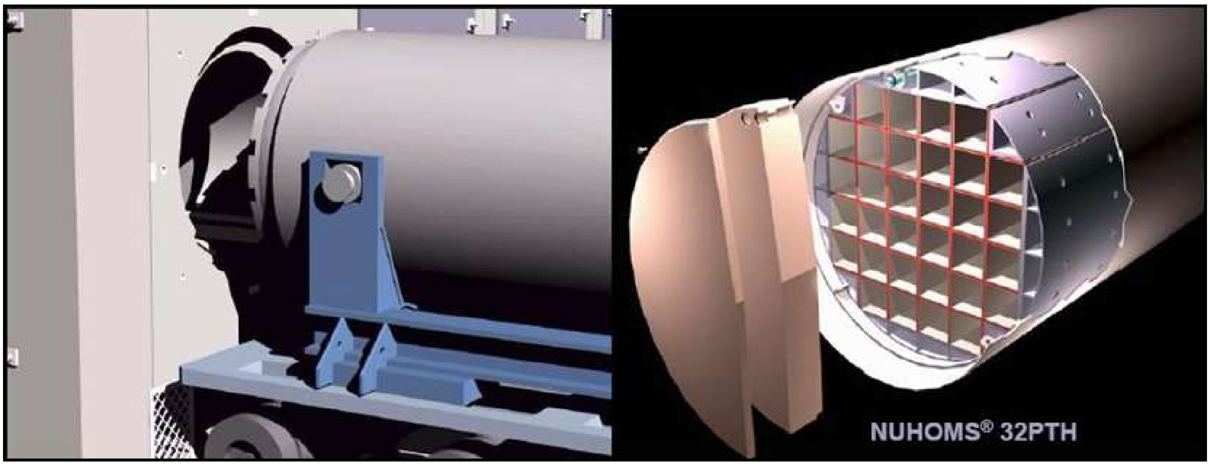

(a) (b)

FIG. 3.9. (a) NUHOMS horizontal storage module, transfer trailer (reproduced courtesy of TN Americas); (b) NUHOMS 32PTH dry shielded canister (reproduced courtesy of TN Americas).

Vacuum drying

Water remaining in the canister after fuel loading at the pool could cause corrosion of the fuel cladding and internal structures or may create a flammable environment within the canister if radiolysis creates free oxygen and hydrogen. Applicable US guidance require less than 0.25 volume percent oxidizing gasses remain in the canister. To provide additional confidence in this criterion, a plan for measuring the quantity of unbound residual water remaining in a canister following vacuum drying was developed.

The typical vacuum drying systems and operational procedures were described in a report [3.15]. This report is intended to provide technical background for a test programme to measure the quantity of unbound residual water in SNF dry storage canisters dried to the criterion recommended in NUREG–1536 [3.16]. The main chapters of this report address the design and operation of systems currently used by industry for vacuum drying, the characteristics of fuel assemblies or canisters that could affect the quantity of residual water, and the measurement concepts that could be employed for the test programme. Information on current industry drying practices was gathered by reviewing safety analysis reports and operational procedures, as well as by visiting vendors who perform vacuum drying services in the industry. Fuel assembly and canister designs were reviewed to identify locations where water could be trapped or difficult to remove during drying.

Cladding stress

The objective is to assess the potential for low temperature creep and DHC failures in HBU SNF cladding during extended dry storage, using a modified version of the US NRC's steady state fuel performance code FRAPCON. FRAPCON calculations were performed to predict cladding creep and the resulting stresses and strains during 300 years of storage. Fuel pellet swelling, as well as decay gas production and release during storage, were taken into account to produce the cladding stress predictions.

Fatigue fracture

The high burnup of nuclear fuel entails hydride precipitation, as well as high levels of irradiation-induced damage to cladding and fuel pellets. Each of these phenomena has an effect on the mechanical behaviour of SNF. HBF rods were tested in this contribution under static and dynamic loading conditions, including both static and cyclic tests, and the results of these tests were compared to the results of tests for defueled rod specimens.

3.3. SUMMARY AND OUTCOMES REFLECTING DATA GAPS FOR LONG TERM STORAGE

The long term performance of the fuel cladding during dry storage and transportation in casks is a very relevant issue, as it provides an additional safe enclosure of the radioactive inventory. The cladding also contributes to maintaining the fuel geometry assumed in the safety cases, under both normal and accident conditions of storage and subsequent transportation. An accurate prediction of the cladding behaviour is key to provide an adequate demonstration of the fuel safety functions fulfilment in the long term.

An issue of concern is the potential loss of ductility of the cladding during storage. Hydrogen dissolved during fuel drying at high temperature will precipitate as the temperature drops during storage. As the cladding is subject to a circumferential (hoop) stress, at least part of the precipitated hydrides will be oriented radially, contributing to cladding embrittlement if temperatures are sufficiently low. Relevant parameters for this phenomenon are the cladding temperature, mainly governed by the decay time, cladding stresses and hydrogen contents. Investigation programmes have been performed, both with irradiated and fresh, pre-hydrided cladding material, to understand the cladding behaviour in the long term, simulating alteration mechanisms under temperature and loading conditions (pressure/stress, static/dynamic) representative of fuel drying, long term storage and subsequent transportation phases.

The majority of the research contributions for fuel rod behaviour have addressed the different effects of the hydrogen accumulated in the cladding during in-reactor operation on the cladding mechanical properties. This fact reflects the importance given to this issue in relation with the preservation of cladding integrity during extended storage and subsequent transportation.

The results obtained identify that hydride reorientation and high hydrogen contents are the major issues needing further research, as they can be the source of cladding failure when subject to high mechanical loads associated with off-normal and accident conditions of fuel storage and transportation. The additional information needed includes the identification of the conditions leading to cladding failure for the set of parameters that define the hydrogen behaviour and hydride formation, such as hydrogen concentration, cladding temperature and cladding stresses for the different cladding alloys currently in operation.

The contributions received seem to indicate that the remaining hydrogen effects, as well as other cladding failure mechanisms, are considered to have a lower impact on cladding integrity. This is the case of the results provided for long term cladding creep or DHC.

Some contributions have produced valuable information on the behaviour of fuel pellet oxidation in air. While the fuel loaded in dry cask is in an inert atmosphere, later phases of the SNF management cycle may include fuel unloading for repackaging, and the guarantee of an inert atmosphere in the repackaging facilities may be difficult to obtain. Still, a more systematic analysis of the impact on the oxidation rate of relevant parameters such as temperature, burnup, enrichment and oxygen concentration in the atmosphere would be desirable.

REFERENCES TO CHAPTER 3

[3.1] INTERNATIONAL ATOMIC ENERGY AGENCY, Behaviour of Spent Fuel During Storage, Extracts from The Final Reports of Coordinated Research Projects on Behaviour of Spent Fuel Assemblies in Storage (BEFAST I–III) and Spent Fuel Performance Assessment and Research (SPAR I–III) 1981–2014, IAEA-TECDOC-1862, IAEA, Vienna (2019).

[3.2] ELECTRIC POWER RESEARCH INSTITUTE, Extended Storage Collaboration Program International Subcommittee Report: International Perspectives on Technical Data Gaps Associated with Extended Storage and Transportation of Used Nuclear Fuel, Rep. 1026481, EPRI, CA (2012).

[3.3] RAYNAUD, P. A., et al. "Influence of hydride microstructure on through-thickness crack growth in Zircaloy-4 sheet", 13th International Conference on Environmental Degradation of Materials in Nuclear Power Systems (Proc. Int. Conf. Whistler, 2007), Canadian Nuclear Society, Toronto (2007).

[3.4] RIGBY, D.B., Evaluation of the Technical Basis for Extended Dry Storage and Transportation of Used Nuclear Fuel, U.S. Nuclear Waste Technical Review Board, VA (2010).

[3.5] INTERNATIONAL ATOMIC ENERGY AGENCY, Spent Fuel Performance Assessment and Research, Final Report of a Coordinated Research Project on Spent Fuel Performance Assessment and Research (SPAR-III) 2009–2014, IAEA-TECDOC-1771, IAEA, Vienna (2015).

[3.6] BILLONE, M.C., BURTSEVA, T.A., EINZIGER, R.E., Ductile-to-brittle transition temperature for high-burnup cladding alloys exposed to simulated drying-storage conditions, Journal of Nuclear Materials 433 (2013) 431–448.

[3.7] BILLONE, M.C., "Update on testing to evaluate radial hydrides", paper presented at 2016 U.S. Nuclear Waste Technical Review Board, Knoxville, TN (2016).

[3.8] WANG, J.-A., WANG, H., Mechanical Fatigue Testing of High-Burnup Fuel for Transportation Applications, Rep. NUREG/CR-7198, Rev. 1, ORNL/TM-2016/689, Nuclear Regulatory Commission, Washington, DC (2017).

[3.9] NUCLEAR REGULATORY COMMISSION, Interim Staff Guidance 11, Rev. 3, Cladding Considerations for the Transportation and Storage of Spent Fuel, USNRC ISG-11, Nuclear Regulatory Commission, Office of Nuclear Material Safety and Safeguards, Spent Fuel Project Office, Washington, DC (2003).

[3.10] McEACHERN, R.J., TAYLOR, P., A review of the oxidation of uranium dioxide at temperatures below 400ºC, Journal of Nuclear Materials 254 (1998) 87–121.

[3.11] UNITED STATES DEPARTMENT OF ENERGY, Commercial Spent Nuclear Fuel Handling in Air Study, Rep. 000-30R-MGR0-00700-000-000, Bechtel SAIC, NV (2005).

[3.12] MORLAES, I., VO VAN, V., ''AREVA solutions for management of defective fuel'', European Nuclear Conference (ENC) 2014 (Proc. Conf. Marseille, 2014), European Nuclear Society, Brussels (2014).

[3.13] RONDINELLA, V.V., PAPAIOANNOU, D., NASYROW, R., Impact test on 67 GWd/tHM LWR spent nuclear fuel rodlet, JRC Technical Report, Joint Research Centre of the European Commission, Brussels (2016).

[3.14] DAS, K., BASU, D., WALTER, G., Thermal Analysis of Horizontal Storage Casks for Extended Storage Applications, Rep. NUREG/CR-7191, Nuclear Regulatory Commission, Washington, DC (2014).

[3.15] MILLER, L., et al., Overview of Vacuum Drying Methods and Factors Affecting the Quantity of Residual Water After Drying, NRC document ML1319A125, Nuclear Regulatory Commission, Washington, DC (2013).
[3.16] NUCLEAR REGULATORY COMMISSION, Standard Review Plan for Spent Fuel Dry Storage Systems at a General License Facility – Final Report, Rep. NUREG-1536, Rev. 1, Office of Nuclear Material Safety and Safeguards, Washington, DC (2010).

4. CONCRETE DEGRADATION IN DRY STORAGE SYSTEMS DURING LONG TERM SPENT FUEL STORAGE

4.1. INTRODUCTION

Dry storage was originally designed to cool down and reduce the radioactive levels from spent nuclear fuel (SNF), so that reprocessing and recovery of valuable fission products can start and as alternative technology to wet storage after the required cooling time of SNF at reactor pools. Current existing dry storage facilities are designed for several decades of operation [4.1] and, among other dry storage systems, concrete casks and vaults have demonstrated to be credible solutions for long term storage of SNF [4.2]. Extending currently licensed storage periods will require licensees and certificate of compliance holders to renew and extend their initial license term. Thus, as part of the revised ageing management programmes, the licensees need to address the potential degradation mechanisms of concrete casks, as well as consider the use of different inspection techniques to detect these mechanisms in order to monitor cask performance throughout this extended period.

There are four different dry storage system designs employing concrete:

(1) Bolted lid cask employing shielding materials in the cask wall (Figs 4.1). In some bolted lid designs, concrete is included in the cask wall;
(2) Steel canisters inside concrete overpacks (horizontal design) (Fig. 4.2);
(3) Steel canisters inside concrete overpacks (vertical design). There are two variants of the vertical design:
    (a) Concrete overpacks exposed to the atmosphere (Fig. 4.3). The exposed concrete surfaces of the concrete cask are coated with a commercial-grade sealant to provide protection to the cask surfaces during current and long term storage operations;
    (b) Concrete overpacks with an outer steel liner (Fig. 4.4);
(4) Concrete vaults (see Figs 4.5 and 4.6 for two examples). This type of storage system uses metal canisters in all-metal silos located inside concrete vaults.

Only types (2), (3)(a) and (3)(b) are considered in this chapter.

FIG. 4.1. Example of a bolted metal storage cask: CONSTOR® (reproduced courtesy of GNS) [4.3].

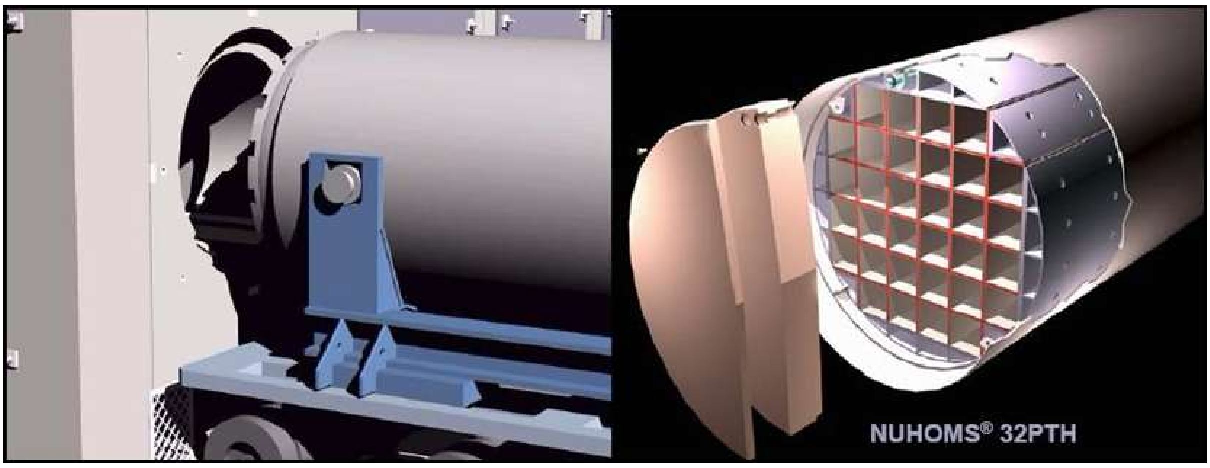

(a) (b)

FIG. 4.2. (a) NUHOMS horizontal storage module, transfer trailer (reproduced courtesy of TN Americas); (b) NUHOMS 32PTH dry shielded canister (reproduced courtesy of TN Americas).

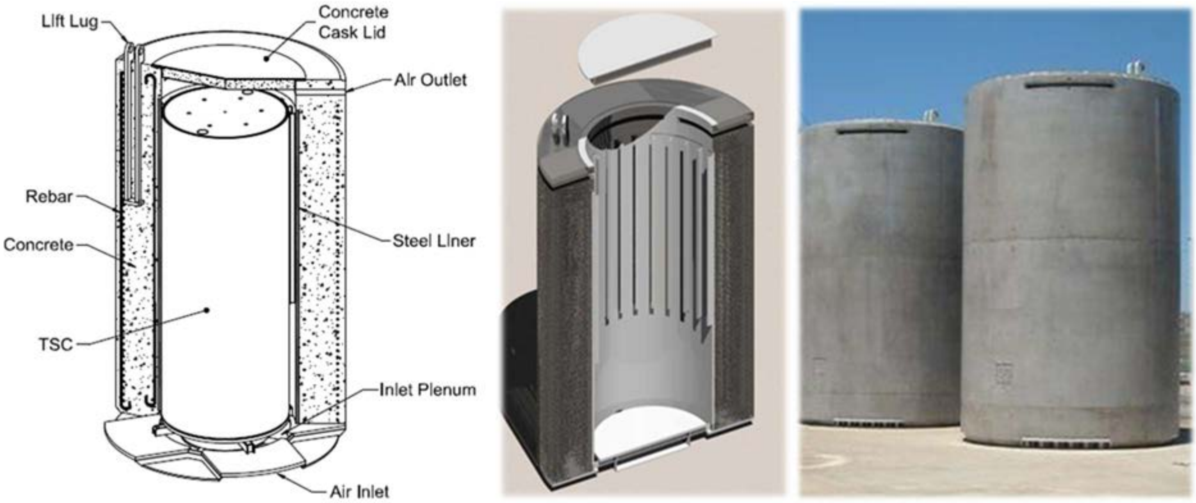

FIG. 4.3. NAC MAGNASTOR system (reproduced courtesy of NAC International) [4.4, 4.5].

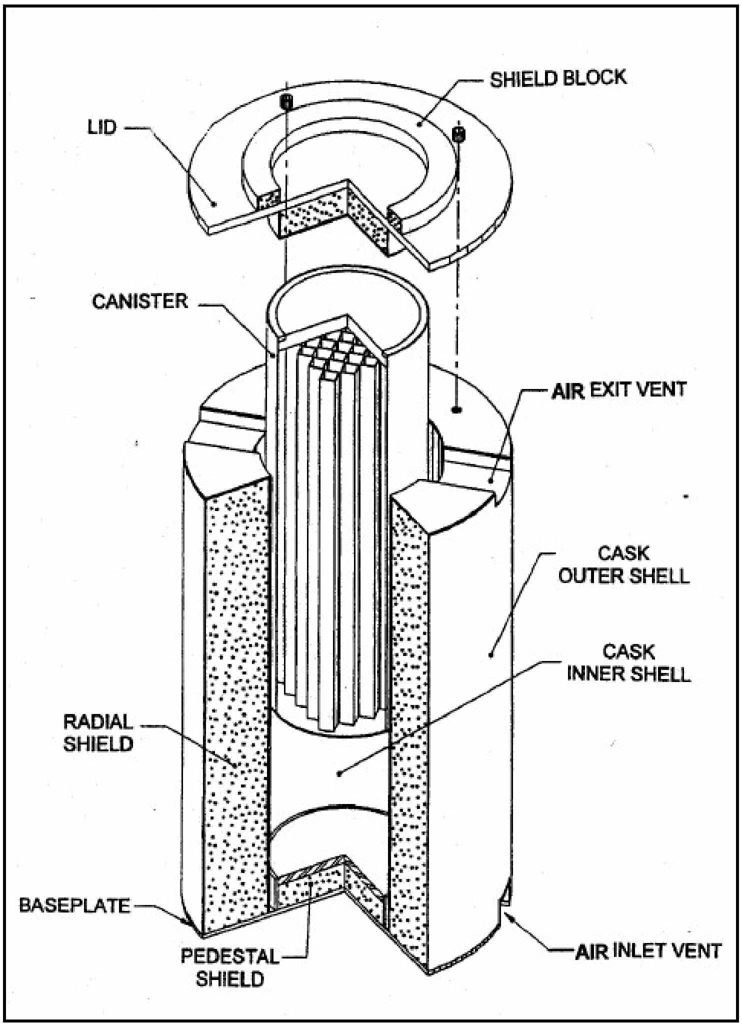

FIG. 4.4. Cross section of the HI-STORM 100 overpack for storage cask (reproduced courtesy of US NRC) [4.6].

FIG. 4.5. Empresa Nacional de Residuos Radiactivos, S.A (ENRESA, Spain) planned vault storage (reproduced courtesy of ENRESA)[4.7].

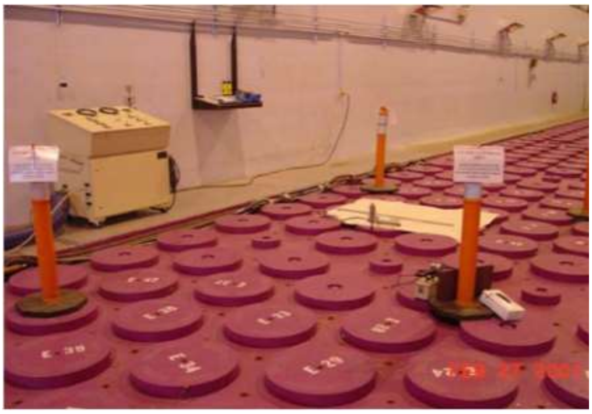

(a) *(b)*

FIG. 4.6. US Department of Energy (US DOE) SNF vault containing SNF from the decommissioned Fort St. Vrain reactor in the US (reproduced courtesy of US DOE) [4.8]: (a) Vault exterior view; (b) Interior charge face.

Concrete overpacks are storage modules that house a horizontal steel fuel container (referred to as a 'canister'). An example of a horizontal design is shown in Fig. 4.7, item 8. Walls are made of reinforced concrete (RC), with front, top and bottom of the vault having thicker walls compared to the sides and back. This is due to the way multiple vaults are positioned next to each other. Main differences between the variations of the NUHOMS® design are their shape, the type of steel rail support structure inside and the location of air inlets and outlets. Outside, air flows through inlets, positioned somewhere along the bottom, and exits through outlets, positioned at the top. This natural airflow helps dissipate heat produced from the radioactive decay of the fuel in the canister.

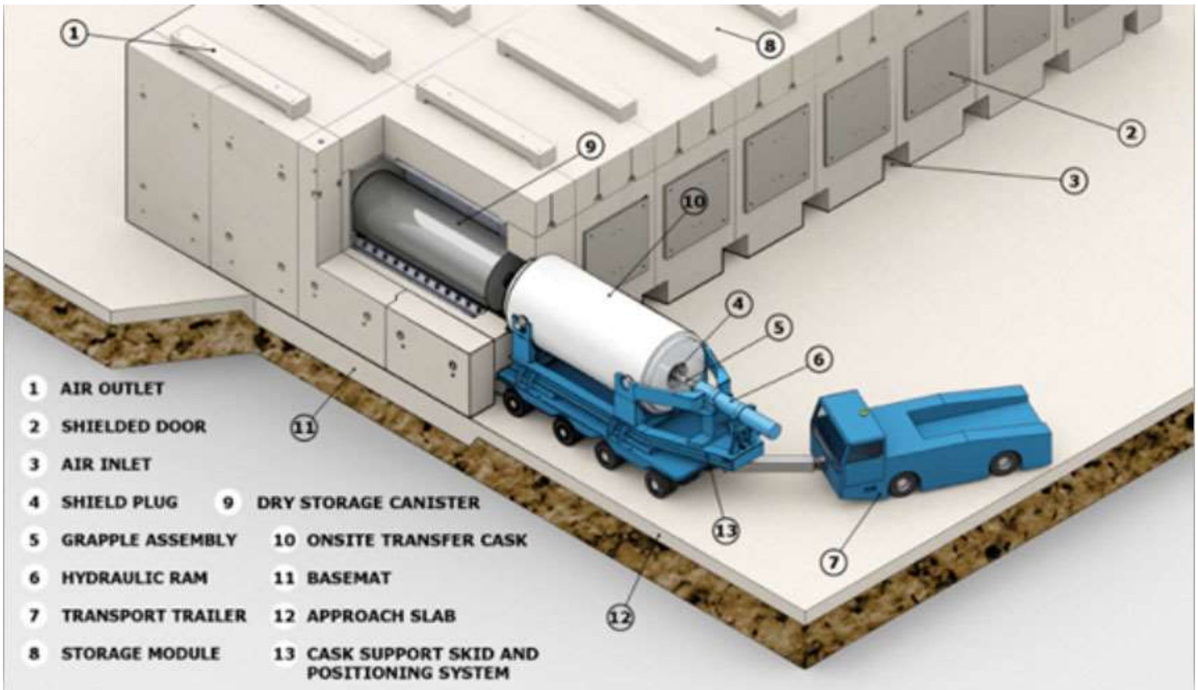

FIG. 4.7. NUHOMS horizontal storage module schematic. Concrete components are part of items 2, 8, 11, and 12 (reproduced courtesy of Orano TN).

Multipurpose canisters (MPC), NAC-UMS® casks, MAGNASTOR® and ventilated storage cask (VSC) are all different designs of vertical RC cylinders, often called ventilated concrete casks. They are made of a thick layer of RC cylinder wall, with inlets at the bottom and outlets at the top. These shafts can be of different shapes and sizes, depending on cask design. The inside of the overpack is covered with a steel liner, which protects the concrete from outside environment. An example of the vertical design is shown in Fig. 4.8.

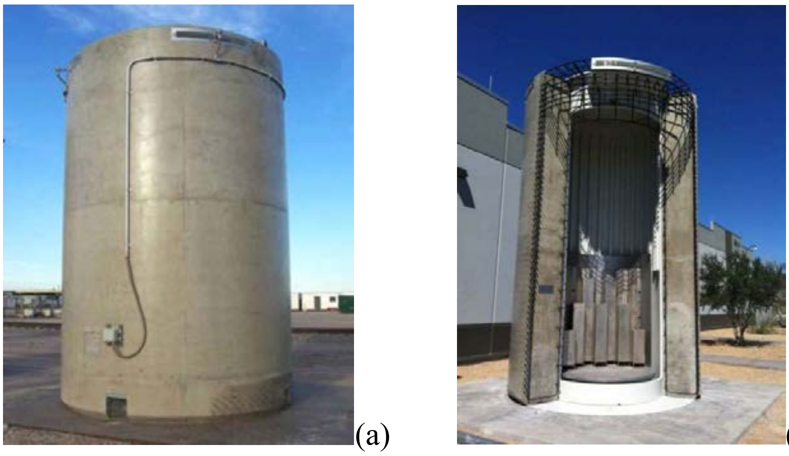

(a) (b)

FIG. 4.8. Vertical RC overpack example (a) UMS ventilated concrete cask (reproduced courtesy of NAC) (b) MAGNASTOR® mock-up at Palo Verde (reproduced courtesy of US DOE).

The third type of concrete casks, such as HI-STORM (Fig. 4.9), are vertical steel-encased concrete cylinders. They consist of steel plates on the inside and outside surfaces of the concrete, and the concrete does not have any embedded reinforcement. The main purpose of the concrete is not to provide structural strength, but radiation shielding. Like in previous designs, cooling is done through natural air convection using inlets and outlets.

(a)

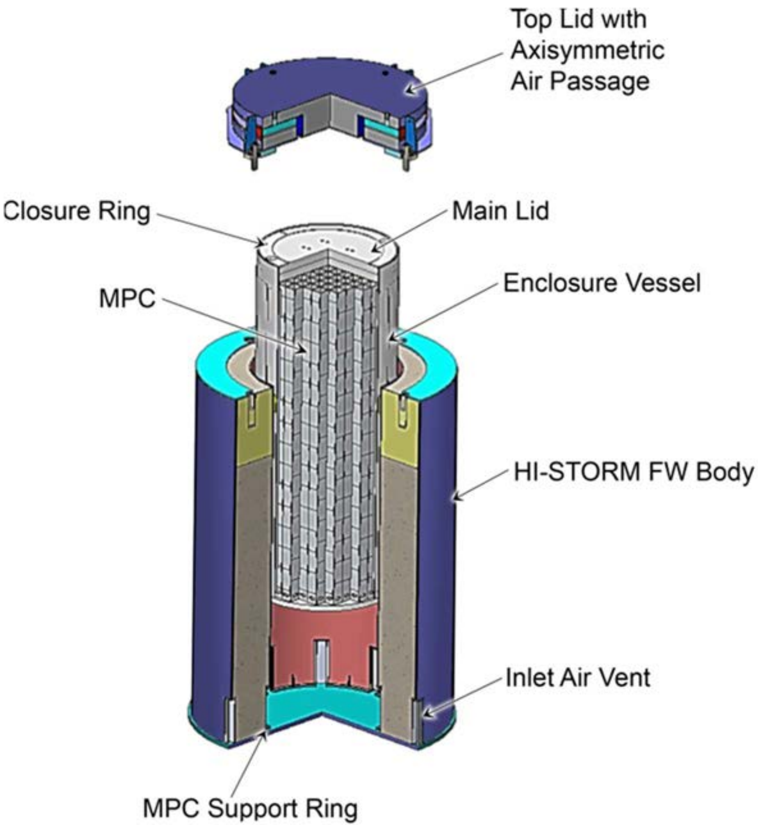

(b)

FIG. 4.9. Vertical steel-encased concrete cask (a) HI-STORMs on Pad (reproduced courtesy of US DOE) (b) HI-STORM schematic (reproduced courtesy of Holtec International).

In addition, almost all storage systems are placed onto concrete pads. The pads are designed with specific structural properties, such as a minimum and maximum strength range, and a minimum and maximum coefficient of static and dynamic friction range.

4.2. DEGRADATION MECHANISMS

The following degradation mechanisms have been identified as potentially harmful to the integrity, stability and durability of concrete casks, vaults, and pads for SNF storage:

- Concrete shrinkage and creep caused by long term dry out;
- Carbonation caused by reaction with CO_2 in the atmosphere;
- Ingress of chlorides via chloride deposition on concrete surfaces and dissolved by rain water;
- Freeze-thaw due to use of concrete in cold environments;
- Alkali-silica reaction (ASR) within the concrete;
- Sulphate attack due to the presence of sulphates inside the concrete and additional sulphates deposited from the environment;
- Effects due to concrete irradiation;
- Thermal degradation;
- Leaching and efflorescence.

Each of these potential degradation mechanisms is described in somewhat more detail in the following subsections.

4.2.1. Drying shrinkage and creep

Hardened cement paste is a porous material that contains physically absorbed water within its pores. If the concrete is exposed to the atmosphere, long term drying of the concrete can occur. As some of the water of hydration that is a fundamental part of the reaction products of concrete curing gets removed over time, the concrete becomes dimensionally unstable and strains. The two main causes for the phenomena are sustained stress and reduction and atmospheric relative humidity. The first results in creep strain, while the second results in drying shrinkage [4.9].

From a durability standpoint, drying shrinkage is the most problematic process. When a structure is restrained, the drying process is unable to deform the concrete, which results in increased tensile stresses. If these stresses are larger than the tensile strength, concrete cracks. This promotes ingress of other deleterious material into concrete. Creep has a favourable effect on restrained structures under sustained load as it causes stress relaxation. This reduces both tensile and compressive stresses which slows down further development of cracks.

4.2.2. Carbonation

When the concrete is still fresh, it exhibits alkaline properties. With time, different influences start neutralizing the concrete. These include acidic substances in the air, soil and water, as well as fire and microbial activity.

The most common form of concrete neutralization is carbonation. Carbonation occurs when CO_2 from the atmosphere starts diffusing through the concrete pores, where it gets in contact with hydration products. Approximately 96% of calcium hydroxide is available for reaction with diffused CO_2 to form calcium carbonate. Consequently, the alkalinity of concrete and, in turn, decreases its pH value from 12.5 all the way down to 7, where concrete is completely carbonized [4.10]. This process is, however, relatively slow and generally different zones in concrete exist: concrete cover is usually complete carbonized, whereas in deeper no reaction has occurred yet. A great part of concrete consists of partially carbonated zones, with pH values between 7 and 12.5.

Impact of carbonation on concrete structures is as follows:

- Reinforcement corrosion: concrete with a pH value above 11.5 creates an environment where steel rebars form passive layers which greatly reduce the corrosion rate. However, carbonation reduces the pH value below that which is required for passivation, such that the passive film becomes unstable and the corrosion rate increases;
- Diffusion of Cl-: the binding capacity of chloride ions with concrete decreases where carbonation process took place. As a result, carbonized concrete contains more free chloride ions. The presence of chlorides is discussed in Subsection 4.2.3;
- Shrinkage: carbonation can also cause shrinkage of the concrete structure. One of possible explanation is related to the dissolution of calcium hydroxide crystals, which forms stress-free calcium carbonate in the pores [4.11]. There are other studies that suggest that carbonation promotes polymerization and dehydration of the calcium silicate hydrate leading to shrinkage [4.12];
- Concrete strength: in a controlled environment, carbonation causes an increase in concrete strength as it compacts the concrete structure. However, the actual strength of carbonized concrete in the construction environment can decline due to wet and dry cycles that cause leaching of specific components.

The main factors affecting concrete carbonation are:

- Relative humidity: H_2O is required as part of the carbonation reaction, so if the concrete moisture is too low, the carbonation process slows down as CO_2 diffusion slows down. The optimal relative humidity to promote carbonisation is estimated between 50% and 70% [4.13];
- Environmental temperature: although higher temperature increases the chemical reaction rate, there is no clear agreement about exact influence on carbonisation;
- CO_2 concentration: generally, higher CO_2 concentrations cause higher carbonation rates;
- Wind pressure: increased air movement and wind pressure can increase the CO_2 diffusion rate;
- Cement: concretes made by slag cement, pozzolanic cement and fly ash cement have higher rates of carbonation than concrete made by normal Portland cement;
- Water-cement ratio: higher water/cement ratios cause formation of more air bubbles as excess water evaporates. Thus, CO_2 diffusion increases, as does the carbonation rate;
- Admixtures: water-reducing and air-entraining agents reduce carbonation rates.

4.2.3. Chloride ingress

Chloride ion penetration can cause corrosion of embedded steel reinforcement. When concrete hardens, it produces an alkaline environment where oxide passive films can form. A film of a few nanometres in thickness is formed spontaneously and remains effective until it is destroyed by either carbonation or chloride ion diffusion. A sufficient concentration of chlorides near steel surface is needed to break the passive film [4.13]. Once steel is depassivated, the corrosion rate greatly increases despite concrete protection, which only acts as a physical barrier providing mechanical protection. Usually, some cracks or other discontinuities in concrete define areas, where critical chloride concentration is exceeded and initiate localized corrosion of embedded steel.

The impact of corrosion on RC is twofold. First is the reduction of steel reinforcement cross section, which reduces the overall carrying capacity of RC. The second is volume expansion of corrosion products which imposes additional stress on concrete. Due to its limited plastic deformation, concrete starts to crack and that leads to reduction of bond strength and loss of serviceability [4.14]. In the case of consequent decrease of cross section area of rebars and reduction of the structural capacity, even the loss of structural integrity could be reached.

The Tuutti model [4.15] is the most widely used when it comes to assessing the loss of serviceability of a concrete structure. The model proposes two stages:

- The initial stage or initiation stage in which steel is passivated, but chloride ion diffusion or carbonation is already taking place;
- The propagation stage which begins when steel is depassivated and ends when a limiting state is reached. Corrosion is very active during this stage.

Using this model, diffusion of chlorides is often used as an indicator to determine remaining service life of a concrete structure. Nowadays, penetration of chloride ions from seawater or de-icing salts into concrete and the associated risk for reinforcement corrosion is in many countries regarded as the most important degradation mechanism for RC infrastructure [4.13].

4.2.4. Freeze-thaw cycle

When water in concrete changes state from liquid to solid (and vice versa) two damaging processes occur. The first is volume expansion which creates additional pressure inside concrete. The volume increase can be up to 9% when water turns into ice under certain temperatures below 0°C. The second physical change is vapour pressure difference that results in seepage pressure. Since water in the pore freezes, its volume expands and creates additional pressure. This, in turn, makes cooled water in the gel pore migrate and redistribute in the microstructure of concrete, adding to the effect [4.16].

The described cyclic change of water state inside concrete is called a freeze-thaw cycle. If concrete is subjected to such cycles, the damage accumulates and degrades concrete properties. Concrete durability, rupture and tensile strength reduction are the most important properties affected. The following factors have been known to affect the freeze-thaw durability of concrete:

- Internal factors: aggregate, cement, additive, water/cement ratio and air content. In general, the quality of the concrete affects the impact of freeze-thaw cycles. As an example, higher air content or lower water cement ratio will result in less strength loss due to freeze-thaw. In addition, air size distribution plays an important role in the freeze-thaw resistance of concrete.
- External factors: freeze-thaw temperature, freeze-thaw velocity and imposed load. These are the environmental conditions that will influence concrete.

4.2.5. Alkali-silica reaction

ASR is a chemical reaction between alkalis in Portland cement paste and amorphous silica found in certain natural aggregate [4.17]. In general, it is a complicated process that involves several stages, but can be summarized in two. The first is the attack of hydroxyl ions to produce alkali silicate and silicic acid. The second is a reaction between the newly formed silicic acid and hydroxyl ions to produce even more alkali silicate. Both chemical reactions produce an amorphous gel, which expands with the absorption of water. As the gel expands, it creates additional pressure inside concrete that causes it to crack, thus reducing its strength and serviceability.

For the ASR to occur in concrete, it is generally known that three conditions must be satisfied:

- The presence of reactive aggregates (amount of reactive silica in the aggregate, reactive level of silica, aggregate particle size and distribution in mixture);
- A high level of alkalinity (amount of cement, cement alkali content, alkali from aggregate, admixtures, etc. and migration leaching of alkalis);
- Sufficient moisture (concrete volume-to-external surface area ratio, water-to-cement ratio, water permeability, climate and exposure. Relative humidity in the concrete pores needs to be at or above approximately 80%.

Additionally, nuclear radiation has an effect on the aggregate that can make it more ASR-sensitive. This can cause ASR to occur more rapidly. Research has been done on the effect of nuclear radiation on quartz based aggregates and plagioclase minerals [4.18]. The former lasted longer for irradiated conditions than when exposed to radiation. Additional radiation effects are discussed in Subsection 4.2.7.

4.2.6. Sulphate attack

Cements with high alumina content contain calcium hydroxide within its hydration products. When sulphate ions come into contact with calcium hydroxide, alumina-containing hydrates are converted to the high-sulphate form called ettringite [4.9]. The new products have a higher specific volume, which cause tensile stresses and subsequent cracking of concrete. Most soils and groundwater contain a certain amount of sulphate ions.

Gypsum can also form in the presence of sulphate and calcium hydroxide. Depending on the cation type associated with the sulphate solution, both calcium hydroxide and the calcium-silica gel can be converted to gypsum. In the process, new hydroxides are formed (e.g. magnesium hydroxide) that can reduce the alkalinity of hardened cement paste, making it unstable (see Subsection 4.2.2).

Delayed ettringite formation is the third form of sulphate attack, with the source of sulphate ions in this phenomenon being internal. The process is known to occur when either a gypsum-contaminated aggregate or cement containing unusually high sulphate content has been used. During high curing temperatures, ettringite gets dissolved and sulphate gets adsorbed on the cement paste surface. After the concrete has cooled, ettringite reforms and causes the increase in specific volume described above. Curing temperatures are usually the highest during steam curing or mass concrete placements.

4.2.7. Nuclear radiation effect

The effect of nuclear radiation on concrete deterioration is not well understood by most structural engineers. It is a mechanism where neutron radiation causes lattice movements and, as a result, aggregate expansion [4.19]. As the aggregate volume changes, tensile strength, compressive strength and modulus of elasticity are affected. Tests have shown that these properties can get reduced significantly in the presence of neutron flux, even without considering the temperature effect. Therefore, studying mechanical properties of RC close to the radiation sources is important.

Concrete storage casks are not the only RC structures in nuclear power plants that are affected by radiation. Other structures potentially affected include the following:

- Containments (primary – leak tightness, secondary – enclosures);
- Containment internal structure (floor slabs, walls, columns, beams, etc.);
- Shielding shear walls (they surround the reactor core);
- SNF storages (effects of long term exposure to high levels of gamma; radiation is similar to those induced by neutron radiation).

4.2.8. Thermal degradation

Concrete exposed to high temperatures for an extended period of time can have its mechanical properties reduced [4.20]. When approaching 100°C, concrete starts drying out as pore water is lost. Cracking and scaling of concrete surfaces can be observed when temperatures go above 149°C. This is the reason why the horizontal concrete overpacks should be protected by 'heat shields' that are placed just below the roof of the overpack. Thermal degradation is a function of the SNF decay heat, the ability of the storage system to remove heat, and atmospheric temperature and wind speed.

4.2.9. Leaching and efflorescence

Certain calcium compounds in concrete can dissolve when in contact with water. As water traverses through cracks and dissolves these calcium compounds ('leaching'), this water-soluble calcium gets deposited on the concrete surface as crystalline white powder, creating efflorescence [4.20]. The consequences of concrete leaching are in reduction in pH (Subsection 4.2.2) and increased porosity, both of which can promote embedded steel corrosion. An increase in porosity causes an increase in the migration of soluble and gaseous species such as hydroxides, chloride, sulphate and CO_2. Therefore, vulnerability to hazardous environments containing such species can also increase with increased porosity.

4.3. INSPECTION TECHNIQUES

Inspection techniques applicable to concrete cask storage systems can be divided into four groups: visual inspection, non-destructive evaluation, invasive techniques and the use of analytical tools. Below is a summary of presently utilized techniques [4.20].

4.3.1. Visual inspection

Visual inspection is usually the first technique used when assessing the state of concrete. It is the most common and basic technique that can detect some of the effects of the described degradation mechanisms, usually surface defects and the presence of efflorescence. Combining acquired data over time can also show the degree of severity and degradation rate. Many assisting tools can be used during visual inspection, such as crack comparators, binoculars, borescope, additional lighting, cameras and other specialized equipment. The usage of such tools becomes a necessity when inspecting some of the more difficult to access areas, such as the interior concrete surface of a storage overpack. It should be noted that the quality of information gathered from such inspections is lower than the information gathered from readily accessible structures. There are also situations where visual inspection is not possible. Concrete overpack designs that are covered with steel lining, or are located next to each other, prevent visual inspection of certain concrete wall sections, although liners can also mitigate several of the degradation mechanisms above that require exposure to the atmosphere to occur.

4.3.2. Non-destructive evaluation

To obtain the condition of concrete that can't be seen on the surface, non-destructive evaluation can be used. These techniques can be used to detect corrosion of reinforcement, delamination, voids and vertical cracks inside concrete. Most of these initial damages evolve during degradation processes into visible destruction, as spalling of concrete. Main goal of non-destructive evaluation is to detect and assess damages in an early stage, but due to specific limitations of individual techniques, not all defects can be detected. Access to at least one side of a concrete surface is required, with some techniques requiring access to both. This makes usage of different methods depending on concrete overpack or storage pad design. If the measuring device is too bulky, it might not fit inside ventilation shafts, making it inappropriate for inspecting interior concrete surfaces.

Listed below are several commercially available techniques for detecting corrosion of embedded steel and delamination. Devices for measuring the depth of naturally generated cracks (perpendicular to the concrete surface) have shown poor reliability, despite manufacturer claims.

Methods for detecting steel corrosion:

- Half-Cell Potential: indicate the risk that corrosion of embedded steel reinforcement may occur. Assessment of the degree of corrosion is not possible. Can be partially destructive, as it requires direct connection to the embedded steel reinforcement. This limitation can be overcome if the rebar is connected to some outside metal surface, like the shaft framing;
- Resistivity: detects susceptibility to corrosion. Does not provide information on whether corrosion is actively occurring or the degree of corrosion;
- Linear polarization resistance: used for measuring the rate of active corrosion, but the interpretation of results due to possible localization of corrosion might not be quite reliable.

Methods for detecting delamination:

- Hammer sounding or chain dragging: this method detects shallow delamination by comparing difference in response sounds on healthy and delaminated concrete surface. It is very fast, operator dependent, meaning it is very subjective, and can be affected by ambient noise. The method does not require any special equipment, only a hammer or some type of chain which can produce sound when dragged over concrete surface;
- Impulse response: this method detects delamination less than a third of the size of concrete thickness. It is very fast, operator dependent, and does not provide the delamination depth;
- Impact echo: this method detects delamination and measures the thickness of the concrete, or the depth to the defect. The technique is very time consuming and has good reliability only when no obstacles like rebar and tendons are present in concrete;
- Ultrasonic shear wave (array): this method detects delamination, voids and measures plate thickness. It has good reliability with the exception of shallow delamination.

4.3.3. Invasive techniques

Techniques in this group require the removal of concrete or the exposure of steel reinforcement to perform testing and observations. The following tests can be performed:

- Determination of chloride content;
- Determination of pH;
- Determination of depth of carbonation;
- Petrographic evaluation;
- Chemical analysis;
- Determination of permeability;
- Void size distribution.

More than one of these methods is usually needed in order to determine the presence of a certain degradation mechanism. They are also combined with other non-destructive methods, since data obtained is localized to a particular region of the entire concrete structure and there are limitations to how many times an invasive technique can be used on a single structure.

Since radiation shielding is one of the primary functions of concrete in dry storage casks, there are concerns about using invasive techniques. Analysis needs to be performed beforehand, to ensure no loss in shielding function takes place.

4.3.4. Analytical methods

When certain areas are inaccessible for other inspection techniques, models, calculations and analysis can be used as a form of evaluation. These methods are often used in combination with non-destructive and invasive techniques to evaluate structural integrity or predict the evolution of certain degradation mechanisms.

4.4. TYPES OF EXPOSED STRUCTURES

Two types of concrete overpacks (horizontal and vertical) and a concrete pad have been identified as structures susceptible to concrete degradation mechanisms in SNF dry storage systems [4.20]. The purpose of the concrete casks is to physically protect the SNF canister from external events, provide radiation shielding to personnel and allow the canister to cool through natural air convection. The concrete pad serves as a base on which these casks and canisters stand on.

4.4.1. Horizontal storage module

All degradation mechanisms described in the previous subsection can affect horizontal storage modules. It should be noted that the inside of the concrete vault does not have steel liners but do have heat shields instead. This means it is also exposed to the atmosphere. Thermal degradation and radiation damage will cause damage on the inside before progressing to the outside. All other mechanisms either work in reverse direction or are present throughout the concrete structure. Visual inspection can be used to detect most concrete degradation. Harder to reach outside places, like the side and the back walls, depend largely on vault positioning, while the inside can be inspected using a borescope camera through the air inlets and outlets. Reinforcement corrosion and delamination require other non-destructive evaluation techniques, which might prove difficult if the area of inspection is hard to access.

4.4.2. Vertical reinforced concrete cylinder

Like horizontal storage modules, all concrete degradation mechanisms can affect vertical RC overpacks, since they are directly exposed to the outside environment. As mentioned, the inside of the casks is not directly exposed to the environment, but the thermal and radioactive degradation can still occur. Multiple casks within a matrix are arranged to ensure ease of access to all external areas to aid inspection. With the inside concrete covered in a steel liner, visual and non-destructive evaluation can only be carried out on the external wall surface.

4.4.3. Vertical steel-encased concrete cylinder

Since the concrete is neither directly exposed to the environment, nor does it have reinforcement, many of the degradation mechanisms described in previous subsections are not a problem as long as water tightness is maintained. Shrinkage, radiation damage and thermal damage still remain an issue, however. Since the concrete is encased in steel, none of the defects related to concrete can be detected visually. At this point in time, there is no verified non-destructive evaluation technique that can accurately detect flaws in concrete encased in steel without access from both sides of the cylinder wall.

4.4.4. Independent spent fuel storage installation concrete pad

A thick RC slab, which provides stable foundation for concrete casks, also needs to be evaluated for concrete degradation. While thermal degradation and radiation damage are not an issue, sulphate attack is a bigger concern due to contact with groundwater. Groundwater monitoring can be used to check for both sulphate and chloride concentrations. Visual inspection can be performed on the top surface only, while the bottom surface requires excavation beforehand.

4.5. CURRENT RESEARCH ON INTERIM STORAGE OF SPENT FUEL

Recently, analysis of the thermal behaviour of concrete casks in dry storage has been carried out. Since the designs employing metal canisters inside concrete overpack designs have air inlets and outlets as shown in the figures above, most of the heat loss is due to natural convection and some due to radiation [4.21, 4.22]. When off-normal scenarios are performed, one or two of the inlets are blocked. In the long term, some regulations require that the concrete cask must remain below 90°C in such conditions. If the requirement is not met, design modifications and material changes would need to be made for satisfactory performance. Two such casks were tested as part of a Central Research Institute of Electric Power Industry (CRIEPI) approved research program for the verification of cask integrity under long term dry storage conditions [4.23]. The two casks were a RC cask similar to that shown in Fig. 4.8, and a concrete filled steel (CFS) cask similar to that shown in Fig. 4.9. The temperature of the former rose up to 91°C, thus not passing the long term heat removal test.

Orientation and position of the storage casks has also shown significant effect on their cooling behaviour and different heat transfer mechanisms become significant based on whether the fuel element is placed vertically or horizontally [4.21].

In dry storage, the casks are generally arranged as free standing structures as opposed to firmly anchored ones. This can lead to stability issues when it comes to seismic activity. Numerous researches are taking place where stability is being analysed for particular designs of casks [4.21, 4.23].

Accident scenarios during storage or transportation have been considered. These include dropping the canister during transportation, impact by aircrafts and external fires. The casks have to be designed so that leak tightness and shielding functions are not affected when accidents occur [4.21]. The typical mechanical testing of such containers involves a drop test, during which the canister is dropped from height or tipped over and the vessel is subsequently examined for dents, rupture, cracks and leakage [4.23]. Some canisters contain Helium gas to enhance heat removal from SNF. Leakage in such canisters could severely decrease its heat removing capabilities [4.22]. Another research [4.24] suggests that loads during accidents on long term stored fuel need to be re-examined. Existing models may fall short in their capability to model the physics and predict the actual load on fuel due to all the effects of long term storage. Therefore, post accident inspection is likely to be required to assess the extent of any degradation.

The combination of chloride attack and high temperature are especially important to steel corrosion in concrete casks. Recent research [4.25, 4.26] shows an increase in depth of chloride ion penetration with increasing temperature in all concrete, regardless of water-cement ratio. Premature deterioration can be expected for concrete structures subjected to salt attack under high temperature.

Monitoring of concrete degradation mechanisms discussed in Subsection 4.3 has also been a topic of ongoing research. The following International Atomic Energy Agency (IAEA) Coordinated Research Project (CRP) relates to the subject.

4.5.1. Outcome of work at National Building and Civil Engineering Institute (ZAG), Slovenia

Research activities on steel corrosion in concrete at ZAG started more than a decade ago, with the main focus on developing monitoring systems that would be capable of following the evolution of corrosion processes under various conditions. It should be mentioned that these activities were not oriented specifically at issues of dry SNF storage, but they opened new possibilities for monitoring the evolution of corrosion damage in SNF/HLW dry storage facilities.

Two relatively new methods were combined during the research period: measuring with electrical resistance (ER) probes and coupled multi-electrodes or coupled multi-electrode arrays (CMEA) [4.27, 4.28]. ER probes are frequently used in corrosion monitoring systems in various industrial fields, especially in the petro-chemical industry. This method is based on measurements of the thickness reduction due to corrosion, so it can be very sensitive to general corrosion. On the other hand, the response of these probes to localized corrosion types and transient events is limited. Measuring with CMEAs and coupled multi-electrodes is by some means an advancement of electrochemical noise (EN). It was confirmed that they can reliably follow the distribution of anodic and cathodic currents over time. The results of both used methods were compared and related to the conditions of rebar, the ER probes and the micro-electrodes that were assessed by X-ray computer tomography (MicroCT) scans.

A total of three experiments were conducted using different RC specimens with embedded probes. The first experiment started in 2007 when several smaller specimens of different cements were made (Fig. 4.10(a)). This was a laboratory experiment where embedded steel was exposed to cyclic wetting and drying using simulated groundwater that is typical for the planned location of the underground low and intermediate level waste (LILW) storage (Vrbina). Galvanostatic pulse and ER probe measurements were done periodically, with select specimens being thoroughly investigated using various methods: MicroCT, visual, and SEM. After 1877 days of exposure, the remaining specimens were switched to simulated saline water (3.5% NaCl). In 2009, large scale RC specimens were produced and exposed to marine environment on the island of Krk (Fig. 4.10(b)). Reinforcing bars, ER probes and coupled multi-electrodes made of carbon steel and different types of stainless steel were embedded in concrete columns. ER probes and coupled electrodes were placed at different heights to monitor the effect of sea level changes on corrosion. Galvanostatic pulse measurements, partial currents on coupled multi-electrodes as well as measurements on the ER probes were performed periodically. Due to deficiencies detected at the columns installed in 2009, a new set of concrete columns were constructed and placed at the Port of Koper. Certain features of the measuring system were upgraded to enable wireless data acquisition.

(a) *(b)*

FIG. 4.10. (a) Laboratory specimens (reproduced courtesy of National Building and Civil Engineering Institute (ZAG)); (b) Concrete columns exposed to marine environment (reproduced courtesy of National Building and Civil Engineering Institute (ZAG)).

The results from the first experiment show that ER probes are reliable for measuring average general corrosion rate, whereas response to pitting is limited. X-Ray tomography was identified as a powerful non-destructive technique for the assessment of corrosion damage of steel in concrete. Certain types of stainless steels behaved significantly better than ordinary steel rebars, showing no corrosion damage after more than 5 years of exposure.

From the exposure of concrete columns to a marine environment it was established that some of the ER probes made of carbon steel embedded in the concrete specimens clearly detected intensive corrosion. Three of them (exposed in the splash zone, tidal zone and the zone below the surface) corroded completely in slightly more than a year. Obviously, also in the zone below the surface due to strong winds and waves, the presence of oxygen was sufficient to support high corrosion rates. No thickness change was measured on the ER probe exposed in the zone in which the specimens were always covered by water. Measurements of coupling currents implied that a certain corrosion pattern was generated: neighbouring electrodes were usually not mutually anodic or cathodic, but they acted as an anode/cathode pair. Results of coupling currents and measurements of the ER probes were generally in agreement, with a few exceptions. Visual inspection was also performed in order to detect cracks and mechanical damage. The most severe cracks on the columns with carbon steel rebars were found close to the plastic spacers, which probably made the ingress of chlorides easier. Some vertical cracks were also detected. It is suspected that these cracks were generated by the growth of corrosion products on vertical rebars. No indications of corrosion could be seen on the specimens with stainless steel rebars.

All the measuring and evaluation techniques used have confirmed that most stainless steel (austenitic, duplex) behaves significantly better that ordinary carbon/black steel. The only exception is low-alloyed steel, which is durable only under mild exposure conditions. These results indicate that use of stainless steel reinforcement in storage casks and related structures would greatly reduce the risk posed by rebar corrosion.

4.5.2. Outcome of work at Comisión Nacional de Energía Atómica (CNEA), Argentina

The research evaluated the ability of emission tomography to detect cracks, voids and eventually the rebar corrosion in concrete containment structures used for SNF storage. Several high performance gamma detectors were used to map the spatial distribution of the radiation to detect variations in levels that would indicate changes in shielding properties and hence indicate degradation of the structure (Fig. 4.11).

The main objective of the present research was to determine whether periodic scanning of the external surface of a concrete cask could be used to provide a useable tomographic image. The selected case of study was a large concrete silo of 2.4 m in diameter and 6 m in height, located at the Embalse NPP facility. The attention was focused on Silo #1 loaded in 1993, because the highest radiation emission rate was expected at the surface of the silo. A total of five experiments and one modelling simulation were conducted.

The first two experiments were conducted in a laboratory where gamma-radiography and the accompanying tomography techniques were evaluated on RC test samples. The first experiment employed a planar gamma camera to acquire a global energy spectrum and an image after enough resolution and contrast was obtained. The second experiment used six of these cameras next to each other, while the specimen was rotating to acquire images from many angles and hence provide tomographic data.

Experiments 3, 4 and 5 were done on the test site. The third experiment used low energy resolution and high efficiency detectors on two casks, one older and one newer, while experiment 4 used higher energy resolution detectors. Experiment 5 evaluated the benefits of sacrificing energy resolution to gain more spatial resolution. The last experiment was a modelling simulation where simplified physical models were used in order to conduct the experiment faster.

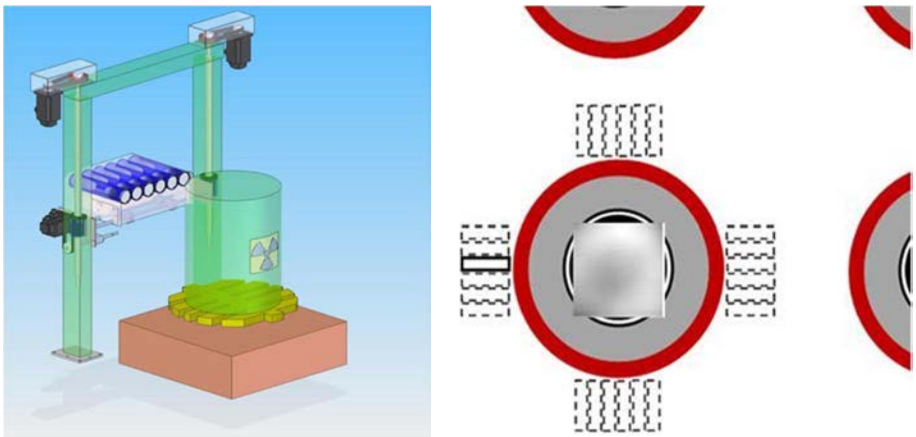

(a) *(b)*

FIG. 4.11. (a) Tomographic Gamma Scanner (reproduced courtesy of CNEA); (b) Position of the tomographic Gamma Scanner around a concrete cask (reproduced courtesy of CNEA).

The result obtained from experiment 1 indicated that it would be possible to use planar scintigraphy using a flat panel scintillator detector, which is similar to the approach used in the digital high energy radiography. No gamma ray point source was available, so instead, there are a certain amount of scattered gamma rays that can be used as backlight illumination. To acquire an image of the rebars with enough resolution to assess corrosion damage, cracks or voids, a high energy collimator is necessary in between the silo surface and the flat panel. At present, a pixelated BGO detector attached to a high energy lead collimator capable of up to 5 mm resolution is under construction. It is expected that in the near future research will be undertaken to assess its effectiveness.

Experiment 2 showed that it was possible to perform tomographic assessment with low energy resolution detectors in low activity radioactive waste containments with compact volume. However, measurements made during experiments 3 and 5 showed the inability of NaI and $LaBr_3$ detectors to discriminate true energy peaks in high Compton background generated in the thicker concrete silos. High resolution $LaBr_3$ detectors have an appropriate energy window that can be selected using scatter subtraction techniques and self-emission elimination. These may be able to provide suitable data for tomographic purposes, but the concept needs further testing to demonstrate whether this is the case.

The measurement of a high resolution spectrum in experiment 4 indicated that peaks suitable for image reconstruction are available for ^{137}Cs and, to a lesser extent, ^{154}Eu. In the case of ^{137}Cs, the count rate in its energy window is less than 1 per second for a single detector, while the same count is six time lower in the case of ^{154}Eu. This means that the data acquisition times for tomographic purpose will be necessarily prolonged. Since the data in this experiment was collected from a small number of angles and linear positions, the reconstructed images were somewhat crude. However, the results would suggest that in a dedicated device for this type of application one should have a greater number of detectors to reduce the acquisition time and increase sensitivity (although this would increase the detector cost as a result). A more suitable device was proposed with an array of 28 high resolution detectors that cover a complete diameter of the silo with spatial resolution of at least 10 cm. If linear movement is added, the estimated acquisition time for a single slice is 15 hours. The ability of this kind of device to detect cracks, voids or hot spots in the bulk of the silo is currently being evaluated by modelling simulations.

4.5.3. Outcome of work at Centro Atómico Constituyentes (CAC), Argentina

The activities carried out during the development of the CRP resulted in development of an electrochemical corrosion monitoring probe that was inserted in two dry storage facilities [4.29, 4.30].

The corrosion monitoring probe, shown in Fig. 4.12, consists of 6 electrodes: a working electrode made of black steel, a titanium rod reference electrode, two inert electrodes, a chloride electrode and a thermometer. All electrodes are covered in epoxy resin. The sensor is capable of measuring corrosion rate, polarization resistance, concrete resistance, chloride concentration, oxygen availability and temperature.

FIG. 4.12. Detailed look at the probe (reproduced courtesy of Elsevier)[4.29].

In order to evaluate the effectiveness of the probe and the evolution of corrosion parameters, a long term test wall was made. As of mid-2016, 2000 days of testing have been performed, and testing is still ongoing. From the current results it became clear that the developed sensor accurately measures the corrosion parameters of a RC structure. The measured values have entered the safe zone with respect to concrete and rebar degradation. Additionally, more experiments were made in preparation to install the sensors in actual storage site facilities. RC specimens made of ordinary Portland and pozzolanic cement were assessed for 1100 days, with both showing similarly acceptable performance. Based on all test results, the sensor was deemed reliable enough to install in silos, near where the SNF is stored. The main building of the dry storage facility for Atucha-1 nuclear power plant had corrosion probes installed in 2014, while monitoring started in 2015.

The second field experiment was done at the same storage facility. Because penetrations would not be allowed into the silo units, a scale model was built in the same environment, to evaluate their behaviour using corrosion probes. Like in the test experiments, various corrosion parameters are being measured. After some 200 days of operation, all the variables are in the range corresponding to moderate to low corrosion probability, but with clear descending tendency.

4.6. STORAGE SITE EXAMPLES

This subsection reviews current research on concrete storage casks, including tests done on in-service storage facilities.

4.6.1. VSC-17 SNF cask

VSC-17 (Fig. 4.13(a)) is a concrete ventilated storage cask system with 17 cells that was designed to contain fuel rods from both intact and consolidated pressurized water reactor (PWR) fuel assemblies [4.31, 4.32]. It has been storing SNF since October 1991. Its general construction conforms to that shown in Fig. 4.8, with a concrete wall thickness of 51 cm, but has an additional inner liner of A-36 steel that is 89 mm thick, which provides structural support and additional shielding. The annular gap between the steel liner and the canister is 76 mm.

Previous measurements taken in 1991 [4.31] and 2003 [4.32] indicated a step-change in the radiation readings at a point approximately 2.5 m above the base of the cask. Radiation hot-spots have also emerged beneath one of the upper vents. The cause of these variable radiation readings was unknown which spurred another examination 2 years later.

In 2005, the cask was extensively studied to determine compressive strength, concrete cracking, concrete thickness and temperature distribution. In order to accomplish this, the following tests were performed:

- Thermocouple measurements with a thermocouple ladder (5.5 m mast with thermocouples attached 30 cm apart) – used to obtain surface temperature measurements;
- Thermal imaging with a camera – used to determine if the external temperature of the cask varied consistently with atmospheric conditions;
- Concrete hammer tests (rebound test, Schmidt hammer test) – an in situ method used for determining the strength of hardened concrete;
- Gamma radiation measurements;
- Ultrasonic testing (wave propagation velocity test) – used to find evidence of cracks not visible on the surface.

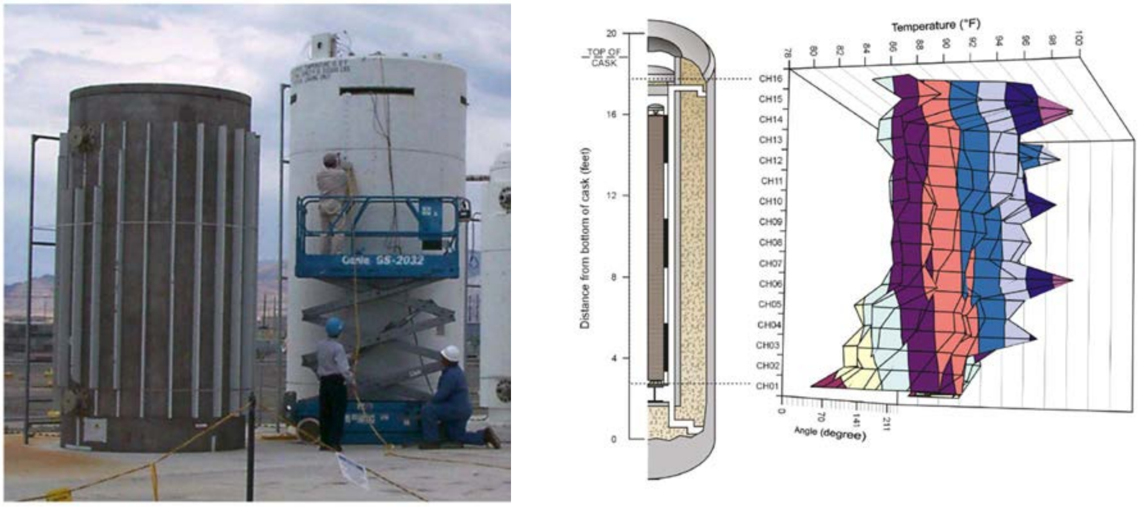

(a) *(b)*

FIG. 4.13. (a) Thermal imaging of the VSC-17 storage system with a camera [4.32]; (b) Temperature profile.
([°F] = [°C] × 9⁄5 + 32; 1 ft = 0.3048 m) (reproduced courtesy of American Nuclear Society) [4.32]

The results show that there was limited variation of temperature throughout the cask. The heat transfer was relatively uniform, and high temperatures occurred at the vents as a result of hot airflow. There was no indication of temperature discontinuity that results from shield component material variability.

The Schmidt rebound hammer tests show minimal variability among the data points on the cask.

There was no conclusive result as to the origin of variations in the radiation field between the lower and upper subsections. There was also no indication that the lower material is denser or stronger based on ultrasonic and hammer testing.

The radiation hot spot found under the 45 to 52-degree upper vent was identified as a construction artefact. This might be a result of a void that was not completely filled in with concrete. Ultrasonic testing also produced anomalous results under the 45-degree vent that could be a product of either manufacturing or ageing.

Overall, early analysis indicated that the VSC-17 ventilated concrete cask shield performance was not significantly affected by the environment or radiation during its more that 15-year lifespan.

4.6.2. Calvert Cliffs

Each horizontal storage module in Calvert Cliffs was visually inspected on the outside surface [4.20]. Less than 1 mm cracks were found, showing signs of minor degradation. Hammer sound testing and internal visual inspections were also performed on select concrete vaults. A borescope camera was used for the accessible internal surfaces. Due to water intrusion through cracks near the air outlets, stalactites had formed on the roof of the storage modules, but their white colour suggests corrosion rebar depth has not been reached. General corrosion was observed on the canister support structure for loading and unloading.

4.6.3. Arkansas Nuclear One

Cracking due to shrinkage was observed on the majority of the VSC-24 concrete casks after visual examination [4.20]. The cracks were small enough to be considered cosmetic. However, the next year, larger cracks were found that needed to be repaired according to standard repair procedures.

4.6.4. Oconee

In 2006, Oconee Nuclear Station performed external visual inspection and internal visual inspection using a borescope camera [4.20]. Coating failure and corrosion was found on welds for the inlet plenum. There were also some construction defects found in areas of heavy steel embedment.

4.6.5. Three Mile Island

Visual inspection, hammer sound testing, ground penetrating radar and petrographic analysis were performed on horizontal storage modules after surface cracks were found a year earlier [4.20]. Radial cracking was present on the roof of all concrete vaults, caused by freeze-thaw near the anchor holes. Anchor holes were filled with polyurethane foam as a countermeasure. To better understand crack growth, crack gages were attached at various locations in 2010.

4.7. FUTURE CHALLENGES

A major challenge in the years to come will be the increasing need for large capacity storage facilities for long term fuel storage. Dry concrete casks were mainly designed to cool down and reduce the radioactive levels from SNF [4.21] and for additional storage capacity to storage pools at reactor site [4.23]. Their size, storage capacity and heat removal capabilities were designed accordingly. Even though concrete vaults are more economical than casks for large fuel storage, cheaper and better storage methods are desired. Larger canisters with pressurized helium gas, which helps with effective heat removal, have already been designed.

Tables 4.1 and 4.2 summarize the more important ‘gaps’ identified [4.33]. While the biggest issues found were hydrogen embrittlement of cladding and corrosion of canister welds, concrete overpacks and the degradation mechanisms present, particularly freeze-thaw and corrosion of reinforcement, were also considered important gaps by most countries. Regardless of the material used, most countries considered cross-cutting technical gaps (Table 4.2), such as monitoring, temperature profiles, drying issues, examination and damage definition as important.

The effects of described degradation mechanisms on concrete storage casks should be studied more thoroughly as specific issues on the subject are still open. In particular, the combination of degradation mechanisms and environmental conditions found at storage sites, such as high temperature and nuclear radiation, can have a negative impact on concrete longevity and durability.

TABLE 4.1. VERY LONG TERM STORAGE TECHNICAL NEEDS FOR STRUCTURES, SYSTEMS AND COMPONENTS (SSCs): SUMMARY OF 'IMPORTANCE TO R&D ASSESSMENTS' (ADAPTED FROM [4.33])

Structures, systems and components (SSCs)	Ageing alteration and/or degradation mechanism	TECDOC chapter in which the gap is addressed
Fuel cladding	Annealing	n.a.
	Hydrogen embrittlement	3
	Hydride cracking	3
	Oxidation	3
	Creep	3
Fuel pellets	Cracking, bonding	n.a.
	Oxidation	3
Fuel assembly hardware	Corrosion and stress corrosion cracking (SCC)	n.a.
Basket	Corrosion, irradiation	n.a.
Neutron shielding	Thermal and radiation ageing	6
	Creep	6
	Corrosion	6
Neutron poison	Creep	n.a.
	Embrittlement	n.a.
	Corrosion	n.a.
Welded canister	Atmospheric corrosion	2
	Aqueous corrosion	n.a.
Moisture absorber	Irradiation, thermal	n.a.
Bolted casks	Fatigue of seals or bolts	5
	Atmospheric corrosion	n.a.
	Aqueous corrosion	n.a.
	Metal seal creep	5
Concrete overpack, cask, or pad	Freeze-thaw	4
	Corrosion (including embedded steel)	4

Note:

A few of these ageing mechanisms are not detrimental to maintaining safety functions.

TABLE 4.2. CROSS-CUTTING DATA NEEDS

Cross-cutting needs note	TECDOC chapter in which the gap is addressed
Monitoring[1] (internal)[2]	7
Monitoring (external)[3]	2, 4, 7
Temperature profile	2–7
Drying issues	3, 7
Subcriticality, burnup credit, moderator exclusion	n.a.
Fuel transfer options	n.a.
Examination[4]	7
Canister weld stress profiles	2, 7
Damage definitions	n.a.
Verification of fuel condition / fuel classification	n.a.

Note:

[1] Monitoring is a general term that includes continuous or periodic measurements or visual observations. This is sometimes referred to as inspection or surveillance.
[2] Internal monitoring is monitoring of the inside of the cask or canister. Examination of the fuel in existing canisters at the Idaho National Laboratory that were put in service in the 1980s into the early 1990s is the one example of internal monitoring that is underway (see Chapter 7).
[3] External monitoring are direct or indirect measurements of the properties of interest. Direct external measurement example: canister exterior surface temperature. Indirect external measurement example: atmospheric chloride concentration as an indication of the amount of chlorides deposited on the outside of canisters.
[4] Examination means post-test measurements or observations of the properties of interest.

REFERENCES TO CHAPTER 4

[4.1] NATO Advanced Research Workshop on Safety Related Issues of Spent Nuclear Fuel Storage, Safety Related Issues of Spent Nuclear Fuel Storage, NATO Security through Science Seri–s - C: Environmental Security (LAMBERT, J.D.B., KADYRZHANOV, K.K., Eds), Proceedings of the NATO Advanced Research Workshop on Safety Related Issues of Spent Nuclear Fuel Storage (Proc. Workshop Almaty, 2005), Dordrecht: Springer: Published in cooperation with NATO Public Diplomacy Division (2007) 356 pp.

[4.2] REITENBACH, G., Dry cask storage booming for spent nuclear fuel, Power 159 (2) (2015) 45–48.

[4.3] GNS, CASTOR® V/19 (2018), http://www.gns.de/language=en/21551/castor-v-19

[4.4] NAC INTERNATIONAL, The MAGNASTOR System: The New Generation in Multipurpose Storage (2014), https://www.nacintl.com/magnastor

[4.5] NAC INTERNATIONAL, MAGNASTOR (2014), https://www.nacintl.com/

[4.6] UNITED STATES NUCLEAR REGULATORY COMMISSION, Final Environmental Impact Statement for the Construction and Operation of an

Independent Spent Fuel Storage Installation on the Reservation of the Skull Valley Band of Goshute Indians and the Related Transportation Facility in Tooele County, Utah, Rep. NUREG-1714, Vol. 1, Office of Nuclear Material Safety and Safeguards, Washington, DC (2001).
[4.7] ZULOAGA, P., ‘‘HLW storage and SL-LLW disposal in Spain’’, paper presented at 19th REFORM Group Meeting, Salzburg (2014).
[4.8] HAIN, K., “Idaho site spent nuclear fuel management”, paper presented at 2010 U.S. Nuclear Waste Technical Review Board, Idaho Falls (2010).
[4.9] MEHTA, P. K., MONTEIRO, P. J. M., Concrete: Microstructure, Properties, and Materials, 3rd ed, McGraw-Hill, New York (2006) 660.
[4.10] LI, Z., WANG, Z., Researches on concrete carbonation, Applied Mechanics and Materials 357–360 (2013) 737–742.
[4.11] POWERS, T.C., A hypothesis on carbonation shrinkage, Journal of the Portland Cement Association (PCA) Research and Development Laboratories Bulletin 146 4 2 (1962) 40–50.
[4.12] SWENSON, E.G., SEREDA, P.J., Mechanism of the carbonation shrinkage of lime and hydrated cement, Journal of Applied Chemistry 18 4 (1968) 111–117.
[4.13] BERTOLINI, L., ELSENER, B., PEDEFERRI, P., REDAELLI, E., POLDER, R.B., Corrosion of Steel in Concrete: Prevention, Diagnosis, Repair, 2nd edn, Wiley-VCH (2013) 434.
[4.14] CABRERA, J.G., Deterioration of concrete due to reinforcement steel corrosion, Cement and Concrete Composites 18 1 (1996) 47–59.
[4.15] TUUTTI, K., Corrosion of Steel in Concrete, Thesis, Swedish Cement and Concrete Research Institute, Stockholm (1982).
[4.16] YOUZHEN, W., Analysis on effects of freeze-thaw cycle on mechanical properties of concrete, Journal of Chemical and Pharmaceutical Research 6 7 (2014) 216–222.
[4.17] PAN, J.W., FENG, Y.T., WANG, J.T., SUN, Q.C., ZHANG, C.H., OWEN, D.R.J., Modeling of alkali-silica reaction in concrete: a review, Frontiers of Structural and Civil Engineering 6 1 (2012) 1–18.
[4.18] ICHIKAWA, T., KIMURA, T., Effect of nuclear radiation on alkali-silica reaction of concrete, Journal of Nuclear Science and Technology 44 10 (2007) 1281–1284.
[4.19] MIRHOSSEINI, S., POLAK, M.A., PANDEY, M., Nuclear radiation effect on the behavior of reinforced concrete elements, Nuclear Engineering and Design 269 (2014) 57–65.
[4.20] ELECTRIC POWER RESEARCH INSTITUTE, Degradation Mechanisms and Inspection Techniques for Concrete Structures in Dry Storage Systems for Spent Nuclear Fuel, Rep. 3002005508, EPRI, CA (2015).
[4.21] BHATTACHARYYA, R., Interim storage of spent nuclear fuel: an assessment of technologies and challenges, Journal of Nuclear Engineering & Technology 4 2 (2014) 1–11.
[4.22] SAEGUSA, T., YAGAWA, G., ARITOMI, M., Topics of research and development on concrete cask storage of spent nuclear fuel, Nuclear Engineering and Design 238 5 (2008) 1168–1174.
[4.23] SAEGUSA, T., et al., Review and future issues on spent nuclear fuel storage, Nuclear Engineering and Technology 42 3 (2010) 237–248.
[4.24] KLYMYSHYN, N.A., ADKINS, H.E., Jr., HANSON, B.D., “Assessing material degradation effects on long term storage structural analyses”, 14th International High-Level Radioactive Waste Management Conference (IHLRWM 2013): Integrating Storage, Transportation, and Disposal (Proc. 14th Int. Conf. Albuquerque, 2013), American Nuclear Society (ANS), La Grange Park, IL (2013).

[4.25] SO, H.-S., CHOI, S.-H., SEO, K.-S., SEO, C.-S., SO, S.-Y., The properties of chloride ion diffusion of concrete under high temperature conditions, with implications for the storage of spent nuclear fuel in concrete casks, KSCE Journal of Civil Engineering 18 7 (2014) 2227–2233.

[4.26] LEE, Y.H., LEE, C.M., LEE, K.J., "A study on durability of reinforced concrete structure for spent fuel storage facility", 12th International High-Level Radioactive Waste Management Conference (IHLRWM 2008): Steps Toward Reality for Safe Disposal (Proc. 12th Int. Conf. Las Vegas, 2008), American Nuclear Society (ANS), La Grange Park, IL (2008) 772–775.

[4.27] LEGAT, A., Monitoring of steel corrosion in concrete by electrode arrays and electrical resistance probes, Electrochimica Acta 52 27 (2007) 7590–7598.

[4.28] ČESEN, A., KOSEC, T., LEGAT, A., Characterization of steel corrosion in mortar by various electrochemical and physical techniques, Corrosion Science 75 (2013) 47–57.

[4.29] DUFFÓ, G.S., FARINA, S.B., Development of an embeddable sensor to monitor the corrosion process of new and existing reinforced concrete structures, Construction and Building Materials 23 8 (2009) 2746–2751.

[4.30] DUFFÓ, G.S., FARINA, S.B., GIORDANO, C.M., Embeddable reference electrodes for corrosion monitoring of reinforced concrete structures, Materials and Corrosion 61 6 (2010) 480–489.

[4.31] ELECTRIC POWER RESEARCH INSTITUTE, Performance Testing and Analyses of the VSC-17 Ventilated Concrete Cask, Rep. TR-100305, EPRI, CA (1992).

[4.32] MORTON, S.L., et al., "Concrete shield performance of the VSC-17 spent nuclear fuel cask", Proceeding of the 11th International High-Level Radioactive Waste Management Conference (IHLRWM 2006): Global Progress Toward Safe Disposal, pp 853-854, ISBN: 978-1-60423-629-3, American Nuclear Society (ANS), La Grange Park, IL (2006).

[4.33] ELECTRIC POWER RESEARCH INSTITUTE, Extended Storage Collaboration Program International Subcommittee Report: International Perspectives on Technical Data Gaps Associated with Extended Storage and Transportation of Used Nuclear Fuel, Rep. 1026481, EPRI, CA (2012).

5. BOLTED CLOSURE SYSTEMS OF DRY STORAGE CASKS

5.1. DESCRIPTION OF TYPICAL BOLTED CLOSURE SYSTEMS

Bolted closure systems are an essential component of dry storage casks ensuring the long term safe enclosure of the radioactive inventory. In general, those casks consist of a thick walled monolithic ductile cast iron or a welded forged steel body closed by a single or double barrier lid system. Often, the cask design is used for transportation and storage purposes (dual purpose casks or DPCs). For transportation, a single barrier lid system is enough to fulfil international and national requirements for the safe enclosure under normal operation and under Type B test conditions, representing severe accident scenarios. For long term interim storage purposes, casks are usually equipped with an additional second barrier lid system including continuous monitoring of proper sealing function. This ensures redundancy in case of a hypothetical loss of seal function and a repair concept is approved concerning primary lid seal change in a nearby hot cell or SNF pool if available, or the double barrier lid system needs to be re-established by a third lid (usually welded) on site.

Bolted closure systems are usually equipped with metal seals to provide the long term confinement function. For proper control of seal function by helium leakage rate measurement during the assembling procedure or later, a second seal adjacent to the first seal is used to evacuate a specific test volume. Therefore, metal seals (e.g. as double metal seal) or also elastomer seals or a combination of both are suitable. Usually, the second seal of each barrier does not belong to the safety-relevant closure system and is necessary for demonstrating proper barrier seal function after lid closure. In any case, the long term proper safety function of the barrier seals has to be demonstrated adequately.

Typical double barrier bolted closure systems are those of CASTOR® cask types (see Fig. 5.1), equipped with a combination of metal and elastomeric auxiliary seals.

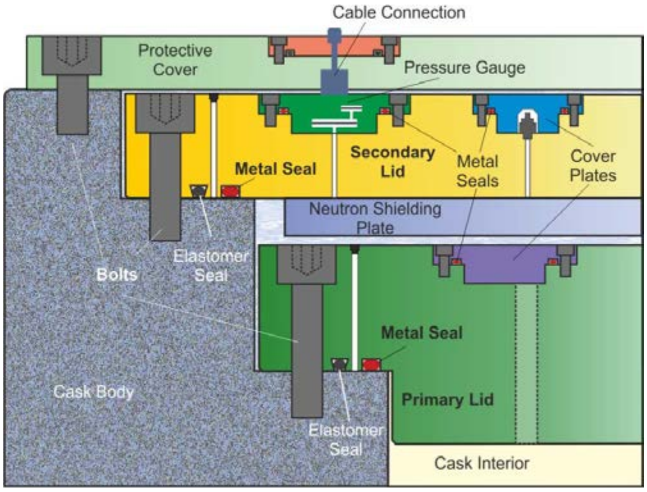

(a) (b)

FIG. 5.1. (a) Typical double barrier bolted closure system of CASTOR® cask types [5.1]; (b) A metal seal of the HELICOFLEX® type (reproduced courtesy of Bundesanstalt für Materialforschung und -prüfung (BAM)).

Due to stringent requirements for barrier seal leak tightness for several decades of operation, constant pressure forces and tight contact conditions between the metal surfaces are essential. Common seal types include an inner helical spring (e.g. made of a nickel alloy) for constant pressure force, an inner layer (e.g. made of stainless steel or nickel alloy) to distribute pressure forces, and a flexible outer layer (e.g. made of aluminium or silver) for the tight contact between the barrier seal and cask body or lid surfaces respectively. Figure 5.1 shows an example of such a typical metal seal of the HELICOFLEX® type. In addition, double metal seals or metal seals with just one aluminium or silver coated steel layer exist. The elastomeric O-rings are usually made of silicon rubber (VMQ), fluorocarbon rubber (FKM) or ethylene propylene diene rubber (EPDM).

5.2. RELEVANCE FOR SAFETY

Casks for transportation and storage (called dual purpose casks or DPCs) usually contain all relevant safety functions for the safe and secure operation whether during public transportation or nuclear site operation. The major safety function of their bolted closure systems is the safe enclosure (confinement) of the radioactive inventory under all relevant operational and accidental conditions during storage and previous or subsequent transportation. In addition, dual purpose casks include shielding and decay heat removal functions, and they ensure subcriticality under all circumstances. Thus, they contain all major safety functions during transportation and storage.

Regulatory requirements exist for public transportation concerning limited potential activity releases under normal operation and test conditions. Usually the internationally-agreed requirements are implemented in the national regulations, e. g. for the safe transportation of dangerous goods. For storage, identical safety goals apply, but in this case specific national regulations and requirements under consideration of site specific or country specific boundary conditions for normal operation and accident scenarios exist. Due to a broad spectrum of inventories, with a potential release of radioactive elements, and the need for standardized system quality demonstrations during the manufacturing and assembling procedures, a specific acceptable leakage rate needs to be defined (e.g. a standard helium leakage rate $Q_{He/St}$ of 10^{-6} or 10^{-8} $Pa{\cdot}m^3{\cdot}s^{-1}$). This required leakage rate does not only consider activity release limitations but also quality assurance aspects regarding proper manufacturing as well as assembling conditions (e.g. adequate surface quality and conditions, complete compression of the bolted lid system) for the specific seal type and lid system. Usually, under storage conditions, DPCs are equipped with a double barrier lid system consisting of two independent lids (primary and secondary lid) to cover a hypothetical barrier seal failure. Additionally, the interspace between the two lids is filled with over-pressurized inert gas and permanently monitored to identify potential pressure loss due to seal failure during storage. Alternatively, some designs use the interspace between double metal seals for leak tightness monitoring.

5.3. POTENTIAL AGEING MECHANISMS AND DATA GAPS FOR EXTENDED STORAGE

For sealing systems, the performance of the barrier seals during long term storage is crucial and ageing effects to the seal function may endanger safety goals. Basically, potential corrosion effects should be principally excluded by qualified assembling procedures to ensure dry and inert conditions. Furthermore, the thermo-mechanical reduction of the initial compressive force in connection with a reduction of the ‘usable resilience’, which is defined as the potential elastic recovery of a seal (in mm) without exceeding the acceptable standard helium leakage rate (see Fig. 5.2), is a major issue. Therefore, for all types of seals the time-dependent sealing performance needs to be determined for the relevant spectrum of thermal and mechanical loads. For elastomeric materials, radiological ageing also has to be considered, whereas metal seals should not be affected by radiation during cask storage because of limited doses and much higher threshold values at which mechanical properties of metals begin to be affected.

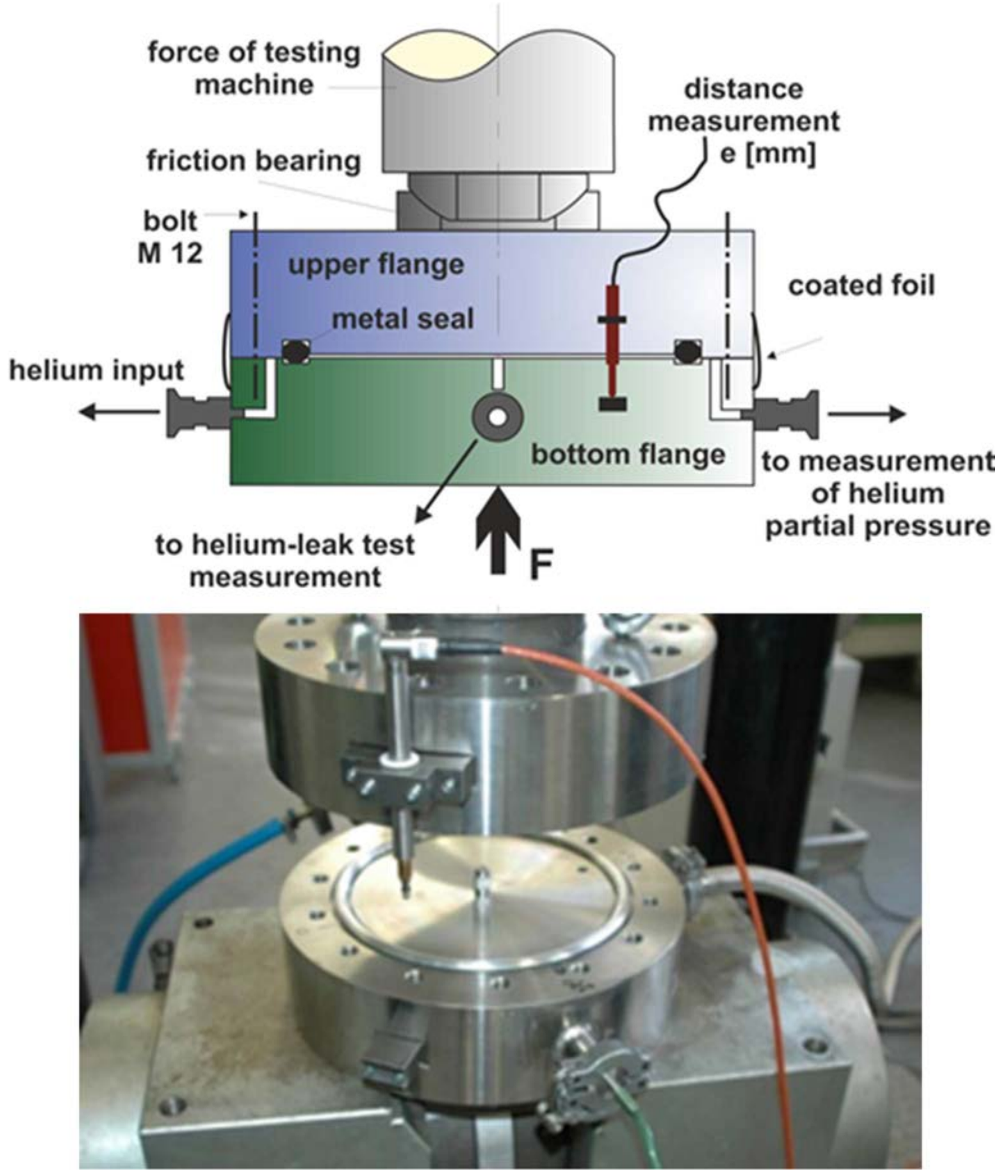

FIG. 5.2. Test equipment for simultaneous measurement of load and leakage rate in a universal testing machine (reproduced courtesy of Taylor&Francis) [5.1].

However, time and temperature effects on metal seals should be carefully assessed to ensure their sufficient long term safety function. Especially degradation of containment functions due to corrosion or creep of metal seals should be taken into consideration. Accordingly, ageing degradation experiments were conducted with metal seals [5.1–5.10]. In addition, a long term containment performance test using full-scale lid models was conducted in Japan from October 1990 until February 2009 [5.11, 5.12]. The results of these experiments are used to develop reliable methods to predict the long term seal performance based on short term test data, such as the Larson-Miller Parameter approach considering the temperature-time relation. This means short term tests at higher temperatures allow extrapolation to longer periods of time at lower temperatures. Usually, maximum seal temperatures during cask operation are around 100°C and decrease significantly over time related to the decay heat descent. However, the Larson-Miller approach needs to be carefully evaluated by experimental data for every specific seal type as there is usually no simple ‘material’ constant available covering the full temperature and time range.

As polymeric materials are more sensitive to radiation and temperature than metals, the radiation exposure conditions for safety-related elastomeric seals should be determined. The primary irradiation alteration mechanisms of polymer material systems are radiation-induced changes by gamma radiation causing polymer chain scission, cross linking, or both, that lead to degradation of the polymer. In addition, the release of gases during degradation, for example, possibly corrosive fluorine or hydrogen from an elastomeric seal must be considered for any potential secondary effect of the gases on safety functions of storage system components such as corrosion of metal barrier seals. It should be outlined again that, usually, elastomer seals do not belong to the safety relevant closure system of DPCs, and in this case, the degradation behaviour of elastomer seals is of minor importance for long term safety. An overview of ageing behaviour studies for elastomer seals can be found in [5.13–5.28]. Regarding the overall gap as shown in Table 5.1, medium (and high) ranked data gaps related to thermo-mechanical creep and degradation effects of metal seals and degradation mechanisms of elastomer seals were partially addressed by the investigations within this Coordinated Research Project (CRP) and as described in Subsections 5.4 and 5.5.

TABLE 5.1. VERY LONG TERM STORAGE TECHNICAL NEEDS FOR STRUCTURES, SYSTEMS AND COMPONENTS (SSCs): SUMMARY OF 'IMPORTANCE TO R&D ASSESSMENTS' (ADAPTED FROM [5.29])

Structures, systems and components (SSCs)	**Ageing alteration and/or degradation mechanism**	**TECDOC chapter in which the gap is addressed**
Fuel cladding	Annealing	n.a.
	Hydrogen embrittlement	3
	Hydride cracking	3
	Oxidation	3
	Creep	3
Fuel pellets	Cracking, bonding	n.a.
	Oxidation	3
Fuel assembly hardware	Corrosion and stress corrosion cracking (SCC)	n.a.
Basket	Corrosion, irradiation	n.a.
Neutron shielding	Thermal and radiation ageing	6
	Creep	6
	Corrosion	6
Neutron poison	Creep	n.a.
	Embrittlement	n.a.
	Corrosion	n.a.
Welded canister	Atmospheric corrosion	2
	Aqueous corrosion	n.a.
Moisture absorber	Irradiation, thermal	n.a.
Bolted casks	Fatigue of seals or bolts	5
	Atmospheric corrosion	n.a.
	Aqueous corrosion	n.a.
	Metal seal creep	5
Concrete overpack, cask, or pad	Freeze-thaw	4
	Corrosion (including embedded steel)	4

Note:

A few of these ageing mechanisms are not detrimental to maintaining safety functions.

5.4. OUTCOME OF WORK AT BUNDESANSTALT FÜR MATERIALFORSCHUNG UND -PRÜFUNG (BAM), GERMANY

The investigation of bolted closure systems for dry storage casks in Germany is mainly performed by BAM. The work is focused on the behaviour of the metal seals being responsible for the safe enclosure and to a certain amount on elastomer seals.

5.4.1. Metal seals

In 2009, an extensive investigation program on the described metal seals of HELICOFLEX® type (Fig. 5.1) was initiated (for details, see [5.1]). HELICOFLEX® metal seals are used in Germany and also in other countries (e.g. France, Japan and USA). The characteristic mechanical behaviour of HELICOFLEX® seals can be illustrated by their load–deformation relationship during compression and relieving procedures (Fig. 5.3 [5.1]). In Germany, the main criteria for sufficient leak tightness of such seals after assembly is the standard helium leakage rate $Q_{He/St}$, which is calculated using Eq. (5.1):

$$Q_{He/St} = \Delta p(V/t) < 10^{-8}\ Pa.m^3.s^{-1} \tag{5.1}$$

where
Δp is the pressure difference (Pa);
V is the volume (m^3);
t is the time (s).

The value of $Q_{He/St}$ has to be demonstrated for each metal seal used in casks and it also sets up the evaluation level for the experimental investigations at BAM. Therefore, the characteristic points Y_0, Y_1 and Y_2 of the load-deformation curve are of special interest (Fig. 5.3). The vertical axis 'Load' represents the seal force per length in N/mm. The distance between Y_2 and Y_1 in terms of the deformation represents the ability of the seal of elastic recovery of its deformation and is denoted as 'useable resilience' r_u. In case of real casks, an exceeding of $Q_{He/St}$ may be caused either by mechanical loads under accident scenarios or by reduction of the restoring seal force F_r due to time depending creeping processes of seals and/or screws.

For the test series seals with a smaller overall diameter compared to full-scale cask lid seal diameters are used to allow appropriate dimensions of the test setup. However, their cross-section diameter of about 10 mm as well as materials and dimensions of spring and jackets are identical to the original cask seals to yield representative test results.

Figure 5.2 displays the BAM test flange system including the screw connection and groove geometry principle for seal compression up to the operating point at the flange surfaces' contact position.

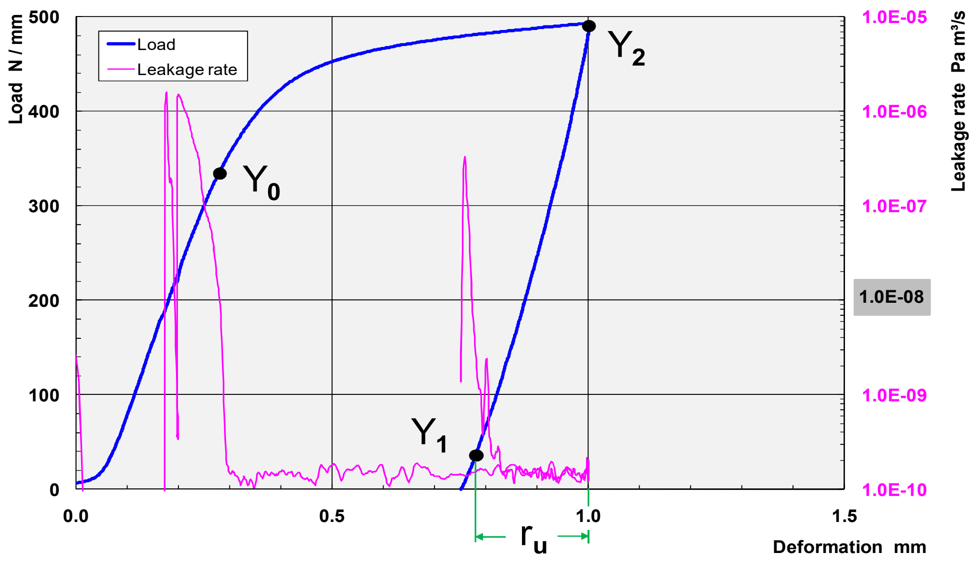

FIG. 5.3. Characteristic load-deformation relationship of a HELICOFLEX® seal with outer silver jacket with respect to standard helium leakage rate $Q_{He/St}$ (reproduced courtesy of Taylor&Francis)[5.1].

The terms in Fig. 5.3 are:

- Y_0: initial amount of deformation to achieve $Q_{He/St}$ during compression;
- Y_1: deformation at which the leakage rate no longer exceeds $Q_{He/St}$ during load relieving;
- Y_2: operation point; and
- r_u: useable resilience during load relief at which the required leakage rate, $Q_{He/St}$, is no longer exceeded [5.1].

The upper portion of the blue curve in this figure is the deformation path according to manufacturer specification.

In a first step of the investigation program test series, tests were performed using various of axial compression loads. A test series with static and dynamic (cyclic) loads were also completed [5.5].

With respect to long term storage, creeping of seals that is dependent on time and temperature is mainly responsible for loss of the sealing function in accordance with the intended use of casks and in case of accident conditions. Regarding compression force reduction at the operating point Y_2 and thus with regard to the reduction of the useable resilience r_u due to time and temperature depending creeping processes, seals with outer jackets made of aluminium and silver are under investigation. Maximum temperatures in the seal area of cask lid systems of about 110°C occur at the beginning of storage. The exact peak seal temperatures depend on cask design and SNF decay heat. Since higher temperatures usually accelerates ageing mechanisms, BAM decided to perform a test series using constant temperatures of 20°C, 100°C and 150°C, which have been started in 2009 and 2010. To rely on a broader data basis, tests at additional temperature levels (75°C and 125°C) have been started in 2014. Measurements of the remaining compression force, useable resilience and leakage rate have been performed periodically. Details of the procedure are described in [5.1]. Example test data gained so far are given in Fig. 5.4.

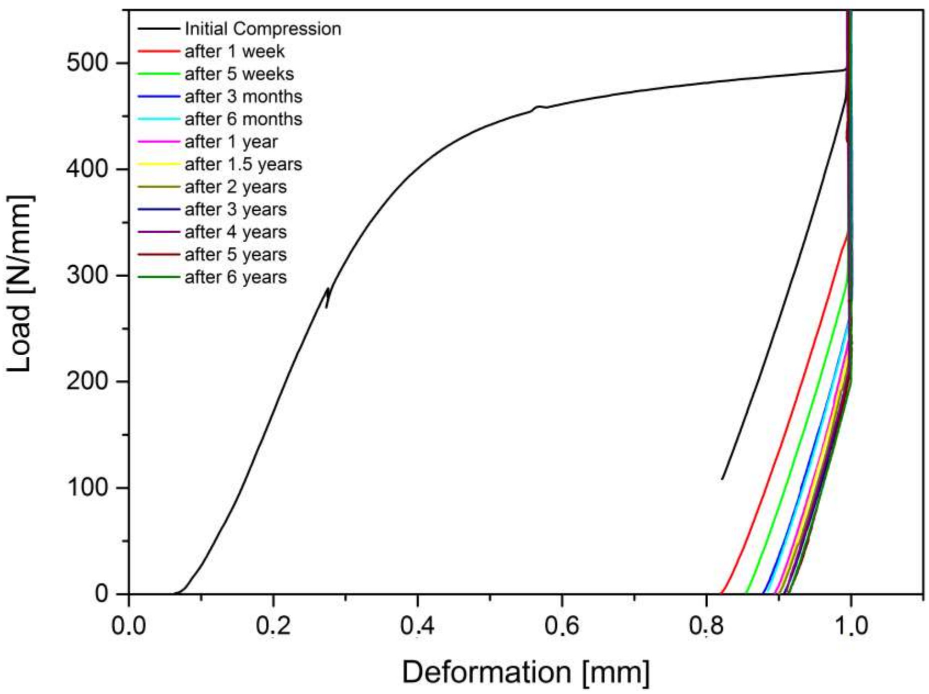

FIG. 5.4. Results of long term experiment of a compressed Ag-seal at 150°C. Reduction of restoring seal force 'load Fr' and useable resilience r_u depending on time and temperature due to creep (reproduced courtesy of Bundesanstalt für Materialforschung und -prüfung (BAM)).

As a consequence of restoring seal force Fr and useable resilience r_u reduction over time, safety margins until loss of the specified leakage rate also diminish. On the other hand, the test results have demonstrated that the specified leakage rate of 10^{-8} $Pa{\cdot}m^3{\cdot}s^{-1}$ is exceeded until nearly complete load relieve due to creeping and plasticization of the outer seal jacket material (Fig. 5.4).

For investigation of the time and temperature dependent F_r and r_u behaviour, Figs 5.5 and 5.6 show exemplary that there could be identified nearly linear correlations in a half-logarithmic scaling. Comparable correlations could be shown for Ag-seals. This allows for an extrapolation to much longer time periods of time in case the trend is confirmed further on by continuation of the test series. In addition, development of a validated predictive model based on the Larson-Miller relationship [5.13] has been started. This would allow correlating time and temperature by an analytical approach. Thus, data from tests at higher temperatures for shorter periods of time could be used to determine the seal behaviour at lower temperature levels for much longer periods of time. The overall aim of the predictive method is to establish accelerated test conditions to generate data with which reliable predictions can be made of the long term behaviour of metal seals used in bolted closure systems of dry interim storage and transportation casks.

There are already several investigations taking account of the Larson-Miller relationship to describe the time and temperature dependent behaviour of metal seals [5.4, 5.12]. Basically, Larson and Miller [5.13] have used the time and temperature relationship to describe rupture and creep stresses by the basic correlation Larson-Miller Parameter LMP as shown in Eq. (5.2):

$$LMP = f\{T\,(C + \ln(t))\} \tag{5.2}$$

where
t is the time (h);
T is the temperature (K);
C is a material constant.

The LMP will be a best-fit straight line on a log-linear plot of either the load versus test time (Fig. 5.5) or the useable resilience versus test time (Fig. 5.6).

A major presumption in that case is a constant material parameter C for the entire test parameter range. As typical metal seals are not just a material but a more or less complex construction from different materials, some test results have shown that C varies with time. Therefore, there is the need for further investigations including long term tests and on the development of a validated analytical approach considering also uncertainties in test data and their effect on extrapolation.

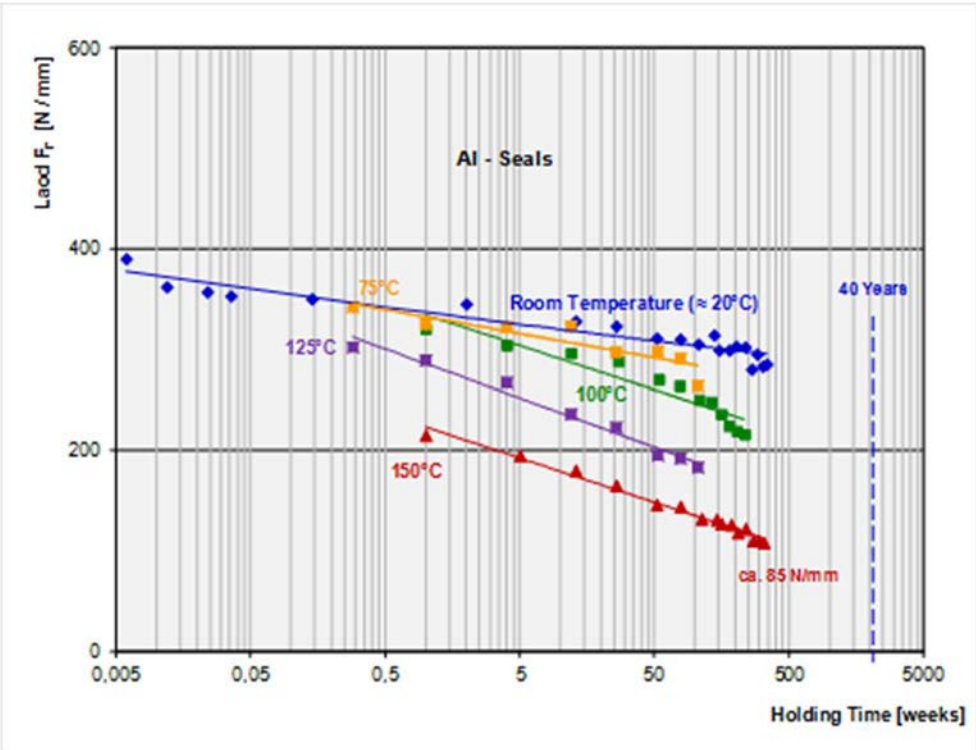

FIG. 5.5. Reduction of restoring seal force F_r depending on holding time and temperature for Al-seals (reproduced courtesy of Bundesanstalt für Materialforschung und -prüfung (BAM)).

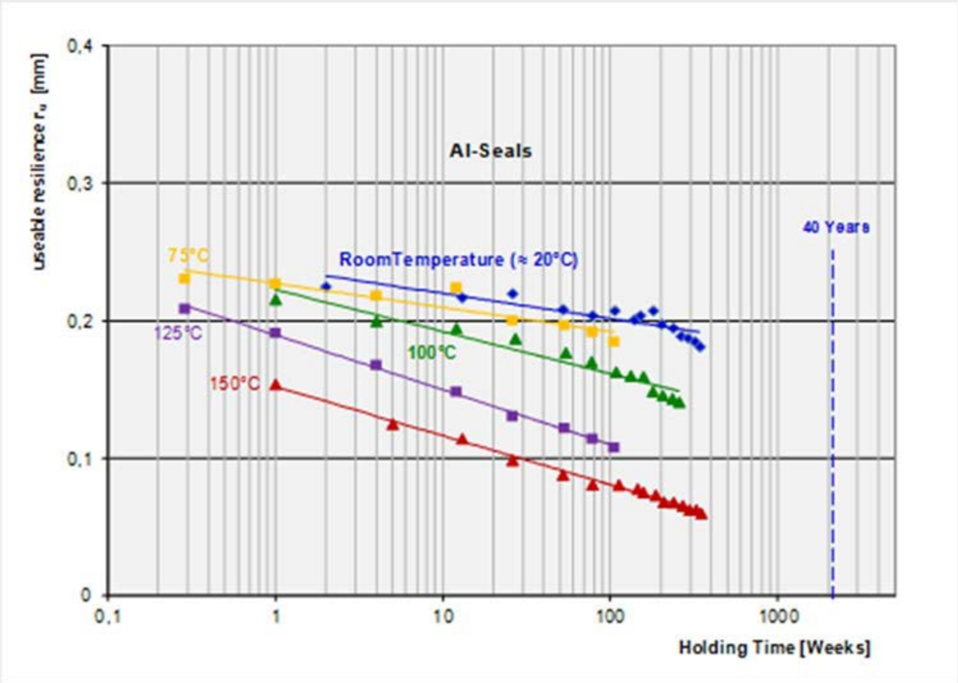

FIG. 5.6. Reduction of useable resilience r_u depending on holding time and temperature for Al-seals (reproduced courtesy of Bundesanstalt für Materialforschung und -prüfung (BAM)).

The performed investigations focus on the time (and temperature) dependent decrease of the restoring seal force F_r and the useable resilience r_u. Up to April 2016, experiments have been running for time periods of up to almost 6 and a half years at three different temperatures (20°C, 100°C and 150°C). The results show mainly linear correlations over time by logarithmic time axis scaling. However, some deviations occurred during the measurements at room temperature (RT) and at 100°C and need to be clarified by continuation of the tests before an extrapolation for longer periods of time is possible. In addition, tests at two more temperatures (75°C and 125°C) were running for two years since early 2014. Their results are consistent with earlier measurements at the other temperatures.

The seal characteristics determined from the investigations were analysed by a time (and temperature) dependent parameterization based upon the Larson-Miller relationship. The presented results indicate that the LMP provides only a rough approximation of the BAM test results. The material parameter C depends at least on temperature but may also depend on time. If applicable, appropriate adjustments or extensions of the Larson-Miller approach should be developed to improve the accuracy and reliability of long term predictions. On this topic, further investigations on, for example, additional seal types and further time-temperature relationships are necessary as well.

More detailed information and results can be found in the final project report (see Annex IV).

5.4.2. Elastomer seals

For investigating the ageing of rubber seals, three materials were selected: HNBR, EPDM and FKM. EPDM and FKM types are used in containers for radioactive waste. However, the tested types were not the ones actually used in the containers. Instead, typical commercially available grades of the respective type were tested. Additionally, a HNBR type seal was investigated as it is another high-performance sealing material that is resistant to oils.

The O-rings used had an inner diameter of 190 mm and a chord diameter of 10 mm. In order to assess the impact of ageing on seal function as well as the influence of compression on degradation, O-rings were aged under compression (25% of the initial chord diameter), both between plates for measuring compression set (Fig. 5.7(a)), and in flanges that allowed leakage rate measurements (Fig. 5.7(b)). In addition, long term compression stress relaxation measurements were performed on O-ring segments. Furthermore, uncompressed O-rings were aged on racks of punched sheets (Fig. 5.7(c)) in order to compare O-rings aged uncompressed and in compression. For investigating some material properties for which the O-ring geometry is not suitable or when O-rings give distorted results because of diffusion-limited oxidation effects, sheets with a thickness of 2 mm were aged and suspended from racks to allow good oxygen access from all sides. Ageing was performed in air-circulating ovens at 75°C, 100°C, 125°C and 150°C. Ageing periods were chosen to be 1 day, 3 days, 10 days, 30 days, 100 days, 0.5 year, 1 year, 1.5 years, 2 years, 2.5 years, 3 years, 3.67 years, 4.33 years and 5 years although it was expected that not all samples would actually have such a long lifetime at the applied temperatures, especially at the highest ageing temperature of 150°C. With these time and temperature data, extrapolations using time-temperature shifts and Arrhenius graphs were possible.

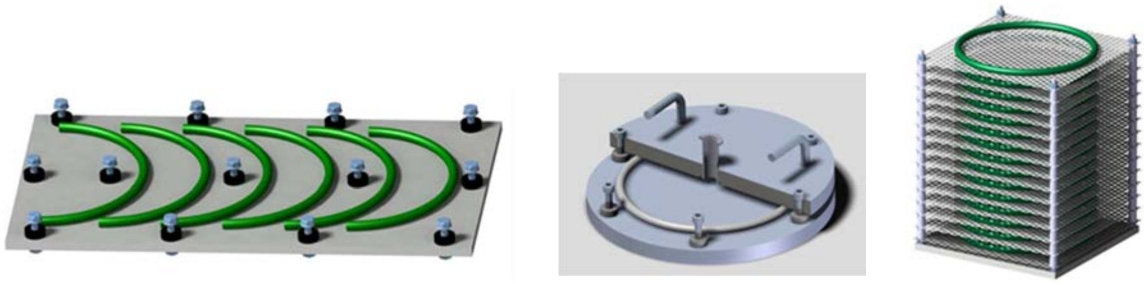

(a) *(b)* *(c)*

FIG. 5.7. (a) Half O-rings ready for compression between plates; (b) O-ring in flange for leakage rate measurements; (c) Uncompressed on punched sheets (reproduced courtesy of Bundesanstalt für Materialforschung und -prüfung (BAM)) [5.19].

Major properties determined from the samples are:

- Hardness based on DIN EN ISO 868 using Shore D hardness;
- Compression stress relaxation based on standard DIN ISO 3384 as a method reflecting the loss of sealing force of a compressed seal over time;
- Compression set (CS) based on standards ASTM D395 and DIN ISO 815-1.

CS gives information about the resilience of a compressed seal and is calculated from the initial seal height, the height of the compressed seal and the measured recovered seal height. A CS of 0% would mean a full recovery back to the initial height, while a CS of 100% would mean no recovery from compression at all. Figure 5.8 illustrates resulting CS depending of material, time, and temperature. Figure 5.9 shows the compression set of the compressed samples after ageing.

Further information is given in the final project report (see Annex IV).

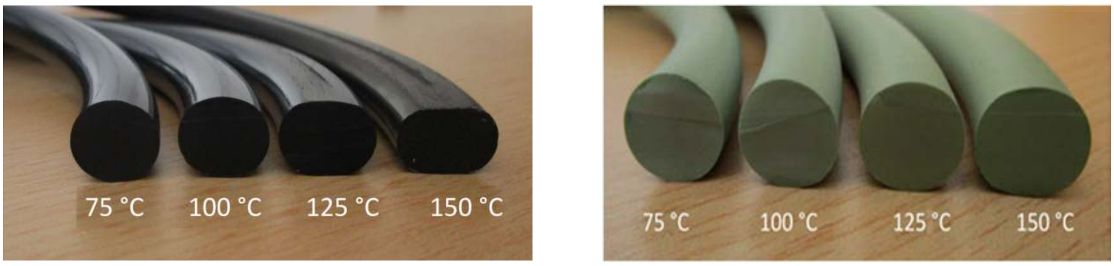

(a) *(b)*

FIG. 5.8. Compression set (CS) after 100 days of ageing at the indicated temperatures for: (a) EPDM; (b) FKM (reproduced courtesy of Bundesanstalt für Materialforschung und -prüfung (BAM)) [5.19].

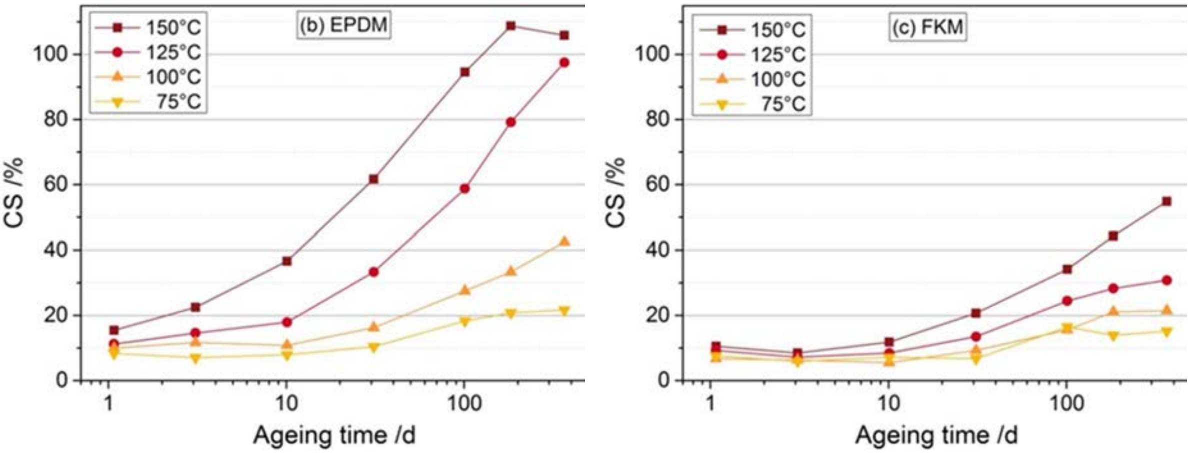

(a) *(b)*

FIG. 5.9. Compression set (CS) vs. ageing time for: (a) EPDM; (b) FKM (reproduced courtesy of Bundesanstalt für Materialforschung und -prüfung (BAM)) [5.24].

A central issue for lifetime predictions is the choice of the end-of-lifetime criteria. For O-rings, leakage rate is the major characteristic determining service life. For this reason, leakage rate measurements were performed. The point of significant increase of leakage rate would mark the end of the seal lifetime. As shown in Fig. 5.10, the leakage rate improved, i.e. decreased with ageing up to 98 days at 150°C although CS values had already reached more than 82% (HNBR) and 95% (EPDM). An explanation of these results could be the strong sticking of the rubber to the flanges, possibly because no lubricant was used. However, after 184 days of ageing at 150°C, when CS values measured on O-rings compressed between plates had exceeded 100%, EPDM O-rings were completely leaky and one HNBR O-ring became leaky during cooling to -30°C. The remaining two HNBR O-rings at 150°C are now tested at shorter intervals of month for detecting a possible increase of leakage rate prior to failure.

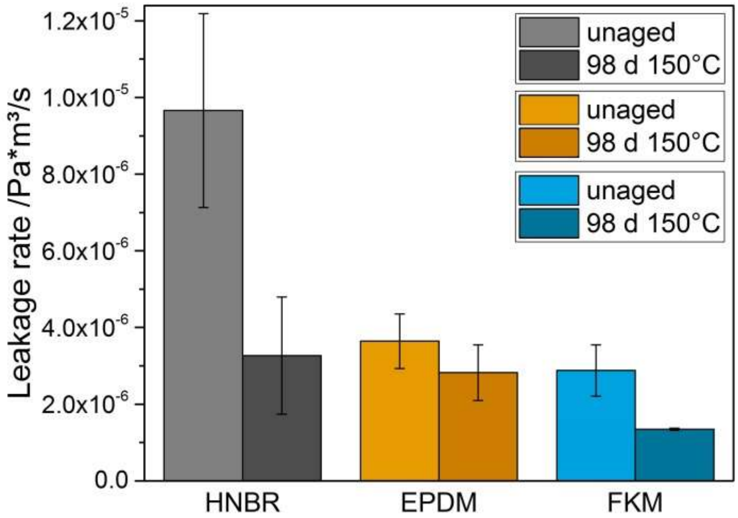

FIG. 5.10. Leakage rates of unaged O-rings and O-rings aged for 98 days at 150°C (reproduced courtesy of Bundesanstalt für Materialforschung und -prüfung (BAM)) [5.24].

In addition to the described study of thermal ageing, the influence of gamma irradiation on low temperature properties of elastomer seals was investigated. These investigations focused on an FKM material produced at BAM (BAM FKM). This compound is based on a copolymer of vinylidene fluoride (VDF) and hexafluoropropylene (HFP). Additionally, a commercial compound was tested (FKM 2). The samples were irradiated by gamma radiation (60Co source) with the following doses: 50 kGy, 100 kGy, 200 kGy, 400 kGy and 600 kGy.

The rubber-glass transition process was studied by differential scanning calorimetry (DSC) and dynamic mechanical analysis (DMA).

Both methods show a continuous increase in the rubber-glass transition temperature with increasing doses. The values of the DMA loss modulus curve lay some degrees higher than the respective values determined from DSC.

The height recovery of an initially compressed seal is emulated by the compression set. As the standardized compression set procedure according to ISO 815-1 and ISO 815-2 is rather time-consuming, an accelerated procedure using DMA was developed and applied to several materials [5.25–5.27]. The compression sample holder was used to measure the DMA compression set CS_{DMA}. With the time-dependent data of the sample height after release d2(t) the CS_{DMA} values can be calculated by using the following Eq. (5.3):

$$CS_{DMA} = \left(\frac{d_0 - d_2(t)}{d_0 - d_1}\right) 100(\%) \tag{5.3}$$

where

d_0 is the initial sample height;

d_1 is the height of the compressed sample;

$d_2(t)$ is the time-dependent data of the sample height after release.

A CS_{DMA} value of 0% means that the sample height returns to its pre-test value after unloading (Fig. 5.11).

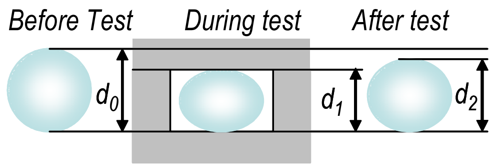

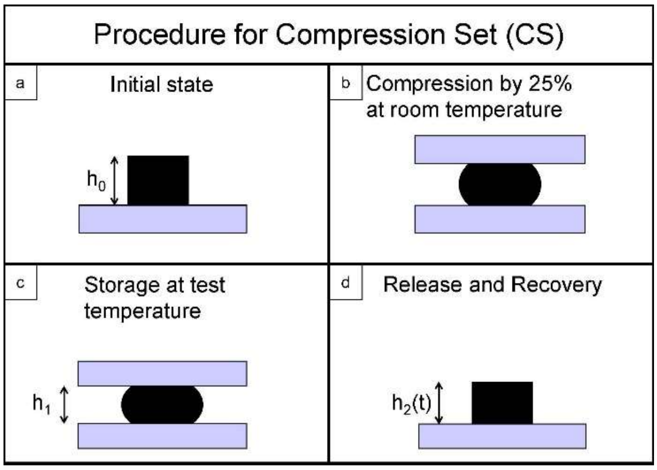

(a) *(b)*

FIG. 5.11. (a) Seal deformation [5.30]; (b) Elastomer seal deformation (reproduced courtesy of Bundesanstalt für Materialforschung und -prüfung (BAM)).

The measurements were performed at various temperatures between RT and a temperature below the rubber-glass transition. A comparison concerning the effect of the irradiation dose is shown in Fig. 5.12 for a temperature of -15°C.

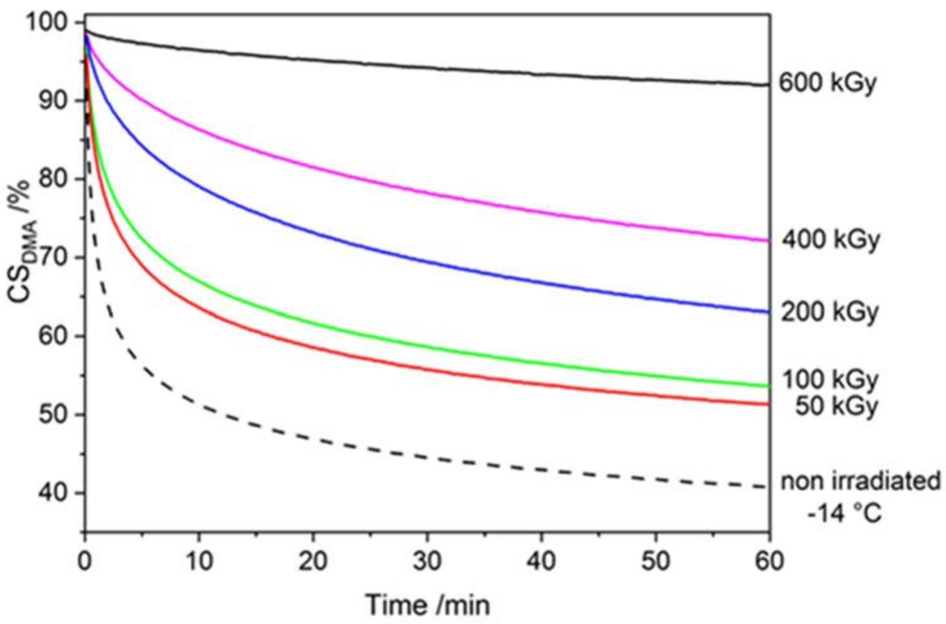

FIG. 5.12. Time dependency of compression set for BAM FKM with varying gamma irradiation dose measured at -15°C (except unirradiated sample) (reproduced courtesy of IAPSAM) [5.28].

The compression set at -15°C rises with increasing irradiation dose. Figure 5.12 shows that, in this temperature range, 30 minutes after release, an unirradiated sample has less than 50% compression set whereas a sample irradiated with 600 kGy shows more than 90% compression set.

Gamma irradiation of fluorocarbon rubbers leads to substantial changes of material properties, e.g. it influences the rubber-glass transition. Due to predominant cross-linking reactions, the rubber-glass transition is shifted to higher temperatures. This effect is not detectable by a standard hardness measurement but can be shown clearly by thermoanalytical methods and compression set measurements.

Leakage rate measurements have shown that O-rings remain leak tight even when other properties, such as CS, already indicate substantial degradation. This highlights that the choice of the end-of-lifetime criterion has a large influence on the predicted lifetime and that standard criteria referring to material properties do not necessarily correlate with component functions such as static leakage rate.

Further ageing especially at the lower ageing temperatures will yield non-diffusion-limited oxidation affected CS values and leakage rates. More CS data will also increase confidence in the time-temperature shifted master curves and resulting Arrhenius diagrams.

The selected ageing conditions have to be considered as rather conservative as in application the available amount of oxygen is limited by the design of a bolted lid closure system. Also, the irradiation doses were chosen rather high to cover the whole range of potential applications.

5.5. OUTCOME OF WORK AT CENTRAL RESEARCH INSTITUTE OF ELECTRIC POWER INDUSTRY (CRIEPI), JAPAN

5.5.1. Long term confinement performance tests of metal seals using small scale and full-scale test models [5.30]

To demonstrate the confinement performance of metal seals, confinement performance tests using full-scale lid models were carried out. Figure 5.13 shows two kinds of cask lid structure models chosen for the tests. The models represent the upper parts of typical full-scale metal casks and were placed in a non-air-conditioned building. In both models, electric heaters were installed in the cask cavities to maintain a constant temperature and the lids were closed in a dry condition.

The design of the Type I model is based on a TN-24 cask design. The cask body and lids were made of forged carbon steel, while the sealing surfaces were overlaid with stainless steel welding (SUS304). For lid sealing, double metal seals with inner Inconel® and outer aluminium jackets and cross-sectional diameters of 6.1 mm were assembled.

The design of the Type II model is based on the CASTOR® cask design. Cask body and lids were made of ductile cast iron and stainless steel, respectively, while the sealing surfaces of the cask body were plated with nickel. For lid sealing, an inner metal seal with an inner Inconel® and outer silver jacket and an auxiliary silicone rubber seal were assembled. The cross-sectional diameter of the seals was 10 mm.

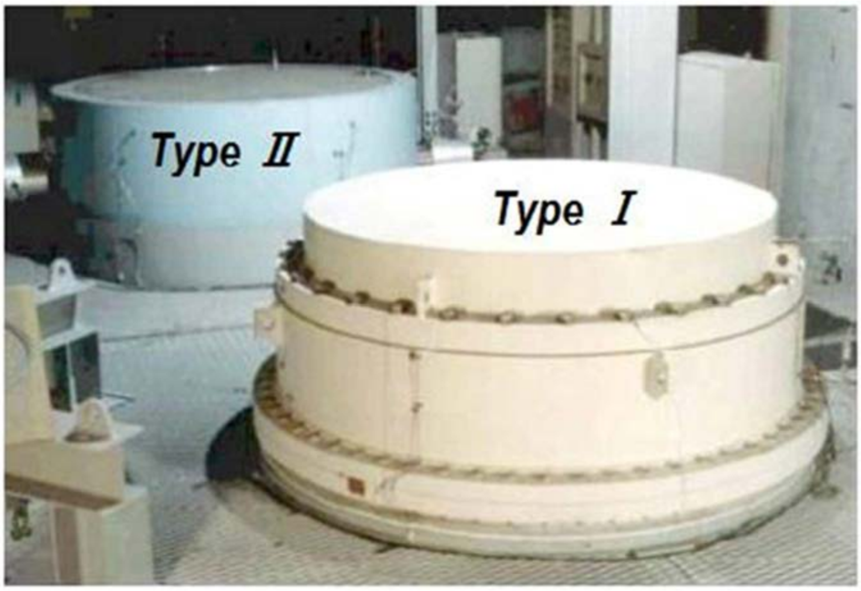

FIG. 5.13. Photograph of test models: Type I representing TN-24 cask design and Type II representing CASTOR® cask design (reproduced courtesy of IAPSAM) [5.30].

To determine appropriate temperature conditions for the tests, thermal analyses were carried out with finite element models using the ABAQUS code. Temperature distributions over time were calculated. Based on the calculated maximum temperature of the primary lid seal, the test temperature of the primary lid seal was set and conservatively kept constant at 160°C during the tests neglecting decay heat decrease over time. After closing the secondary lid, the inner spaces between the primary and secondary lids were filled with helium gas at 0.4 and 0.6 MPa for Types I and II, respectively. To permanently control seal and ambient temperatures and pressure levels between the lids, thermocouples and pressure sensors were installed. The helium leakage rates of the secondary lid seals were measured up to twice a month. For technical reasons, measurements of primary lid leakage could not be performed.

Test results: temperatures of the primary and secondary lids, although slightly affected by seasonal changes of ambient temperatures, remained approximately constant. The secondary lid temperatures of Types I and II were 140°C and 130°C, respectively. The measured helium leakage rates of Types I and II were mainly in the order of 10^{-9} and 10^{-10} $Pa{\cdot}m^3{\cdot}s^{-1}$, respectively, with the lower levels for the seal with the outer silver jacket. The measured helium leakage rates of both secondary lid seals stayed almost constant for more than 19 years (see Fig. 5.14).

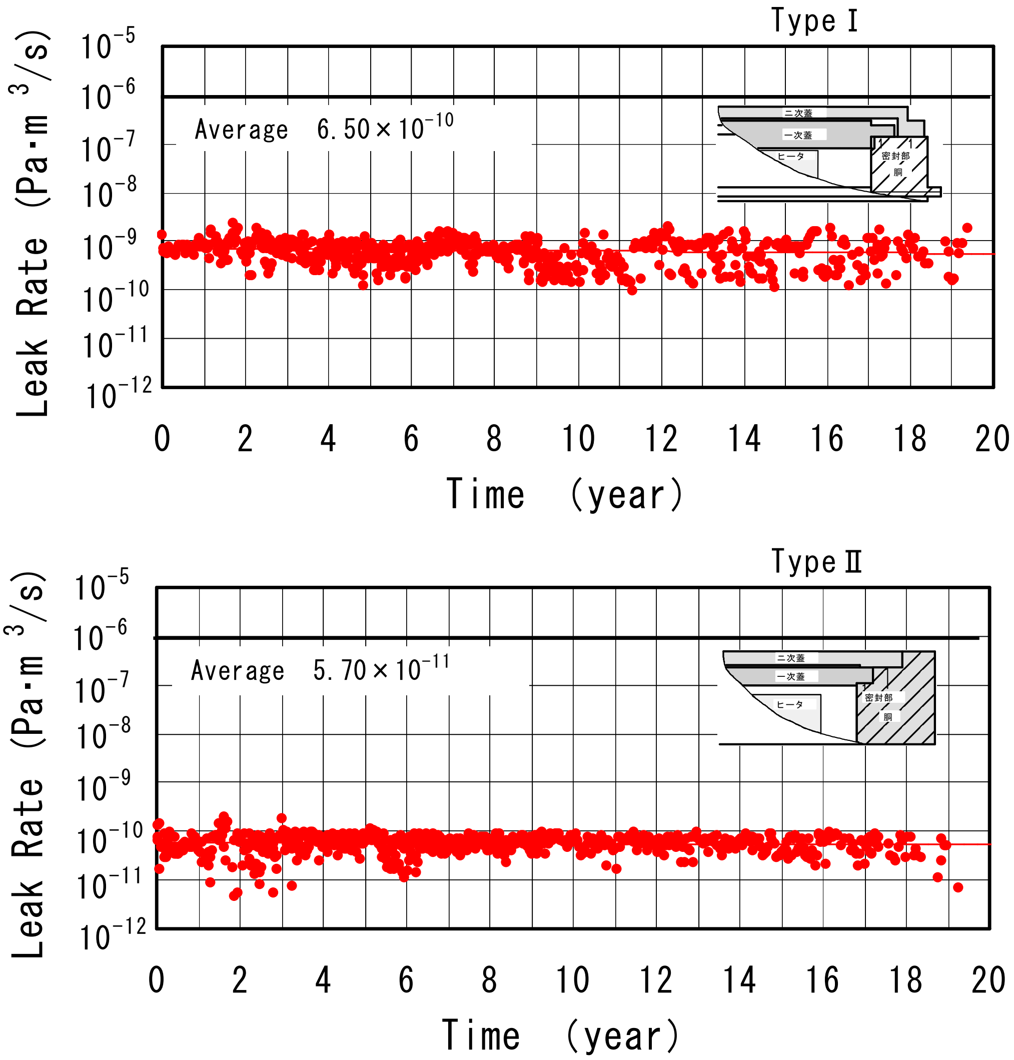

FIG. 5.14. Secondary lid helium leakage rate profiles of test setups: Type I (Al-seal) and Type II (Ag-seal) (reproduced courtesy of IAPSAM)[5.30].

To obtain the leakage threshold, confinement tests using small flange models were carried out under accelerated conditions as shown in Fig. 5.15. This test setup consisted of two bolted stainless steel flanges containing a single metal seal with an outer aluminium jacket and a cross-sectional diameter of 5.5 mm. The test flanges were placed into a heating chamber for a maximum duration of 10 000 hours with a maximum temperature of up to 300°C. Because the melting temperature of aluminium is rather low (660°C), maximum test temperatures above 150°C are critical with regard to an application of the LMP approach to predict the long term performance at lower temperatures.

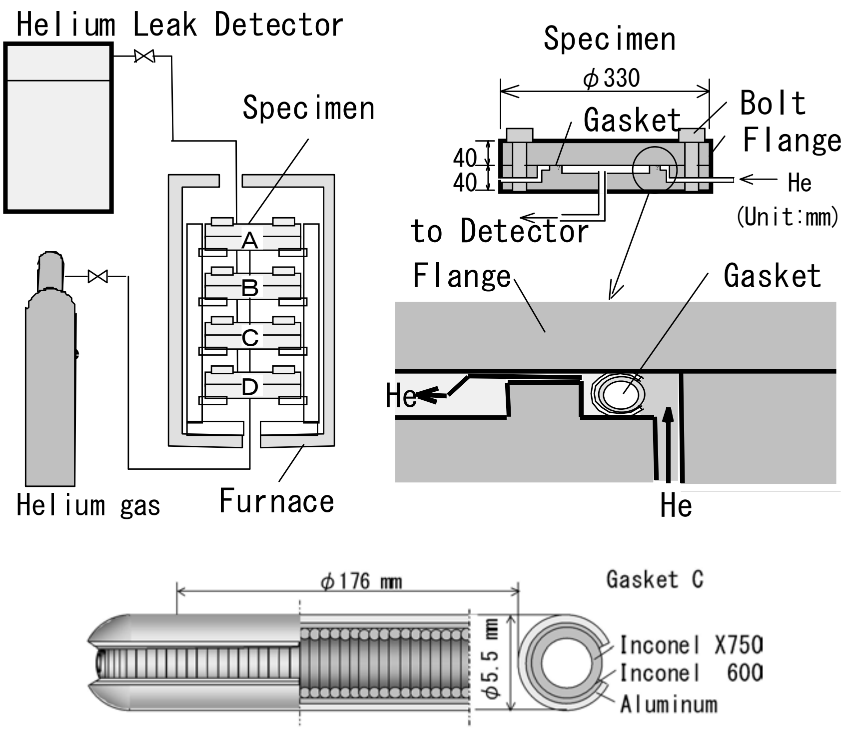

FIG. 5.15. Test setup for accelerated small scale aluminium seal tests (reproduced courtesy of IAPSAM) [5.30].

Figure 5.16 shows an almost linear relationship between the LMP (Eq. (5.2)) and the compression set. In this case, the constant C was set to 14. This C value was tentatively developed by CRIEPI from metal seal tests under consideration of a specific aluminium creep law. For a more accurate determination of the C value which is quite sensitive to the LMP approach, it would be necessary to generate a much broader data base by performing many more seal tests. Figure 5.17 shows the relationship between the LMP and the measured helium leakage rate showing an increase in the helium leakage rate for LMP exceeding about 8000 hours.

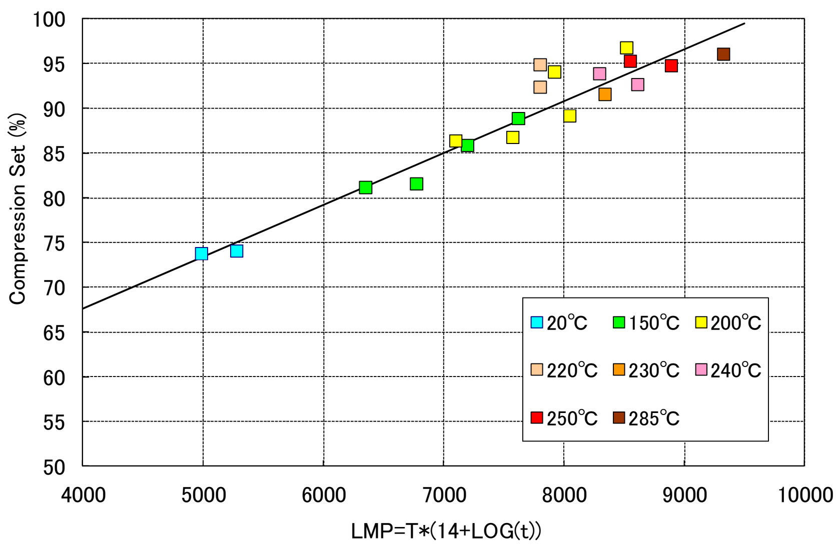

FIG. 5.16. Relation between LMP and compression set (reproduced courtesy of IAPSAM) [5.30].

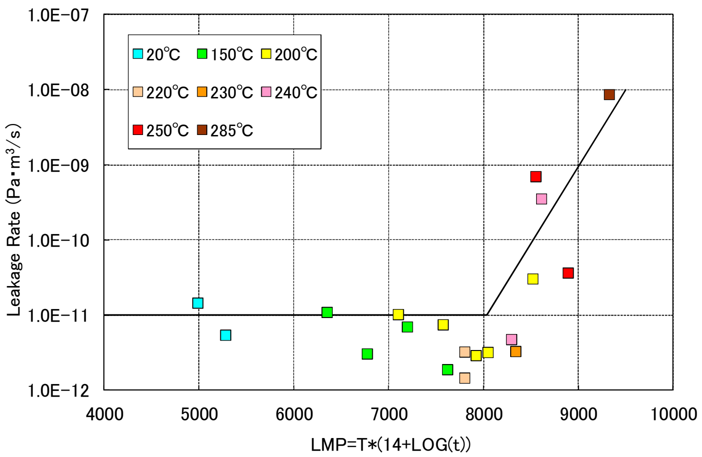

FIG. 5.17. Relation between LMP and helium leakage rate (reproduced courtesy of IAPSAM) [5.30].

The calculated LMP for the secondary lid metal seals of the full-scale tests of Types I and II using the measured temperatures were 7942 (aluminium seal) and 7781 (silver seal). As mentioned before, the constant value C was set to 14. Due to the lack of enough material data concerning silver, the same C value was used for both materials. The LMP of 7942 is below the threshold value taken from Fig. 5.17 and hence the measured leak-tightness consistent with the small scale tests.

To investigate the potentially critical increase of leakage rates due to time-temperature effects of the seal materials, an experimental long term ageing test programme was conducted with a large number of mock-ups consisting of two symmetric flanges holding tightened HELICOFLEX® seals as shown in Fig. 5.18. This test programme was a collaboration between Commissariat ’ l'énergie atomique et aux énergies alternatives (CEA) Technetics Group (France), Gesellschaft für Nuklear-Service (GNS, Germany) and Central Research Institute of Electric Power Industry (CRIEPI, Japan). Further details can be found in [5.8].

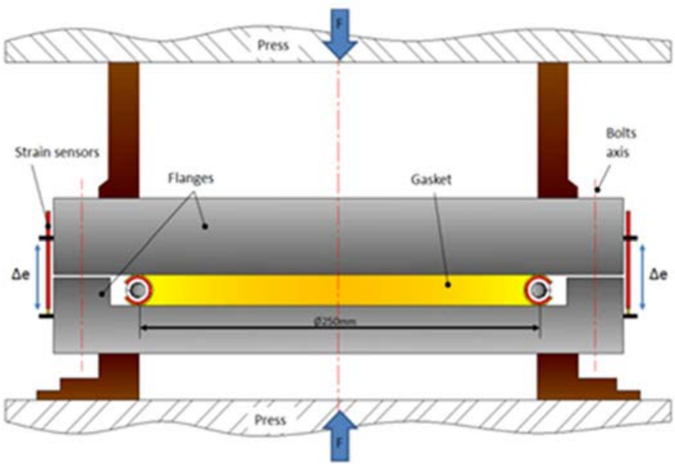

(a) (b)

FIG. 5.18. Long term metal seal test mock-up: (a) Schematic; (b) In a heating chamber (reproduced courtesy of Institute of Nuclear Materials Management (INMM))[5.8].

The inner helical spring of the seals tested in this study is made of Nimonic 90, and the 0.3 mm-thick outer linings consist of pure silver. Two different cross-sectional of diameters 6.2 mm and 8.4 mm are studied. The inner seal jackets consist of 304L stainless steel with a thickness of 0.3 mm and 0.4 mm, respectively. These tests add data regarding the minimum residual linear compressive seal load that can be reached after a certain time at certain temperatures. Concerning the influence of temperature levels on creep kinetics and thus on seal relaxation, the test mock-ups are placed in heating chambers (see Fig. 5.18(b)) at three different constant temperatures: room temperature (RT), 100°C and 200°C. About 40 mock-ups were used for each of the three selected temperatures.

Residual compressive loads and useable resiliencies have been measured after taking the mock-ups from the heating chambers and placing them in a testing machine. Measurements were performed after 10 000, 25 000, 50 000 and 75 000 hours.

Figure 5.19 illustrates the reduction of the compressive seal load when the leakage rate exceeds its threshold value (parameter Y_{2R}) depending on time and temperature. This reduction is mainly driven by plastic deformation of the outer silver lining. Only a few measurements were performed after 5000 hours and below. The data after 10 000 hours were gathered from a different test series compared to the test data after 25 000 hours and beyond (25 000 hours, 50 000 hours and 75 000 hours). The experimental campaign has been continued to up to 100 000 hours so far and will be further continued to gain additional data for a more accurate long term prediction of the seal behaviour. More detailed information is given in the references [5.8, 5.31].

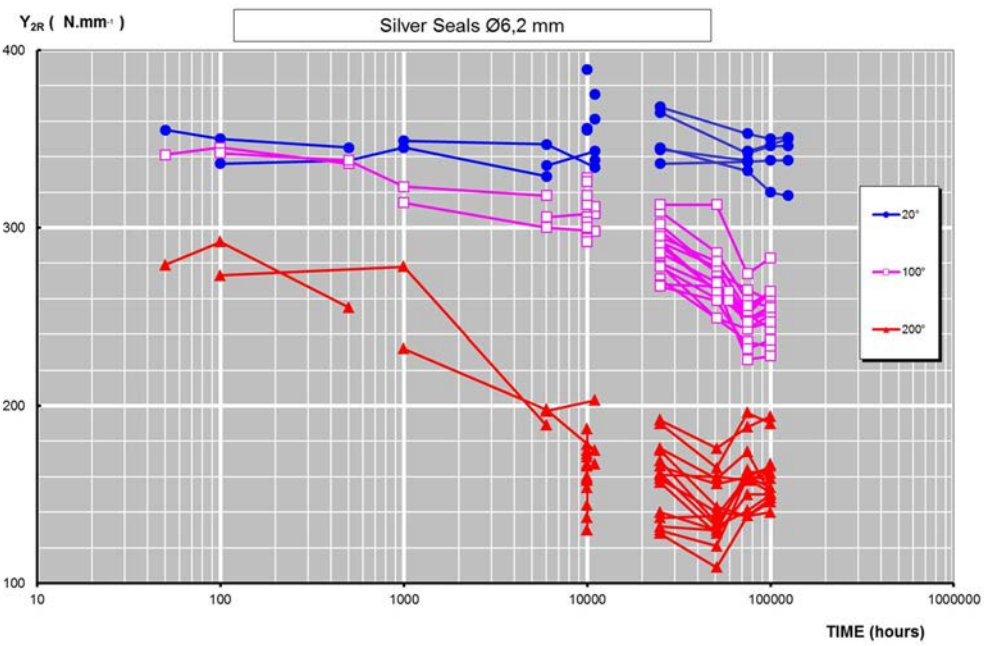

FIG. 5.19. Results from CEA-GNS-CRIEPI long term test programme with HELICOFLEX® metal seals with outer silver jackets: Y_{2R} depending on time and temperature (reproduced courtesy of Institute of Nuclear Materials Management (INMM)) [5.31].

5.5.2. Numerical approach to predict the long term performance of metal seals [5.32]

CRIEPI is developing a numerical analysis method to determine the confinement performance of metal seals. For that purpose, it is important to grasp predominantly the creep characteristics of outer jacket materials. According to the creep strain curves, the strain hardening creep equation can be expressed, referring to the Sassoulas's creep equation, as follows:

$$\varepsilon = (C_1)(e^{C_2 \cdot \sigma})({\varepsilon_c}^{C_3})(e^{-C_4/T}) \tag{5.4}$$

$$\varepsilon_c = (\alpha t)^{1/(1-C_3)} \tag{5.5}$$

where:

ε is the creep strain rate (%/hour);
ε_c is the creep strain (mm/mm);
σ is von Mises stress (N/mm^2);
t is the time (h);
T is the temperature (K);
e is Napier's constant;

$$\alpha = (C_1)(e^{C_2 \cdot \sigma})((1 - C_3)/e^{C_4/T} \tag{5.6}$$

To obtain the coefficient values C1, C2, C3, C4 for silver seals, CRIEPI performed compressive creep tests. According to those test results, these coefficient values were obtained as follows:

$C_1 = 4.30 \times 10^{-8}$;
$C_2 = 0.637$;
$C_3 = -2.01$;
$C_4 = 9120$.

For the numerical relaxation analysis, a non-linear, two-dimensional axis symmetric model was developed according to Fig. 5.20. Outer and inner jackets, upper and lower flanges and the helical spring were modelled with isotropic material, rigid body and equivalent ring pipe, respectively. The maximum deformation of the seal complex was set to the design value of 1.1 mm as well as in the relaxation tests.

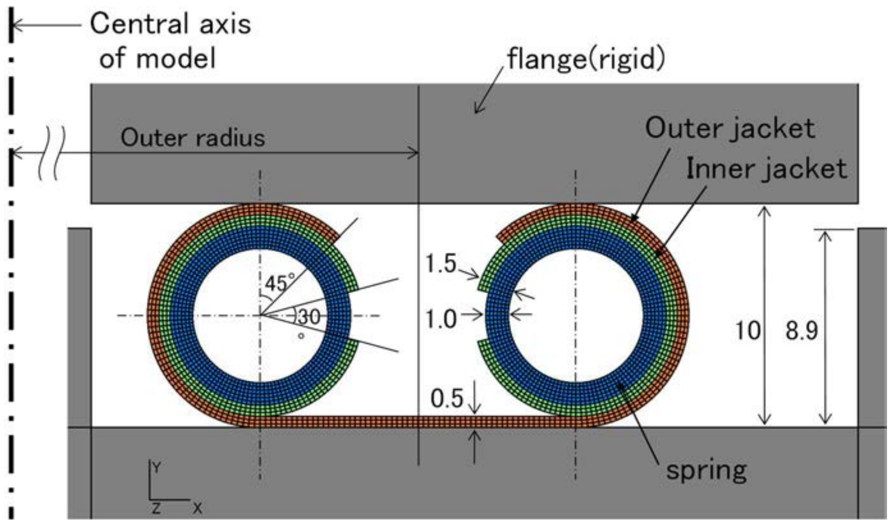

FIG. 5.20. Non-linear two-dimensional axis symmetric metal seal model for numerical relaxation analysis (reproduced courtesy of Institute of Nuclear Materials Management (INMM)) [5.32].

Calculations for the sealing performance residual linear load and spring-back distance caused by the relaxation of the metal seal complex under compressive load and depending on temperature were performed. The applicability of the numerical method was confirmed by comparison of the calculated data and with the relaxation test results.

CRIEPI carried out relaxation tests using metal seals with outer aluminium jackets. The double O-ring test seals had full-scale cross section but smaller circumferential diameter. The seal was compressed to the design value of 1.1 mm and heated to 160°C for 1079 hours. As relevant data the vertical linear seal load, deformation, residual linear load after heating (Y_2), residual linear load when leakage rate exceeds 10^{-8} Pa·m^3·s^{-1} (Y_1) during load relieving, and effective useable resilience distance (r_u) from maximum deformation up to a leak rate exceeding 10^{-8} Pa·m^3·s^{-1}, were measured as shown in Fig. 5.21. The results from the three tests indicate that the residual linear load decreased from 350 N/mm to 212 N/mm due to the relaxation of the heated seal complex. Measurements of Y_1 and r_u resulted in 12 N/mm and 0.12 mm, respectively. For comparison, Fig. 5.21 also illustrates the calculated load-deformation curve showing good accordance with the experimental results concerning Y_{20} and Y_2 values. Just in the early load (deformation phase), the experimental values show a delayed increase due to small initial gaps between the seal components. By estimating the Y_1 value to ~12 N/mm from the numerical analysis, the resulting useable resilience r_u was determined to 0.11 mm which is close to the experimental results. In total, the results show good agreement between the chosen numerical approach and test data for the selected parameters and seal type. The method should generally be applicable to other configurations as well.

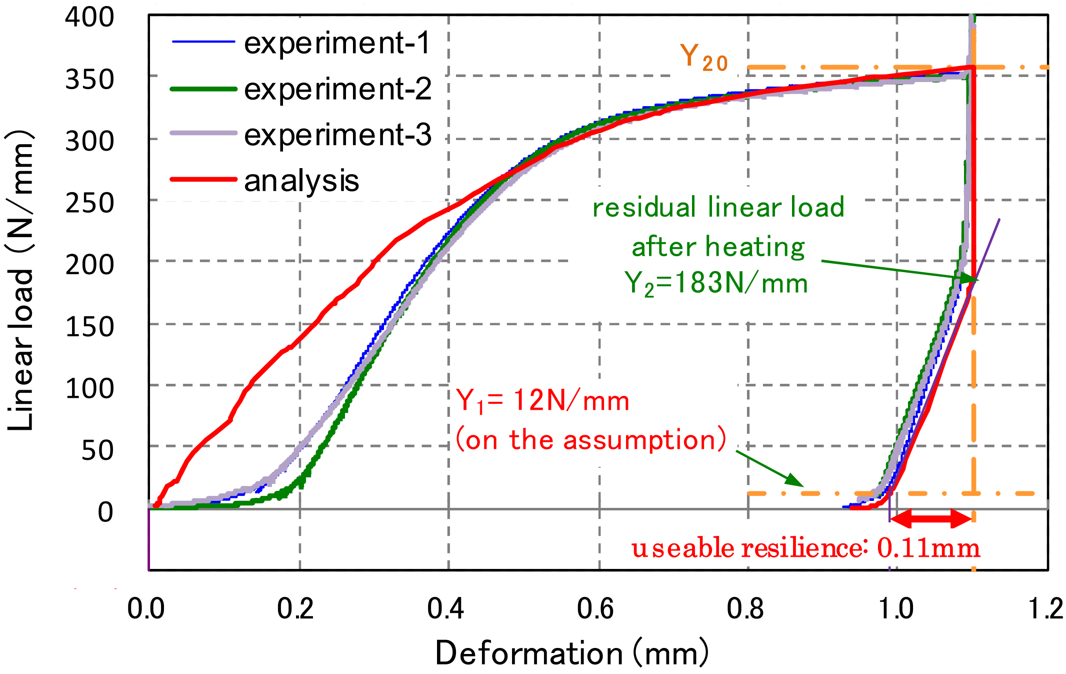

FIG. 5.21. Relaxation test results and numerical simulation of aluminium seals after 1079 hours at 160°C; linear load over deformation (reproduced courtesy of Institute of Nuclear Materials Management (INMM)) [5.32].

5.5.3. Transportation loads on bolted lid systems concerning aged metal seals [5.33]

Transportation loads during sea transport of dual purpose casks equipped with double barrier lid systems may cause critical lid opening displacements for aged metal seals. For that purpose, a finite element calculation was performed under consideration of acceleration measurements set on a cask support frame during actual marine transportation. For the numerical analyses, a full-scale model of the 120-tonne transport and storage cask with an outer diameter of 2.3 m and a length of 5.4 m including the double barrier lid system and the cask inventory was developed. The finite element code used was LS-DYNA.

The calculated lid opening displacements were reasonably low with just up to a few µm. Compared to the remaining useable resilience of r_u = 0.09 mm of aged seals after 60 years at a temperature level of almost 100°C, a sufficient safety margin could be demonstrated. The r_u threshold value was gained from metal seal aging tests at higher temperatures after shorter time periods by applying the Larson-Miller relationship as defined by Eq. (5.2). More detailed information is given in [5.33].

In another test programme, the effects on aged metal seals caused by horizontal sliding of flanges representing bolted lids due to vibration loads during transportation of packages were studied. This investigation addresses potential effects of cyclic metal seal sliding on the leak-tightness. In order to obtain a relationship between the size of lateral lid sliding displacement and the leakage rate, a 1/10-scale model of a lid structure of a typical metal cask was fabricated and assembled with a double O-ring metal seal of the HELICOFLEX® type with an outer aluminium jacket as shown in Fig. 5.22. The seal diameter was 10 mm. The test setup consisted of three flanges bolted together and helium gas with a pressure of 2 atm was filled into the space between the flanges. Eddy current displacement sensors with an accuracy of ± 0.01 mm were used to measure flange displacements. Sliding load and relative displacements were applied to the middle flange by a universal test machine. In order to simulate thermal ageing of the metal seal due to the SNF decay heat during cask operation, prior to the tests the flanges with the assembled metal seal were put in a heating chamber at 180°C for 20 hours. According to the Larson-Miller relationship (Eq. (5.2)), this represents almost 180 days (1/2 year) of storage before transportation for typical seal temperatures (~120°C) of a loaded cask. Leakage rate and axial bolt forces were continuously measured.

During the tests, three loading conditions were applied:

- A quasi-static displacement velocity of 0.01 mm/s up to 3.0 mm sliding displacement;
- Secondly, a dynamic displacement velocity of 85 mm/s also up to 3.0 mm sliding displacement;
- Thirdly, cyclic loading with a displacement amplitude of ~0.02 mm at a displacement velocity of 0.01 mm/s which results in a frequency of 0.125 Hz.

All tests were carried out three times with always fresh seals.

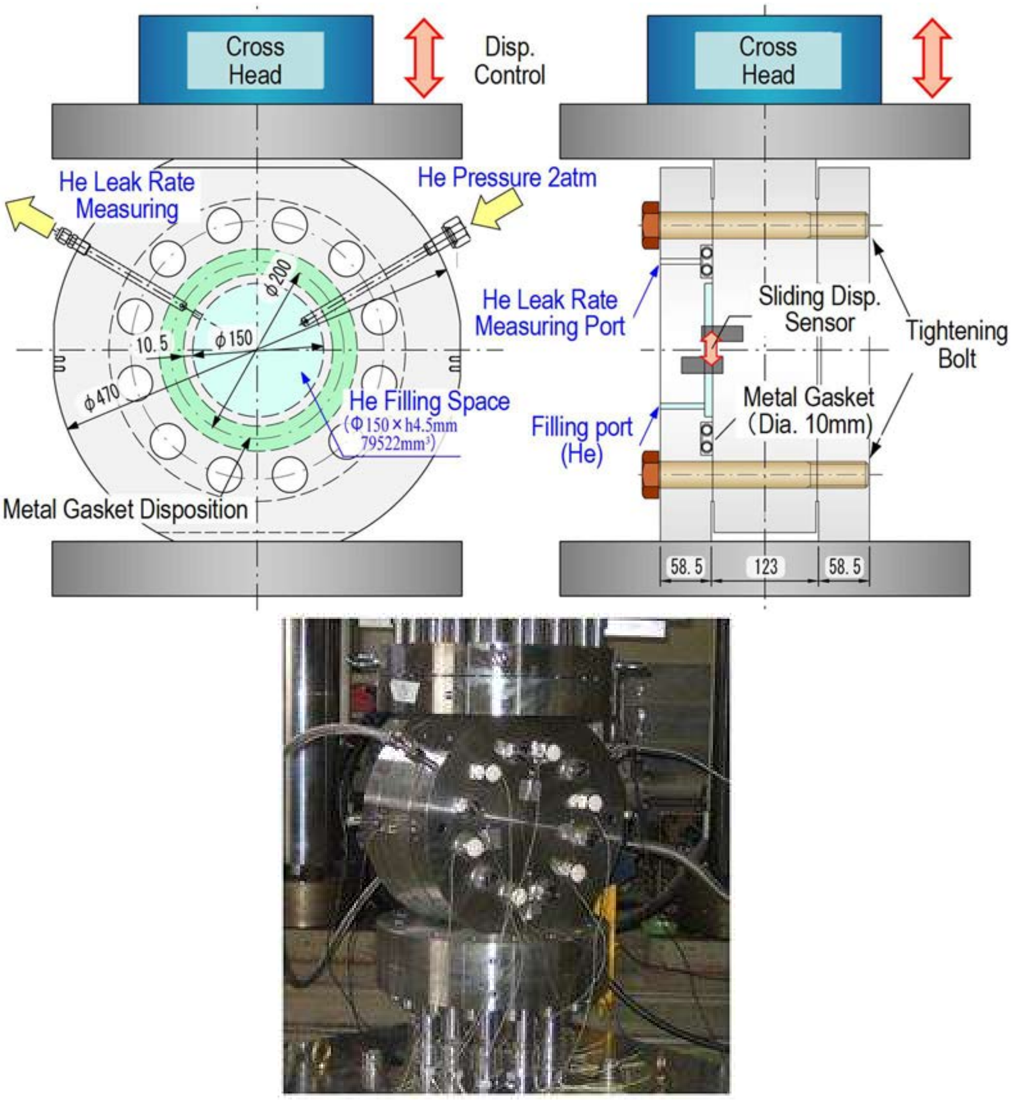

FIG. 5.22. Test setup representing a 1/10-scale model of a bolted lid system with a metal seal (reproduced courtesy of Institute of Nuclear Materials Management (INMM)) [5.33].

For the quasi static tests, Figure 5.23 shows rapidly increasing helium leakage rates starting from initially 10^{-10} $Pa \cdot m^3 \cdot s^{-1}$ to up to 10^{-6} $Pa \cdot m^3 \cdot s^{-1}$ after a 3.0 mm sliding displacement. A helium leakage rate of 10^{-8} $Pa \cdot m^3 \cdot s^{-1}$ is already exceeded after 0.2 mm to 0.3 mm sliding displacement. For the dynamic tests at 85 mm/s displacement velocity the same helium leakage rate increases to 10^{-6} $Pa \cdot m^3 \cdot s^{-1}$ was found after 3.0 mm sliding displacement showing that there is no significant dependency on the loading speed. At the same time initial bolt forces always decreased just slightly.

Finally, cyclic tests [5.33] have shown results that are specific to the test setup. Additional tests would be needed to identify systematic effects on real sealed lid systems under cyclic loading conditions.

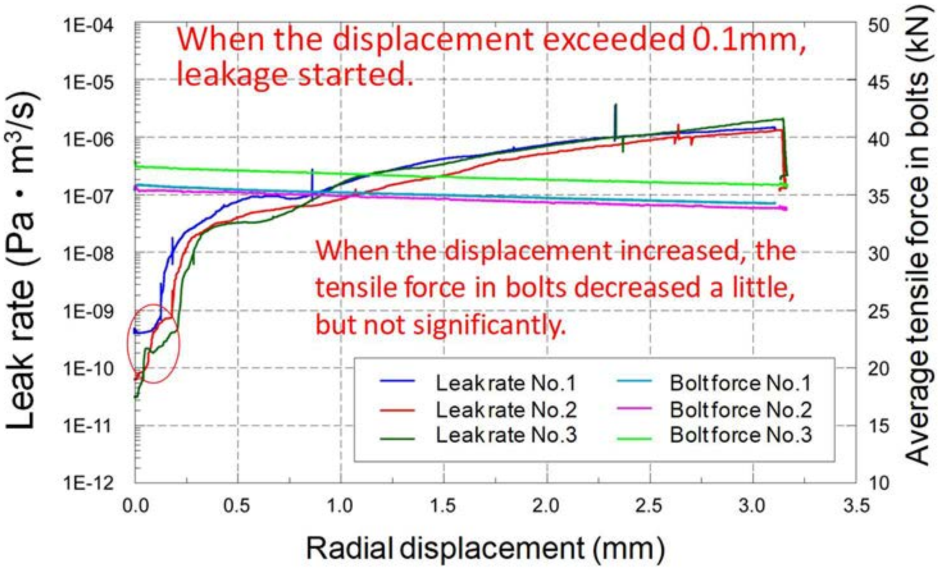

FIG. 5.23. Results from three quasi-static load tests; helium leakage rate and bolt forces over sliding displacement (reproduced courtesy of Institute of Nuclear Materials Management (INMM)) [5.33].

5.6. SUMMARY AND OUTCOMES REFLECTING DATA GAPS FOR LONG TERM STORAGE

The long term performance of bolted closure systems of transport and storage casks is essential to the safe enclosure of the radioactive inventory during storage and subsequent transportation under normal operation conditions as well as under accident scenarios. Most relevant and also most sensitive components to provide sufficient long term leak-tightness are metal seal consisting of a helical metal spring and covered by two outer metal jackets.

Research programmes have been performed to address the thermo-mechanical behaviour of metal seal in the long term. Relevant parameters are the temperature and time. To accelerate ageing mechanisms and to potentially extrapolate to longer periods of time, seal tests at higher temperatures can be generally used but material and test parameters have to be determined and validated carefully. Outcomes from the test programs shown in this report generally demonstrate proper performance of metal seals regarding leak tightness even though pressure forces and useable resilience decrease significantly. For the establishment of reliable models to predict the long term light tightness for many decades taking into consideration the Larson-Miller approach, additional investigations are needed. In addition, numerical approaches are going to be developed for analyzing and predicting the mechanical behaviour of bolted lid systems under various loading conditions. But also, in this case more experimental and numerical investigations are needed to develop and validate sufficient finite element simulations. Other effects to be investigated are not just quasi-static loads in the long term, but also dynamic loads during transportation and impact loads in accidental scenarios on aged metal seals. Some investigations have been performed successfully, providing valuable information but more detailed investigations are needed to get a more comprehensive and precise picture.

In general, the findings of various series of test explained in this report have shown good congruence regarding sufficient long term metal seal function. Further investigations should improve the ability to predict their long term behaviour under various static and dynamic loading conditions during storage, handling and subsequent transportation more precisely and validated for several decades of further storage.

Additionally, degradation mechanisms on elastomer seals have been investigated to understand their ageing mechanisms depending on time, temperature and irradiation. As they are used just as auxiliary seals without safety function in case of SNF and high level waste casks, just to provide a test vacuum for measuring the leakage rate of the primary metal seals, potential side effects on other safety relevant components have to be addressed. Related investigations on ageing and degradation of elastomer seals by thermo-mechanical loads and irradiation should be continued.

REFERENCES TO CHAPTER 5

[5.1] VÖLZKE, H., PROBST, U., WOLFF, D., NAGELSCHMIDT, S., SCHULZ, S., Long term performance of metal seals for transport and storage casks, Packaging, Transport, Storage & Security of Radioactive Material 25 (2013) 8–15.

[5.2] WOLFF, D., PROBST, U., VÖLZKE, H., DROSTE, B., RÖDEL, R., Safety aspects of long-term dry interim storage of Type-B spent fuel and HLW transport casks, Packaging, Transport, Storage & Security of Radioactive Material 15 (2004) 207–213.

[5.3] YOKOYAMA, T., KAWAKAMI, H., UCHIYAMA, N., YASUDA, M., MATSUOKA, S., Assessment of integrity of a dual-purpose metal cask after long-term interim storage: seal performance under transport conditions, Packaging, Transport, Storage & Security of Radioactive Material 16 (2005) 189–197.

[5.4] SASSOULAS, H., MORICE, L., CAPLAIN, P., ROUAUD, C., MIRABEL, L., BEAL, F., Ageing of metallic gaskets for spent fuel casks: century-long life forecast from 25,000-h-long experiments, Nuclear Engineering and Design 236 (2006) 2411–2417.

[5.5] PROBST, U., HAGENOW, P., VÖLZKE, H., WOLFF, D., WOSSIDLO, P., ABBASI, B., ACHELPÖHLER-SCHULTE, A., SCHULZ, S., Investigation of seal effects according to axial compression variation of metal seals for transport and storage casks, Packaging, Transport, Storage & Security of Radioactive Material 19 (2008) 47–52.

[5.6] VÖLZKE, H., PROBST, U., WOLFF, D., NAGELSCHMIDT, S., SCHULZ, S., Investigations on the Long Term Behavior of Metal Seals for Spent Fuel Storage Casks, Institute of Nuclear Material Management, Deerfield, IL (2011).
[5.7] VÖLZKE, H., PROBST, U., WOLFF, D., NAGELSCHMIDT, S., SCHULZ, S., ‘‘Seal and closure performance in long term storage’’, 11th International Probabilistic Safety Assessment and Management Conference and the Annual European Safety and Reliability Conference 2012 (PSAM11 ESREL 2012) (Proc. Conf. Helsinki, 2012), IAPSAM & ESRA, New York (2012).
[5.8] BÉZIAT, A., et al., “Ageing of HELICOFLEX® metallic gasket for spent fuel cask: results and analysis of sealing performances of a 75,000h campaign”, PATRAM 2013, 17th Int. Symp. on the Packaging and Transportation of Radioactive Materials (Proc. Int. Symp. San Francisco, 2013), Omnipress, Madison, WI (2013).
[5.9] SHIRAI, K., NAMBA, K., WATARU, M., VÖLZKE, H., WOLFF, D., PROBST, U., JAUNICH, M., SCHULZ, S., “Numerical evaluation of the long-term sealing performance of the Silver gasket for dual purpose metal cask under high temperature”, PATRAM 2013, 17th Int. Symp. on the Packaging and Transportation of Radioactive Materials (Proc. Int. Symp. San Francisco, 2013), Omnipress, Madison, WI (2013).
[5.10] NAGELSCHMIDT, S., HERBRICH, U., PROBST, U., WOLFF, D., VÖLZKE, H., “Test results and analyses in terms of aging mechanisms of metal seals in casks for dry storage of SNF’’, Waste Management Symposia (WM Symposia) (Proc. Symp. Phoenix, 2014), WM Symposia, Phoenix (2014).
[5.11] WATARU, M., SHIRAI, K., SAEGUSA, T., ITO, C., ‘‘Long-term containment test using two full-scale lid models of DPC with metal gaskets for interim storage’’, paper presented at Third East Asia Forum on Radwaste Management: 2010 EAFORM, Gyeongju, Republic of Korea, (2010).
[5.12] SHIRAI, K., WATARU, M., SAEGUSA, T., ITO, C., “Long-term containment performance test of metal cask”, 13th International High-Level Radioactive Waste Management (IHLRWM) Conference (Proc. Int. Conf. Albuquerque, 2011), American Nuclear Society, La Grange Park, IL (2011).
[5.13] LARSON, F.R., MILLER, J., A time-temperature relationship for rupture and creep stresses, Trans. ASME 74 (1952) 765–771.
[5.14] KOWALEWSKY, H., DROSTE, B., NEUMEYER, T., BURNAY, S.G., BALL, M.H., MORTON, D.A.V., SMITH, P.N., TUSON, A.T., “Safety assessment of leak tightness criteria for radioactive materials transport packages”, PATRAM 1998, 12th Int. Conf. on the Packaging and Transportation of Radioactive Materials (Proc. Int. Conf. Paris, 1998), Société Français’ d'Energie Nucléaire, Paris (1998).
[5.15] BERNSTEIN, R., GILLEN, K.T., Fluorosilicone and Silicone O-ring Aging Study, Rep. SAND2007-6781, Sandia Natl Labs, NM (2007).
[5.16] HOFFMAN, E.N., SKIDMORE, T.E., DAUGHERTY, W.L., DUNN, K.A., Long Term Aging and Surveillance of 9975 Package Components, Rep. SRNL-STI-2009-00733, Savannah River Natl Lab., SC (2009).
[5.17] SKIDMORE, T.E., Performance Evaluation of O-ring Seals in the SAFKEG 3940A Package in KAMS (U), Rep. WSRC-TR-2003-00198, Rev. 0, Savannah River Technology Center, SC (2003).
[5.18] VERST, C., SINDELAR, R.L., SKIDMORE, T.E., DAUGHERTY, W.L., “Performance of bolted closure joint elastomers under cask aging conditions”, ASME 2015 Pressure Vessels and Piping Conference (PVP 2015) (Proc. Conf. Boston, 2015), The American Society of Mechanical Engineers, New York (2015).

[5.19] KÖMMLING, A., JAUNICH, M., WOLFF, D., "Aging of elastomeric seals for storage casks", Waste Management Symposia (WM Symposia) (Proc. Symp. Phoenix, 2015), WM Symposia, Phoenix (2015).

[5.20] JAUNICH, M., WOLFF, D., Influence of gamma irradiation on low temperature properties of rubber seal materials, KGK Kautschuk Gummi Kunststoffe 68 (2015) 85–89.

[5.21] JAUNICH, M., WEBER, M., KÖMMLING, A., ZENCKER, U., WOLFF, D., VÖLZKE, H., "Performance of elastomer seals in transport and storage casks", Int. Conf. on Management of Spent Fuel from Nuclear Power Reactors – An Integrated Approach to the Back-End of the Fuel Cycle, Vienna (2015).

[5.22] FERRY, J.D., Viscoelastic Properties of Polymers, 3rd edition, John Wiley & Sons (1980).

[5.23] GILLEN, K.T., WISE, J., CELINA. M., CLOUGH, R.L., Evidence that Arrhenius High-Temperature Aging Behavior for an EPDM O-ring Does Not Extrapolate to Lower Temperatures, Sandia Natl Labs, NM (1997).

[5.24] KÖMMLING, A., JAUNICH, M., WOLFF, D., Ageing of HNBR, EPDM and FKM O-rings, KGK Kautschuk Gummi Kunststoffe 69 (2016) 36–42.

[5.25] JAUNICH, M., STARK, W., WOLFF, D., A new method to evaluate the low temperature function of rubber sealing materials, Polymer Testing 29 (2010) 815–823.

[5.26] JAUNICH, M., STARK, W., WOLFF, D., Comparison of low temperature properties of different elastomer materials investigated by a new method for compression set measurement, Polymer Testing 31 (2012) 987–992.

[5.27] JAUNICH, M., STARK, W., WOLFF, D., Low temperature properties of rubber seals, KGK Kautschuk Gummi Kunststoffe 64 (2011) 52–55.

[5.28] WOLFF, D., JAUNICH, M., PROBST, U., NAGELSCHMIDT, S., ''Understanding the long-term behavior of sealing systems and neutron shielding material for extended dry cask storage'', Probabilistic Safety Assessment and Management (PSAM) 12 Conf. (Proc. Conf. Honolulu, 2014), CreateSpace Independent Publishing Platform (2016).

[5.29] ELECTRIC POWER RESEARCH INSTITUTE, Extended Storage Collaboration Program International Subcommittee Report: International Perspectives on Technical Data Gaps Associated with Extended Storage and Transportation of Used Nuclear Fuel, Rep. 1026481, EPRI, CA (2012).

[5.30] WATARU, M., SHIRAI, K., SAEGUSA, T., ITO, C., "Long-term containment performance test of metal cask for spent nuclear fuel storage", 11th International Probabilistic Safety Assessment and Management Conference and the Annual European Safety and Reliability Conference 2012 (PSAM11 ESREL 2012) (Proc. Conf. Helsinki, 2012), IAPSAM & ESRA, New York (2012).

[5.31] WATARU, M., SHIRAI, K., BÉZIAT, A., LEDRAPPIER, F., VULLIEZ, K., DESCHAMPS, B., JULIAA, J.F., MIRABEL, L., WINKLER, H-P., HÜEGGENBERG, R., "Ageing of HELICOFLEX® metallic gasket for spent fuel cask: results of sealing performances of a 100,000h campaign", PATRAM 2016, 18th Int. Symp. on the Packaging and Transportation of Radioactive Materials (Proc. Int. Symp. Kobe, 2016), The Japan Society of Mechanical Engineers, Tokyo (2016).

[5.32] NAMBA, K., SHIRAI, K., WATARU, M., SAEGUSA, T., "Evaluation of sealing performance of metal gaskets used in dual purpose metal cask under normal transport condition considering ageing of metal gaskets under long-term storage", PATRAM 2013, 17th Int. Symp. on the Packaging and Transportation of

Radioactive Materials (Proc. Int. Symp. San Francisco, 2013), Omnipress, Madison, WI (2013).

[5.33] SAEGUSA, T., SHIRAI, K., TAKEDA, H., WATARU, M., NAMBA, K., “Influence of mechanical vibration in transport on leak-tightness of metal gasket in transport/storage cask for spent nuclear fuel”, PATRAM 2010, 16th Int. Symp. on the Packaging and Transportation of Radioactive Materials (Proc. Int. Symp. London, 2010), London (2010) CD-ROM

6. NEUTRON SHIELDING IN DRY STORAGE SYSTEMS

6.1. STORAGE/TRANSPORT REGULATION AND GAMMA AND NEUTRON SHIELDING

Transport and storage of nuclear and radioactive material must fulfil general principles of safety to control hazards, prevent accidents and mitigate any harmful consequences of ionizing radiations. One aspect of hazard control is radiological protection to workers and members of the public. As described in Subsection 6.3 below, dose rate limits are prescribed for storage and transportation activities. Therefore, systems to transport and/or store nuclear and radioactive material include shielding materials that are interposed between the source of radiation and persons or environment in order to absorb radiation and thereby reduce radiation exposure of public and workers. For existing shielding designs in dry storage systems, dose rate calculations are performed during the storage period to verify that the shielding performance meets the applicable radiation protection criteria, especially in the case of extension of storage period.

6.2. DESCRIPTION OF NEUTRON SHIELDING OPTIONS

All the neutron shielding materials have a high content of hydrogen for attenuation and capture of neutrons. As such, it is important for neutron shielding material to maintain adequate hydrogen content as long as the storage and transportation system remains in operation. This chapter is focussed on the behaviour of neutron radiation shielding during periods of extended operation.

Neutron shielding is incorporated into whatever storage and transportation system design considered. For bolted lid storage and transportation systems, typical neutron shielding materials are [6.1]:

- Water in leak-tight compartments;
- Polymers and corresponding polymer compounds with high hydrogen content such as polyethylene or polyester. Some polymers may be borated for neutron capture. The shielding performance of polymers is given by their chemical composition, density and thickness;
- Concrete. Although the hydrogen content is lower than for polymers (four times less than polyethylene), leading to an increase of the thickness of shielding layer, it is possible to increase concrete shielding performance by adding fillers.

For welded stainless steel canister inside concrete overpack storage systems, both neutron and gamma shielding are provided by the overpack that is primarily composed of a thick layer of concrete.

6.3. SAFETY FUNCTIONS AND KNOWLEDGE GAPS

Radiological protection safety function: International Atomic Energy Agency (IAEA) dose rate limits

From general regulations and standards, the shielding of any dry storage system or shipping cask must reduce the external dose rate from the largest expected source to below specified tolerance levels. The IAEA requirements for a 'Type B package' are applicable for transport packages as defined by the IAEA safety standards [6.2]. Some countries may have different radiation limits due to a different regulation in their country. According to the IAEA safety standards [6.2], normal conditions of transport and accident conditions of transport must be justified for safety.

During storage, the dose rate shall be less than 2 mSv/h at any point on the external surface of the package and less than 0.1 mSv/h at a distance of 2 m from the package. In accident conditions of storage, the dose rate shall be less than 10 mSv/h after regulatory test sequences at a distance of 1 m from package.

For normal conditions of transport, the dose rate shall be less than 2 mSv/h at any point of external surface of the package and the dose rate shall be less than 0.1 mSv/h at a distance of 2 m from the package. The tests required for normal conditions of transport are specified in the IAEA safety standards [6.2]. The package design must meet these dose rate limits when submitted to these tests. In accident conditions of transport, the dose rate shall be less than 10 mSv/h after regulatory test sequences at a distance of 1 m from the package.

6.4. KNOWLEDGE GAPS FOR VERY LONG TERM STORAGE FOLLOWED BY TRANSPORTATION

Shielding performance must be maintained in operation in normal conditions. This is the reason why the neutron shielding layer in bolted lid systems is often contained in a metal sheet or box to retain as much of the hydrogen content in the neutron shielding material as possible. Thus, the neutron shielding layer is protected from the external environment in normal conditions.

In accident conditions of transport, to comply with regulatory requirements, behaviour in case of fire needs to be checked since polymeric material can be flammable, and all hydrogen-containing materials can lose hydrogen at elevated temperatures. Therefore, the ignition temperature of the polymeric material is important. A self-extinguishing material is preferable in order to prevent addition of energy to the fire with burnable material.

Radioactivity decreases with time due to decay, so the highest shielding performance is required at the start of the storage period. Nevertheless, a continuous shielding capability is required for the entire storage period even in the case of a long term period. Changes in the properties of neutron shielding materials occur during time and are caused by elevated temperatures, thermal cycling, irradiation and mechanical load. Each of the shielding material types has its own properties, degradation mechanisms and degradation rates.

In case of interim storage and subsequent transport, the package characteristics and especially the shielding performance during storage, the normal conditions of transport and the accident conditions of transport must be maintained, considering potential ageing and degradation. The primary ageing mechanisms for neutron shielding materials during long term storage are degradation of shielding materials due to prolonged elevated temperatures and prolonged exposure to neutron and gamma fluxes (Table 6.1). However, for storage conditions, depending on the shielding material, degradation through irradiation is a second order mechanism. Experimental results have shown that thermal degradation or oxidation with temperature is the predominant degradation process for neutron shielding materials.

TABLE 6.1. SHIELDING MATERIAL: KNOWLEDGE GAPS

Safety function	Corresponding effect
Radiation protection	Thermal and radiation ageing

Since the properties and performance of these shielding materials are temperature-sensitive, it is necessary to verify that these shielding materials will not be subjected to temperatures above their design limits during either normal or accident conditions of transport that could cause a rapid loss of hydrogen content. During normal conditions of storage and/or transport, temperatures are typically the highest at early times. In addition, it is possible that shielding materials may experience hydrogen loss during the prolonged elevated temperatures typical of normal storage conditions. This potential for long term hydrogen loss needs to be considered. Less data exists to evaluate the behaviour of neutron shielding materials under somewhat elevated but prolonged temperatures than for short term behaviour at design limit temperatures.

In addition to possible degradation of neutron shielding materials due to elevated temperatures, polymeric neutron shielding materials are known to degrade in the presence of gamma and neutron irradiation[14]. Since the amount of polymer degradation is partially dependent on the gamma and neutron fluence, it is likely that at least some additional polymeric material degradation would occur with increasing storage time. As for long term thermal effects, less data exists for the properties of polymeric shielding materials under fluence levels associated with long term storage periods than for lower fluence levels.

6.5. COORDINATED RESEARCH PROJECT (CRP) CONTRIBUTORS SCOPE AND OUTCOMES

6.5.1. Long term performance justification/methods

To evaluate the adequacy of neutron shielding during dry storage in the long term followed by transport, first SNF modelling and calculation of gamma and neutron source evolution and thermal power evolution are necessary. Then the performance of the shielding material and its potential degradation due to prolonged elevated temperature conditions and increasing gamma and neutron fluence must be evaluated. Experimental methods are used to assess the degradation of shielding materials. Accelerated ageing tests are carried out on neutron shielding samples at different temperatures. Then, characterization of aged polymeric neutron shielding material samples is performed using mostly differential scanning calorimetry (DSC), thermo mechanical analysis (TMA), dynamic mechanical analysis (DMA), thermo gravimetric

[14] The neutron shielding capability of concrete is primarily provided by the presence of bound water in the concrete matrix. Loss of water is primarily governed by temperature either due to direct volatilization of water or replacement of water by carbonates due to reaction of hydroxides in the concrete with CO_2. Hence, degradation of concrete neutron shielding properties due to irradiation is a secondary effect.

analysis (TGA), attenuated total reflectance (µATR) and Fourier transformed infrared (FTIR) spectroscopy. In addition to these techniques, gravimetric analysis, oxidation profiling and O_2 permeation tests are also carried out to estimate both O_2 diffusivity and solubility into neutron shielding films.

To investigate the long term properties, a non-empirical model may be applied. In this regard, oxidation kinetic is coupled with oxygen diffusion. For example, some models shown hereafter simulate very confidently weight losses (which are then converted into hydrogen atoms loss) and oxidation profiles.

6.5.2. Investigations by countries

Three studies related to neutron shielding material degradation were part of the CRP that is the subject of this TECDOC (Table 6.2). Two studies were focused on the potential degradation of polymeric neutron shielding performance during extended dry storage. A third study calculated gamma and neutron dose rates as a function of time. The conclusion that can be drawn from these three studies is that existing neutron shielding designs using polymeric materials will continue to meet the IAEA neutron dose rate limits in the long term.

TABLE 6.2. CRP CONTRIBUTIONS TO ADDRESS KNOWLEDGE GAPS IN THE LONG TERM PERFORMANCE OF NEUTRON SHIELDING MATERIALS

Knowledge gap related to shielding	CRP contributor (CRP report number (see Annexes))
Chemical composition, density and hydrogen release of polymeric materials	Germany (GFR 17307 - Annex IV), France (FRA 17270 - Annex III)
Expansion coefficient and shear modulus of polymeric materials	Germany (GFR 17307 - Annex IV)
Modelling evolution of source term	Lithuania (LIT 17275 - Annex VII)

Detailed information on the investigations is given in country reports found in the annexes. A summary of each of the three CRP contributions is provided below.

6.5.2.1. France

In France the investigations on degradation of shielding performance of a specific polymeric neutron shielding material were performed and published by Orano TN[15] (see Annex III). Recent work [6.3–6.6] has been performed on oxidative mechanisms of a thermoset matrix-based neutron shielding, called 'resin' (TN® Vyal B) used in dual purpose casks (Fig. 6.1). Oxidation can cause the loss of hydrogen.

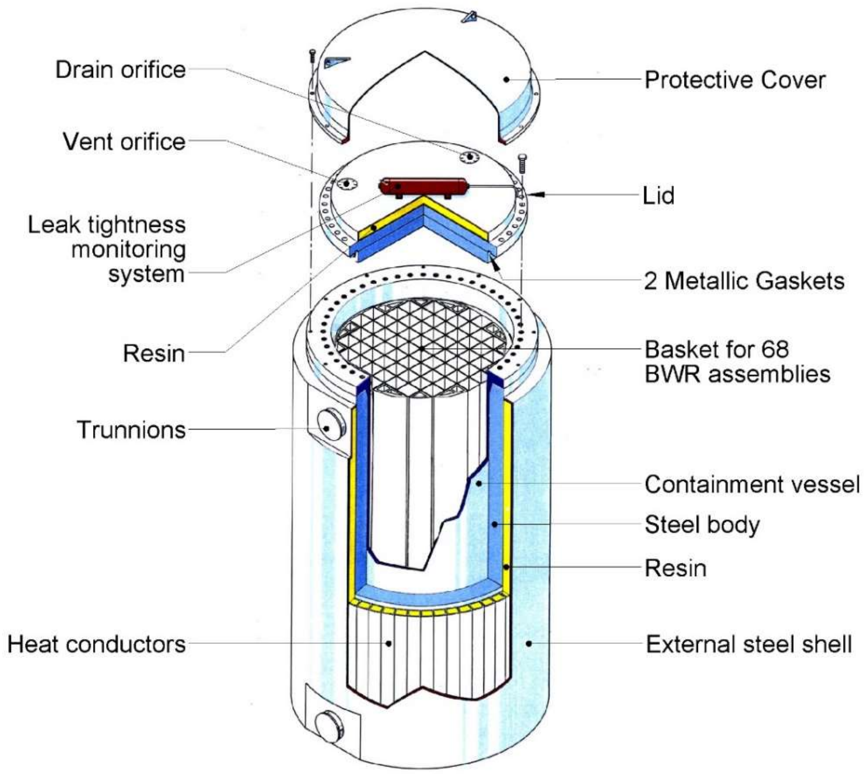

FIG. 6.1. TN-68 dual purpose cask, with resin neutron shielding (reproduced courtesy of TN Americas).

The objective of the study was to investigate the material's thermal degradation mechanism using accelerated ageing tests and to validate a non-empirical model for predicting long term in-service properties.

The main conclusions are the following:

The consequence of ageing of TN® Vyal B is a superficial modification of the chemical composition in the matrix by cutting fragments of the molecular chain or network that leads finally to a superficial oxidative layer build-up, suggesting a diffusion-limited oxidation effect.

[15] Orano TN was formerly AREVA TN International.

IR measurements, described in FRA 172–0 - Annex III, show a slight decrease of C-H groups (hydrogen abstraction) followed by an increase in carbonyl groups (C=O) in the oxidized layer.

Exposure of free films to high temperatures and oxygen caused early mass uptake (due to O_2 grafting on polymer chain) followed by a dramatic drop of mass due to loss of volatile oxidation products (most of which contain hydrogen). Based on these observed modifications, the appropriateness of the thermodynamic chemical equations involved used to model the degradation of TN® Vyal B and build the kinetic model of the degradation can be confirmed. The kinetic model was used to predict oxidation-induced weight loss as a function of temperature and time, which is a critical parameter of the shielding performance for samples exposed to different temperatures and oxygen pressure. For instance, in Fig. 6.2, a quite acceptable agreement is shown for composite samples exposed to 140°C and 2×10^5 Pa of O_2.

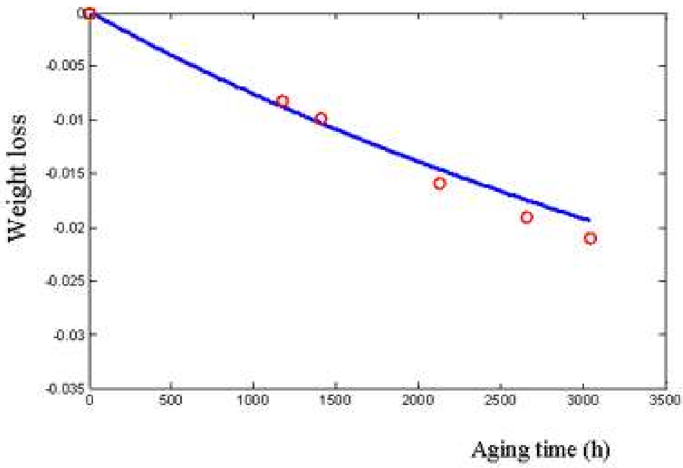

FIG. 6.2. Weight loss curve obtained for vinylester composite TN® Vyal B at 140°C under 2×10^5 Pa of O_2: experimental (o), model (—) (reproduced courtesy of Springer) [6.4].

As a conclusion, a good correlation of experimental and simulated data is obtained on weight changes as well as oxidation profiles (Fig. 6.3).

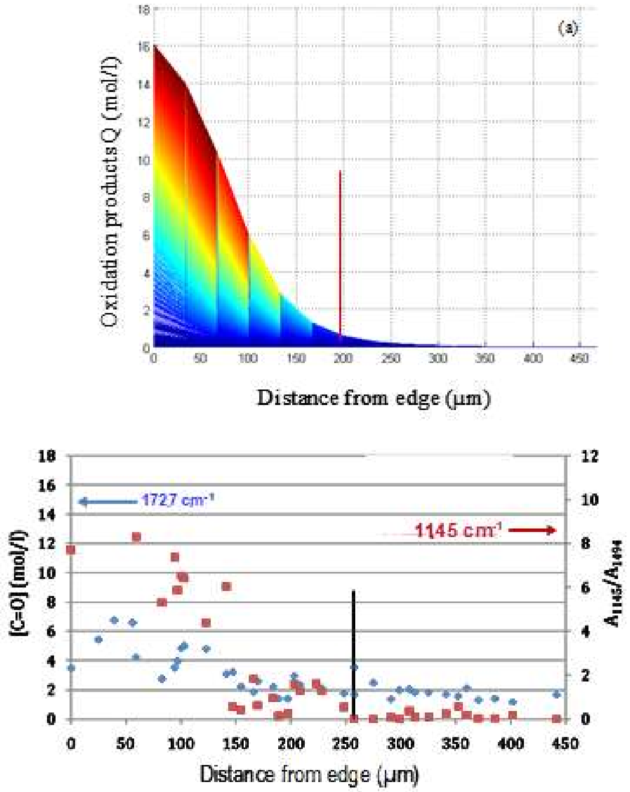

FIG. 6.3. Example of simulated and experimental oxidized layer thickness for composite samples exposed to 160°C / 2 × 10^5 Pa O_2 (reproduced courtesy of Springer)[6.4, 6.5].

The new approach allows a great understanding of thermoset neutron shielding long term performance.

6.5.2.2. Germany

In Germany the investigations were performed and published mainly by the Bundesanstalt für Materialforschung und -prüfung (BAM; see GFR 173–7 - Annex IV).

As shown in Fig. 6.4, polyethylene for neutron radiation shielding in the CASTOR® V-cask by GNS is used in the form of rods in cylindrical boreholes in the cask side wall plates between the primary and secondary lids and below bottom of cask body [6.7, 6.8].

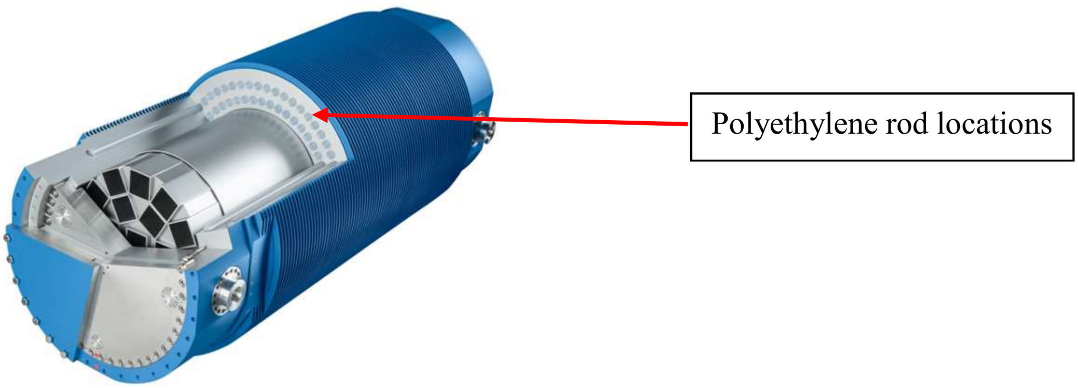

FIG. 6.4. CASTOR® V-cask by GNS with polyethylene (PE)-rods in the cask side wall and a plate between the lids (reproduced courtesy of GNS Gesellschaft für Nuklear-Service mbH).

Polyethylene shielding materials used in this study are high density polyethylene HMW-PE (e.g. LUPOLEN 5261Z) and ultra high molecular weight polyethylene (U)HMW-PE (e.g. GUR 4120).

Thermo-oxidative ageing and irradiation effects are considered as degradation mechanisms. The purpose of these studies is to better understand and quantify the characteristics of the shielding material that play a significant role in the radiation safety and are time- and temperature-dependent and/or radiation-dependent [6.10].

Several subjects are addressed (see GFR 173–7 - Annex IV and relevant references [6.8, 6.10–6.20]):

- With regard to the position of neutron moderator rods in the wall of the cask an important aspect is the expansion at thermal equilibrium. Expansion behaviour has been evaluated. For (U)HMW-PE shielding rods, geometrical changes in relative lengths and diameters over all the cycles are relatively small;
- During ageing, hydrogen gas production is taken into consideration;
- Another subject is the chemical composition and hydrogen release. The results show very small changes in the concentration of carbon or hydrogen.

With the applied methods it is possible to detect radiation-induced structural changes of polyethylene (PE) [6.9]. With regard to the special application of (U)HMW-PE as neutron shielding material in casks for storage and transport of radioactive material, the detected changes do not impact the ability to meet neutron dose rate limits over a period of 40 years. Investigations are in progress to obtain information for longer periods of time [6.7, 6.9].

Irradiation leads to broken chemical bonds and thus radical formation. This can result in the loss of hydrogen. These radicals can either recombine (resulting in additional crosslinks), terminate via a disproportionation reaction (leading to chain scission and the formation of double bonds), or react with oxygen that is present in the amorphous regions and form oxidation products such as carbonyls. Side-effects of chain scission reactions can be the formation of low molecular weight fragments and recrystallization [6.8, 6.10].

Moreover, radiation induced ageing of PE was studied by means of terahertz (THz) and mid-infrared (Mid-IR) Fourier transform spectroscopy. THz and Mid-IR reveals modifications in PE chemical bonding induced by γ-irradiation processes and a subsequently applied thermal load cycle covering a temperature range above and below the melting point. Changes in the spectrum point towards chain scission and crosslink formation. This effect results initially in a slight increase of the degree of crystallinity. An amorphization of the HMW-PE and (U)HMW-PE can be observed if recrystallization has been initiated by a thermal load cycle. (U)HMW-PE shows a higher stability against 60Co γ-irradiation in comparison to HMW-PE.

The density of HMW-PE as well as of (U)HMW-PE increases with an increasing dose of gamma irradiation (Fig. 6.5). This is a positive aspect since the density is an important criterion for the shielding properties of polyethylene. Crosslinking and a higher degree of crystallinity can both contribute to a density increase.

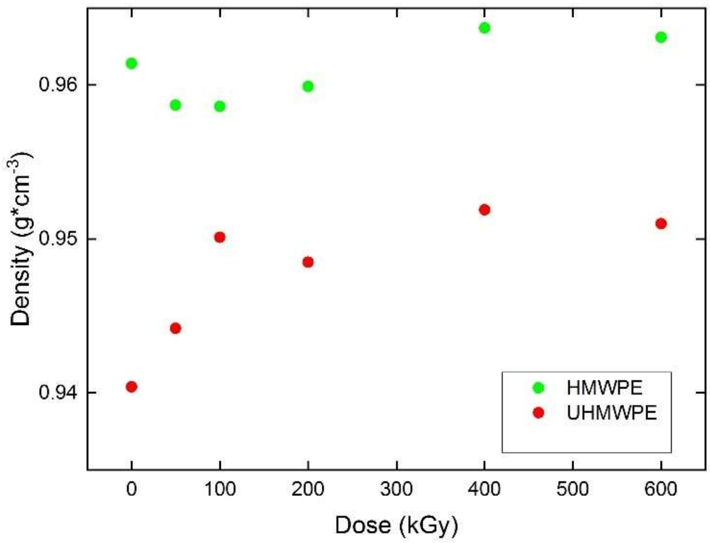

FIG. 6.5. Density values of HMW-PE and (U)HMW-PE in dependence of gamma irradiation dose (reproduced courtesy of Bundesanstalt für Materialforschung und -prüfung (BAM) based on data published in [6.21]).

In addition, the evaluation of shear modulus, especially the height and temperature dependence of the plateau value gives information about the mechanical properties of the crosslinks of the material. The measurements reveal that the degree of cross-linking is increased through irradiation, and it can be distinguished between physical crosslinks (e.g. entanglements) and chemical crosslinks. As crosslinks can strongly increase the viscosity of the polymer melt a possible stress build up has to be considered for the material within the container wall during accident conditions.

6.5.2.3. Lithuania

In Lithuania, the investigations were performed and published by the Lithuanian Energy Institute (LEI) [6.22–6.24] (see LIT 172–5 - Annex VII). The objective of the study was to perform numerical modelling related to long term storage of spent RBMK-1500 fuel at Ignalina NPP. The detailed study is presented in LIT 172–5 - Annex VII and in relevant references [6.25–6.39]. The study estimated neutron and gamma fluxes and neutron and gamma dose rates in a storage cask model as a function of time.

Spent RBMK-1500 nuclear fuel characteristics, dose rate variation of CASTOR®RBMK-1500 and CONSTOR®RBMK-1500 storage casks, neutron transport and activation of the components of these storage casks for long term storage periods have been estimated. Fuel rod characteristics such as radionuclide content, gamma and neutron sources, and residual heat are used in the radiation safety and decay heat removal analysis.

Dose rate calculations for CASTOR®RBMK-1500 and CONSTOR®RBMK-1500 storage casks have revealed that for long term storage periods, the dose rate caused by neutrons becomes dominant. Therefore, appropriate materials for maintenance of adequate long term neutron shielding is important.

Results of the neutron activation modelling of the heavy concrete wall of a CONSTOR®RBMK-1500 cask have provided the activities of specific radionuclides in the concrete. Even neutron-induced activities in the cask's components for CASTOR®RBMK-1500 and CONSTOR®RBMK-1500 storage casks meet the free release conditions after 300–600 years of decay. It must be considered that the modelling was done for RBMK fuel that has a relatively low enrichment and burnup.

Modelling of spent RBMK-1500 nuclear fuel characteristics (radionuclide content, gamma and neutron sources, decay heat) has been performed using the SAS2H sequence of the SCALE 5.0 computer code system. Later with the newer version of SCALE 6.1.2 all characteristics have been re-evaluated using the TRITON code.

The results obtained in the calculation address/deal with:

- Radionuclide concentration variation with burnup and comparison with the experimental data [6.35, 6.36];
- Gamma and neutron sources for RBMK-1500 spent nuclear fuel (SNF);
- Activities of actinides and fission products and residual decay heat.

Despite the differences in the model descriptions, the SAS2H and TRITON codes provide rather similar modelling results. Measured and calculated results also are in a rather good agreement.

Gamma and neutron sources for different types of RBMK-1500 spent fuel after 300 years of cooling time are presented in this TECDOC.

The general outcome of induced activities modelling results is the fact that total induced activity in every component of the CASTOR®RBMK-1500 cask is higher compared to the same component of CONSTOR®RBMK-1500 cask during all analyzed time period.

All components for both casks met the free release conditions for the 300–600 years decay period which was analyzed, i.e. specific activities of all radionuclides in each component are lower than their clearance levels and met the free release criterion. However, it should be noted that possible surface contamination of the casks components is not accounted in this case, so the presented outcomes are conditional and applicable only to induced activities.

6.6. SUMMARY AND OUTCOMES

For storage extension, source term and dose evaluation have been addressed. On the other hand, degradation mechanisms and evaluation which were identified as knowledge gaps were studied and new contributions have been delivered and published.

The performance of neutron shielding in the long term was evaluated through specific tests. The ageing phenomena and mechanisms are thermal or thermo-oxidative degradation, eventually coupled with irradiation. Some tests addressed temperature effects and other irradiation effects. Major results and outcomes from the studies presented in this chapter show that the relevant changes related to safety are small and that the shielding performance modification corresponding to the situation of dry storage and subsequent transport are very limited in all cases. A modelling approach allows for prediction of shielding efficiency after long term storage.

REFERENCES TO CHAPTER 6

[6.1] ISSARD, H., ‘‘Radiation protection by shielding in packages for radioactive materials’’, Safe and Secure Transport and Storage of Radioactive Materials, B. K. Sorenson, Elsevier Woodhead, Woodhead publishing services in Energy: Number 78 (2015) Ch. 9.

[6.2] INTERNATIONAL ATOMIC ENERGY AGENCY, Regulations for the Safe Transport of Radioactive Material, 2012 Edition, IAEA Safety Standards Series No. SSR-6, IAEA, Vienna (2012).

[6.3] NIZEYIMANA, F., ALAMI, A., ISSARD, H., BELLENGER, V., “Ageing of a neutron shielding used in transport/storage casks”, 6th Int. Conf. on Times of Polymers (TOP) & Composites (Proc. Conf. Ischia, 2012), American Institute of Physics (AIP), Melville, NY (2012) 120–122.

[6.4] NIZEYIMANA, F., ISSARD, H., ‘‘A kinetic model for predicting polymeric neutron shieldings lifetime’’, Service Life Prediction of Polymeric Materials: Vision for the Future conference (Proc. Conf. Monterrey, 2013), Springer, Cham, Switzerland (2015).

[6.5] NIZEYIMANA F., ALAMI A., ISSARD H., “Neutron shielding materials long term performance: a new approach for modeling thermo-oxidative aging”, PATRAM 2013, 17th Int. Symp. on the Packaging and Transportation of Radioactive Materials (Proc. Int. Symp. San Francisco, 2013), Omnipress, Madison, WI (2013).

[6.6] NIZEYIMANA F., ISSARD H., ‘‘Thermoset-based materials radio-oxidation challenges’’, 11th Meeting of the Ionizing Radiation and Polymers Symposium (IRaP 2014), Jeju Island, 2014.

[6.7] VON DER EHE, K., JAUNICH, M., WOLFF, D., BÖHNING, M., GOERING, H., “Radiation induced structural changes of (U)HMW polyethylene with regard to its application for radiation shielding”, PATRAM 2010, 16th Int. Symp. on the Packaging and Transportation of Radioactive Materials (Proc. Int. Symp. London, 2010), London (2010) CD-ROM.

[6.8] ZHAO, Y., LUO, Y., JIANG, B., Effect of irradiation on crystallinity and mechanical properties of ultrahigh molecular weight polyethylene, J. Appl. Polym. Sci. 50 (1993) 1797–1801.

[6.9] WOLFF, D., JAUNICH, M., PROBST, U., NAGELSCHMIDT, S., ‘‘Understanding the long-term behavior of sealing systems and neutron shielding material for extended dry cask storage’’, Probabilistic Safety Assessment and Management (PSAM) 12 Conf. (Proc. Conf. Honolulu, 2014), CreateSpace Independent Publishing Platform (2016).
[6.10] BHATEJA, S., ANDREWS, E., YOUNG, R., Radiation-induced crystallinity changes in linear polyethylene, Journal of Polymer Science: Polymer Physics Edition 21 (1983) 523–536.
[6.11] VON DER EHE, K., KÖMMLING, A., WOLFF, D., ‘‘Neutron radiation shielding material polyethylene: consequences of gamma irradiation’’, Waste Management Symposia (WM Symposia) (Proc. Symp. Phoenix, 2015), WM Symposia, Phoenix (2015) 15062, 15061–15010.
[6.12] WOLFF, D., VON DER EHE, K., JAUNICH, M., BÖHNING, M., GOERING, H., (U) HMWPE as neutron radiation shielding materials: impact of gamma radiation on structure and properties, Effects of Radiation on Nuclear Materials: 25th Volume, ASTM International (2012).
[6.13] WOLFF, D., VON DER EHE, K., JAUNICH, M., BÖHNING, M., ‘‘Performance of neutron radiation shielding material (U)HMW-PE influenced by gamma radiation’’, 11th International Probabilistic Safety Assessment and Management Conference and the Annual European Safety and Reliability Conference 2012 (PSAM11 ESREL 2012) (Proc. Conf. Helsinki, 2012), IAPSAM & ESRA, New York (2012).
[6.14] BECKMANN, J., SCHADE, U., VON DER EHE, K., JAUNICH, M., WOLFF, D., AZIZ, E.F., ‘‘THz and Mid IR Fourier transform spectroscopy on polyethylene irradiated with gamma-Co60 radiation’’, IRMMW-THz 2014, 39th International Conference on Infrared, Millimeter, and Terahertz Waves (Proc. Int. Conf. Tucson, 2014), IEEE, Piscataway, NJ (2014).
[6.15] EHRENSTEIN, G.W., RIEDEL, G., TRAWIEL, P., Praxis der thermischen Analyse von Kunststoffen, Hanser (2003).
[6.16] ORAL, E., BECKOS, C.G., MURATOGLU, O.K., Free radical elimination in irradiated UHMWPE through crystal mobility in phase transition to the hexagonal phase, Polymer 49 (2008) 4733–4739.
[6.17] STEPHENS, C., BENSON, R., MARTINEZ-PARDO, M.E., BARKER, E., WALKER, J., STEPHENS, T., The effect of dose rate on the crystalline lamellar thickness distribution in gamma-radiation of UHMWPE, Nuclear Instruments and Methods in Physics Research Section B: Beam Interactions with Materials and Atoms 236 (2005) 540–545.
[6.18] SPIEGELBERG, S., Analytical techniques for assessing the effects of radiation on UHMWPE, Cambridge Polymer Group, Application Note 8 (2001).
[6.19] SLOUF, M., SYNKOVA, H., BALDRIAN, J., MAREK, A., KOVAROVA, J., SCHMIDT, P., DORSCHNER, H., STEPHAN, M., GOHS, U., Structural changes of UHMWPE after e-beam irradiation and thermal treatment, Journal of Biomedical Materials Research Part B: Applied Biomaterials 85 (2008) 240-251.
[6.20] AMRHEIN, E.-M., MÜLLER, F., Zur Absorption von Polymeren im Fernen Infrarot, Kolloid-Zeitschrift und Zeitschrift für Polymere 234 (1969) 1078–1082.
[6.21] KOEMMLING, A., VON DER EHE, K., WOLFF, D., JAUNICH, M., Effect of high-dose gamma irradiation on (U)HMWPE neutron shielding materials, Radiation Physics and Chemistry 142 (2018) 29–33.

[6.22] ŠMAIŽYS, A., POŠKAS, P., NARKŪNAS, E., BARTKUS, G., Numerical modelling of radionuclide inventory for RBMK irradiated nuclear fuel, Nuclear Engineering and Design 277 (2014) 28–35.

[6.23] NARKŪNAS, E., ŠMAIŽYS, A., POŠKAS, P., RAGAIŠIS, V., Modelling of RBMK-1500 SNF storage casks activation during very long term storage, Applied Radiation and Isotopes 115 (2016) 100–108.

[6.24] ŠMAIŽYS, A., POŠKAS, P., NARKŪNAS, E., ‘‘Evaluation of radiation characteristics of spent RBMK-1500 nuclear fuel storage casks during very long term storage’’, paper presented at Int. Conf. on Management of Spent Fuel from Nuclear Power Reactors – An Integrated Approach to the Back-End of the Fuel Cycle, Vienna, 2015.

[6.25] KOSTYUCHENKO, A. N., Distribution of an oxide film over the outer surface of cylindrical elements of spent VVÉR and RBMK fuel assemblies, Atomic Energy 102 6 (2007) 480–483.

[6.26] SMIRNOVA, I. M., KUCHKINA, I. N., KOSTYUCHENKO, A. N., KUPRIENKO, M.V., Determination of the composition of the deposits and thickness of the oxide film on the surface of VVÉR and RBMK fuel elements, Atomic Energy 98 1 (2005) 46–49.

[6.27] SMIRNOVA, I. M., MARKOV, D. V., Results from studies of surface deposits on the claddings of fuel rods used in RBMK-1000 reactors, Thermal Engineering 57 7 (2010) 560–565.

[6.28] SMIRNOVA, I. M., FILYAKIN, G. V., KUZMIN, S.V., Post-reactor investigations of deposits on RBMK fuel-element cladding, Atomic Energy 105 2 (2008).

[6.29] COLEMAN, C., GRIGORIEV, V., INOZEMTSEV, V., MARKELOV, V., ROTH, M., MAKAREVIČIUS, V., KIM, Y., ALI, K., CHAKRAVARRTY, J., MIZRAHI, R., LALGUDI, R., The effect of microstructure on delayed hydride cracking behavior of zircaloy-4 fuel cladding—An International Atomic Energy Agency Coordinated Research Program, Journal of ASTM international 7 5 (2010).

[6.30] COLEMAN, C., GRIGORIEV, V., INOZEMTSEV, V., MARKELOV, V., ROTH, M., MAKAREVIČIUS, V., KIM, Y.S., KANWAR LIAGAT, ALI, CHAKRAVARTTY, J.K., MIZRAHI, R., LALGUDI, R., Delayed hydride cracking in zircaloy fuel cladding – an IAEA coordinated research programme, Nuclear Engineering and Technology 41 2 (2009).

[6.31] MARKELOV, V.A., Delayed hydride cracking of zirconium alloys: appearance conditions and basic laws, Russian Metallurgy (Metally) 2011 4 (2011).

[6.32] NIKULINA, A.V., MALGIN, A.G., Impurities and their effect on the structure and properties of zirconium parts in nuclear reactors, Atomic Energy 105 5 (2008).

[6.33] KALIATKA, T., ‘‘Adaptation of FEMAXI-6 code for modelling of RBMK-1500 fuel rod’’, paper presented at the 5th Annual Conf. of Young Scientists on Energy Issues CYSENI 2008, Kaunas, Lithuania, 2008.

[6.34] TREPULIS, M., KALIATKA, T., ‘‘Analysis of processes in RBMK-1000 fuel rods during reactivity initiated accident using FEMAXI-6 code’’, paper presented at the 8th International Conf. of Young Scientists on Energy Issues CYSENI 2011, Kaunas, Lithuania, 2011.

[6.35] KORENKOV, A.G., MAKAROVA, T.P., STEPANOV, A.V., PEVTSOVA, E.V., BELYAEV, B.N., VORONKOV, A.A., Destructive analysis determination of neutron emission from spent RBMK fuel, Atomic Energy 93 4 (2002) 815–822.

[6.36] MAKAROVA, T.P., BIBICHEV, B.A., DOMKIN, V.D., Destructive analysis of the nuclide composition of spent fuel of WWER-440, WWER-1000, and RBMK-1000 reactors, Radiochemistry 50 4 (2008) 414–426.

[6.37] PLUKIENĖ, R., PLUKIS, A., GERMANAS, D., REMEIKIS, V., Numerical sensitivity study of irradiated nuclear fuel evolution in the RBMK reactor, Lithuanian Journal of Physics 49 4 (2009) 461–469.

[6.38] ŠMAIŽYS, A., POŠKAS, P., ‘‘Analysis of radiation characteristics for casks loaded with spent RBMK-1500 nuclear fuel’’, Int. Conf. Nuclear Energy in Central Europe 2001 (Proc. Int. Conf. Slovenia, 2001), Nuclear Society of Slovenia, Ljubljana (2001).

[6.39] POŠKAS, P., ŠIMONIS, V., ŠMAIŽYS, A., ‘‘Comparison of the main characteristics for CASTOR® and CONSTOR® casks loaded with spent RBMK-1500 nuclear fuel’’, Int. Conf. on Storage of Spent Fuel from Power Reactors (Proc. Int. Conf. Vienna, 2003), International Atomic Energy Agency Publication, 1 CD-ROM as IAEA–CSP–20/CD, ISBN 92–0–109603–8, ISSN 1562–4153, IAEA, Vienna (2003), 270–282 .

7. LONG TERM DEMONSTRATION PROGRAMMES

7.1. INTRODUCTION

A significant number of experimental studies, including those discussed in previous chapters and in the annexes[16] of this TECDOC, have been conducted to determine the expected behaviour of dry storage systems over extended storage times greater than the duration of the test project. Usually these tests are made under conditions that are small scale (e.g. laboratory tests of relatively short duration) and accelerate the expected degradation phenomena that might affect the overall behaviour of the system. In some cases, the laboratory scale tests are conducted using 'surrogate' materials (materials that are not the same as those in actual storage systems but are intended to simulate their performance). A common example of use of surrogate materials is substituting unirradiated material, such as fuel pellets and cladding, so that experiments can be conducted without the use of hot cells[17]. Based on these small scale tests, models are developed to extrapolate the results to real systems and for longer time frames. Hence, there is value in conducting larger scale (in dimensions and time) tests. Larger scale tests are commonly termed 'demonstration' tests or projects. In some cases, such demonstration tests may scale up just part of dimensions or time, termed 'partial demonstration'. A 'full demonstration' would be one for which both time and dimensions are full-scale, and no surrogate materials are used. A demonstration project of significant size and duration accomplishes several important goals:

- It provides monitored testing of an integrated system of many components to determine if the projected behaviour of components from individual models work in conjunction with each other, as intended by the storage system design;
- It allows the individual models to be tested under representative conditions removing the uncertainty of changing degradation modes by the acceleration process or use of surrogate materials;
- It may identify new modes of degradation that might not have been preconceived and modelled;
- It provides information whether the system actually works in a safe manner over longer periods of time.

The difference between laboratory scale experiments potentially using surrogate materials under atypical conditions and fuller scale demonstrations is the prototypical conditions under which a demonstration test is performed. Prototypical conditions are dependent on the guidance given by the country storing the fuel and doing the demonstration, the type of dry storage system(s) being used, and the types of SNF to be stored. The Table 7.1 below compares the attributes of a laboratory scale test, a partial demonstration and a full demonstration. A partial demonstration is one that has many, but not all, of the attributes of a full demonstration but still maintains the capability to evaluate any unanticipated experimental artefacts introduced in the

---

[16] The Annexes of this report are provided as supplementary material. The names of the files are composed by the country abbreviation followed by the code of the CRP and the number of the Annex. The annexes included are: ARG 17338 – Annex I, ARG 17339 – Annex II, FRA 17270 – Annex III, GFR 17307 – Annex IV, JPN 17308 – Annex V, JPN 17486 – Annex VI, LIT 17275 – Annex VII, PAK 17283 – Annex VIII, POL 17290 – Annex IX, SLO 17810 – Annex X, SPA 17305 – Annex XI, SPA 18996 – Annex XII, UK 17420 – Annex XIII USA 19249 – Annex XIV.

[17] See Chapter 3 for examples of substitute unirradiated materials regarding SNF long term behaviour.

smaller scale experiments when applied to modelling actual storage systems over long time periods.

TABLE 7.1. ATTRIBUTES OF A DEMONSTRATION

Attribute of the demonstration	Laboratory scale test	Partial demonstration	Full demonstration
Purpose	Identify and study some mechanisms, develop sub-models	Identify some unexpected mechanisms, confirm sub-models (integration of effects), scaling effects	Identify unexpected mechanisms, develop and confirm total system models (integration of effects), scaling effects
Physical scale (e.g. specimen size, rod length, components size)	Generally small	SSCs of interest are near full-scale	Full
Time scale	Usually short	Long enough to extrapolate data	Long enough to extrapolate data
Instrumented or inspection capability	Yes	Mostly yes	Partial
Acceleration of effects (e.g. time, stress, temperature, bounding conditions)	Yes	Sometimes, depends on purpose	No
Test conditions (e.g. stress, atmosphere, chemical, thermal)	Can be varied, including use of ‘bounding’ conditions	Most of the conditions are realistic	Realistic
Actual material and condition (e.g. irradiation, surrogate materials)	If possible, but often not	Mostly	Yes
Cost	Low	Moderate	High

This chapter will provide a brief discussion of previous demonstration projects that were conducted. It will then discuss the ongoing demonstration projects, including ones not directly part of the Coordinated Research Project (CRP) such as the US Department of Energy (US DOE) high burnup fuel (HBF) demonstration project, with their varied goals and conditions. Two contributions were developed during the CRP dealing specifically with overall demonstrations: one by the Japanese (see JPN 174–6 - Annex VI) describing their ongoing HBF demonstration, and one by the US Nuclear Regulatory Commission (US NRC, see USA 192–9 - Annex XIV) dealing with an overview of considerations that need to be accounted for in order to develop a useful demonstration. Finally, a few opportunities for improving full scale demonstrations are identified.

7.2. PREVIOUS DEMONSTRATIONS NOT PART OF THE CRP

Previous demonstration projects give an indication of the variety of conditions that SNF and SNF storage systems can be exposed to. They also indicate what data can be obtained from demonstrations, and problems associated with obtaining this data. This TECDOC only discusses demonstration projects relevant to normal conditions of storage.

There are thousands of dry storage systems that have been deployed on concrete pads for many years. A case could be made that these systems could be considered demonstrations if at least some information on their condition can be obtained. These are not considered demonstrations for this TECDOC since the storage conditions (internal and external atmospheres or temperatures) have not been monitored, and the initial condition of the fuel is largely unknown.

In many cases there is information on the atmosphere and temperatures that outer components of dry storage systems are exposed to, but the only direct information available for the SNF stored in them have come from monitoring of the double seal systems in the lids of bolted casks. A small number of bolted lid metal casks that have had a loss of seal such that they needed to be returned to the SNF pool for seal replacement. In some of these instances, the SNF assemblies that were in the cask that were returned to the pool were removed, and a visual inspection of some of the rods was conducted. Indirect rod integrity information was provided by measuring the gas inside the casks being returned to the pools for the presence of ^{85}Kr prior to reflooding the cask. After the returned casks were reflooded and the lids removed, the storage systems sealing surfaces and seals were inspected and seals replaced if necessary.

7.2.1. Canadian CANDU irradiated fuel demonstration

Canada had a three-part demonstration to confirm the long term behaviour of CANDU fuel. The programme was conducted at the former Whiteshell Nuclear Research Establishment [7.1, 7.2]. A variety of CANLUB and non-CANLUB fuel bundles were used in 28- and 37-element bundles. Both fresh and spent CANDU fuel with intentional defects in the form of pre-drilled small holes through the cladding were stored. The real casks were equipped to monitor both the cladding temperatures and the composition of the cask cover gas. One demonstration was conducted in dry air at ~55°C, another in dry air at 150°C and the third one in an air-moisture saturated atmosphere at 150°C. Initially, approximately 100 mL of water for each assembly was added to the test canister. The burnup of the spent fuel ranged from 7.5 to 10.8 GWd/t(HM) and had been cooled from 1.5 to 9 years after reactor discharge [7.3]. No fluence level was specified. Examination of the spent fuel occurred 22.5 and 99.5 months after test initiation [7.4]. No change was visually observed in any of the intact rods. Profilometry on selected intact and defected rods indicated no significant creep.

A few rods were removed for destructive examination including metallography and ceramography. No degradation or additional failure of the intact rods was observed.

This demonstration used several different atmospheres and types of CANDU fuel that are experienced in the Canadian dry cask storage programme. As a result, comparisons were able to be made of the effects of the variables such as linear power, CANDU fuels versus CANLUB fuels, and moisture content of the cask atmosphere. The comparisons are discussed in detail by Wasywich [7.1–7.4]. The results of the final examination in 1992 [7.4] are summarized below by He [7.5]:

– There were no significant changes to spent nuclear fuel (SNF) rods, equivalent hydrogen concentration, outer surface of stainless steel pressure vessels, and dimension. For the case of multiple fracture areas, the end-cap element showed up to a 1.2% increase in diameter over the pre-demonstration value. However, it was suspected that the fracture damage had been introduced during the pre-demonstration period;
– There was no migration of fission products from the SNF pellet matrix to the gap region during storage. There was no apparent movement of radionuclides for both intact and defected bundles;
– Grain boundary oxidation occurred for defected SNF rods when water was introduced into the test cell. A very thin oxide layer was present on the oxidized SNF fragments when the test was conducted in dry air only. For both cases, there was no evidence of bulk oxidation of the individual UO_2 grains for intact or defected SNF. The extent of fuel oxidation agreed with oxidation measurements made in the laboratory on SNF.

Wasywich [7.1] found that the water in the casks became very acidic due to radiolysis of the air and water. Additional information on these demonstrations and the analysis of the results can be found in [7.5].

The first time this demonstration was attempted in air was to prove the ability to store defected fuel in air at temperatures below 150°C. Initial results were very promising until it was found that, very early in the demonstration, the oxygen in the air was depleted, so the results didn't represent long term storage in air. However, the results were very useful for storage of fuel in a sealed, nearly oxygen-free gas atmosphere. This illustrated the importance of the proper design of the demonstration and control of the conditions [7.2].

7.2.2. US demonstration of low burnup fuel performance (US Nuclear Regulatory commission, US Department of Energy and the Electric Power Research Institute)

In the USA, Section 218 of the Nuclear Waste Policy Act [7.6] required the Secretary of Energy to establish a demonstration programme, in cooperation with the private sector, for dry storage of SNF at civilian nuclear power reactor sites. The objective of this demonstration programme was to establish storage technologies that the US NRC could approve by rulemaking for use at reactor sites without the need for additional site-specific NRC approvals.

Starting in 1984, a monitored dry storage demonstration programme was conducted at the Idaho National Environmental and Engineering Laboratory (INEEL). Five casks instrumented with thermocouples were loaded with PWR fuel with burnups up to approximately 35 GWd/t(HM) [7.7] to determine the thermal characteristics of the casks. Another cask containing BWR fuel was instrumented at the General Electric Morris Facility [7.8]. The casks were backfilled with nitrogen, helium or a vacuum, and the temperature was measured with the casks oriented horizontally and then vertically. The fuel was characterized visually and/or by sipping to determine the integrity of the rod cladding. No breached rods were put into the casks tested. In May 1985, fuel rods from two of the casks were removed from the original assemblies and then consolidated to reduce the volume by a factor of two and placed back in the TN-24P and VSC-17 casks. A complete description of the tests is presented in [7.9].

The cover gas in the casks was monitored and analysed to determine changes in atmospheric composition and for ^{85}Kr, which, in sufficient quantity can indicate a leaking rod. ^{85}Kr indications were found during the three-month testing of the Cooper BWR fuel in the REA-2023 cask at the GE Morris storage facility and in the TN-24P cask when it held unconsolidated fuel. It is thought that the leak in the TN-24P cask occurred when the cask was rotated. In neither case the leaker was able to be visually identified at the end of the test. The size of the ^{85}Kr indication along with the lack of visible identification indicates that the breaches were very small and would not be considered as 'gross damage' as referred to in the NRC Regulation 10 CFR 72 and described in more detail in NRC's Interim Staff Guidance 1, Rev. 2 [7.10]. No leakers have been identified in the CASTOR-V/21 cask holding 21 PWR assemblies since September 1985 (Figs 7.1, 7.2 and 7.3), the VSC-17 cask holding 17 consolidated PWR assemblies since September 1990, or the MC-10 cask [7.11] holding 12 to 24 PWR assemblies since 1986. Up to 10 leakers appeared in the TN-24P cask [7.12] after it was loaded with consolidated PWR fuel in 1986 [7.13]. These leakers are probably a result of aggravation of the irradiation-induced incipient cladding defects when the rods were pulled from the assembly for consolidation.

The US Department of Energy (US DOE) and the Electric Power Research Institute (EPRI) also signed a cooperative agreement with Carolina Power and Light Company (CP&L, now Duke Energy) to demonstrate the NUHOMS technology at the H.B. Robinson plant for at-reactor dry storage. The project started in 1983 and culminated in July 1989 with the loading of SNF into the eight NUHOMS-07P storage modules, following receipt of a site-specific ISFSI license [7.14]. CP&L and EPRI documented the results of this demonstration programme as shown in [7.15, 7.16].

In the early 2000s, the CASTOR-V/21 cask was opened after approximately 14 years of storage to examine the condition of the interior components, seals and fuels. Other than basket cracks that were originally present, the interior components were in excellent condition. The seals showed some indications of wear. There was very little flaking of CRUD from the rod cladding. A number of rods were removed for non-destructive and destructive examination. Rod puncture indicated no additional fission gas release and profilometry indicated that within the uncertainty caused by the lack of pre-testing rod diameters no cladding creep had occurred. The temperature measurements were sporadic, so it was difficult to determine the time-dependent profile and correlate the measured creep with calculated creep. A deficiency in this demonstration was lack of characterization of the rods prior to testing, causing an uncertainty in the interpretation of the results for cladding creep. If more creep had been observed this might have negated a significant amount of the findings. Full accounts of the post-demonstration observations can be found in [7.17, 7.18]. The results of these confirmatory tests provided data upon which the US NRC partially relied in granting licenses for longer term storage and transportation of low burnup fuel (<45 GWd/t(HM)).

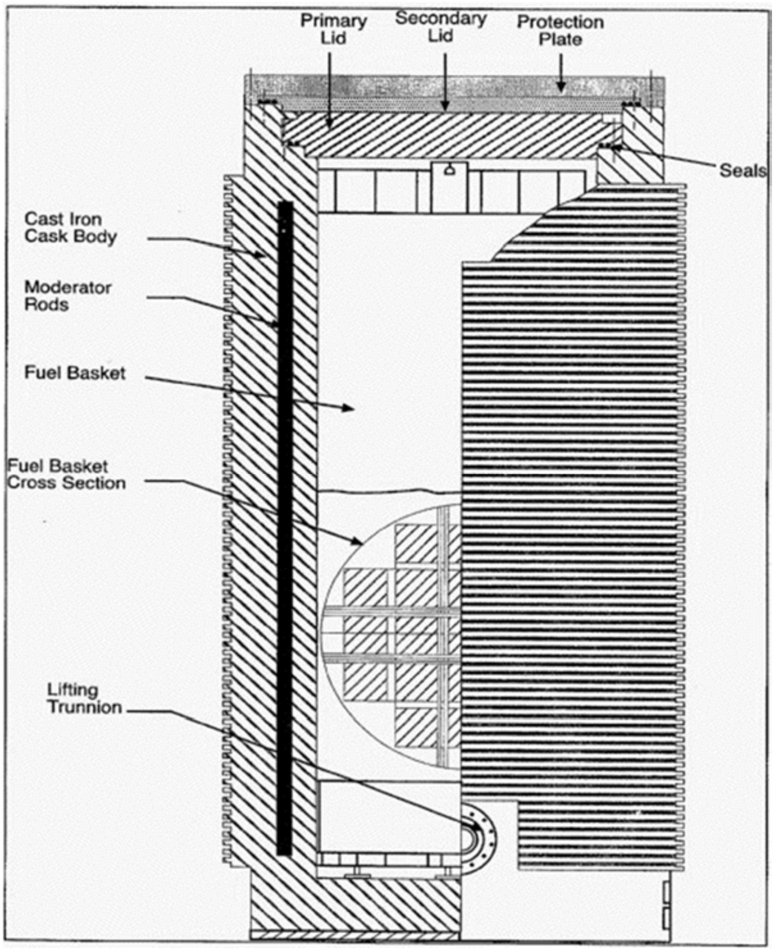

FIG. 7.1. CASTOR V/21 metal storage cask (adapted from [7.19]).

The canister or cask designs for the demonstrations were somewhat modified to collect cask internal temperature and gas composition data during initial cask/canister drying. An example of the modification for the CASTOR V/21 bolted lid system for the testing at INL is shown in Figs 7.2 and 7.3. The tests provided valuable data to benchmark thermal and shielding models used for dry storage system development. This is an example of the need to depart slightly from a completely realistic full-scale demonstration test to allow for data collection (see Table 7.1). However, given the limited modifications made to collect the data, all of the important design features of the cask were unaltered such that essentially no departure from realism for the conditions affecting the SNF, shielding, or factors affecting heat transfer and temperature distribution in the full-scale demonstration was caused due to the instrumentation added.

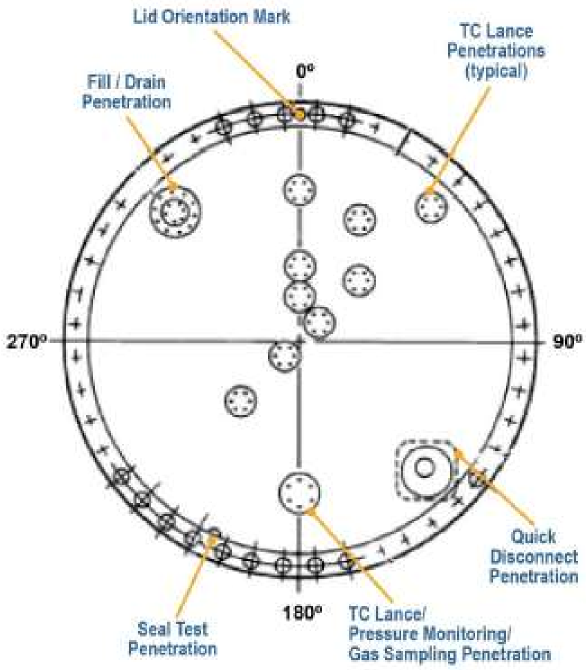

FIG. 7.2. Diagram of the modified CASTOR V/21 lid showing the thermocouple (TC) lance and pressure monitoring/gas sampling penetrations (reproduced courtesy of EPRI) [7.20].

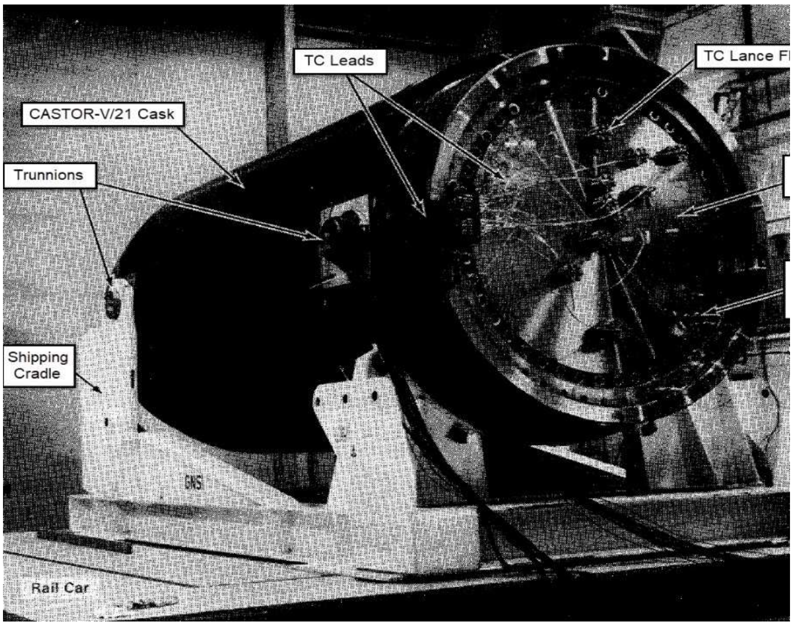

FIG. 7.3. CASTOR V/21 showing the thermocouple (TC) leads through the modified lid (reproduced courtesy of EPRI)[7.21].

7.2.3. US Department of Energy (US DOE) transport-vibration demonstration

The US DOE conducted a demonstration at Sandia National Laboratories (SNL) to determine the vibration loading on a fuel assembly as it was transported by truck over a typical transportation route (see Fig. 7.4). An unirradiated fuel assembly with rods having similar weights to the real rods in a basket with an actual truck cask PWR basket configuration on a truck trailer which replicated the weight of a real cask was run over 64 km to determine the vibration spectra transmitted to the PWR assembly and fuel rods [7.22]. The system was fully instrumented to determine the strain and accelerations on the assembly and rods. The test showed that the expected stress amplitude was based on shock strain of 213 µm/m (213 µin/in). The estimated range of vibration cycles in a 3200 km rail trip was < 2×10^6 cycles, and 3×10^4 shock cycles. In both situations, the number of vibration cycles prior to fatigue failure in the laboratory tests [7.23] was at least a factor of 5 times greater than the number of cycles measured in the road test [7.24]. Furthermore, the amount of strain applied to the laboratory samples was higher than the strains measured during the truck test. The truck test results were used to model the expected normal conditions of transport fuel rods would encounter. This demonstration had trade-offs (departures from actual materials, materials properties, vibrations, or environmental conditions from those that are typical of actual properties and conditions of SNF being transported in transportation overpacks) made due to availability of a cask, unirradiated nature of the fuel, difficulty of instrumenting an actual fuel assembly, etc. These trade-offs are shown in USA 192–9 - Annex XIV. Trade-offs require a detailed interpretation of how the demonstration results relate to the transport of an actual assembly. This demonstration is an excellent example of how trade-offs are handled.

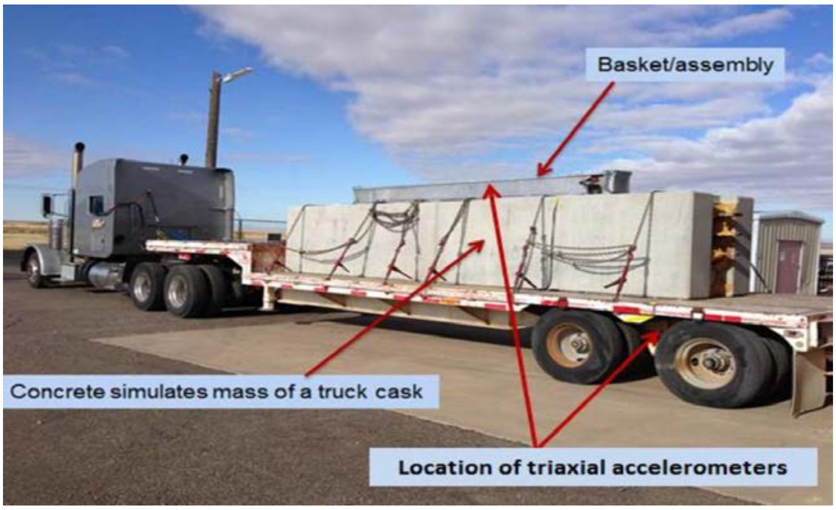

FIG. 7.4. Over-the-Road Truck Test- Simulated Over-the-Road Test conducted over 64 km to simulate various road conditions and speeds (reproduced courtesy of US DOE)[7.22].

Multimodal Testing

In 2017, the US DOE, in cooperation with Equipos Nucleares, S.A. (ENSA) of Spain, Empresa Nacional de Residuos Radiactivos, S.A (ENRESA) of Spain, Korea Radioactive Waste Agency (KORAD) and the Korea Atomic Energy Research Institute (KAERI), conducted a multimodal transportation demonstration in an ENSA transportation cask (the ENUN-32P (Fig. 7.5)) via truck, railcar, barge, and ocean-going ship. Three surrogates, unirradiated, instrumented assemblies were placed in the cask [7.25]. These assemblies are listed below along with the source of the surrogate assemblies:

- Sandia National Laboratories (USA): the same assembly of the Westinghouse 17 × 17 configuration used in the shaker table tests with one Zircaloy-4 clad rod with lead pellets and another Zircaloy-4 clad rod with molybdenum pellets. The remaining rods are copper clad and contained lead rope. The assembly was instrumented with eighteen strain gages and six accelerometers;

– ENRESA (Spain): an assembly of the Westinghouse 17 × 17 design with fuel rods having Zirlo cladding containing molybdenum pellets. The assembly was instrumented with eighteen strain gages and six accelerometers;
– KORAD/KAERI (Republic of Korea): a Korean PWR assembly containing fuel rods with Zirlo cladding containing metal simulated pellets. The assembly had one strain gage and three tri-axial accelerometers.

UO_2 pellets were not used because the environmental safety and health requirements were prohibitive and put the project at risk of not happening. The remaining 29 spaces in the basket inside the cask were filled with concrete 'dummy assemblies' that mimicked the weight of real assemblies. An actual rail cask basket and cradle were used, although the basket didn't experience the ageing that might occur during extended storage. The basket, cask, cradle and skid were instrumented with three, six, eight and seven accelerometers respectively. Modelling was used to identify the optimal places within the cask for the surrogate assemblies.

The cask and test assemblies were shipped from Maliaño Santander, Spain to the Transportation Technology Center in Pueblo, Colorado, USA (Fig. 7.6), where they underwent testing over various controlled track conditions. In addition to the transport legs, data (strain, acceleration, number of cycles and temperature) were collected during intermodal transfers from truck to barge, barge to ship, and ship to rail [7.25]. Pictures of the various transport vehicles are shown in [7.26]. Eight different tests encompassing 125 separate events including road crossings and track switches were conducted over nine days. Data was also obtained during the return rail trip to Baltimore. Complete details of the test, instrumentation, data acquisition system and cask design are given in the ENSA/DOE Cask Shock and Vibration Test Plan [7.27]. The cask was returned to Spain without monitoring and the demonstration concluded in October 2017. A significant amount of data analysis, including modelling the effects of the surrogate components from the testing is required to draw definitive conclusions from these tests.

This should be considered a partial demonstration because of the number of surrogates used for some components such as concrete non-instrumented assemblies and the fuel rods in the instrumented assemblies. Due to contractual agreements and operational limitations, the test programme wasn't optimized. If a rod breach occurred during transport, there wasn't a way to determine in which leg of the journey it occurred or if the breach would have occurred in actual irradiated fuel. The ability to say with confidence that other HBF can be transported under normal conditions while maintaining its configuration depends on successfully developing and benchmarking a structural model of the transportation system.

There are still questions about how changes to the cladding and assembly components due to the irradiation, such as loosening of the retention force of the grid springs on the rods, irradiation hardening of the spacer grid springs, embrittlement of the grid spacers and potential collapse of the support guide tubes in the horizontal transport configuration will affect the input data used in the models. Finite element analyses were conducted to evaluate the effects of guide tube collapse, grid collapse and vibration impact of the assembly with the basket wall [7.28]. The results showed that the grid spacers and guide tubes, which are the main components bearing the gravitational and vibrational load when transport is in the horizontal orientation, are at risk of failure during normal conditions of transport, which will affect the vibration modes and intensity during transport.

The model should consider resonance and enhanced stress on the fuel under certain combinations of components and material performance of the SNF fuel rods or assembly hardware. This later point is important if the SNF will need to be stored again after transport. Once validated, these models should also be used to estimate the sensitivity of measured road and rail test loads and frequency results to changes in design of the cask, basket and fuel.

The strain and vibration data recorded during the trip will inform computer models to support future licensing and safe, secure transport of SNF. As of early 2018, the data was still being analysed prior to publication.

FIG. 7.5. Design of the ENSA ENUN 32P cask (reproduced courtesy of ENSA) [7.27].

FIG. 7.6. Transportation route for the ENSA test cask (reproduced courtesy of ENSA) [7.27].

7.2.4. German testing

Ispra

Germany conducted full-scale dry storage cask demonstrations with 10 irradiated PWR and 15 BWR fuel rods in the Research Center at Ispra, Italy [7.29, 7.30]. The primary focus of the demonstrations was to determine if fuel rods would degrade under storage temperatures at or somewhat above the maximum expected temperatures of in-service storage systems. Data was also collected that shed light on the amount of water left in the cask after the drying process. All the rods were characterized before the demonstration. Tests lasted up to 17 months in an oxygen-free atmosphere. The isothermal temperature was raised in 6-month increments from

400 to 450°C[18]. Visual and eddy current examinations confirmed the integrity of the rods. The main conclusions were that no rods breached, HT (hydrogen tritiated gas) and HTO (tritiated water) were found in the cask atmosphere, and the creep strain after each temperature change and the total creep strain were below 1%, at which time cladding creep stopped. Over a long duration the pressure, temperature, and decay heat in the fuel rod dropped. Therefore, the researchers think that since the driving force for cladding degradation has been sufficiently removed after two years, it is of no consequence whether the storage period is 20 or 100 years as long as an inert atmosphere is maintained. Calculations were conducted to compare the results with theory [7.29, 7.31]. Shorter term tests using a whole assembly are described in [7.30]. These tests used both single rods and whole assemblies. These short term tests ran longer than 6 years at temperatures as high as 440°C. Several effects were measured such as defective fuel rod behaviour, drying efficiency, fuel fragmentation, cladding oxidation and creep. These tests are 'part scale' (see Table 7.1); the tests did not use a storage system that was full-scale but ran substantially longer than laboratory tests under typical storage conditions.

CASTOR cask demonstrations [7.32]

Demonstrations in an inert atmosphere were conducted in 3 models of CASTOR casks using over 3000 PWR and BWR fuel rods. They lasted between 24 and 30 months. The rod burnups were between 6 and 30 GWd/t(HM). Maximum temperatures ranged from 250°C to 430°C. Pre- and post-examinations were conducted on select fuel rods to determine rod integrity and cladding creep. During the tests the temperature distribution inside the cask was measured, and the cover gas was sampled for ^{85}Kr and ^{3}H. There was no significant cladding creep, and no indication of rod failure. Additional information can be found in [7.32]. These were full-scale demonstrations as they used actual fuel in actual casks under actual storage conditions.

7.2.5. Japanese demonstrations

Seal performance

An approximately 19-year demonstration test of the ability of a metal seal to hold leak-tightness was conducted by the Central Research Institute of Electric Power Industry (CRIEPI) for defining the design lifetime of a metal seal. Two full-scale lids were tested at a constant temperature (temperature of the secondary lid gasket is about 130°C and 140°C for each lid model). Since the lid temperature will drop with time the demonstration under constant temperature, this test could be considered to be accelerated. The seal maintained a constant, long term leak rate over the duration of the storage demonstration. This demonstration is continuing and is discussed in Chapter 5 "Bolted closure systems of dry storage casks".

Long term demonstration of fuel rod behaviour

A demonstration was conducted on 5 BWR-MOX rods and one PWR-UO_2 rod stored for 20 years after discharge. The BWR-MOX rods had a burnup of ~20 GWd/t(HM) and the PWR-UO_2 rod had a burnup of ~58 GWd/t(HM). Three of the MOX rods were stored in water (wet condition) and 2 were cut into segments and stored in air (dry condition). In all cases, the rods were stored with other rods to provide heat. Sibling rods[19] of BWR-MOX before storage were

[18] No indication was given how the temperature was raised.

[19] A sibling rod is one from the same or another assembly that has seen a nearly the same irradiation history and manufacturing history.

examined (visual, gas puncture, pellet and cladding ceramography and metallography respectively, and pellet density) to form a baseline for comparison. Similar examinations were conducted on the stored rods after 20 years at ambient temperature (60°C). No substantial change in the fuel condition was observed. Full details can be found in [7.5, 7.33]. One major deficiency in this demonstration is that the temperature at the commencement of storage was not measured.

Impacts of the earthquake

Although not controlled, the behaviour of the dry cask storage systems at Fukushima Daiichi Nuclear Power station which was hit by a huge tsunami caused by Tohoku Pacific Ocean earthquake on 11 March 2011 could be considered a full-scale demonstration since prior to the earthquake the fuel was stored under normal conditions and both the cask and fuel were examined after the earthquake. Nine all-metal, bolted lid casks containing Zircaloy-2-clad BWR fuel rods with a burnup of approximately 30.0–33.5 GWd/t(HM) had been stored horizontally for 15 years prior to the earthquake. No temperature measurements were made, but the maximum fuel cladding temperature was calculated to be below 270°C. Before opening after the accident, an analysis of the cover gas in all nine casks was conducted. All nine casks were opened, and the metallic O-ring seals were inspected. Visual inspection was conducted on fuel rods withdrawn from two of the casks. The inspections showed no degradation of the fuels, casks, or seals during the 15-year storage period or due to the earthquake [7.34].

(a) *(b)*

FIG. 7.7. Dry storage cask building immediately after the earthquake (reproduced courtesy of Institute of Nuclear Materials Management (INMM)) [7.35]: (a) Cask custody building; (b) Dry casks.

7.3. SYNOPSIS OF THE CRP DEMONSTRATION WORK

7.3.1. US Nuclear Regulatory Commission (US NRC) considerations in developing a demonstration programme

The US NRC made a presentation on elements and considerations for a good demonstration programme. The full presentation details are in USA 192–9 - Annex XIV. There are several considerations before a demonstration is started. Foremost is why one is doing the demonstration, i.e. its purpose. It might be confirmation of existing models, gaining operating experience or as input to an ageing management programme. Once that is established the type of demonstration ('demo') can be determined keeping in mind all the trade-offs and restrictions that might be necessary to physically accomplish the demo in a way that can provide data that are interpretable and can be modelled if necessary. The presentation discusses a number of different types of demonstrations along with their pros and cons. They range all the way from using many new casks for redundancy to doing a demonstration in a controlled hot cell. The US DOE evaluation of constraints and compromises developed by Sandia National Laboratories is discussed [7.36]. This includes a discussion of the ramifications of the constraints and trade-offs on the potential usefulness of the results. This must include the stresses and conditions that influence the behaviour of the demonstration and the auxiliary testing and modelling that is necessary.

The remainder of the presentation dealt specifically with demonstrations for long term irradiated fuel behaviour in dry storage. The NRC Interim Staff guidance ISG-24, Rev. 0, ''The Use of a Demonstration Program as a Surveillance Tool for Confirmation of Integrity for Continued Storage of High Burnup Fuel Beyond 20 Years'' [7.37] deals with the variety of variables that must be controlled, fuel variables that must be specified, and pre-, post-, and in-progress examinations and data gathering that is necessary for the most optimum demonstration that can support an ageing management programme. Because breaking containment to access the SNF in storage usually extracts a severe penalty in terms of time, dose, and cost, if the demo is to be conducted at a utility, the economic and worker dose costs are usually prohibitive such that a demo is only done if a known safety issue must be resolved[20]. Examination of the fuel to gather data on its behaviour is usually not done. Therefore, the demonstration may be for the purpose of providing operational experience on the behaviour of the fuel for an ageing management programme. The way the demonstration fits into the elements of the ageing management programme is discussed. Additional discussion of these issues can be found in [7.38].

7.3.2. Japanese demo

In Japan, interim storage of SNF in dual purpose dry metal casks is planned for a maximum of 50-years until reprocessing. During the interim storage period, cladding integrity of SNF will be maintained and the safety of transportation after the storage will be ensured based on the knowledge and experience concerning integrity of SNF during dry storage in Japan and overseas. To ensure safety of transportation after the storage, some of Japanese electric companies (The Japan Atomic Power Company, The Kansai Electric Company and Kyusyu Electric Company (hereinafter called 'the utilities')) are conducting a long term storage test for PWR spent fuel assemblies, which have not been used for dry storage in Japan in the similar environment of actual casks and to confirm maintenance of the SNF integrity. In this test, the utilities have installed a compact test container in the research facility that can store two 17 × 17 PWR spent fuel assemblies (see Figs 7.8 and Fig. 7.9 and JPN 174–6 - Annex VI). The utilities will take gas samples from inside the container every 5 years for a maximum of 60 years to determine if any of the fuel rods have begun leaking, and it will confirm the fuel cladding integrity (see JPN 174–6 - Annex VI). The utilities have completed thermal testing of the container using heaters in order to test the thermocouples and develop thermal models. Starting in 2016, the first of the two assemblies (a PWR with a burnup of 42 GWd/t(HM)) was inserted and the testing began. The utilities plan to add the second assembly (burnup of 55 GWd/t(HM)) in 2026.

[20] Three times bolted casks have been opened because leaks were detected in the seals.

This test is a ‘part scale’ demo (see Table 7.1): two full-size assemblies will be used in a special container. The time scale is ‘full-scale’ while the dimensions are partially full-scale (actual irradiated assemblies) and partially part scale (smaller canister).

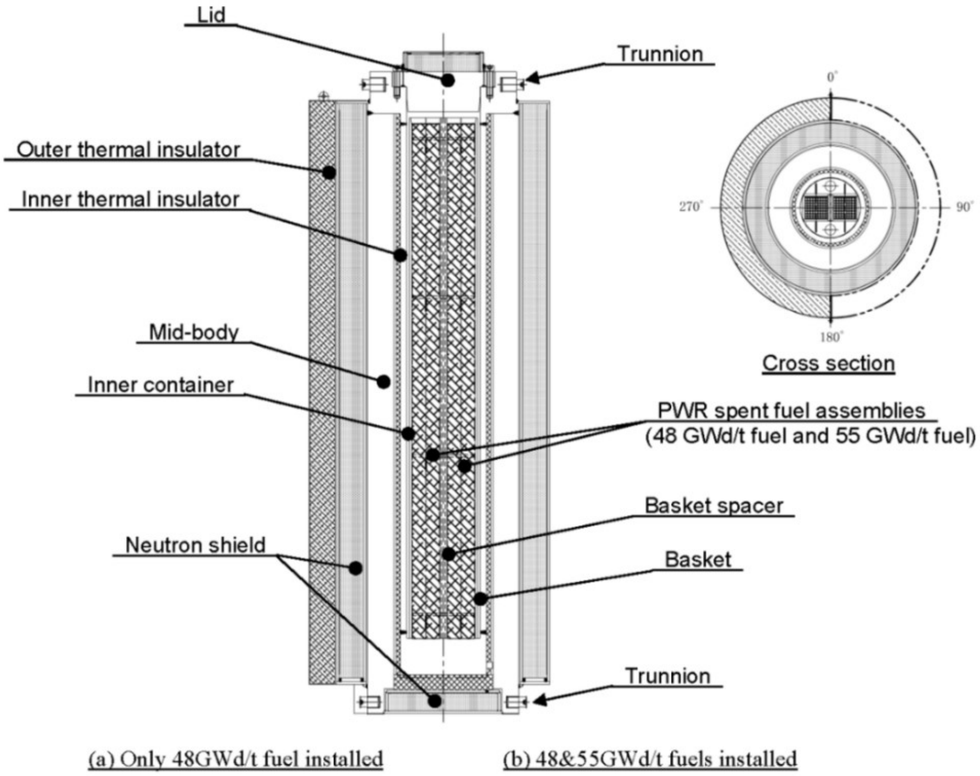

FIG. 7.8. Schematic of the Japanese demo test container (reproduced courtesy of JAPC, Kansai Electric Power Company and Kyushu Electric Power Company).

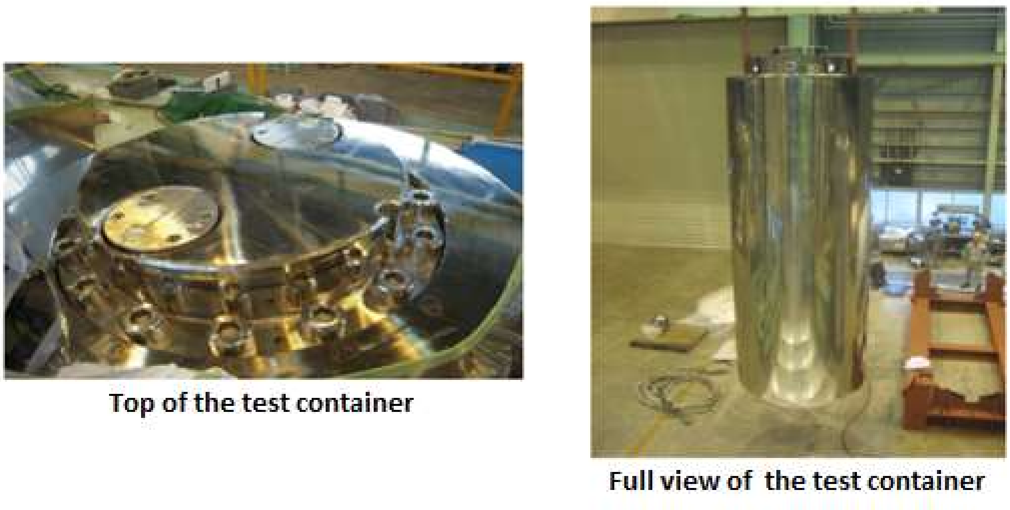

FIG. 7.9. Photos of the Japanese demo test container (reproduced courtesy of JAPC, Kansai Electric Power Company and Kyushu Electric Power Company).

7.3.3. Other demonstrations being planned or in progress

7.3.3.1. US Department of Energy (US DOE)/Electric Power Research Institute (EPRI)

In November 2017, the US DOE and EPRI started a full-scale cask demonstration of high burnup (> 45 GWd/t(HM)) PWR fuel at the North Anna Nuclear Power Station in Mineral, Virginia USA. The purpose of the demonstration is to determine if the predictions of long term, HBF behaviour that was based on short term testing are correct. In a TN-32 storage cask with a modified lid for diagnostics, 32 PWR assemblies will be loaded. Prior to loading, some rods will be removed from either the test assemblies or sibling assemblies for baseline characterization. The fuel burnup is between 50 and 58 GWd/t(HM). The rods have either Zircaloy-4, low tin Zircaloy-4, Zirlo, or M5 cladding. After drying by standard means, and backfilling with helium, the system is being continuously monitored to obtain temperature profile data (axial and radial temperatures), and occasionally monitored for water, fission gases, hydrogen and air. It is expected that the maximum fuel cladding temperature will be about 270°C during drying and slightly lower during storage. The demonstration will run for approximately ten years after which it will be transported to a hot cell for removal of rods for examination. As of January 2016, 25 'sibling' rods[21] were extracted from either the same assemblies that are being used in the demo or rods from other assemblies with a similar irradiation history. These rods have been shipped to the Oak Ridge National Laboratory (ORNL). The non-destructive examinations (profilometry, visual, etc.) have been completed. Destructive examination of the rods will be conducted at ORNL, Pacific Northwest National Laboratory (PNNL) and Argonne National Laboratory (ANL). The examinations on the sibling rods will be used to establish the condition of the fuel prior to initiation of dry storage. After the storage period, additional rods from the demo cask will be extracted and tested and compared to the results of the sibling rods to determine the long term performance of HBF in long term storage, and to determine if the predictions from short term testing models can be confirmed. Examinations will include visual, puncture for gas analysis and pressure, profilometry and microscopic examination of the cladding and fuel. Complete details can be found in the test plan [7.20].

Along with almost all of the demos described in Subsection 7.2.2 above, this demo most closely fits the definition of a truly 'full-scale' test.

7.3.3.2. Republic of Korea ("DrySim6")

This demonstration has the purpose of assessing potential degradation effects on PWR spent fuel under dry storage conditions by focusing on rod creep and other material property changes that could affect cladding mechanical properties including the concentration and orientation of zirconium hydrides. The test will consist of using six irradiated fuel rods contained in a sealed stainless steel vessel placed in a pool for shielding purposes (Figs 7.10 and 7.11). It will contain 12 thermal heaters surrounding the SNF rods to control the outer temperature of SNF cladding and to maintain a given storage temperature profile. The system will be instrumented to continuously measure the rod temperature. After 3 years of testing, the rods will be removed and measured to identify any signs of cladding creep. It is expected that in 2018 the system will be installed in the KAERI post-irradiation examination pool, and initial performance testing without SNF rods will be conducted. Extensive pre-demonstration characterisation, as

[21] A 'sibling' rod is one that closely resembles the characteristics of the rods in the demonstration, such as burnup distribution, reactor operating history, and cladding type.

indicated in Table 7.2, for 6 sister rods just located next to the demonstration test rods in the assemblies has been completed [7.39]. The test rods have Zircaloy-4 cladding and a burnup in the range of 43 to 52 GWd/t(HM). Further work will depend on national funding levels. Details of the test are given in the Table 7.2, Figs 7.9 and 7.10 [7.40, 7.41].

The DrySim6 test is part scale: the rods are full length; the testing period will exceed that of most laboratory tests; the temperatures will partially mimic real rod temperatures during storage; and the rest of the test system is smaller scale.

FIG. 7.10. KAERI experimental chamber (reproduced courtesy of KAERI).

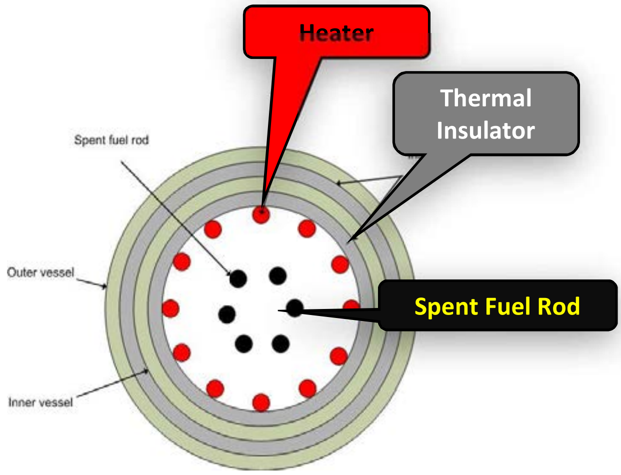

FIG. 7.11. KAERI arrangement of rods and heaters (reproduced courtesy of KAERI)[7.42].

7.3.3.3. Bolted lid seal performance

The Bundesanstalt für Materialforschung und -prüfung (BAM) is conducting long term tests on bolted lid seals to evaluate potential degradation of the seals during long term storage. The long term tests on seals are discussed in Chapter 5 on bolted closure systems.

7.3.4. Comparison of demonstrations

A comparison of the relevant details of the active or planned fuel demonstrations is given in Table 7.2 below. The same information, where available for completed demonstrations, is given in Table 7.3 below. The US demonstration on road vibrations and Japanese and German demonstrations on gasket durability have not been included because they are one-of-a-kind and have a different set of characteristics than the fuel that need to be specified to interpret the results.

None of the demonstrations clearly stated why the particular fuels or conditions of the demonstrations were chosen. There is a wide range of fuels and conditions used in these demonstrations. Sometimes, the conditions are chosen to demonstrate the behaviour if a particular condition exists in the cask, such as the Canadian demonstration of defected fuel in an air atmosphere. Many of the demonstrations are designed to show how the intact fuel would behave under normal conditions of storage. Common to all the demonstrations is an intensive post-demonstration characterization of the fuel. No systematic evaluation of the cumulative demonstrations has been made.

TABLE 7.2. COMPARISON OF ACTIVE OR PLANNED FUEL DEMONSTRATIONS

	United States	**Japan**	**Republic of Korea**
Start date	November 2017	42 GWd/t(HM) – 2015 55 GWd/t(HM) – 2025	2018
Scale	Full	Part	Part
# assemblies	32	2	6 rods
Assembly type	PWR	PWR	PWR
Cladding types	Zry-4, Zirlo, M5, low tin Zry-4	Zry-4 (2016), MDA or Zirlo (2026)	Zry-4
Max cladding temperature	~270°C (drying)	~230°C	~400°C
Duration	Approximately 10 years	42 GWd/t(HM)– 35 years 55 GWd/t(HM)–10 years	3 years
Atmosphere	Vacuum dry, then He	He+10% moisture	Vacuum dry, then He
Pre-test exams	Visual, rod internal gas analysis and pressure, profilometry, metallography, and ceramography	Confirm no leaking rods, visual of assembly exterior rods	Visual, rod internal gas analysis and pressure, profilometry, metallography, and ceramography
Post-test exams	Same as pre-test	Visual, rod pressure, ^{85}Kr in cask	Same as pre-test, ^{85}Kr in cask
Exams during test	Temperature spatial distribution (continuous, multiple combinations of axial and radial positions), fission gas, H_2O, H_2, O_2 inside the cask (all intermittent)	Periodic (5 yr) container cavity fission gas ^{85}Kr, leak tightness. Internal temperature calculations based on models developed during the initial thermal testing using external temperature measurements	Rod surface temperatures, gas sampling
Burnup range	50 < BU < 58 GWd/t(HM)	42 < BU < 55 GWd/t(HM)	43–53 GWd/t(HM) (rod average)
Reference	[7.20]	JPN 174–6 - Annex VI	[7.39–7.41]

TABLE 7.3. COMPARISON OF CONDITIONS AND EXAMINATIONS FOR COMPLETED FUEL DEMONSTRATIONS

	Canada	United States-Low burnup fuel	Germany-ISPRA	Germany-CASTOR	Japan
Scale	Part	Full	Part	Part	Part
Start date	~1978	1986 (Castor V/21)	Early 1980s	Early 1980s	~1988
# assemblies or rods	Full cask load	21 assemblies	10 PWR rods 15 BWR rods	~3000 rods	# rods: 5-BWR-MOX 1-PWR-UO_2
Assembly type	CANLUB, non-CANLUB	PWR	PWR and BWR	BWR, PWR rods	2 BWR-MOX 1 PWR-UO_2
Cladding types	Zry-2, -4	CWSR Zry-4	Zry-2, -4	Zry- 2, -4	n.a.
Max temperature	150°C	420°C	400–450°C	250–430°C raised in steps	Not stated
Duration	Up to 93 months	~14 years at time of examination (continuing)	17 months	24–30 months	20 years
Atmosphere	H_2O added to air (*4)	Dry He (*7)	Dry, oxygen-free (*3)	Inert	MOX: cut rods, dry air; PWR: air/He
Pre-test exams	Some rods punctured	None other than confirmation rods were intact	Visual, eddy current	Rod integrity, creep	(*1)
Post-test exams	(*5)	(*6)	Visual, eddy current, creep < 1%	Rod integrity, creep	(*2)
Measurements during test	Temperature, cover gas analysis	Occasional temperature measurements and gas sampling	Unknown	Temperature, gas analysis	n.a.
Burnup range GWd/t(HM)	7–10	~36 maximum	n.a.	6–30	MOX ~20 UO_2 ~58
Reference	[7.1]	[7.17]	[7.29]	[7.30, 7.32]	[7.5, 7.33]

Note:

(*1) Visual, gas puncture, pellet ceramography, cladding metallography, pellet density.
(*2) Same as Note 1 plus cladding tensile tests, H_2 redistribution.
(*3) Reference says dry air, but this may not be the case since the demonstration was in a pool over water.
(*4) Upon 1st examination it was noted that the oxygen in the cask had been depleted.
(*5) Visual, end-plate torque, dimensional, gamma scan, ceramography, metallography, fuel pellet surface analysis.
(*6) Visual, gamma-scan, neutron radiography, gas analysis, profilometry, ceramography, metallography, creep testing, hardness, hydride reorientation, SEM.
(*7) Approximately six months with partial air ingress.

7.4. SUMMARY

7.4.1. Information gained from the studies to address data needs gaps that influence the way a demonstration would be conducted

It is important to understand the range of likely materials and conditions to be encountered in service as well as typical and bounding parameter values to ensure that the demonstration addresses relevant conditions as well as providing a robust case for model validation. Because of the complex inter-relationships between many of these parameters, partial demonstration projects are likely to require very careful design to ensure that important aspects being tested are clearly prototypic. Most of the part scale tests discussed above and within the annexes[22] were conducted with this in mind such that the parameters of interest in each test do represent conditions expected over the course of years to decades. The value of the full-scale tests is that such tests can determine if the part scale tests do, indeed, represent expected conditions governing the parameters of interest over the long term.

7.4.2. Findings

This CRP has identified a number of demonstration issues that need to be considered in order to increase the value of demonstration test plans with a particular set of goals in mind. Addressing these issues would potentially expand the applicability of the present and future demonstrations. Potential additional issues include:

- How demonstrations can be used to improve our understanding of long term degradation of the storage systems and stored SNF under a variety of conditions applicable to all participating countries. The potential need for additional demonstrations should be identified along with the parameters of interest. For example, demonstrations using other types of dry storage systems (e.g. vaults, SNF pools) would impose different environmental conditions (temperature, coolant properties (e.g. water instead of an inert gas), radiation) than those characteristics of dry cask storage systems. Use of other fuel types (e.g. MOX, WWER, Magnox, metallic) that are or would be placed into long term storage could identify different degradation mechanisms due to differences in materials and environmental conditions;
- If relevant data can come from just one demonstration or if data from multiple demonstrations are needed. The Japanese demonstration described in Subsection 7.3.2 is an example of, potentially, the need for just one relevant demo for the limited purpose of determining spent LWR fuel behaviour in dry storage systems with peak cladding temperatures limited to 230°C over longer time periods since it involved the use of two different types of fuel assemblies at bounding cladding temperatures. The Japanese regulator has taken the steps to lower their maximum allowable SNF cladding temperatures to 230°C to avoid any amount of hydride reorientation. This limits the usefulness of the Japanese data for those countries using a higher cladding temperature limit, such as 400°C. As long as there is no degradation that fails the cladding in either of the two types of assemblies in the current demonstration (described in Subsection

[22] The Annexes of this report are provided as supplementary material. The names of the files are composed by the country abbreviation followed by the code of the CRP and the number of the Annex. The annexes included are: ARG 17338 – Annex I, ARG 17339 – Annex II, FRA 17270 – Annex III, GFR 17307 – Annex IV, JPN 17308 – Annex V, JPN 17486 – Annex VI, LIT 17275 – Annex VII, PAK 17283 – Annex VIII, POL 17290 – Annex IX, SLO 17810 – Annex X, SPA 17305 – Annex XI, SPA 18996 – Annex XII, UK 17420 – Annex XIII USA 19249 – Annex XIV.

7.3.2), a single demonstration may be enough to establish confidence in the robust behaviour of LWR spent fuel in long term dry storage followed by transportation, but potentially only for fuel whose cladding temperature never exceeds 230°C;

- How data obtained from multiple demonstrations can be used to expand the number of storage system properties that can be determined over the long term. Pre- and post-test data for SNF and some of the common dry storage and transportation system components are likely to have more universal value. Measurements of SNF properties such as cladding creep and mechanical properties for various cladding types are just a few examples. Data for irradiation-related degradation of multiple storage system components (fuel, neutron shielding, neutron absorbers, other basket materials), as well as temperature-related degradation phenomena could also have more universal value;
- How models developed from 'separate effects' or 'small scale' test data can be confirmed by the demonstration;
- The benefit of developing novel measurement techniques that could expand the value of future demos by either improving the accuracy of some measurements, being able to measure some of the conditions inside the storage system during the demo or increase the number of long term degradation mechanisms that can be investigated. If so, explore the techniques, and what R&D that would need to be developed to make them ready for future demos or even routine use in future storage systems;
- Fuel characterisation and data that is gathered during a demonstration are not consistent and many times not presented in enough detail in reports to make the data from the demonstration useful to other situations. It would be of value to consider development of common fuel characterisation and minimum data gathering needs. Examples of areas where this is potentially needed for LWR spent fuel under dry storage conditions are for:
  - Cladding testing: pre- and post-demonstration rod properties (e.g. hydride concentration and distribution, oxide thickness, pellet-cladding interaction, ductility (e.g. Charpy, 'pinch', axial bending);
  - Test environments: ^{85}Kr, water vapor, hydrogen gas sampling (last two require a 'typical' drying scenario);
  - Cask/canister internals: visual, use of coupons.
- Dry storage systems are often designed for both storage and transportation (commonly referred to as 'dual purpose' designs). If some degradation of the dual purpose systems or the SNF stored in them occurs over longer periods of storage, this could affect the ability of these systems to be transported. It could be valuable to identify opportunities for the existing or planned storage demos (in whole or in part) to be designed or modified to be used for subsequent transportation testing.

REFERENCES TO CHAPTER 7

[7.1] WASYWICH, K.M., FROST, C.R., ''Update on the Canadian experimental program to evaluate used-fuel integrity under dry-storage conditions'', Second International Conference on CANDU Fuel (Proc. Int. Conf. Pembroke, 1989), Canadian Nuclear Society, Toronto (1989).

[7.2] WASYWICH, K.M., TAYLOR, P., FROST, C.R., ''The Canadian long-term experimental used fuel storage program'', 1993 International Conference on Nuclear Waste Management and Environmental Remediation (Proc. Int. Conf.

Prague, 1993), Vol. 1, The American Society of Mechanical Engineers, New York (1993) 549–557.

[7.3] WASYWICH, K.M., et al., "Examination of intact and defected irradiated CANDU fuel bundles stored up to ~30 months in moist air at 150°C'', Third International Spent Fuel Storage Technology Symposium/Workshop (Proc. Int. Symp./Workshop Seattle, 1986), Vol. 1, Pacific Northwest Labs, Richland, WA (1986) S-231–S252.

[7.4] WASYWICH, K.M., HOCKING, W.H., SHOESMITH, D.W., TAYLOR, P., Differences in oxidation behavior of used CANDU fuel during prolonged storage in moisture-saturated air and dry air at 150°C, Nuclear Technology 104 (1993) 309–329.

[7.5] HE, X., TIPTON, L., PAN, Y., JUNG, H., TAIT, J., EINZIGER, R.E., GONZALEZ, H., Development and Evaluation of Cask Demonstration Programs, Nuclear Regulatory Commission, Washington, DC (2011).

[7.6] UNITED STATES DEPARTMENT OF ENERGY, The Nuclear Waste Policy Act, As Amended, With Appropriations Acts Appended, DOE/RW-0438, Rev. 1, USDOE Office of Civilian Radioactive Waste Management, U.S. Govt. Printing Office, Washington, DC (1995).

[7.7] McKINNON, M.A., CUNNINGHAM, M.E., Dry Storage Demonstration for High-Burnup Spent Nuclear Fuel–Feasibility Study, Rep. PNNL-14390, Pacific Northwest Natl Lab., WA (2003).

[7.8] McKINNON, M.A., DOMAN, J.W., TANNER, J.E., GUENTHER, R.J., CREER, J.M., KING, C.E., BWR Spent Fuel Storage Cask Performance Test-Volume I-Cask Handling Experience and Decay Heat, Heat Transfer, and Shielding Data, Rep. PNL-5777 Vol. 1, Pacific Northwest Lab., WA (1986).

[7.9] McKINNON, M.A., DeLOACH, V.A., Spent Nuclear Fuel Storage-Performance Tests and Demonstrations, Rep. PNL-8451, Pacific Northwest Lab., WA (1993).

[7.10] NUCLEAR REGULATORY COMMISSION, Interim Staff Guidance-1, Revision 2, Classifying the Condition of Spent Nuclear Fuel for Interim Storage and Transportation Based on Function, NRC document ML 071420268, Nuclear Regulatory Commission, Washington, DC (2007).

[7.11] ELECTRIC POWER RESEARCH INSTITUTE, The MC-10 PWR Spent-Fuel Storage Cask: Testing and Analysis, Rep. EPRI NP-5268, EPRI, CA (1987).

[7.12] ELECTRIC POWER RESEARCH INSTITUTE, The TN-24P PWR Spent-Fuel Storage Cask: Testing and Analyses, Rep. EPRI NP-5128, EPRI, CA (1987).

[7.13] McKINNON, M.A., DOHERTY, A.L., Spent Nuclear Fuel Integrity During Dry Storage- Performance Tests and Demonstrations, Rep. PNNL-11576, Pacific Northwest Lab., WA (1997).

[7.14] ELECTRIC POWER RESEARCH INSTITUTE, An Independent Spent-Fuel Storage Installation at Surry Station: Design and Operation, Rep. EPRI NP-6032, EPRI, CA (1989).

[7.15] ELECTRIC POWER RESEARCH INSTITUTE, NUHOMS Modular Spent-Fuel Storage System: Design, Licensing, and Construction, Rep. EPRI NP-6940, EPRI, CA (1990).

[7.16] ELECTRIC POWER RESEARCH INSTITUTE, NUHOMS Modular Spent-Fuel Storage System: Performance Testing, Rep. EPRI NP-6941, EPRI, CA (1990).

[7.17] EINZIGER, R.E., TSAI, H.C., BILLONE, M.C., HILTON, B.A., Examination of spent pressurized water reactor fuel rods after 15 years in dry storage, Nuclear Technology 144 2 (2003) 186–200.

[7.18] ELECTRIC POWER RESEARCH INSTITUTE, Dry Cask Storage Characterization Project, Rep. 1002882, EPRI, CA (2002).
[7.19] BARE, W.C., TORGERSON, L.D., Dry Cask Storage Characterization Project-Phase 1: CASTOR V/21 Cask Opening and Examination, Rep. NUREG/CR-6745, Nuclear Regulatory Commission, Washington, DC (2001).
[7.20] ELECTRIC POWER RESEARCH INSTITUTE, High Burnup Dry Storage Cask Research and Development Project: Final Test Plan, Contract No.: DE-NE-0000593, EPRI, CA (2014).
[7.21] ELECTRIC POWER RESEARCH INSTITUTE, The CASTOR-V/21 PWR Spent-Fuel Storage Cask: Testing and Analyses, Rep. EPRI NP-4887, EPRI, CA (1986).
[7.22] McCONNELL, P., WAUNEKA, R., SALTZSTEIN, S., SORENSON, K., Normal Conditions of Transport Truck Test of a Surrogate Fuel Assembly, Rep. SAND2014-20495, Rep. FCRD-UFD-2014-000066, Rev. 0.1, Sandia Natl Labs, NM (2014).
[7.23] WANG, J.-A., WANG, H., JIANG, H., YAN, Y., BEVARD, B., "CIRFT testing of high burnup used nuclear fuel from PWR and BWRs", paper presented at 2016 U.S. Nuclear Waste Technical Review Board, Knoxville, TN (2016).
[7.24] McCONNELL, P., "Sandia shaker table and over-the-road vibration studies", paper presented at 2016 U.S. Nuclear Waste Technical Review Board, Knoxville, TN (2016).
[7.25] SORENSON, K., SALTZSTEIN, S., McCONNELL, P., AMMERMAN, D., ROSS, S., HANSON, B., KLYMYSHYN, N., JENSEN, P., ENGLAND, J., "Full-scale rail-cask tests with surrogate PWR assemblies", SAND2016-4379C, paper presented at EPRI Extended Storage Collaboration Program (ESCP) 2016 International Subcommittee Meeting, Charlotte, NC, 2016.
[7.26] SALTZSTEIN, S., SORENSON, K., McCONNELL, P., ROSS, S., "ENSA ENUN 32P rail cask transport tests", paper presented at the U.S. NRC Division of Spent Fuel Management (DSFM) Regulatory Conference (REG CON) 2017, Rockville, MD, 2017.
[7.27] McCONNELL, P., et.al., Rail-Cask Tests: Normal-Conditions-of-Transport Tests of Surrogate PWR Fuel Assemblies in an ENSA ENUN 32P Cask, Rep. SFWD-SFWST-2017-000004, Sandia Natl Labs, NM (2018).
[7.28] WANG, J.-A., JIANG, H., WANG, H., BEVARD, B.B., SCAGLIONE, J.M., Dynamic Deformation Simulation of Spent Nuclear Fuel Assembly and CIRFT Deformation Sensor Stability Investigation, Rep. ORNL/SPR-2015/662, Oak Ridge Natl Lab., TN (2015).
[7.29] PEEHS, M., KASPAR, G., STEINBERG, E., ''Experimentally based spent fuel dry storage performance criteria'', Third International Spent Fuel Storage Technology Symposium/Workshop (Proc. Int. Symp./Workshop Seattle, 1986), Vol. 1, Pacific Northwest Labs, Richland, WA (1986) S-316–S-332.
[7.30] PEEHS, M., BOKELMANN, R., FLEISCH, J., ''Spent fuel dry storage performance in inert atmosphere'', Third International Spent Fuel Storage Technology Symposium/Workshop (Proc. Int. Symp./Workshop Seattle, 1986), Vol. 1, Pacific Northwest Labs, Richland, WA (1986) S-215–S-230.
[7.31] SCHNEIDER, K.J., MITCHELL, S.J., Foreign Experience on Effects of Extended Dry Storage on the Integrity of Spent Nuclear Fuel, Rep. PNL-8072, Pacific Northwest Lab., WA (1992).
[7.32] FLEISCH, J., PEEHS, M., ''Analysis of spent fu174ehaviourour in dry storage cask demonstrations in the FRG'', Third International Spent Fuel Storage Technology

Symposium/Workshop (Proc. Int. Symp./Workshop Seattle, 1986), Vol. 1, Pacific Northwest Labs, Richland, WA (1986) S-253–S-262.

[7.33] SASAHARA, A., MATSUMURA, T., Post-irradiation examinations focused on fuel integrity of spent BWR-MOX and PWR-UO2 fuels stored for 20 years, Nuclear Engineering and Design 238 (2008) 1250–1259.

[7.34] SAEGUSA, T., “Roadmap of spent fuel management and report of investigation and maintenance of the dry casks at Fukushima Daiichi NPS – Tokyo Electric Power Company”, PATRAM 2013, 17th Int. Symp. on the Packaging and Transportation of Radioactive Materials (Proc. Int. Symp. San Francisco, 2013), Omnipress, Madison, WI (2013).

[7.35] TOKUMORI, R., MATSUKURA, J., “Spent fuel management at Fukushima-Daiichi NPS”, PATRAM 2016, 18th Int. Symp. on the Packaging and Transportation of Radioactive Materials, (Proc. Int. Symp. Kobe, 2016), The Japan Society of Mechanical Engineers, Tokyo (2016).

[7.36] McCONNELL, P., et al., Surrogate Fuel Assembly Multi-Axis Shaker Tests to Simulate Normal Conditions of Rail and Truck Transport, Rep. SAND2016-4576R, Rep. FCRD-UFRD-2015-00128, Rev. 1, Sandia Natl Labs, NM (2016).

[7.37] NUCLEAR REGULATORY COMMISSION, Interim Staff Guidance-24, Revision 0, The Use of a Demonstration Program as a Surveillance Tool for Confirmation of Integrity for Continued Storage of High Burnup Fuel beyond 20 Years, Nuclear Regulatory Commission, Washington, DC (2014).

[7.38] EINZIGER, R.E., An aging management plan for spent fuel dry storage and transportation, Radwaste Solutions 20 1 (2013) 38–45.

[7.39] KOOK, D., YANG, Y., YANG, J., KOO, Y., “Spent fuel storage status in Korea and KAERI’s R&D activities”, paper presented at EPRI Extended Storage Collaboration Program (ESCP) 2016 International Subcommittee Meeting, Charlotte, NC, 2016.

[7.40] KIM, D., SHIN, C., YANG, Y., KOOK, D., KWON, H., JANG, J., CHOI, J., ‘‘Design concept of integrated test system (SFFA) for safe long-term storage of SNF’’, Korean Nuclear Society (KNS) 2012 Spring Meeting (Proc. Spring Mtg Jeju Island, 2012), Korean Nuclear Society, Daejeon (2012).

[7.41] KIM, D., SHIN, C., YANG, Y., KOOK, D., KOO, Y., ‘‘Performance and durability test of DrySim6’’, Korean Nuclear Society (KNS) 2014 Spring Meeting (Proc. Spring Mtg Jeju Island, 2014), Korean Nuclear Society, Daejeon (2014).

8. CONCLUSIONS

Currently there are no disposal facilities for SNF in operation which is causing the foreseen period for wet and dry SNF storage to be extended. Furthermore, in some countries there is considerable activity related to extending the operating period of existing nuclear power reactors up to 80 years. In all cases the SNF pools at reactor sites would need to maintain their safety functions over the same time period. Given the relative complexity of nuclear power plants compared to wet and dry storage systems, if this can be achieved for nuclear plants, it is likely that wet and dry storage systems could be demonstrated to remain safe for at least the same length of time as the reactors themselves and adjacent SNF pools. As part of the US Nuclear Regulatory Commission (US NRC)'s 'Continued Storage' ruling, NRC evaluated the very long term environmental impacts of time-unlimited storage and found the impacts generally 'low' to 'medium' ('NRC 2014') [8.1]. The 'NRC 2014' analyses assumed monitoring the storage systems for signs of degradation, and mitigation of any degradation that could result in the loss of safety functions[23]. 'NRC 2014' also assumed near-complete replacement of SNF storage systems would occur every century. These assumptions lead to the need to develop and maintain capabilities to design, monitor, mitigate, and replace SNF storage systems over the course of many decades.

The overall objective of this Coordinated Research Project (CRP) is to support and share improvements in the nuclear power community's technical basis for LWR SNF management licences as dry storage durations extend. This involves developing:

- A network of experts working on current research projects to demonstrate the long term performance of SNF storage and transportation systems;
- Capability to assess the impact of high burnup fuel (HBF) on very long term storage prior to or followed by transportation.

This report provides results from the International Atomic Energy Agency (IAEA) CRP T13014 on experimental data and plans for demonstration testing on the very long term performance of SNF and related storage system components to guide the development of a demonstration programme. Experiments such as those reported here will help the future development of computational and additional experimental methods to adequately demonstrate and evaluate very long term performance.

This work contributes to technical basis documentation for demonstrating the performance of SNF and related important storage system components over long durations (CRP results are also expected to facilitate subsequent transport and disposal) and thereby facilitate the transfer of this knowledge to others including to newcomer countries.

The IAEA Spent Fuel Management Conference in 2015 [8.2] noted the growing worldwide awareness of the increasing need for long term SNF storage and recommended that the interface issues between storage and transport should be resolved and should be addressed in ageing

[23] 'Safety functions' include: radiological protection (via shielding, confinement of radioactive species inside the dry storage system, and maintaining sub-criticality); thermal performance (maintaining temperatures of specified structures, systems and components (SSCs) below thermal limits); and maintaining structural integrity.

management/in-service inspections. This CRP contributes to this objective and the sharing of information between Member States.

This TECDOC provides a general discussion of medium -to high- priority data 'gaps' that must be filled to provide the technical bases for the behaviour of SNF storage systems over the long term storage (Tables 8.1 and 8.2). Though the work conducted within the IAEA CRP, described in this TECDOC, provides data to partially close many of the data gaps listed in Table 8.1. Scientific and engineering efforts should be continued to accumulate the knowledge under the international framework. This chapter summarizes the major conclusions and identifies opportunities for further work.

TABLE 8.1. VERY LONG TERM STORAGE TECHNICAL NEEDS FOR STRUCTURES, SYSTEMS AND COMPONENTS (SSCs): SUMMARY OF 'IMPORTANCE TO R&D ASSESSMENTS' (ADAPTED FROM [8.3])

Structures, systems and components (SSCs)	Ageing alteration and/or degradation mechanism	TECDOC chapter in which the gap is addressed
Fuel cladding	Annealing	n.a.
	Hydrogen embrittlement	3
	Hydride cracking	3
	Oxidation	3
	Creep	3
Fuel pellets	Cracking, bonding	n.a.
	Oxidation	3
Fuel assembly hardware	Corrosion and stress corrosion cracking (SCC)	n.a.
Basket	Corrosion, irradiation	n.a.
Neutron shielding	Thermal and radiation ageing	6
	Creep	6
	Corrosion	6
Neutron poison	Creep	n.a.
	Embrittlement	n.a.
	Corrosion	n.a.
Welded canister	Atmospheric corrosion	2
	Aqueous corrosion	n.a.
Moisture absorber	Irradiation, thermal	n.a.
Bolted casks	Fatigue of seals or bolts	5
	Atmospheric corrosion	n.a.
	Aqueous corrosion	n.a.
	Metal seal creep	5
Concrete overpack, cask, or pad	Freeze-thaw	4
	Corrosion (including embedded steel)	4

Note:

A few of these ageing mechanisms are not detrimental to maintaining safety functions.

The gaps shown in Tables 8.1 and 8.2 can be addressed initially via small scale tests. In this TECDOC 'small scale' means tests that are performed for relatively short periods of time compared to actual SNF storage times or are performed using test materials that are smaller in scale and/or use substitute materials than that for real dry storage systems. Usually, models are developed from such smaller scale tests. Ultimate 'validation'[24] of smaller scale tests and associated models would therefore involve longer time scales and full-size systems.

TABLE 8.2. CROSS-CUTTING DATA NEEDS

Cross-cutting needs note	TECDOC chapter in which the gap is addressed
Monitoring[1] (internal)[2]	7
Monitoring (external)[3]	2, 4, 7
Temperature profile	2–7
Drying issues	3, 7
Subcriticality, burnup credit, moderator exclusion	n.a.
Fuel transfer options	n.a.
Examination[4]	7
Canister weld stress profiles	2, 7
Damage definitions	n.a.
Verification of fuel condition / fuel classification	n.a.

Note:

[1] Monitoring is a general term that includes continuous or periodic measurements or visual observations. This is sometimes referred to as inspection or surveillance.
[2] Internal monitoring is monitoring of the inside of the cask or canister. Examination of the fuel in existing canisters at the Idaho National Laboratory that were put in service in the 1980s into the early 1990s is the one example of internal monitoring that is underway (see Chapter 7).
[3] External monitoring are direct or indirect measurements of the properties of interest. Direct external measurement example: canister exterior surface temperature. Indirect external measurement example: atmospheric chloride concentration as an indication of the amount of chlorides deposited on the outside of canisters.
[4] Examination means post-test measurements or observations of the properties of interest.

Chapter 7 discusses the characteristics of useful system demonstration(s). As described above, the difference between laboratory experiments and demonstration is the prototypical conditions under which a demonstration test should be performed. Prototypical conditions are dependent on the guidance given by the country storing the fuel and doing the demonstration, the type of dry storage system(s) being used, and the types of SNF to be stored. A comparison of the attributes of various types of tests from the smallest scale ('laboratory scale') to partially full-scale in either time or size ('partial' demonstration) to full-scale in both time and size ('full' demonstration) is provided in Table 8.3. The details provided in this table are discussed in detail in Chapter 7.

[24] The term 'validation' is commonly used in this context, although the meaning is to provide an 'evaluation' of the behaviour of the full-scale storage systems to determine if the models developed from smaller scale testing adequately project full-scale system behaviour. Such an evaluation is accomplished via 'demonstration' test(s).

TABLE 8.3. ATTRIBUTES OF TESTS AT VARIOUS TIME AND SIZE SCALES WITH RESPECT TO DEVELOPMENT OF MODELS INCORPORATING IMPORTANT MECHANISMS INFLUENCING LONG TERM BEHAVIOUR OF ACTUAL SPENT FUEL DRY STORAGE SYSTEMS

Attribute of the demonstration	Laboratory scale test	Partial demonstration	Full demonstration
Purpose	Identify and study mechanisms, develop models	Identify unexpected mechanisms, confirm models (integration of effects), scaling effects	Identify unexpected mechanisms, confirm models (integration of effects), scaling effects
Physical scale (specimen size) (e.g. rod length, components size)	Generally small	Structures, systems and components (SSCs) of interest are near full-scale	Full
Time scale	Short	Long enough to extrapolate data	Long enough to extrapolate data
Instrumented or inspection capability	Yes	Mostly yes	If possible
Acceleration of effects (e.g. time, stress, temperature, bounding conditions)	Yes	Depends on purpose	No
Test conditions (e.g. stress, atmosphere, chemical, thermal)	Can be varied	Most of the conditions are realistic	Realistic
Specimen material and condition (e.g. irradiation, surrogate materials)	If possible	Yes, if possible	Yes
Cost	Low	Moderate	High

Hence, it is important to be able to evaluate the relevance of the smaller scale test results to actual dry storage conditions (long time periods and full-size systems). Figure 8.1 illustrates the linkage between smaller scale tests, the models developed from the smaller scale tests, and full-scale behaviour. Laboratory scale experiments (usually short term, small dimensions, and/or substitute materials) are often designed to investigate the effect of individual factors that may contribute to long term alteration of one or more SSCs. These are termed 'separate effects' tests in Fig. 8.1. Predictions are made using models developed from separate effects tests to estimate long term, full-scale behaviour of the actual storage systems. A 'system demonstration' is a full-scale test to evaluate the adequacy of the models. Data obtained from the system demonstration(s) are compared to the model predictions. If the models are determined to be adequately 'correct', then the models can be more confidently used to estimate long term behaviour of other dry storage systems. If the models are judged to be deficient ('incorrect'), then the data from the system demonstration(s) can be used to improve the models. Another type of testing that can be applied to evaluation of models is collection of inspection data from in-service dry storage systems. Chapters 2 through 6 discussed some separate effects tests and inspection data generated as part of this CRP and other data that can be used in the development of models.

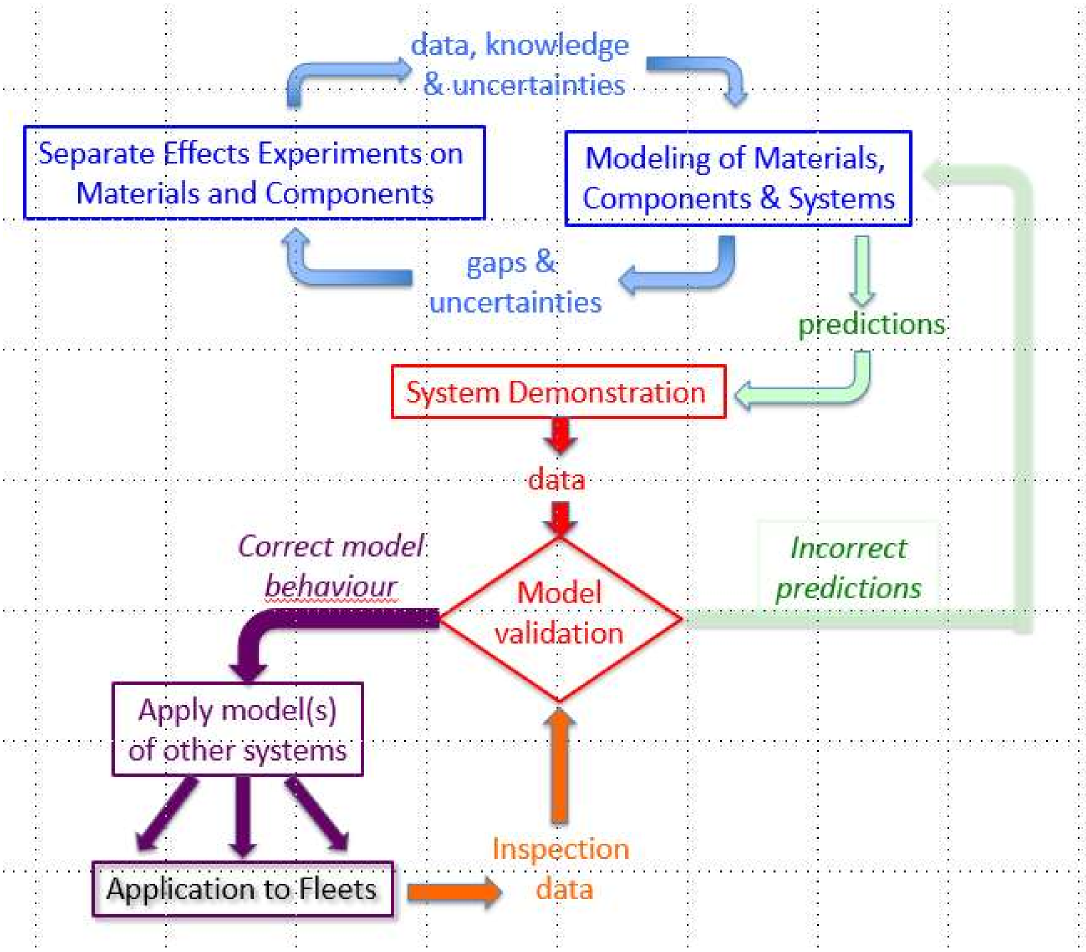

FIG. 8.1. Linkage between separate effects testing, modelling, 'demonstration' large scale, long term testing and inspection data, evaluation criteria, and determination of the extent of application to the fleet of SNF storage systems and the SNF stored in those systems.

The role of a demonstration test or project is to provide evidence as to whether scientific knowledge developed from separate effects experiments and modelling can provide reliable prediction for complex, long term phenomena, so that predictions can reliably be made for a wide range of industrial settings.

It is important to note that modelling in this context represents the use of best available scientific knowledge to:

- Demonstrate that phenomena observed in experiments can be explained by theories and physically-based correlations;
- Evaluate the uncertainty associated with predictions.

There are a number of topics covered in this report where data are primarily derived from a single organization or laboratory. Whilst international co-operation is valuable in eliminating duplications, much greater confidence in important outcomes can be gained when these are validated by independent investigation or round-robin testing.

Though experimental data on the long term performance of SNF and related important system components (such as ageing effect on the canister confinement and the metal cask lid systems) are being accumulated, there are still important uncertainties associated with corrosion of the canisters and the integrity of high burnup fuel during transport after storage. Therefore, there is a need to develop an adequate demonstration methodology relevant to these very long term performance issues.

A thorough fulfilment of the gaps shown in Tables 8.1 and 8.2 require an approach that will involve laboratory scale and small scale ‘separate effects’ experiments on materials and components and modelling. A larger scale (in both space and time) system demonstration is useful to evaluate the validity of the models to provide reliable predictions of long term system behaviour. The models should be flexible enough to be able to be used for a variety of SSCs and operating conditions so that they can be applied across the range of storage systems over long timescales in any specific regulatory environment. Figure 8.1 shows the linkage between experiments, models and system demonstrations that need to be considered when planning necessary activities to close the data gaps. These considerations formed the basis for the following conclusions.

8.1. DEMONSTRATION TESTS

Plans for future demonstration testing can be developed with a particular set of goals that would potentially expand the applicability of the past, and present demonstrations described in Chapter 7.

If the purpose of a demonstration is to determine how systems or components will perform after being stored for a significant period of time, then aged materials and components are necessary to provide reliable data. This requires that materials can be ‘reliably aged’. Approaches using ‘artificially aged’ material will eventually require longer term, larger scale ‘demonstrations’ to evaluate whether accelerated testing has introduced any artefacts.

In addition to the development of monitoring technologies that are addressed in this CRP, further work should focus on the implementation of advanced technologies to improve the methods for identification, measurement, and mitigation of long term system degradation.

8.2. STRESS CORROSION CRACKING OF AUSTENITIC STAINLESS STEEL DRY STORAGE CANISTERS

Conclusions

The results of work conducted within this CRP have provided evidence that gamma radiation is unlikely to influence canister/cask material properties during expected lifetimes and hence confirms that this is not a mechanism of concern.

Results on chloride induced stress corrosion cracking (CISCC) initiation conditions have contributed to new data by several of the organizations participating in this CRP, which is resolving some of the inconsistencies in previously reported data. An important outcome is evidence of similarity in CISCC initiation between laboratory tests under relevant stress conditions and a large scale test. Evaluation of temperature predictions used in work on CISCC has demonstrated the importance of having best-estimate models to avoid making predictions where the effects of bias are not understood, and prediction of conservative models are not conservative for a new application.

Development of monitoring and inspection techniques within the CRP (LIBS for salt concentration, temperature profiling for loss of canister integrity and instrumented coupons) has shown progress towards systems that are deployable and useful for monitoring canister integrity, although further development and qualification work remains before full value can be obtained in relation to long term management of loaded canisters. Work on acoustic emission indicated that it is unlikely to be sufficiently discriminating in real systems to warrant further development at the moment.

Future opportunities to close relevant data gaps

Technical bases to support SNF dry storage for the first few decades are mostly in place such that licensing of dry storage systems is proceeding. For very long time periods of storage followed by transportation, further work is required on SCC susceptibility, initiation times and crack growth rates under conditions that are relevant for SNF storage canisters.

To provide relevant test data to be used in the development of ageing management programmes, experimental work should be undertaken to obtain data required for mechanistically based models of crack initiation and growth so that the implications of separate effects tests for industrial canisters can be evaluated.

Given the challenges faced in obtaining reliable data on the conditions under which SCC will occur, the rate of crack growth and resulting characteristics, further work to develop monitoring and inspection systems for canister is warranted. Such work should include activities to raise the technology readiness level of existing techniques and work to demonstrate viability of new techniques.

8.3. SPENT FUEL DEGRADATION

Conclusions

The long term integrity/performance of the fuel cladding within the storage and transportation casks is essential as the first barrier to the safe confinement of the radioactive inventory during drying, storage and subsequent transportation under normal, abnormal and postulated accident conditions. The main degradation mechanisms compromising cladding integrity are those induced by the presence of hydrogen in the cladding: hydrogen embrittlement, hydride cracking and oxidation.

Burnup is a factor for the hydrogen effects in the cladding. Because of the potentially high hydrogen content accumulated during operation and the rod internal pressure, high-burnup fuel is more susceptible to radial hydride formation. Likewise, the reduction of the fuel temperature with time during the storage period will promote formation of radial hydrides, and the cladding behaviour may be brittle if the temperature is sufficiently low.

Investigation programmes have been performed to address the cladding behaviour in the long term, both with fresh pre-hydrided cladding material as well as with irradiated material. The parameters relevant to these mechanisms have been identified with an adequate level of understanding of the phenomena.

Future opportunities to close relevant data gaps

Work is still required to address the lack of knowledge and data to define the limiting parameters that determine the cladding integrity under realistic combinations of cladding material conditions and operational loads.

The most limiting mechanical loads on the cladding are produced during postulated normal operation and accident scenarios of subsequent transportation. A combined effort to adequately represent the irradiated cladding condition after storage and the realistic loads on the cladding during the hypothetical scenarios is needed, based on additional experimental data and on the development of advanced failure analysis methodologies.

The water remaining in the cask cavity after the drying process may lead to cladding oxidation during storage, and hence is a key factor to avoid fuel degradation in long term storage. Additional experimental data and analytical work is needed on this matter.

8.4. CONCRETE CASKS, OVERPACKS, AND PAD DEGRADATION

Conclusions

While the biggest issues found were hydrogen embrittlement of cladding and corrosion of canister welds, concrete overpacks and the degradation mechanisms present, particularly freeze-thaw and corrosion of reinforcement, were also considered as important gaps by several countries.

Inspection techniques applicable to concrete cask storage systems can be divided into four groups: visual inspection, non-destructive evaluation, invasive techniques and the usage of analytical tools. Visual inspection is usually the first technique used when assessing the state of concrete. There are also situations where visual inspection is not possible. Concrete overpack designs that are covered with steel lining, or are located next to each other, prevent visual inspection of certain concrete wall sections.

Non-destructive evaluation techniques can be used to detect corrosion of reinforcement, delamination, voids and vertical cracks inside concrete. However, due to limitations of the techniques, not all potential defects can be detected. Access to at least one side of a concrete surface is required, with some techniques requiring access to both. This makes the use of different methods depending on concrete casks design necessary. If the measuring device is too bulky, it might not fit inside ventilation shafts, making it inappropriate for inspecting interior concrete surface.

Invasive methods are usually needed in order to determine presence of a certain degradation mechanism. They are also combined with other non-destructive methods, since data obtained is localized and there are limitations to how many times an invasive technique can be used on a single structure.

When certain areas are inaccessible for other inspection techniques, models, calculations and analysis should be used as a form of evaluation. These methods are often used in combination with non-destructive and invasive techniques to evaluate structural integrity or predict the evolution of certain degradation mechanisms.

Other general conclusions

- The implementation of stainless steel reinforcement would, minimize any corrosion issues in concrete elements or structures;
- The use of an emission tomography system using an array of gamma detectors to detect concrete cracks and voids was investigated. As of mid-2016, the potential ability of this kind of device to detect cracks, voids or hot spots in the bulk of the silo is currently being evaluated by simulations;

- A corrosion monitoring probe that would be embedded in the concrete structure was developed and tested in the laboratory, and a part scale test was conducted in the field. After 200 days of operation, the probes are still functioning and obtaining valuable data.

Future opportunities to close relevant data gaps

The effects of the degradation mechanisms on concrete storage casks discussed in Chapter 4 could be studied more thoroughly as little research exists on the subject. In particular, the combination of degradation mechanisms and environmental conditions found at storage sites, such as high temperature and nuclear radiation, can have a negative impact on concrete longevity and durability.

8.5. BOLTED LID CASK BOLTS AND SEALS DEGRADATION

Conclusions

The long term performance of bolted closure systems of transportation and storage casks is essential to the safe enclosure of the radioactive inventory during storage and subsequent transportation under normal operation conditions as well as under accident scenarios. Most relevant and also most sensitive components to provide sufficient long term leak-tightness are metal seals consisting of a helical metal spring that is covered by two outer metal jackets. Investigation programmes have been performed to address the thermo-mechanical metal seal behaviour in the long term. Relevant parameters are the temperature and time. Accelerated ageing tests to potentially extrapolate to longer periods of time seal tests at higher temperatures can be generally used, but material and test parameters have to be determined and validated carefully. Outcomes from the test programmes shown in this report generally demonstrate proper performance of metal seals regarding leak tightness even though pressure forces and useable resilience decrease significantly.

Future opportunities to close relevant data gaps

- For the establishment of reliable models to predict the long term leak tightness of metal seals for many decades taking into consideration the Larson-Miller approach, additional investigations are needed;
- In addition, numerical approaches using finite element models are being developed for analysis and prediction of the mechanical behaviour of bolted lid systems under various loading conditions. However more experimental and numerical investigations are needed to develop and validate such finite element models;
- Other effects to be investigated are not just quasi-static loads in the long term but also dynamic loads during transportation and impact loads in accidental scenarios on bolted lid systems equipped with aged metal seals. Although some investigations have been performed successfully providing valuable information, more detailed investigations are needed to get a more comprehensive and precise understanding.

8.6. NEUTRON SHIELDING DEGRADATION

Conclusions

Typical neutron shielding materials are: water, polymers and polymeric compounds, and concrete. Shielding performance must be maintained in operation in normal conditions. This is the reason why the neutron shielding layer is often contained in a metal sheet or box. Thus, the neutron shielding layer is protected from the external environment in normal conditions. The potential for shielding material to experience changes in densities at higher temperature at some time during their in-service life needs to be taken into account. High temperatures may reduce hydrogen content through loss of weight. Since sufficient neutron shielding must continue to function even after a transportation accident involving a fire, the ignition temperature and fire resistance is important.

Various methods were employed in this CRP to measure ageing of neutron shielding materials. One method used successfully measured changes in cross-linking in polymeric materials. An optical technique was also employed to observe oxidation of polymeric materials. A third technique measured changes in polymeric material density.

For storage extension, source term and dose evaluation were addressed.

On the other hand, degradation mechanisms and evaluation which were identified as knowledge gaps were studied and new contributions have been published.

Neutron shielding performance in the long term has been evaluated through specific tests. The ageing phenomena and mechanisms are thermal or thermo-oxidative degradation eventually coupled with irradiation. Some tests are addressing temperature effects and others irradiation effects. Major results and outcomes from the studies presented in this chapter show that the safety relevant changes are small and that the shielding performance modification corresponding to the situation in dry storage and subsequent transport are very limited in all cases. Modelling approach allow for prediction of shielding efficiency after long term storage.

Future opportunities to close relevant data gaps

Data and models are already available to address this question. In order to justify the shielding performance in the long term, more tests on specimen of materials with measurement of weight loss would be useful. Additional tests for longer period could confirm existing test results and enable the designer to give more accurate predictions. The comparison of weight loss given by the model and weight loss from samples taken from an actual cask used for a demonstration, would reinforce the safety justification.

8.7. LONG TERM DEMONSTRATION TESTS

Conclusions

- Demonstration tests allow the validity of conclusions about the performance of systems and components. These are drawn from separate effects tests that are sometimes accelerated, to the performance of the components or systems under actual storage or transportation conditions;
- Successful demonstrations take careful consideration of many questions that are elucidated in the USA 192–9 - Annex XIV. Many times, the answers to these questions

involve compromises. The effect of these compromises on the potential use of the data from the demonstration should be carefully considered;

- A demonstration only confirms the component performance for one set of conditions. Prior to starting any demonstration, researchers should develop predictive models to broaden the application of the demonstration results to SNF with different cladding types or irradiation histories, in different storage systems, and under different storage and transportation conditions. Establishing the models prior to the demonstration will allow the researchers to determine what additional information will be needed to conduct the demonstration properly and interpret the demonstration results;
- If the demonstrations purpose is to confirm the performance of components that have been in storage for extended periods of time, methods must be developed to age the component in such a manner that the aged component will have properties similar to the component if it aged naturally;
- Without characterization of the test components prior to the start of a demonstration, one risks getting uninterpretable results. The amount of characterization should be guided by the models.

Future opportunities to close relevant data gaps

In addition, this CRP has identified several demonstration shortcomings that need to be addressed that could potentially expand the applicability of the past, present and future demonstrations described above. Potential questions and issues that could be considered when developing future demonstrations include:

- How can demonstrations be used to improve our understanding of long term degradation of the storage systems and stored SNF under a variety of conditions?
- Can relevant data come from just one of the demonstrations, or are data from multiple demonstrations needed?
- How might models developed from smaller scale (in both space and time) test data be confirmed by the demonstration?
- Is there any benefit of developing novel measurement techniques that could expand the value of future demos by either improving the accuracy of some measurements, being able to measure some of the conditions inside the storage system during the demo, or increase the number of long term degradation mechanisms that can be investigated?
- Fuel characterization and data that are gathered during a demonstration are not consistent and many times not presented in enough detail in reports to make the data from the demonstration useful to other situations. Common fuel characterization and minimum data to be gathered could be developed and identified.

Dry storage systems are often designed for both storage and transportation. If some degradation of the dual purpose systems or the SNF stored in them occurs over longer periods of storage, this could affect the ability of these systems to be transported. It could be valuable to identify opportunities for the existing or planned storage demonstrations (in whole or in part) to be designed or modified to be used for subsequent transportation testing. Additional information on these concerns can be found in the conclusions of Chapter 7.

REFERENCES TO CHAPTER 8

[8.1] UNITED STATES NUCLEAR REGULATORY COMMISSION, Generic Environmental Impact Statement for Continued Storage of Spent Nuclear Fuel – Final Report, Rep. NUREG-2157, Vol. 1, Office of Nuclear Material Safety and Safeguards, Washington, DC (2014).

[8.2] INTERNATIONAL ATOMIC ENERGY AGENCY, Int. Conf. on Management of Spent Fuel from Nuclear Power Reactors – An Integrated Approach to the Back-End of the Fuel Cycle, Vienna, 2015.

[8.3] ELECTRIC POWER RESEARCH INSTITUTE, Extended Storage Collaboration Program International Subcommittee Report: International Perspectives on Technical Data Gaps Associated with Extended Storage and Transportation of Used Nuclear Fuel, Rep. 1026481, EPRI, CA (2012).

LIST OF ABBREVIATIONS

μATR	Attenuated total reflectance
AE	Acoustic emission
ANL	Argonne National Laboratory
ASR	Alkali-silica reaction
BAM	Bundesanstalt für Materialforschung und -prüfung
CAC	Centro Atómico Constituyentes
CEA	Commissariat ’ l'énergie atomique et aux énergies alternatives
CFD	Computational fluid dynamics
CFS	Concrete filled steel
CGR	Crack growth rate
CIEMAT	Centro de Investigaciones Energéticas Medioambientales y Tecnológicas
CISCC	Chloride induced stress corrosion cracking
CMEA	Coupled multi-electrode arrays
CNEA	Comisión Nacional de Energía Atómica
CRIEPI	Central Research Institute of Electric Power Industry
CRP	Coordinated Research Project
CS	Compression set
CSN	Consejo de Seguridad Nuclear
CWSR	Cold-worked, stress relieved
DBTT	Ductile-to-brittle transition temperature
DHC	Delayed hydride cracking
DIC	Digital image correlation
DMA	Dynamic mechanical analysis
DPC	Dual purpose cask
DSC	Differential scanning calorimetry
ECM	Environmental control monitor
EDM	Electrical discharge machining
EN	Electrochemical noise
ENRESA	Empresa Nacional de Residuos Radiactivos, S.A.
ENSA	Equipos Nucleares, S.A.
EPDM	Ethylene propylene diene monomer rubber
EPRI	Electric Power Research Institute
EPS	Equivalent plastic strain

ER	Electrical resistance
FIP	Fuel Integrity Project
FKM	Fluorocarbon rubber
FSM	Field signature method
FTIR	Fourier transformed infrared
GNS	Gesellschaft für Nuklear-Service
HAZ	Heat affected zone
HBF	High burnup fuel
HBU	High burnup
HFP	Hexafluoropropylene
HLW	High level waste
HT	Hydrogen titrated water
HTO	Titrated water
IAEA	International Atomic Energy Agency
IAPSAM	International Association for Probabilistic Safety Assessment and Management
INEEL	Idaho National Environmental and Engineering Laboratory
ISFSI	Independent spent fuel storage installation
JAPC	Japan Atomic Power Company
KAERI	Korea Atomic Energy Research Institute
KORAD	Korea Radioactive Waste Agency
LEI	Lithuanian Energy Institute
LIBS	Laser-induced breakdown spectrometry
LILW	Low and intermediate level waste
LPB	Low plasticity burnishing
LWR	Light water reactor
MID-IR	Mid-infrared
MPC	Multipurpose canister
NCBJ	National Centre for Nuclear Research
NNL	National Nuclear Laboratory
ORNL	Oak Ridge National Laboratory
PHWR	Pressurized heavy water reactor
PINSTECH	Pakistan Institute of Nuclear Science and Technology
PNNL	Pacific Northwest National Laboratory
PRE	Pitting resistance equivalent

PWR	Pressurized water reactor
RC	Reinforced concrete
RCT	Ring compression test
RDCPD	Reverse direct current potential drop
RH	Relative humidity
RT	Room temperature
SED	Strain energy density
SEM	Scanning electron microscopy
SFE	Spent fuel element
SFP	Spent fuel pool
SNF	Spent nuclear fuel
SNL	Sandia National Laboratories
SPT	Small punch testing
SS	Stainless steel
SSCs	Structures, systems and components
TGA	Thermo gravimetric analysis
TLAA	Time-limited aging analyses
TMA	Thermo mechanical analysis
US DOE	US Department of Energy
US NRC	US Nuclear Regulatory Commission
US NWTRB	US Nuclear Waste Technical Review Board
VCC	Ventilated concrete cask
VDF	Vinylidene fluoride
VMQ	Silicon rubber
VSC	Ventilated storage cask
XRD	X-ray diffraction
ZAG	National Building and Civil Engineering Institute

ANNEXES I-XIV[25]. PROVIDED AS SUPPLEMENTARY MATERIAL

[25] The Annexes of this report are provided as supplementary material. The names of the files are composed by the country abbreviation followed by the code of the CRP and the number of the Annex. The annexes included are: ARG 17338 – Annex I, ARG 17339 – Annex II, FRA 17270 – Annex III, GFR 17307 – Annex IV, JPN 17308 – Annex V, JPN 17486 – Annex VI, LIT 17275 – Annex VII, PAK 17283 – Annex VIII, POL 17290 – Annex IX, SLO 17810 – Annex X, SPA 17305 – Annex XI, SPA 18996 – Annex XII, UK 17420 – Annex XIII USA 19249 – Annex XIV.

CONTRIBUTORS TO DRAFTING AND REVIEW

Alejano, C.	Consejo de Seguridad Nuclear (CSN), Spain
Bevilacqua, A.	International Atomic Energy Agency (IAEA)
Cobos, J.	Centro de Investigaciones Energéticas Medioambientales y Tecnológicas (CIEMAT), Spain
Conde, J.M.	ENUSA Industrias Avanzadas (ENUSA), Spain
Einziger, R.E.	US Nuclear Waste Technical Review Board (US NWTRB), United States of America
Fukuda, S.-I.	Japan Atomic Power Company (JAPC), Japan
González Espartero, A.	International Atomic Energy Agency (IAEA)
Gouzy-Portaix, S.	International Atomic Energy Agency (IAEA)
Haddad Andalaf, R.E.	Centro Atómico Constituyentes (CAC), Argentina
Hambley, D.	National Nuclear Laboratory (NNL), United Kingdom of Great Britain and Northern Ireland
Issard, H.	Orano TN, France
Kessler, J.	Electric Power Research Institute (EPRI), United States of America
Kurpaska, L.	National Centre for Nuclear Research (NCBJ), Poland
Legat, A.	National Building and Civil Engineering Institute (ZAG), Slovenia
Qureshi, A.H.	Pakistan Institute of Nuclear Science and Technology (PINSTECH), Pakistan
Ruiz, J.	Universidad Politécnica de Madrid (UPM), Spain
Shirai, K.	Central Research Institute of Electric Power Industry (CRIEPI), Japan
Šmaižys, A.	Lithuanian Energy Institute (LEI), Lithuania
Verrastro, C.A.	Comisión Nacional de Energía Atómica (CNEA), Argentina
Völzke, H.	Bundesanstalt für Materialforschung und -prüfung (BAM), Germany
Wolff, D.	Bundesanstalt für Materialforschung und -prüfung (BAM), Germany

Research Coordination Meetings

Córdoba, Argentina: 15-18 April 2013

Abiko, Japan: 10-14 November 2014

Santander, España: 11-15 April 2016

Consultants Meetings

Vienna, Austria: 27-29 March 2012

Workington, UK: 24-28 August 2015

Vienna, Austria: 22-24 February 2017

IAEA
International Atomic Energy Agency

No. 26

ORDERING LOCALLY

IAEA priced publications may be purchased from the sources listed below or from major local booksellers.

Orders for unpriced publications should be made directly to the IAEA. The contact details are given at the end of this list.

NORTH AMERICA

Bernan / Rowman & Littlefield

15250 NBN Way, Blue Ridge Summit, PA 17214, USA
Telephone: +1 800 462 6420 • Fax: +1 800 338 4550
Email: orders@rowman.com • Web site: www.rowman.com/bernan

Renouf Publishing Co. Ltd

22-1010 Polytek Street, Ottawa, ON K1J 9J1, CANADA
Telephone: +1 613 745 2665 • Fax: +1 613 745 7660
Email: orders@renoufbooks.com • Web site: www.renoufbooks.com

REST OF WORLD

Please contact your preferred local supplier, or our lead distributor:

Eurospan Group

Gray’s Inn House
127 Clerkenwell Road
London EC1R 5DB
United Kingdom

Trade orders and enquiries:

Telephone: +44 (0)176 760 4972 • Fax: +44 (0)176 760 1640
Email: eurospan@turpin-distribution.com

Individual orders:

www.eurospanbookstore.com/iaea

For further information:

Telephone: +44 (0)207 240 0856 • Fax: +44 (0)207 379 0609
Email: info@eurospangroup.com • Web site: www.eurospangroup.com

Orders for both priced and unpriced publications may be addressed directly to:

Marketing and Sales Unit
International Atomic Energy Agency
Vienna International Centre, PO Box 100, 1400 Vienna, Austria
Telephone: +43 1 2600 22529 or 22530 • Fax: +43 1 26007 22529
Email: sales.publications@iaea.org • Web site: www.iaea.org/books

19-00421

International Atomic Energy Agency
Vienna
ISBN 978–92–0–103319–2
ISSN 1011–4289